

Please cite the Published Version

Bin Ammar, Albandari (2019) Investigation of the potential effect of AGEs inhibitors for improvement of diabetics wound healing. Doctoral thesis (PhD), Manchester Metropolitan University.

Downloaded from: <https://e-space.mmu.ac.uk/623722/>

Usage rights:  Creative Commons: Attribution-Noncommercial-No Derivative Works 4.0

Enquiries:

If you have questions about this document, contact openresearch@mmu.ac.uk. Please include the URL of the record in e-space. If you believe that your, or a third party's rights have been compromised through this document please see our Take Down policy (available from <https://www.mmu.ac.uk/library/using-the-library/policies-and-guidelines>)

Investigation of the Potential Effect of AGEs Inhibitors for Improvement of Diabetics Wound Healing

Albandari Bin Ammar

A thesis submitted in partial fulfilment of the requirements
of Manchester Metropolitan University for the degree of
Doctor of Philosophy

School of Healthcare Science
Manchester Metropolitan University

2019

Abstract

Impaired wound healing is associated with hyperglycaemia in patients suffering from diabetes mellitus. Hyperglycaemia induces protein glycation and the formation of advanced glycation endproducts (AGEs). The accumulation of AGEs in the body leads to structural and functional modifications of tissue proteins. Protein glycation is believed to play an important role in the development of diabetic complications. Thus, inhibition of AGE formation may have a role in the prevention of diabetic complications. This thesis was set out to evaluate the potential effects of compounds with antiglycation activities. The investigated compounds include S-allyl cysteine (SAC), N-acetylcysteine (NAC), as well as the synthesised derivative known as compound A. The extent of glycation in the presence and absence of a number of inhibitors include SAC/NAC and compound A were assessed by several methods including fluorescence, sodium dodecyl sulphate-polyacrylamide gel electrophoresis (SDS-PAGE)-silver stain, western blotting and enzyme-linked immunosorbent assays (ELISA).

Moreover, this work aimed to evaluate and quantify the potential of human adipose mesenchymal stem cells (hADMSCs) to release these ‘drugs’ as potential therapeutics, and therefore hADMSCs were primed with SAC/NAC, compound A and concentration analysed using high performance liquid chromatography (HPLC). The SAC/NAC and compound A showed protective effects against AGEs formation. These inhibitors reduced the cell migration and tube formation of cultured bovine aortic endothelial cells (BAECs) while conditioned medium from SAC/NAC- and compound A-loaded hADMSCs induced the cell migration and tube formation in BAECs. hADMSCs provide a unique opportunity for developing a novel targeting and drug delivery system, which could effectively deliver therapeutics to specific regions of wounds or other damaged tissues. The results show the potential of hADMSCs as a drug delivery method with potential to improve wound healing. The findings from the *in vitro* study suggest that dietary supplementation with SAC, NAC, and compound A may offer protection against the damage from cross-linked AGEs and therefore would be a potential therapeutic targeting for the development of diabetic complications.

Table of Contents

Chapter 1 -Introduction	20
1.1 Diabetes.....	20
1.2 High blood sugar level complications for diabetes sufferers.....	21
1.3 Investigating the reaction between amino acids and reducing sugars.....	21
1.4 Three stages of the Maillard reaction.....	23
1.5 Maillard reaction during cooking.....	25
1.5.1 Flavour, colour, texture and aroma	26
1.5.2 Irreversible compounds and end products.....	26
1.6 Identifying AGEs.....	26
1.6.1 Major AGE structure.....	27
1.6.2 Minor AGE structure	27
1.6.3 Non-fluorescent non-cross-linked AGEs	27
1.6.4 Fluorescent non-cross-linked AGEs	27
1.7 Regulation of the Maillard reaction through physical factors.....	28
1.7.1 Influence of pH	28
1.7.2 Influence of temperature on the browning reaction	29
1.7.3 How dehydration impacts the Maillard reaction.....	29
1.8 Reducing sugars and reactive AGEs.....	30
1.9 Biological effects of AGEs	30
1.10 Receptor for advanced glycation end products	31
1.11 Diabetes mellitus and oxidative-stress signalling pathways.....	32
1.12 Advanced glycation end products and complications.....	34
1.12.1 Complications associated with damage to smaller blood vessels.....	35
1.12.1.1 Most common complications.....	36
1.12.1.2 Development of cataracts.....	36
1.12.1.3 Kidney damage in diabetic patients	37
1.12.1.4 The impact of diabetes on the nervous system.....	37
1.12.2 The impact of AGEs on major blood vessels.....	38
1.12.2.1 The impact of AGEs on arteries.....	38
1.13 Wound healing.....	39
1.13.1 The impact of diabetes on wound healing.....	44
1.14 Recognising and measuring AGEs	48
1.15 Using medicinal plants for diabetes.....	49
1.15.1 The origins and medicinal properties of garlic	50
1.15.1.1 Garlic – a closer look into the key compounds	51
1.15.1.2 Use and properties of aged garlic extract.....	53

1.15.1.3 Recommended daily garlic intake.....	54
1.16 Using synthetic compounds for diabetic complications.....	55
1.17 The role of mesenchymal stem cells.....	55
1.17.1 The use of MSCs as a mean to deliver drugs.....	57
1.17.2 The role MSCs play in healing wounds.....	59
1.17.3 Ability of MSCs to express pro-angiogenic factors.....	63
1.17.4 The impact of MSCs on immune modulation.....	64
1.17.5 Skin regeneration improvements with the application of MSCs.....	65
1.18 Uses method of analysis with chromatography.....	66
1.18.1 Selection and developing of the chromatography method.....	68
1.19 Aims and objectives.....	69
The aims and objectives of this study were:.....	69
Chapter 2 – Materials and methods.....	70
2.1 Materials.....	70
2.2 Equipment.....	72
2.3 Buffer solutions.....	73
2.4 Methods.....	75
2.4.1 Methods for <i>in vitro</i> protein glycation.....	75
2.4.1.1 Preparation of AGEs.....	75
2.4.1.2 Measurement of cross-linked AGEs using SDS – PAGE.....	76
2.4.1.3 Coomassie Brilliant Blue staining.....	77
2.4.1.4 Silver stain.....	78
2.4.1.5 Preparation of bovine serum albumin-derived advanced glycation end products (BSA-AGEs).....	78
2.4.1.6 Endotoxin removal from BSA-AGEs.....	79
2.4.1.7 Determination of endotoxin content in BSA–AGE solutions.....	79
2.4.1.8 Glycated protein dialysis.....	79
2.4.1.9 Imaging SDS-PAGE gels.....	80
2.4.1.10 Percentage inhibition of cross-linked AGEs.....	80
2.4.1.11 Measurements of fluorescent AGEs.....	80
2.4.1.12 Measurement of cross-linked AGE by Western blotting.....	81
2.4.1.13 Measurement of AGEs using ELISA.....	81
2.4.2 Methods for cell culture techniques.....	82
2.4.2.1 Preparation of cell culture medium for BAECs.....	83
2.4.2.2 Cell culture techniques for BAECs.....	83
2.4.2.3 Sub-culture of BAECs.....	84
2.4.2.4 Preparation of freezing medium.....	84

2.4.2.5	Freezing of cells.....	84
2.4.2.6	Thawing of cells.....	85
2.4.2.7	Cell counting.....	85
2.4.2.8	Protein extraction.....	85
2.4.2.9	Protein estimation.....	86
2.4.2.10	Cell migration – wound healing assay.....	86
2.4.2.11	Matrigel™ tube formation assay.....	87
2.4.2.12	Preparation of cell growth medium for human adipose-derived mesenchymal stem cells (hADMSCs).....	87
2.4.2.13	Subculture of stem cells MSCs.....	88
2.4.2.14	Cytotoxicity of the compounds on hADMSCs.....	88
2.4.3	High performance liquid chromatography (HPLC) analysis.....	89
2.4.3.1	Preparation of the mobile phase.....	89
2.4.3.2	Preparation of calibration solution.....	89
2.4.3.3	Sample preparation and derivatisation.....	89
2.5	Statistical analysis.....	90
Chapter 3	– Results.....	91
3.1	AGE formation of lysozyme induced by MG.....	91
3.1.1	Lysozyme glycation by MG after 24 hours.....	91
3.1.2	Lysozyme glycation by MG after 72 hours.....	92
3.2	Detection of AGEs.....	94
3.2.1	Detection of AGEs by fluorescence.....	94
3.2.2	Detection of AGEs by SDS-PAGE-silver stain.....	95
3.2.2.1	The effect of SAC on MG-derived AGE formation.....	95
3.2.2.2	The effect of NAC on MG-derived AGE formation.....	97
3.2.2.3	The effect of SAC/NAC on MG-derived AGE formation.....	99
3.2.2.4	Comparison between mimic compounds A, B and C on MG-derived AGE formation.....	101
3.2.2.5	The effect of compound A on MG-induced AGE formation.....	103
3.2.2.7	Effect of SAC/NAC-primed hADMSCs CM on MG-induced cross-linked AGE formation.....	107
	Figure 3.18: SDS-PAGE gel showing the effect of SAC/NAC-primed hADMSCs CM on MG-induced cross-linked AGE formation.....	108
3.2.2.8	Effect of compound A-primed hADMSCs CM on MG-induced cross-linked AGE formation.....	109
3.2.2.9	Effect of SAC/NAC- and compound A- loaded hADMSCs CM on MG-induced cross-linked AGE formation.....	111
3.2.3	Detection of AGEs by Western blot.....	113
3.2.3.1	Protein determination.....	113

3.2.3.2	The effect of MG on BAEC glycation after 24 hours	114
3.2.3.3	The effect of MG on BAEC glycation after 72 hours	116
3.2.3.4	The effect of MG on BAEC glycation after 120 hours	118
3.2.3.5	The effect of SAC/NAC on BAEC glycation.	120
3.2.3.6	The effect of compound A on BAEC glycation.	122
3.2.3.7	The effect SAC/NAC and compound A on BAEC glycation.	124
3.2.3.8	The effect of SAC/NAC- and compound A-loaded hADMSCs CM on BAEC glycation.....	126
3.2.4	Detection of AGEs by ELISA.....	128
3.2.4.1	Standardisation of ELISA for measurement of AGE.....	128
3.2.4.2	The effect of SAC/NAC and compound A on AGE levels.....	129
3.3	Cytotoxicity study of SAC/NAC using CellTiter-Blue® Cell Viability Assay.....	130
3.4	Cell Angiogenesis Assay	132
3.4.1	Effect of glucose on BAEC migration	132
3.4.2	Effect of glucose on tube formation.....	134
3.4.3	Effect of SAC/NAC in the presence of glucose on BAEC wound healing.....	136
3.4.4	Effect of SAC/NAC in the presence of glucose on BAEC tube formation.....	138
3.4.5	Effect of compound A in the presence of glucose on BAEC wound healing	140
3.4.6	Effect of compound A in the presence of glucose on BAEC tube formation	142
3.4.7	Effect of BSA-AGEs on BAEC wound healing	144
3.4.8	Effect of BSA-AGEs on BAEC tube formation	146
3.4.9	Effect of SAC/NAC in the presence of BSA-AGEs on BAEC wound healing..	148
3.4.10	Effect of SAC/NAC in the presence of BSA-AGEs on BAEC tube formation	150
3.4.11	Effect of compound A in the presence of BSA-AGEs on BAEC wound healing	152
3.4.12	Effect of compound A in the presence of BSA-AGEs on BAEC tube formation	154
3.4.13	Effect of SAC/NAC on BAEC wound healing.....	156
3.4.14	Effect of SAC/NAC on BAEC tube formation.....	158
3.4.15	Effect of compound A on BAEC wound healing.....	160
3.4.16	Effect of compound A on BAEC tube formation.....	162
3.4.17	Effect of SAC/NAC-loaded hADMSCs CM on BEAC wound healing	164
3.4.18	Effect of SAC/NAC-loaded hADMSCs CM on BAEC tube formation	166
3.4.19	Effect of compound A-loaded hADMSCs CM on BAEC wound healing.....	168
3.4.20	Effect of compound A-loaded hADMSCs CM on BAEC tube formation.....	170
3.5	Analysis of hADMSCs-loaded CM with high performance liquid chromatography (HPLC).....	172
3.5.1	HPLC method development and optimisation	172

3.5.2 Calibration curves	173
3.5.3 Detection of NAC by UV-DAD.....	174
3.5.4 HPLC analysis of NAC.....	175
Chapter 4 - Discussion.....	177
4.1 Detection of AGEs.....	177
4.2 Angiogenesis.....	181
4.3 HPLC	188
Chapter 5 – Conclusion and Future work.....	192
5.1 Conclusion	192
5.2 Limitations	192
5.3 Future work.....	193
References.....	194
Appendices.....	227
Appendix A.....	227
1. AGE formation of lysozyme induced by MG.....	227
2. Detection of AGEs by SDS-PAGE-silver stain	228
3. Detection of AGEs by Western blot	231
Appendix B: Angiogenesis	234
Appendix C: HPLC.....	243

List of Figures

Figure 1.1: A graphic timeline for some of the key discoveries made in the Maillard reaction literature	23
Figure 1.2: Formation of AGEs in three stages	25
Figure 1.3: Chemical structures of four types of AGEs:	28
Figure 1.4: Structure of RAGE. The extracellular part of RAGE contains one of the V-type immunoglobulin domains, followed by two C-type immunoglobulin domains. Dominant negative RAGE (DN-RAGE) is located inside the membrane and is functionally blunted in regulating RAGE pathways (Hallam <i>et al.</i> , 2010).	32
Figure 1.5: Signal transduction pathways activated by AGE-RAGE interaction.	34
Figure 1.6: Major microvascular and macrovascular complications associated with diabetes mellitus.	35
Figure 1.7: Schematic representation of the phases of cutaneous wound healing	40
Figure 1.8: Comparison of wound healing in healthy and diabetic people.	46
Figure 1.9: Molecular basis of debridement.	48
Figure 1.10: S-allyl cysteine chemical structure.	52
Figure 1.11: N-acetylcysteine chemical structure.	53
Figure 1.12: Structure of mimic compound A, B and C.	55
Figure 1.13: The involvement of MSCs in healing cutaneous wounds.	63
Figure 1.14: Diagram of the general structure of an HPLC system	67
Figure 2.1: Reaction of NPM with thiols to form fluorescent adducts.	90
Figure 3.1: SDS-PAGE gel showing lysozyme glycation by MG after 24 hours	91
Figure 3.2: Lysozyme glycated by different concentrations of MG after 24 hours.	92
Figure 3.3: SDS-PAGE gel showing lysozyme glycation by MG after 72 hours.	93
Figure 3.4: Lysozyme glycated by MG after 72 hours.	94
Figure 3.5: Effect of MG on fluorescent AGE formation.	95
Figure 3.6: SDS-PAGE gel showing the effect of SAC on MG-derived AGE formation.	96
Figure 3.7: The effect of SAC on MG-derived AGE formation.	97
Figure 3.8: SDS-PAGE gel showing the effect of NAC on MG-derived AGE formation.	98
Figure 3.9: The effect of NAC on MG-derived AGE formation.	99
Figure 3.10: SDS-PAGE gel showing the effect of SAC/NAC on the formation of cross-linked AGEs.	100
Figure 3.11: The effect of SAC/NAC on the formation of cross-linked AGEs.	101
Figure 3.12: SDS-PAGE gel showing the effect of compounds A, B and C on MG-induced cross-linked AGE formation.	102
Figure 3.13: The effect of compounds A, B and C on MG-induced cross-linked AGE formation.	103
Figure 3.14: SDS-PAGE gel showing the effect of compound A on MG-induced cross-linked AGE formation.	104
Figure 3.15: The effect of compound A on MG-induced cross-linked AGE formation.	105
Figure 3.16: SDS-PAGE gel showing the effect of SAC/NAC and compound A on MG-induced cross-linked AGE formation.	106
Figure 3.17: The effect of SAC/NAC and compound A on MG-induced cross-linked AGE formation.	107
Figure 3.18: SDS-PAGE gel showing the effect of SAC/NAC-primed hADMSCs CM on MG-induced cross-linked AGE formation.	108
Figure 3.19: The effect of SAC/NAC-primed hADMSCs CM on MG-induced cross-linked AGE formation.	109
Figure 3.20: SDS-PAGE gel showing the effect of compound A-primed hADMSCs CM on MG-induced cross-linked AGE formation.	110
Figure 3.21: The effect of compound A-primed hADMSCs CM on MG-induced cross-linked AGE formation.	111
Figure 3.22: SDS-PAGE gel showing the effect of SAC/NAC- and compound A-primed hADMSCs CM on MG-induced cross-linked AGE formation.	112
Figure 3.23: The effect of SAC/NAC- and compound A-primed hADMSCs CM on MG-induced cross-linked AGE formation.	113

Figure 3.24: Calibration graph of protein estimation for Western blot analysis.	114
Figure 3.25: SDS-PAGE gel showing the effect of MG on BAEC glycation after 24 hours.	115
Figure 3.26: The effect of MG on BAEC glycation after 24 hours.	116
Figure 3.27: SDS-PAGE gel showing the effect of MG on BAEC glycation after 72 hours.	117
Figure 3.28: The effect of MG on BAEC glycation after 72 hours.	118
Figure 3.29: SDS-PAGE gel showing the effect of MG on BAEC glycation after 120 hours.	119
Figure 3.30: The effect of MG on BAEC glycation after 120 hours.	120
Figure 3.31: SDS-PAGE gel showing the effect of SAC/NAC on BAEC glycation.	121
Figure 3.32: The effect of SAC/NAC on BAEC glycation.	122
Figure 3.33: SDS-PAGE gel showing the effect of compound A on BAEC glycation.	123
Figure 3.34: The effect of compound A on BAEC glycation.	124
Figure 3.35: SDS-PAGE gel showing the effect of SAC/NAC and compound A on BAEC glycation.	125
Figure 3.36: The effect of SAC/NAC and compound A on BAEC glycation.	126
Figure 3.37: SDS-PAGE gel showing the effect of SAC/NAC- and compound A- loaded hADMSCs CM on BAEC glycation.	127
Figure 3.38: The effect of SAC/NAC and compound A loaded hADMSCs CM on BAEC glycation.	128
Figure 3.39: Standard curve of BSA-AGE.	129
Figure 3.40: Interaction of SAC/NAC and compound A on MG induced AGEs' production.	130
Figure 3.41: The effect of SAC/NAC and compound A on hADMSCs viability using the alamarBlue assay.	131
Figure 3.42: Photomicrographic showing the effect of glucose on BAEC wound healing.	133
Figure 3.43: Effect of glucose on BAEC wound healing.	134
Figure 3.44: Photomicrographic showing the effect of glucose on BAEC tube formation.	135
Figure 3.45: Effect of glucose on BAEC tube formation.	136
Figure 3.46: Photomicrographic showing the effect of SAC/NAC in the presence of glucose on BAEC wound healing.	137
Figure 3.47: Effect of SAC/NAC in the presence of glucose on BAEC wound healing.	138
Figure 3.48: Photomicrographic showing the effect of SAC/NAC in the presence of glucose on BAEC tube formation.	139
Figure 3.49: Effect of SAC/NAC in the presence of glucose on BAEC tube formation.	140
Figure 3.50: Photomicrographic showing the effect of compound A in the presence of glucose on BAEC wound healing.	141
Figure 3.51: Effect of compound A in the presence of glucose on BAEC wound healing.	142
Figure 3.52: Photomicrographic showing the effect of compound A in the presence of glucose on BAEC tube formation.	143
Figure 3.53: Effect of compound A in the presence of glucose on BAEC tube formation.	144
Figure 3.54: Photomicrographic showing the effect of BSA-AGEs on BAEC wound healing.	145
Figure 3.55: Effect of BSA-AGEs on BAEC wound healing.	146
Figure 3.56: Photomicrographic showing the effect of BSA-AGEs on BAEC tube formation.	147
Figure 3.57: Effect of BSA-AGEs on BAEC tube formation.	148
Figure 3.58: Photomicrographic showing the effect of SAC/NAC in presence of BSA-AGEs on BAEC wound healing.	149
Figure 3.59: Effect of SAC/NAC in the presence of BSA-AGEs on BAEC wound healing.	150
Figure 3.60: Photomicrographic showing the effect of SAC/NAC in the presence of BSA-AGEs on BAEC tube formation.	151
Figure 3.61: Effect of SAC/NAC in the presence of BSA-AGEs on BAEC tube formation.	152
Figure 3.62: Photomicrographic showing the effect of compound A in the presence of BSA-AGEs on BAEC wound healing.	153
Figure 3.63: Effect of compound A in the presence of BSA-AGEs on BAEC wound healing.	154
Figure 3.64: Photomicrographic showing the effect of compound A in the presence of BSA-AGEs on BAEC tube formation.	155
Figure 3.65: Effect of compound A in the presence of BSA-AGEs on BAEC tube formation.	156
Figure 3.66: Photomicrographic showing the effect of SAC/NAC on BAEC wound healing.	157
Figure 3.67: Effect of SAC/NAC on BAEC wound healing.	158

Figure 3.68: Photomicrographic showing the effect of SAC/NAC on BAEC tube formation.	159
Figure 3.69: Effect of SAC/NAC on BAEC tube formation.	160
Figure 3.70: Photomicrographic showing the effect of compound A on BAEC wound healing.....	161
Figure 3.71: Effect of compound A on BAEC wound healing.....	162
Figure 3.72: Photomicrographic showing the effect of compound A on BAEC tube formation.....	163
Figure 3.73: Effect of compound A on BAEC tube formation.....	164
Figure 3.74: Photomicrographic showing the effect of SAC/NAC-loaded hADMSCs CM on BAEC wound healing.	165
Figure 3.75: The effect of SAC/NAC-loaded hADMSCs CM on BAEC wound healing.	166
Figure 3.76: Photomicrographic showing the effect of SAC/NAC-loaded hADMSCs CM on BAEC tube formation.	167
Figure 3.77: Effect of SAC/NAC-loaded hADMSCs CM on BAEC tube formation.	168
Figure 3.78: Photomicrographic showing the effect of compound A-loaded hADMSCs CM on BAEC wound healing.	169
Figure 3.79: Effect of compound A-loaded hADMSCs CM on BAEC wound healing.....	170
Figure 3.80: Photomicrographic showing the effect of compound A-loaded hADMSCs CM on BAEC tube formation.	171
Figure 3.81: The effect of compound A-loaded hADMSCs CM on BAEC tube formation.	172
Figure 3.82: Chromatograms representing the specificity of the developed HPLC method.	173
Figure 3.83: Calibration curves of NAC with water.	174
Figure 3.84: HPLC-DAD.	175
Figure 3.85: Chromatograms of derivative samples.....	176

List of Tables

Table 2.1: Preparation of separating gel.....	76
Table 2.2: Preparation of stacking gel.....	77
Table 2.3: Volume of the standard to dilute and sample diluent buffer required to establish the standard curve	82
Table 2.4: Preparation of cell culture medium supplemented with 0.1 – 15% of FBS.....	83
Table 2.5: The volume of BSA, dH ₂ O and Bio-Rad solution required to establish the standard curve	86

Declaration

I hereby declare that this work has been composed by myself, and has not been accepted for any degree before and is not currently being submitted in candidature for any degree other than the degree of Doctor of Philosophy of the Manchester Metropolitan University.

Albandari Bin Ammar

Acknowledgements

First and foremost, I would like to thank God Almighty for giving me the strength, knowledge, ability and opportunity to undertake this research study and to persevere and complete it satisfactorily. Without his blessings, this achievement would not have been possible.

I feel highly privileged to express my heartiest gratitude to the worthy and kind supervisor, Professor Mark Slevin for his dynamic supervision, constructive criticism and affectionate behaviour throughout this study. I would like to express my deep and sincere gratitude to him for his understanding and personal guidance. His wide knowledge and logical way of thinking have been of great value for me. I also would like to thank my Co-supervisor, Dr Nessar Ahmed was always there to listen and give advice.

Special thanks should be given to Dr Donghui Liu, an excellent study adviser who helped me learn several laboratory techniques and provided quotes for ordering laboratory materials. He has made his support available in a number of ways, especially towards the completion of this thesis.

I am thankful to Dr Catharine for her help in teaching me the step by step in hADMSC cell culture prepare of the MSCs medium and her outstanding attitude and vast knowledge helped me to carry on my laboratory work.

I would like to express my deep gratitude and respect to Dr Hakeem who gave me great tips on how to write up my thesis and for his valuable comments and important support throughout this work.

My acknowledgement would be incomplete without thanking the biggest source of my strength, my husband Dr Abdulmohsen, for his untiring support and endless encouragement, especially through the difficult times, who has been by my side throughout this PhD, living every single minute of it. Thank you for giving me the freedom and confidence to pursue my dreams. My children: Saud, Samar, Abdullah,

Saad and Aaliah who had to bear long hours of my absence from home, also deserve the credit for the successful completion of my thesis.

My sincere deepest gratitude to my Mum, Dad, brothers and sisters for always believing in me and encouraging me to follow my dreams. Without their encouragement and understanding, it would have been impossible for me to finish this work.

A very special thank you to my best friends Dr Sumayh and Dr Noufa for helping me enormously, especially with the mammoth task of doing the final formatting of this thesis.

Finally, I would also like to extend my greatest thanks to my sponsor (Ministry of Higher Education). Thank you for the financial and moral support throughout my course, without you this work could not have been possible.

List of Publications

1. Albandari Bin Ammar, Mark Slevin, Nessar Ahmed, and Donghui Liu. School of Healthcare Sciences, Manchester Metropolitan University, Manchester, UK. Development of a Novel Wound Dressing Coated with Drug-loaded Mesenchymal Stem Cells to Promote Wound Healing in Diabetics. *International Journal of Food Engineering Vol. 4, No. 3, September 2018*. Copenhagen, Denmark, April 9-11, 2018 *ICFSN 2018*

List of posters

1. Albandari Bin Ammar, Prof. Mark Slevin, Dr Nessar Ahmed, Dr. Donghui Liu.
Development of a novel wound dressing coated with drug-loaded mesenchymal stem cells to promote wound healing in diabetics. mmu.ac.uk. 2017
2. Albandari Bin Ammar, Prof. Mark Slevin, Dr Nessar Ahmed, Dr. Donghui Liu.
Assessment of the Ability of Compounds from AGE_{Ext} to Inhibit Protein Glycation. MMU.ac.uk. 09-2016

List of Abbreviations

AB	ankle-brachial
AF-MSCs	amniotic fluid-derived stromal cells
AGEs	advanced glycation end products
ALT	aspartate aminotransferase
ANOVA	analysis of variance
APS	APS ammonium persulphate
AR	aldose reductase
ASCs	adipose-derived stromal cells
AST	alanine aminotransferase
a_w	water activity
BAECs	bovine aortic endothelial cells
BFGF	basic fibroblast growth factor
BM-MSCs	bone marrow- derived mesenchymal stem cells
BSA	bovine serum albumin
CAT	Catalase
CEL	carboxyethyllysine
CHO	chinese hamster ovary
CM	conditioned medium
CML	carboxymethyllysine
CVD	cardiovascular disease
DAD	diode array detector
DADS	diallyl disulfide
DAS	diallyl sulphide
DATS	diallyl trisulfide
DFUs	diabetic foot ulcers
DM	diabetes mellitus
DMEM	dulbecco's modified eagle's medium
DMSO	dimethyl sulfoxide
ECM	extracellular matrix
eGFR	estimated glomerular filtration rate
ELISA	enzyme-linked immunosorbent assay
EPCs	endothelial progenitor cells

ERK	extracellular regulated kinase
FBS	Foetal bovine serum
FGF-2	Fibroblast growth factor 2
GDM	gestational diabetes mellitus
GOLD	glyoxal-lysine dimer
GPx	glutathione peroxidase
H ₂ O ₂	hydrogen peroxide
HaCaT	human adult keratinocyte
hADMSCs	human-derived adipose mesenchymal stem cells
HCl	Hydrochloric acid
HGFs	human gingival fibroblast cells
HMF	hydroxymethylfurfural
HPLC	high-performance liquid chromatography
IDDM	insulin-dependent diabetes mellitus
IL-1 α	interleukin-1 α
LDL	low-density lipoprotein
MAPK	mitogen-activated protein kinases
MG	Methylglyoxal
MMPs	membrane metalloproteinases
MOLD	methylglyoxal-lysine dimer
M _r	relative molecular weight
MSCs	mesenchymal Stem Cells
Na Cl	sodium chloride
NAD	nicotinamide adenine dinucleotide
NADPH	nicotinamide adenine dinucleotide phosphate
NF- κ B	nuclear factor kappa B
NIDDM	non-insulin-dependent diabetes mellitus
NO	nitric oxide
NO \cdot	nitric oxide radical
NPM	n-(1-pyrenyl)maleimide
O ₂ \cdot	superoxide radical
OH \cdot	hydroxyl radical
PBS	phosphate buffer saline

PDGF	platelet-derived growth factor
PKC	protein kinase c
PSG	pencillin, streptomycin and l-glutamine
RAGE	receptor for advanced glycation end products
RIPA	radioimmunoprecipitation assay
ROS	reactive oxygen species
SAC	s-allyl cysteine
SACS	s-allyl cysteine sulfoxide
SAMC	s-allylmercaptocysteine
SD	standard deviation
SDF-1 α	stromal-derived factor-1 α
SDS	sodium dodecyl sulphate
SDS-PAGE	sodium dodecyl sulphate-polyacrylamide gel electrophoresis
SEC	s-ethyl cysteine
SOD	superoxide dismutase
SPM	serum-poor medium
SPSS	statistical package for the social sciences
TBS-Tween	tris buffered saline and Tween
TEMED	N, N, N', N'-tetramethylethylenediamine
TNF- α	tumour necrosis factor- α
UCB-MSCs	umbilical cord blood-derived mesenchymal stem cell
VCAM-1	vascular cell adhesion molecule-1
VEGF	vascular endothelial growth factor

List of Units

%	Percentage
μg	Microgram
μL	Microliter
μm	Micrometre
cm	Centimetre
Da	Dalton
h	Hour
g	Gram
k	Kilo
L	Litre
mg	Milgram
min	Minute
ml	Millilitre
mm	Millimetre
mM	Millimolar
ng	Nanogram
°C	Degree Celsius

Chapter 1 -Introduction

1.1 Diabetes

Diabetes mellitus (DM) refers to a collection of chronic conditions that result from poor insulin production or insulin resistance causing hyperglycaemia. This high blood sugar and lack of insulin cause metabolic disorders impacting the ability to metabolise proteins, lipids and carbohydrates (Association, 2015; Yazdanpanah *et al.*, 2015). The pathogenesis of DM seems to be influenced by a variety of factors including autoimmune disease, viral infection and environmental factors as well as genetic factors (Fu *et al.*, 2013; Ott *et al.*, 2014).

Over recent years, diabetes has become increasingly widespread and established. This is thought to be caused by several factors from the extensive increase in consuming diets that are very calorie-rich to sedentary lifestyles, obesity and ageing populations (Ott *et al.*, Caliceti *et al.*, 2017). In 2000, diabetes was in the top five causes of death indicating how common this chronic disease is. It then became mankind's third most common cause of death, ranking behind cancer and cerebrovascular and cardiovascular diseases (Diabetes, 2011; Durstine *et al.*, 2013). In 2015, the figure indicating the number of global diabetic patients was 415 million but the World Health Organisation predicted this number to rise up to 642 million by 2040 (Bommer *et al.*, 2018).

Diabetes has been classified into four subtypes by the World Health Organisation and the National Diabetes Data Group. Type 1 refers to insulin-dependent diabetes mellitus (IDDM). This results from insulin deficiency due to pancreatic β -cells being destroyed by the autoimmune system. Around 10% of diabetes cases are IDDM. Type 2 is non-insulin-dependent diabetes mellitus (NIDDM) and results from multiple factors. NIDDM is when the glucose homeostasis regulation is abnormal as a result of resistance to insulin or a defect in insulin secretion, or a combination of the two (Ozougwu *et al.*, 2013). Type 3 is Gestational diabetes mellitus (GDM) presents due to physiological stress or the inability to tolerate glucose normally during pregnancy (Appiah *et al.*, 2016). GDM often resolves after the baby is born (Parsons *et al.*, 2018). It is also possible for Type 4 to be present as a secondary to other conditions; it can

occur as a result of biological events, metabolic events, various drugs/chemicals, genetic abnormalities and environmental factors (Yanling Wu *et al.*, 2014). Diabetic complications are not unusual and often represent a large cause of illness and death. Such complications impact the life quality of the patient and also add strain to healthcare authorities (Dart *et al.*, 2014).

1.2 High blood sugar level complications for diabetes sufferers

Diabetic complications have been recognised as being caused primarily by prolonged high blood sugar levels. The "Diabetes Control and Complications Trial" research group and the "United Kingdom Prospective Diabetes Study" both studied the relationship between diabetic complications and the severity and duration of hyperglycaemia in type 1 and type 2 diabetic patients. The studies found a significant relationship between them, confirming prolonged hyperglycaemia as the principal factor for developing complications (Giacco and Brownlee, 2010). It has also been found that it is possible to delay the start and advancement of complications by controlling the levels of glucose in the blood (Chaudhury *et al.*, 2017).

Although the links between prolonged hyperglycaemia and damage to tissues have not been completely understood and there are several mechanisms that could link the two. These possible links include hyperactivity of the sorbitol-aldose reductase pathway or polyol pathway that converts glucose to fructose (Yan, 2014), hyperactivity of protein kinase C (Feng *et al.*, 2012; Yan, 2014), hexosamine flux increase and the role of protein glycation biochemically (Fattori *et al.*, 2016b). Before looking further into diabetic complications, we must first understand protein glycation's background as well as its biological significance and chemistry.

1.3 Investigating the reaction between amino acids and reducing sugars

The Maillard reaction, or protein glycation reaction, are the names for a well-known and widely studied chemical reaction between amino acids and reducing sugars that is accelerated by heat (Echavarría *et al.*, 2012; Newton *et al.*, 2012). The Maillard reaction was first discovered in the early twentieth century by Louis Maillard and began as an observation of colour formation. Since these humble beginnings, the

reaction now has its own research capacity and within food chemistry is considered an incredibly important reaction (Echavarría *et al.*, 2012). There have been numerous studies on the reaction in an attempt to reveal details as to how it occurs and how it results in colour and flavour changes. In 1925, Mario Amadori made a discovery, termed the Amadori rearrangement that identified the N-glycosides as the unstable products of Schiff bases. In 1942, H Doob studied the influence of moisture on the protein glycation reaction and its ability to control colour formation. The influence of components including iron and copper were also recognised for their ability to enhance the reaction and, in contrast, sulphates sulfates did the opposite by preventing the reaction (FINOT, 2005; Doob Jr *et al.*, 1942). Research groups also identified that the sugar and amino acid decomposition actively aromatic aldehydes by-products (Figure 1.1) (Hellwig and Henle, 2014). The decomposition was named Strecker degradation in 1948 after Adolph Strecker. John Hodge studied the chemistry of non-enzymatic browning reactions in dehydrated foods and in 1953 presented a complete structure of the browning reaction (Hodge, 1953). These findings created an abundance of literature on the subject. It was not until the 1960s that researchers began to explore what the reaction generated in terms of harmful products. In 1968, this led to glycated haemoglobin being discovered. This caused the focus to shift from the chemistry and nutritional aspects of the reaction to the role it plays within the human body. A range of advanced glycation end products (AGEs) was identified and this has been characterised and linked to various conditions including diabetes and Alzheimer's disease. Within Maillard reaction research, its role within medicine is thought of as a distinct, independent matter (Gerrard, 2006). There has been another collection of reaction products produced by the Maillard reaction called process-induced toxicants that have been identified and researched in the last couple of decades. These unwanted products have drawn attention to foods processed by heat and in 1990 heterocyclic amines were identified, followed by a 2002 discovery of acrylamide in heat-processed food (FINOT, 2005).

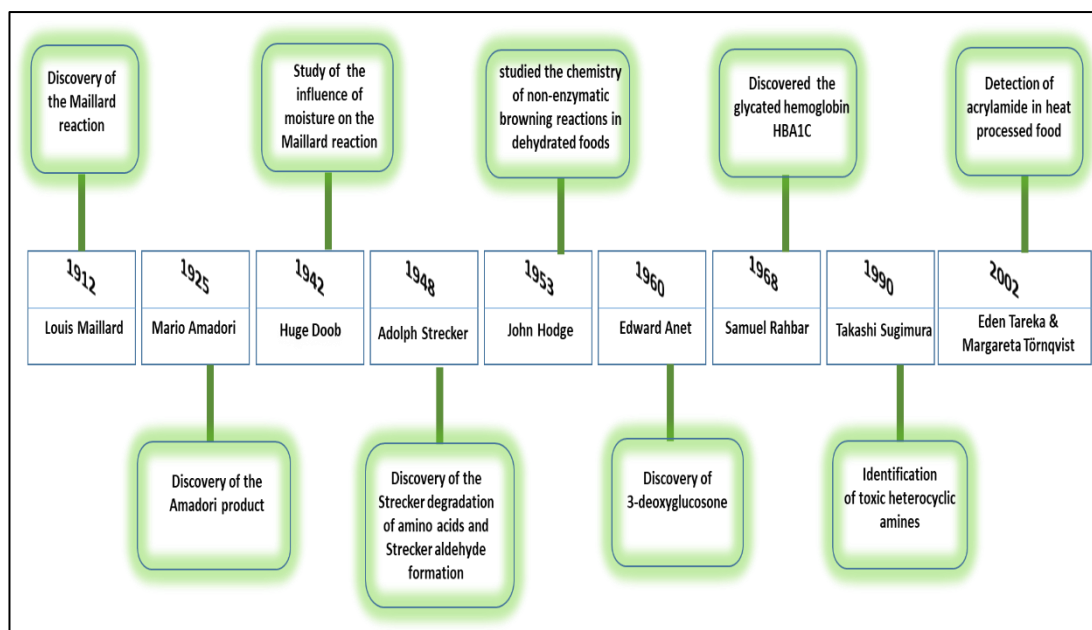


Figure 1.1: A graphic timeline for some of the key discoveries made in the Maillard reaction literature

1.4 Three stages of the Maillard reaction

The protein glycation reaction first begins with an amino compound starting a basic nucleophilic attack on an electrophilic centre, for example, a carbonyl moiety, and this causes a generation of intermediates significant in producing the changes in taste, colour, texture and aroma of foods (Luevano-Contreras and Chapman-Novakofski, 2010).

It is also well known that the reaction causes harmful by-products including furans, heterocyclic amines, acrylamide and advanced biological and dietary glycation end products (Troise and Fogliano, 2013). Despite the varying routes that can occur in different reaction products, Hodge provided the general scheme of the Maillard reaction in 1953 and this continues to be understood as an accurate representation of the processes that occur (Hodge, 1953). The scheme of the reaction is split into three stages (Figure 1.2). The reaction first begins when glycosylamine forms and dehydrates into a Schiff base, it then slowly rearranges into a more stable product known as a ketosamine adduct. This product, when the reducing sugar involved is an aldose, is known as an Amadori Rearrangement Product. If it is ketose that is the reducing sugar, then it is called the Heyn's Rearrangement Product (Hodge, 1953;

Newton *et al.*, 2012). The next stage of the reaction is the transformation that occurs of the products that were generated earlier, and this section is dependent on the pH. If the pH is up to but not including 7, the rearrangement compounds will produce 3-deoxyosone after a 1,2-enolization resulting in elimination occurring. If the sugar that is involved is glucose rather than ketose or aldose, then a 3-deoxyglucosone will be converted to 5-hydroxymethylfurfural (HMF) when dehydration occurs. If, however, the pH is 7 or higher, the reactions will differ. Instead, the Amadori/ Heyn's rearrangement products will go through a 2,3-enolization, something that is irreversible. This 2,3-enolization then has two possible routes, it can branch out to become 1-deoxyosone or 4-deoxyosone. This route results in the generation of dicarbonyls, reductones and several other products. There is also a sub-reaction that occurs at this stage, named Strecker degradation, and this can produce aldehydes, carbon dioxide and aminoketones by branching between the α -dicarbonyl compounds and amines. The production of aldehyde by Strecker degradation, as well as the products created from the condensation of aminoketones, are deemed to be important for the aroma of food. There are many chemical reactions that occur in this second phase of the Maillard reaction and they include; retroaldol reactions, aldol, enolization, dehydration, decarboxylation and Michael additions. The late stage of this reaction begins with the reaction of dicarbonyl compounds with free amino groups of proteins. This reaction undergoes a series of complex cascades of repeated dehydrations, condensations, fragmentations, oxidations and cyclisation reactions within the amino-carbonyl reaction system (Schleicher *et al.*, 2001). The formation of dicarbonyl compounds appears to be the rate-determining step for the cross-linking reaction, which subsequently leads to the formation of an extremely heterogeneous group of compounds called 'advanced glycation endproducts' (Nursten, 2005).

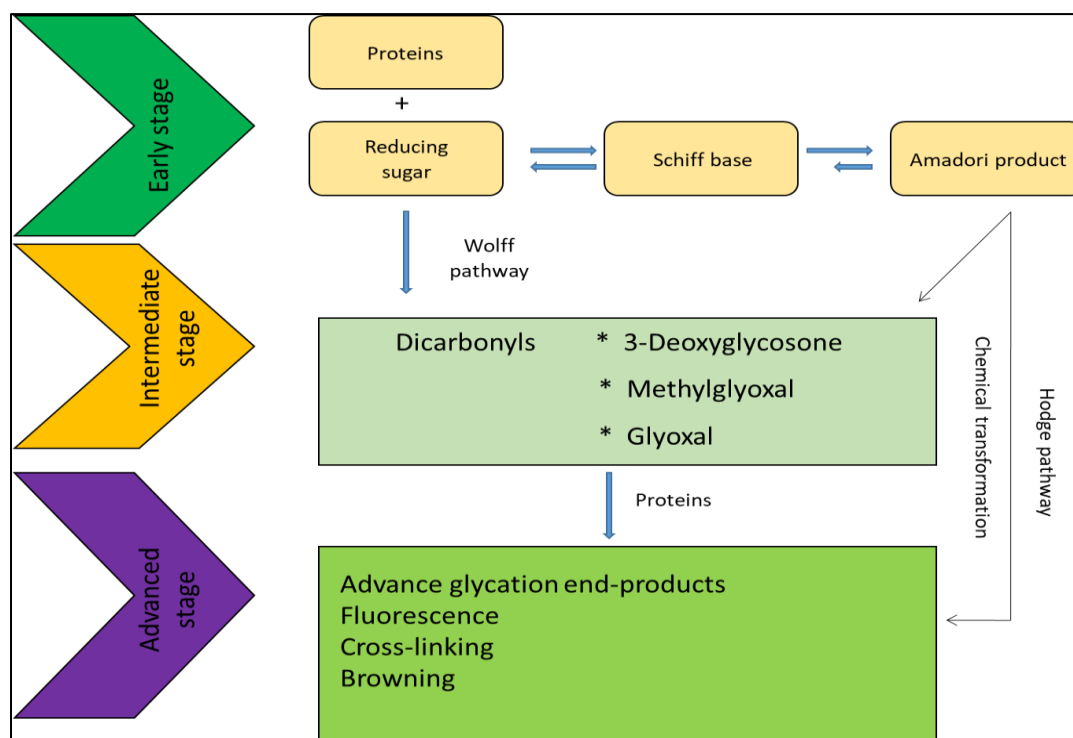


Figure 1.2: Formation of AGEs in three stages

i.e., early, intermediate and advanced. In the early stage, sugars react with a free amino group to form a Schiff base which undergoes a rearrangement to a more stable product known as an Amadori product. In an intermediate stage, the Amadori product degrades to a variety of reactive dicarbonyl compounds. In the advanced stage of the glycation process, AGEs (irreversible compounds) are formed (Tsekovska *et al.*, 2016).

1.5 Maillard reaction during cooking

We can see evidence of this reaction in a wide range of locations from foodstuff to textiles, biological systems, pharmacological preparations and soils, all allowing the reaction to occur at moderately low temperatures (Luevano-Contreras and Chapman-Novakofski, 2010). However, the main focus, particularly for the food industry and food scientists themselves, is when the protein glycation reaction occurs during the processing of food with a focus on frying, roasting, baking, grilling and cooking food (Newton *et al.*, 2012). The reaction causes several enhancing attributes particularly when it comes to the taste, aroma and texture of foods. However, it also brings undesired effects. Therefore, the results of the Maillard reaction can be separated into two groups; desired and undesired.

1.5.1 Flavour, colour, texture and aroma

The Maillard reaction has been a key point of the study of scientists for decades. The food industry aims to provide food that is healthy and safe while also appealing in several ways. The Maillard reaction alters foodstuffs in various ways and the products that are generated include amino sugars, Strecker aldehydes, pyrroles, pyrazines, furanones and more. The various products that are created play a substantial role in the end result of the food, particularly in terms of flavours (Yu and Zhang, 2010).

1.5.2 Irreversible compounds and end products

Protein glycation, *in vivo*, often occurs over an extended time period when excess glucose or other sugars within the body react with proteins due to the Maillard reaction. At the start of the reaction, the process can sometimes be reversible although this is dependent on the concentrations of glucose that are present. The process takes place over time and intermediates are formed over varying periods of time spanning from hours to weeks. HbA1C is an example of an Amadori reaction product that takes only a matter of days to form; the build-up of these products leads to the next stages of the reaction to take place, which are more advanced. Studies have shown that it is the final phase of the Maillard reaction where the advanced glycation end products are formed alongside melanoidins (Poulsen *et al.*, 2013). The advanced glycation end products require an oxidative pathway so this is through either the Wolff pathway (autoxidation of glucose), the Namiki pathway (Schiff base) or the Hodge pathway (Amadori products) (Nursten, 2005). This can also include the peroxidation of lipids. Typically, oxidative stress is present, and this leads to reactive dicarbonyl compounds being generated. These compounds include 3-deoxyglucosone, methylglyoxal (MG) and glyoxal. These reactive dicarbonyl compounds will often react with amino acids such as lysine, arginine, proteins or peptides.

1.6 Identifying AGEs

These complex, heterogeneous molecules were originally recognised by their fluorescent yellow-brown colouring and their capability to cross-link between amino groups (Singh *et al.*, 2014). With the AGEs chemistry remaining unclear, it has been

determined that the majority of the structures are *in vitro* as opposed to the few that have been identified *in vivo*. Based on the structures' chemical and physical characteristics, AGEs have been catalogued into four separate groups, these are; non-fluorescent cross-linked, fluorescent cross-linked, non-fluorescent non-cross-linked and fluorescent non-cross-linked (Figure 1.3).

1.6.1 Major AGE structure

The non-fluorescent cross-linked AGEs are thought to be the major AGE structures which hold a fundamental role *in vivo* protein cross-linking. Methyl-glyoxal-lysine dimers (MOLD) are a common type as well as glyoxal-lysine dimers (GOLD) (Ahmed, 2005; Elosta *et al.*, 2012).

1.6.2 Minor AGE structure

The fluorescent cross-linked AGEs are considered the minor structures as they account for no more than 1% of all of the cross-linking molecules. Some fluorescent cross-linked structures have been identified *in vitro* under physiological conditions such as vesperlysine A- B- C, pentosidine and crossline (Elosta *et al.*, 2012).

1.6.3 Non-fluorescent non-cross-linked AGEs

This collection of AGEs are made under physiological conditions from protein glycation. Examples include carboxyethyllysine (CEL), carboxymethyllysine (CML), imidazolones and pyrraline (Elosta *et al.*, 2012)

1.6.4 Fluorescent non-cross-linked AGEs

Fluorescent non-cross-linked AGEs have been found in the blood of patients with diabetes. A typical example of this would be argpyrimidine (Mashilipa *et al.*, 2011; Elosta *et al.*, 2012).

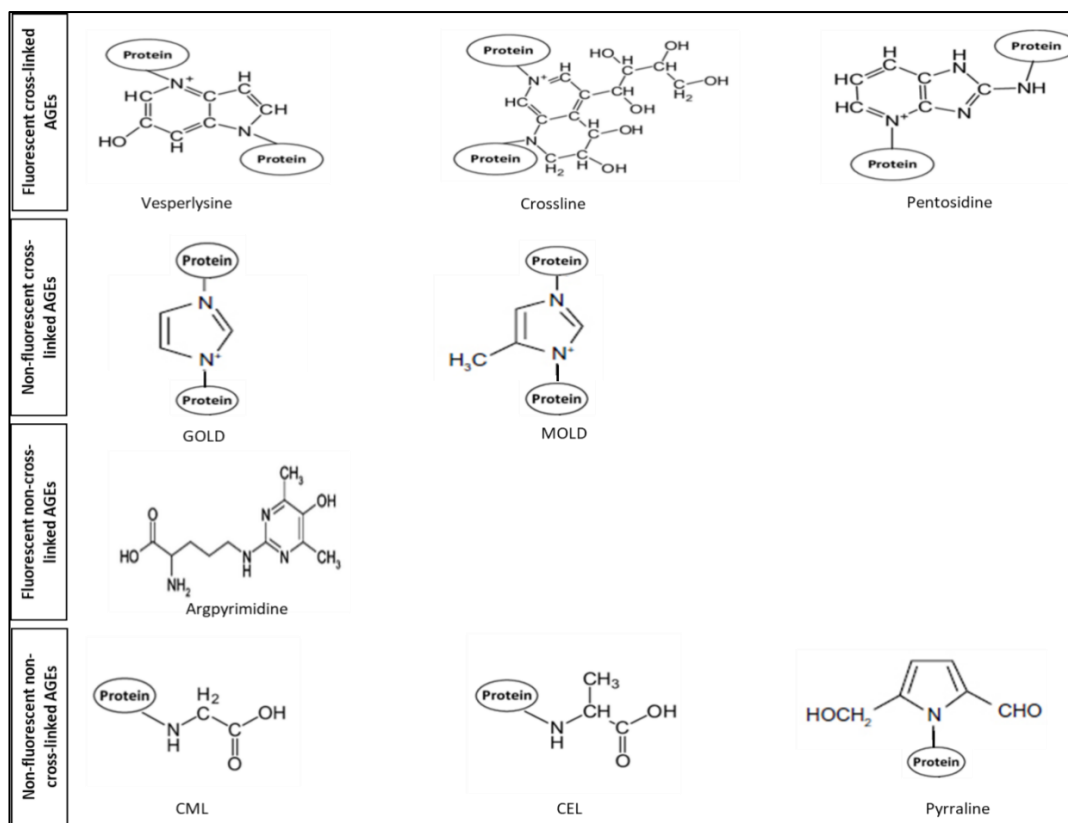


Figure 1.3: Chemical structures of four types of AGEs:

(A) Fluorescence cross-linking AGEs such as vesperlysine; pentosidine and crossline. (B) Non-fluorescent cross-linking AGEs such as GOLD: glyoxal-lysine dimers and MOLD: methyl-glyoxal-lysine dimers. (C) Fluorescent non-cross-linked AGEs such as argpyrimidine. (D) Non-fluorescent non-cross-linked AGEs such as CEL: N-carboxyethyl-lysine; CML: N-carboxymethyllysine and pyridine.

1.7 Regulation of the Maillard reaction through physical factors

1.7.1 Influence of pH

pH seems to have a very large influence on the rate of reaction as well as the production of reactive intermediates. The effect pH has on the Maillard reaction has been a particular focus for many studies due to its substantial function in controlling, as well as impacting, the reaction. In the early stages, pH impacts the degradation of the Heyn's/Amadori rearrangement compounds as well as their progressions into the applicable enolization route. Studies have shown the optimum pH in terms of the browning rate is between 6 - 10. In aqueous systems, acidic and basic buffer solutions are used to control the pH and the browning will often increase as the pH increases up to a high of 9 or 10. A low pH yields a low development of browning (Nursten, 2005). pH values from 8 to 10 have been found to enhance the browning and polymerisation of sugar-amino acid mixtures (Ajandouz *et al.*, 2001). A pH of between 4.6 and 8

almost double the glucose degradation (Martins and Van Boekel, 2005a). This is likely due to the reactive materials of both the amino acid and the sugar being in ideal alkaline conditions (Newton *et al.*, 2012). When non-aqueous reaction materials are considered, switching the neutral amino acids and sugars with charged counterparts, can control the acidity. This is a practical option, particularly in situations such as pyrolytic experiments where the non-aqueous model systems are being studied. In a 2008 study on the influence of basic and acidic sugars in modifying the Maillard reaction in a monosaccharide-cysteine system, it was found that a more complex Maillard reaction profile was formed and, compared to the neutral monosaccharides, the charged sugars produced more volatile compounds (Kraehenbuehl *et al.*, 2008).

1.7.2 Influence of temperature on the browning reaction

Temperature, like pH, can have a direct influence on the Maillard and the browning reactions (Martins and Van Boekel, 2005a). Maillard studied how increasing the temperature and duration of the reaction actually increased the reaction rate. A temperature from 125°C up to 160°C is considered the optimum temperature when it comes to browning (Coghe *et al.*, 2006). End product formation and the depletion of reactants are considered to increase with the temperature rise. The Arrhenius equation is heavily relied upon in kinetic studies in order to determine the influence temperature has on the reaction rate (Martins and Van Boekel, 2005b). An increase of 10°C can cause the reaction to double in speed, however, this causes not only the rise in the speed of the browning process but also leads to products that are potentially harmful being formed. For example, a reactive carbonyl compound and asparagine reacting at 120°C or more cause acrylamide to be produced (Stadler *et al.*, 2002).

1.7.3 How dehydration impacts the Maillard reaction

Water activity (a_w) also plays a big role in the Maillard reaction as it takes place through dehydration. However, the reaction rate actually decreases when moisture levels are higher as well as when the moisture levels are lower due to a larger dilution of reactants or an increase in diffusion resistance (Ames, 1990). There have been many studies that have focused on controlling the water levels and activity in order to stabilise the reaction. Another study found that the reactions of acrylamide formation

and elimination were enhanced when the water activity was decreased to 0.43 from 0.972 (Bassama *et al.*, 2011).

1.8 Reducing sugars and reactive AGEs

AGE molecules are generated as a result of Amadori products being oxidated as well as by lipid peroxidation. It has been indicated in several studies that, in addition to glucose, there are other reducing sugars that are also involved and more reactive that play a part in AGE formation (Ahmad *et al.*, 2007). Forming via non-oxidative glyceraldehyde-3-phosphate fragmentation, the reducing sugars that are more reactive also produce AGEs that are more reactive in the intercellular compartment (Brownlee, 2005). These findings led to further studies that took place using AGE inhibitors thiamine and benfotiamine. Benfotiamine, a lipid-soluble precursor to thiamine, has a higher bioavailability and has been found to reduce diabetes-associated complications in terms of severity due to its ability to prevent AGEs from being produced. The complications that were reduced in severity included nephropathy, neuropathy, angiopathy and retinopathy (Balakumar *et al.*, 2010). By administering 7 days of glucose exposure to the endothelial cells, the level of AGEs was alleviated 14-fold. The increase is likely to have resulted from glycation by the highly reactive reducing sugars including fructose, glucose-6-phosphate and MG (Ahmed, 2005).

1.9 Biological effects of AGEs

Several pathological conditions are generated from aggregations and alterations of a variety of proteins that may cause tissue damage. For instance, accumulation of AGE formation leads to an accumulation of AGEs in tissues (Bohlender *et al.*, 2005). AGE-related tissue injury occurs as a result of the cross-linking of AGEs, increased free radical production, blocking particular functions of proteins and cross-talk with receptors for glycation end products (RAGEs) and accumulation of proteins (Rojas and Morales, 2004).

1.10 Receptor for advanced glycation end products

AGE formation activates different signalling cascades mediated by the multi-ligand receptor RAGE. RAGE has a mass of 45-kDa and belongs to an immunoglobulin superfamily (Hudson and Schmidt, 2004; Srikanth *et al.*, 2011). RAGE is a transmembrane receptor composed of 394 amino acids, with one hydrophobic transmembrane helix consisting of 19 amino acids, and a short cytoplasmic tail of 43 amino acids. The extracellular part of RAGE comprises V-type and C-type immunoglobulin domains (Figure 1.4). The V-domain is important for ligand binding whereas the cytosolic tail regulates RAGE-mediated intracellular signalling (Srikanth *et al.*, 2011). Molecular analysis of RAGE-transfected 293 cells showed a majority of bands with a molecular weight of ~ 50 kDa due to post-translational processing (Neeper *et al.*, 1992). RAGE is highly expressed and particularly present in organs such as heart, lung, and skeletal muscle and different types of cells such as endothelial cells, macrophages, smooth muscle cells, mesangial cells and epithelial cells, lymphocytes, monocytes and neurons (Basta *et al.*, 2004). Previous studies identified several AGE receptors, including lactoferrin, oligosaccharyltransferase complex protein 48 (AGE-R1), 80K-H protein (AGE-R2), galectine-3 (AGE-3), SRA, CD-36 and receptors for AGE (RAGEs), which act as signal transducers for AGEs (Hudson and Schmidt, 2004; Bohlender *et al.*, 2005). Moreover, RAGE is localised in different cell types, including another form of RAGE receptor called DN-RAGE, which is a dominant negative form, not of full length, which lacks the cytosolic tail. It is located inside the membrane and functionally is blunted in mediating RAGE intracellular signalling pathways as shown in Figure 1.4 (Hallam *et al.*, 2010).

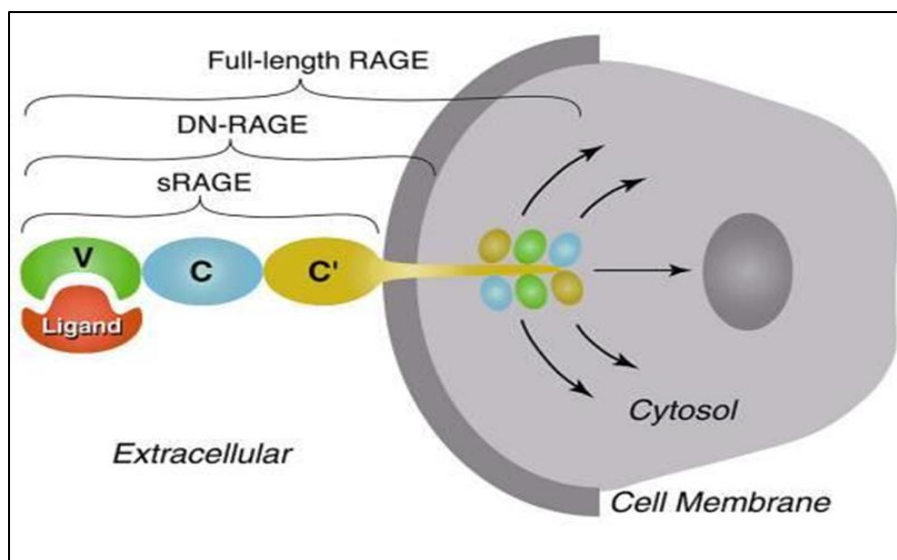


Figure 1.4: Structure of RAGE. The extracellular part of RAGE contains one of the V-type immunoglobulin domains, followed by two C-type immunoglobulin domains. Dominant negative RAGE (DN-RAGE) is located inside the membrane and is functionally blunted in regulating RAGE pathways (Hallam *et al.*, 2010).

1.11 Diabetes mellitus and oxidative-stress signalling pathways

The production of AGEs is a consequence of hyperglycaemia and contributes to the generation of oxidative stress in several tissues (Elosta *et al.*, 2012). Generation of reactive oxygen species (ROS) causes injury to cell components such as proteins, lipids and nucleic acids (DNA and RNA). Thus, the presence of natural, endogenous antioxidant enzymes such as catalase (CAT), superoxide dismutase (SOD) and glutathione peroxidase (GPx) is crucial to engulf ROS and maintain normal cellular functions. When the endogenous antioxidant system is inhibited, the restoration of cellular redox decreases the complications of DM (Tang *et al.*, 2012).

Binding AGEs to RAGEs leads to the generation of a variety of biological effects such as the elevated secretion of cytokines, and inflammatory cytokines (e.g. tumour necrosis factor- α (TNF- α), interleukin-1 α (IL-1 α) and interleukin-6 (IL-6 α)) (Bierhaus *et al.*, 2005; Elosta *et al.*, 2012) as well as to intercellular ROS formation. Initially, ROS production is triggered by the activation of the NADPH-oxidase system (NOX) (NOX family including NOX1, 2, 3, 4, 5 and DOX1 and DOX2) (Frey *et al.*, 2009; Cho *et al.*, 2013). It was found that the development of diabetic complications in organs is associated with the stimulation of a glucose-metabolising pathway that is orchestrated by aldose reductase (AR), a key enzyme in the polyol pathway, which

catalyses the nicotinamide adenosine dinucleotide phosphate-dependent reduction of glucose to sorbitol and sorbitol dehydrogenase. In cells cultured under high glucose conditions, many studies have demonstrated similar AR-dependent increases in ROS production, confirming AR as an important factor for the pathogenesis of many diabetic complications. Moreover, a study carried out by Tang *et al.* have shown that AR inhibitors may be able to prevent or delay the onset of cardiovascular complications such as ischemia/reperfusion injury and atherosclerosis (Tang *et al.*, 2012). Many studies have indicated that production of ROS and elevated oxidative stress trigger signal transduction and change the gene expression (Cui *et al.*, 2012; Cho *et al.*, 2013; Nita and Grzybowski, 2016). Moreover, the transcription factor NF- κ B has been identified as an intercellular target of hyperglycaemia and ROS production (Calcutt *et al.*, 2009).

In addition, hyperglycaemia and oxidative stress potentiate AGE formation and accumulation. AGE-RAGE interaction triggers signal transduction pathways including mitogen-activated protein kinases (MAPK) such as p38, extracellular regulated (ERK)-1/2, c-Jun N-terminal kinase (JNK), Cdc42/rac, and Jak/Stat pathways (Figure 1.5) (Cho *et al.*, 2013). The consequence is the generation of gene products, such as vascular endothelial growth factor (VEGF), vascular cell adhesion molecule-1 (VCAM-1) and others, which all contribute to the development of cellular injury and the long-term complications of diabetes mellitus (Basta *et al.*, 2004).

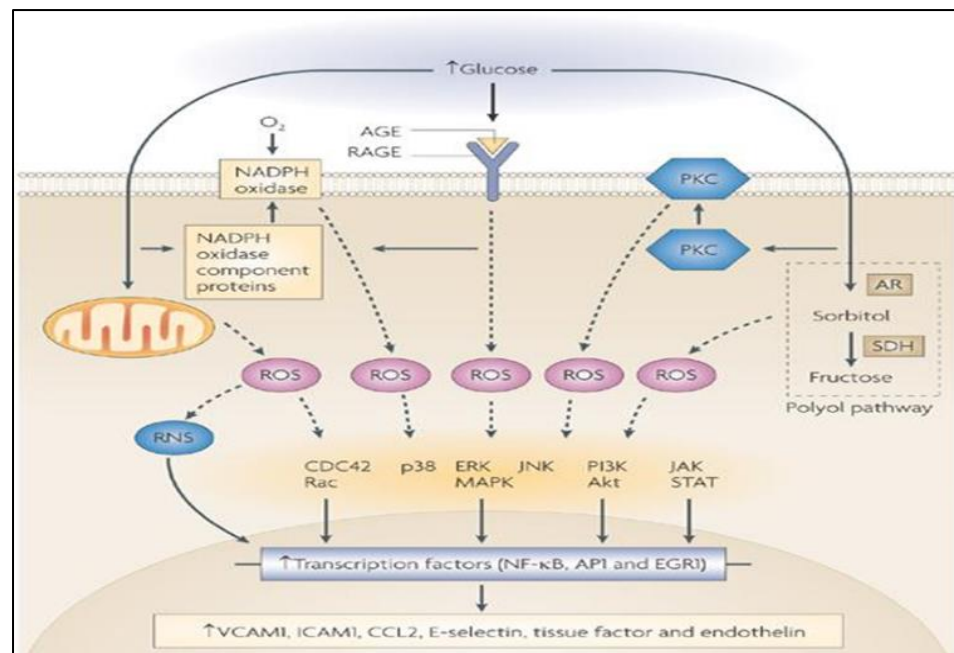


Figure 1.5: Signal transduction pathways activated by AGE-RAGE interaction. Stimulation of RAGE by AGEs formation increases the production of ROS by different signalling pathways (Calcutt *et al.*, 2009).

1.12 Advanced glycation end products and complications

The main complication types experienced by diabetic patients can be split into microvascular, which refers to damage to small blood vessels (including eyes, kidneys, neuropathy), and macrovascular, which refers to damage to larger blood vessels (including brain, heart and extremities) (Figure 1.6). Although there has been a large quantity of literature written on the topic of diabetic complications, it remains unknown what the root of most complications actually is. It seems that a significant aspect leading to complications is the raised development and build-up of AGEs resulting from chronic exposure to hyperglycaemia (Rhee and Kim, 2018). Equally, intensive management of glycaemia causes a reduced formation of AGEs and can help to decrease vascular complications (Ahmed, 2005; O'sullivan and Dinneen, 2009)

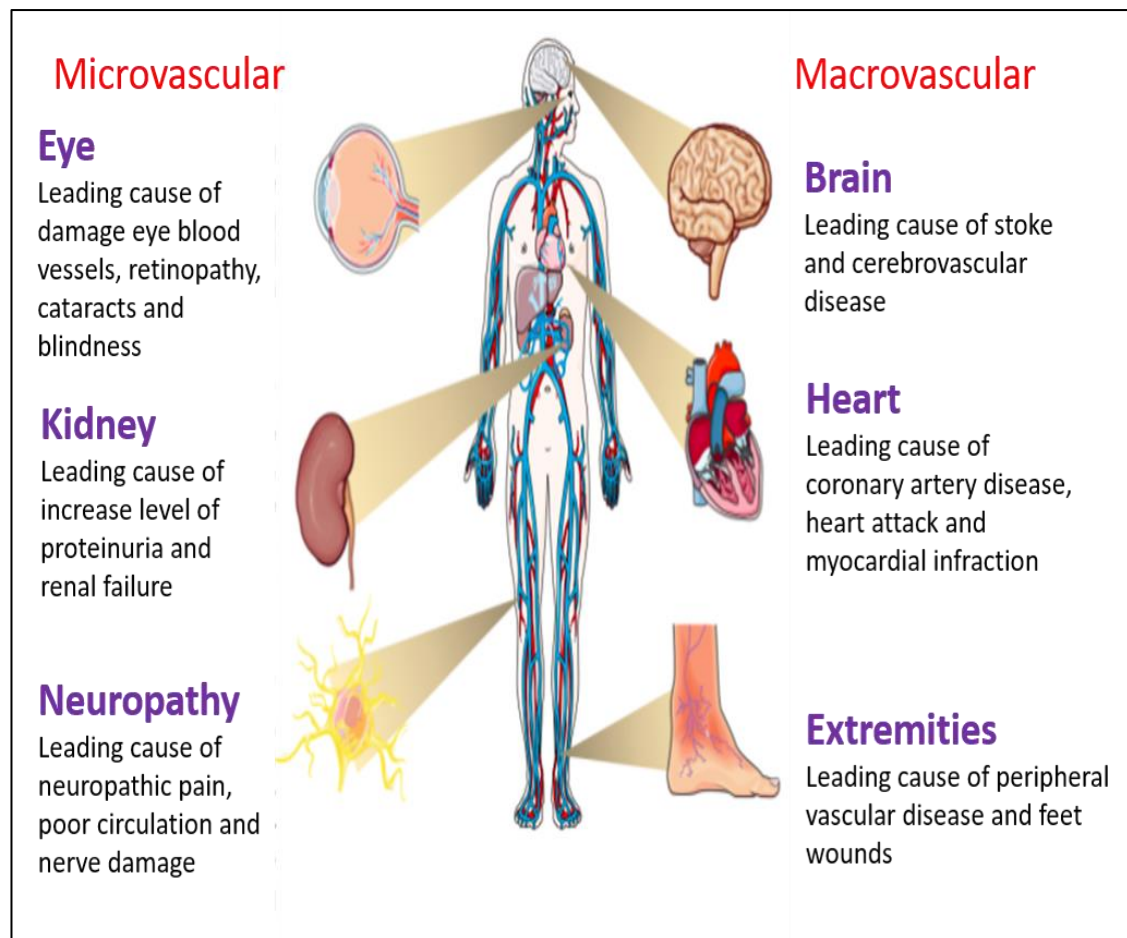


Figure 1.6: Major microvascular and macrovascular complications associated with diabetes mellitus.

Diabetic complications are divided into (1) microvascular, due to damage to small blood vessels and include damage to eyes, kidneys and the nerves and (2) macrovascular, due to damage to larger blood vessels, and includes cardiovascular diseases such as heart attacks, strokes and insufficiency of blood-flow to the legs.

1.12.1 Complications associated with damage to smaller blood vessels

Microvascular complications are generally what is called ‘dysfunctional alterations’ that occur in the microvascular bed. When looking at microangiopathy, the most often seen types are neuropathy, retinopathy and nephropathy (Chawla *et al.*, 2016). To develop this kind of complication in a diabetic patient generally takes 10 to 15 years. Microangiopathy is characterised by the vascular permeability increasing and the basement membranes thickening, resulting in decreased blood flow, otherwise known as a prothrombotic state. (Chawla *et al.*, 2016). To date, there has been no effective treatment for such complications in association with diabetes (Ahmed and Thornalley, 2007).

1.12.1.1 Most common complications

Among the most common complications in terms of microangiopathy is diabetic retinopathy, which can cause blindness if left undiagnosed and untreated. The chance of suffering from retinopathy rises with the amount of time diabetes has been present in the patient. Nearly all type 1 diabetes sufferers, and over 60% of type 2 diabetes patients, experience retinopathy to some degree after 20 years. Studies have shown that increased AGEs play a substantially important role in the growth and advancement of diabetic retinopathy (Fowler, 2008). The increased production of AGEs can also cause retinal microvascular endothelial cells to experience abnormal proliferative reactions resulting in an irregular expression of eNOS (endothelial nitric oxide synthase) (Giacco and Brownlee, 2010). In addition to this, the production of AGEs also impacts the pericyte growth negatively, causing a decrease in pericytes. This decrease is actually the earliest hallmark (histological) of diabetic retinopathy. The decrease in pericytes then causes thickening of the basement membrane, contributing significantly to the inner blood-retinal barrier breakdown (Bianchi *et al.*, 2016). Diabetic retinopathy may also include neural dysfunction/ depletion due to the production and build-up of AGEs (Stitt *et al.*, 2016). It appears as though growth factors such as transforming growth factor beta, VEGF vascular endothelial growth factor and growth hormone also have an impact (Fowler, 2008). A study on animals indicated that suppression of the VEGF is complemented by a lessened development of retinopathy (Fowler, 2011), thus demonstrating a link between the two. It is a matter of conjecture as to what the impact of increased growth factor production can have on the body's response to a lack of oxygen reaching the tissues.

1.12.1.2 Development of cataracts

Diabetes and hyperglycaemia are significant risk factors in regards to developing cataracts; a patient who suffers from diabetes is likely to experience cataracts a whole decade earlier than healthy individuals (Jeng *et al.*, 2018). Methylglyoxal and other AGE precursors play a crucial part in the formation of cataracts. Lens crystallins and other long-lived proteins have a higher probability of glycation taking place (Fowler, 2011). When a lens crystallin experiences glycation, it can cause oxidation, protein crosslinking and high molecular weight aggregates being produced which in turn

cause cataracts to develop (Pescosolido *et al.*, 2016). Cataract formation in diabetic patients may also be significantly contributed to by the glycation of the sodium-potassium pump and channel proteins (Williamson and Ido, 2012).

1.12.1.3 Kidney damage in diabetic patients

Diabetic nephropathy, or diabetic kidney disease, is a significant cause of the last stage of chronic kidney disease. A three-fold increase in the number of AGEs indicates it is present and the disease plays a substantial role in the increased illness and mortality of diabetic patients (Lim, 2014). Diabetic nephropathy is accountable for up to half of all end-stage renal disease cases (Haller *et al.*, 2017). Complications that are connected to diabetic nephropathy include the thickening and expansion of the mesangial matrix, coagulation of basement membranes (specifically glomerular and tubular), leading over time to microvascular impairment, vascular occlusion and fibrotic conversion. This causes a hardening of the glomeruli in the kidneys, also referred to as scarring of the small blood vessels of the kidney (Kolset *et al.*, 2012). Playing a very important role, the kidney is a significant site where AGE clearance takes place, however, it is equally a target for damage caused by AGEs (Mallipattu and Uribarri, 2014). A large number of AGEs that are present in diabetic nephropathy can be linked to reduced clearance, as opposed to an elevated formation of AGEs by glycation of proteins (Stinghen *et al.*, 2015). It has been recently discovered that the renal tissues of diabetic patients contain increased levels of CML and pentosidine regardless of whether the end-stage renal disorder is present (Beisswenger *et al.*, 2013).

1.12.1.4 The impact of diabetes on the nervous system

Over half of all diabetes sufferers experience complications relating to nerve damage; this is a major cause of illness and mortality (Edwards *et al.*, 2015). It is known that diabetic neuropathy causes the peripheral nervous system to be damaged (Beisswenger *et al.*, 2013), often impacting nerves in the patients' legs and feet. AGEs have an important contribution to the development of diabetic neuropathy due to their biochemical pathways (Singh *et al.*, 2014). The impact of AGEs on neuropathy has been widely studied, with a recent study indicating that peripheral nerve myelin that has been modified by AGEs is vulnerable to phagocytosis by macrophages, which

causes segmental demyelination. Subsequently, AGEs have an impact on the main axonal cytoskeletal proteins and this leads to axonal degeneration, which is an expression of diabetic neuropathy the degenerated axonal express in diabetic neuropathy (Cashman and Höke, 2015). More evidence suggests that if the expression levels of eNOS (the inducible form) are altered due to AGEs, then this affects the flow of blood to the nerves and causes a lack of oxygen to the peripheral nerves (Zhao *et al.*, 2015). Despite the precise role of RAGE and AGEs interactions being unknown, there is a contribution to endoneurial vascular dysfunction which causes microangiopathy in peripheral nerves (Yagihashi *et al.*, 2011).

1.12.2 The impact of AGEs on major blood vessels

Complications involving the macrovascular system are alterations within the body that impact the major blood vessels resulting in abnormalities in both function and structure (Chawla *et al.*, 2016). Endothelial dysfunction, reduction of vascular compliance and artery wall thickening are all caused by the glycation of wall structures. Atherosclerosis is considered to be the highest risk factor causing macrovascular complications in diabetic patients, these include myocardial infarction, peripheral vascular disorders and stroke (Funk *et al.*, 2012).

1.12.2.1 The impact of AGEs on arteries

Atherosclerosis is a build-up of plaque within arteries; this seems to be the result of multiple factors and causes limited blood flow. This is the fundamental cause of what is currently the number one killer of humans in the world. Studies have found links between the development of atherosclerosis and AGE production in patients with diabetes (Rai *et al.*, 2016). It is also possible that interactions between AGEs and RAGEs also cause an increase in endothelial impairment, neointimal proliferation, delayed wound healing and increased plaque destabilisation (Hallam *et al.*, 2010; Karmakar and Goswami, 2012). Therefore, it is unsurprising that the interactions between AGEs and RAGEs are considered to be a significant cause in the development of atherosclerosis in sufferers of diabetes (Singh *et al.*, 2014). AGEs also activate nuclear factor-kB and protein-1 transcription factors within vascular wall cells causing increased expression of several atherosclerosis-related genes (Laakso, 2010).

1.13 Wound healing

Wound healing occurs in three stages. The first is inflammation, followed by proliferation and finally maturation and remodelling (Figure 1.7). Each of the phases has distinct functions and characteristics. For the regulatory events to be carried out, there is a reliance on the cell growth factors, cytokines, chemical mediators and chemokines (Eming *et al.*, 2014; You and Han, 2014). In order for the re-establishment of homeostasis to occur, the acute inflammatory response must begin so the tissues can start the healing process (Slavich and Irwin, 2014). When an injury first occurs, the body must react so that it can clot the blood and prevent further blood loss. This is done by various substances including thromboxane A₂, prostacyclin and serotonin being released. Then the coagulation cascade is activated by signals from the exposed collagen, this causes haemostasis to begin as platelets cling to blood vessels that are damaged then a thrombin and fibrin buffer forms. The buffer plays a significant role in preventing micro-organisms from entering the wound, preventing further loss of cellular elements and to assist by creating a provisional matrix, growth factors and cytokine deposit, something that is vital for the later stages of wound healing (Demidova-Rice *et al.*, 2012).

At the start of the inflammation phase, vasodilation occurs in order to immediately decrease blood pressure. This is stimulated by the release of soluble factors including histamine, bradykinin, E and I series prostaglandins and nitric oxide. The blood flow is reduced by the vascular permeability increasing and this allows leukocytes, primarily neutrophils, to interact with the endothelium. This interaction involves multiple levels and events taking place including margination, rolling, adhesion, transmigration and targeting leukocytes so they can focus on the lesion (this occurs with inflammatory mediators, chemotactic activity and vascular endothelial membrane protein alterations (MacLeod *et al.*, 2014).

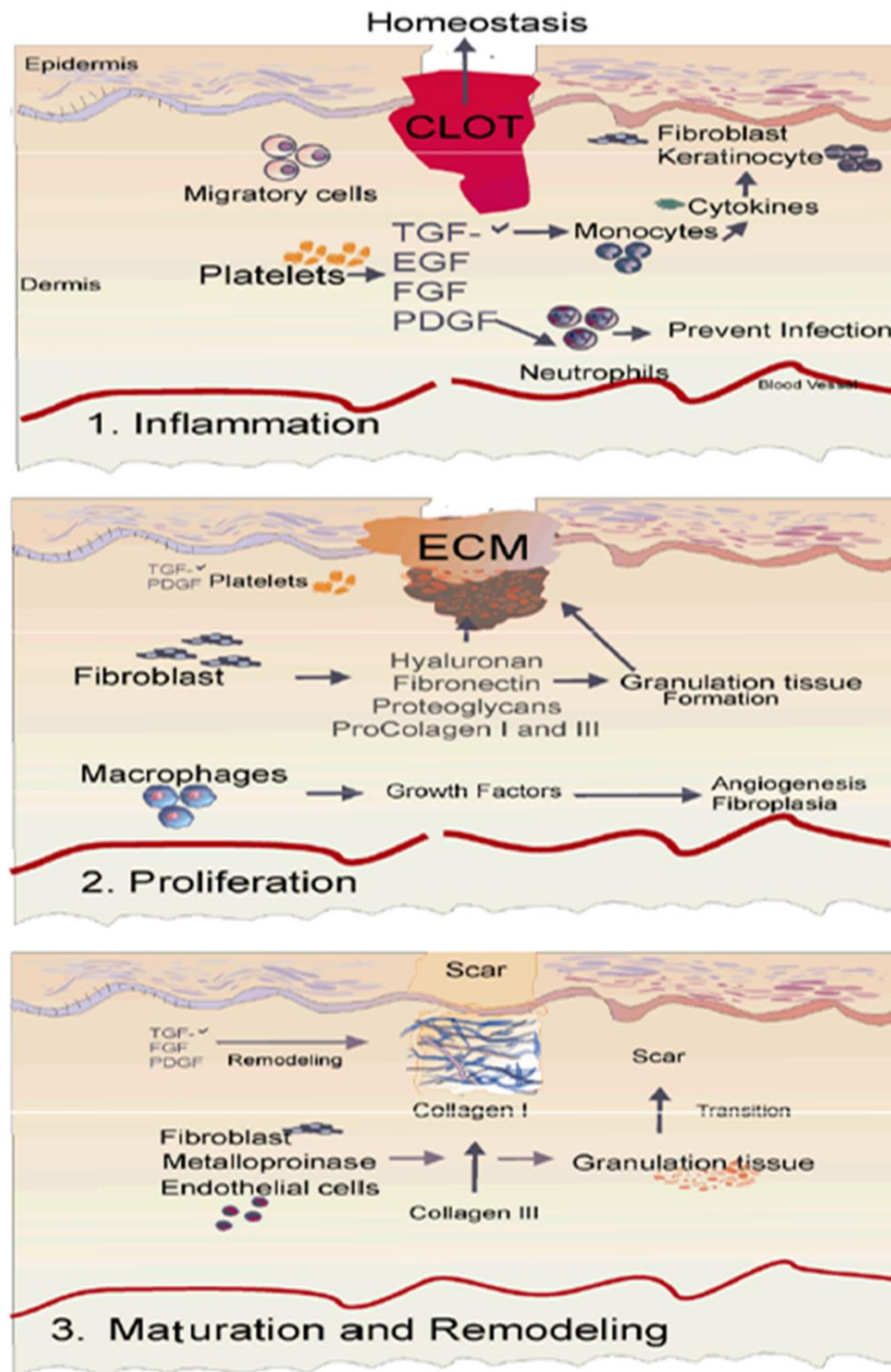


Figure 1.7: Schematic representation of the phases of cutaneous wound healing

(1) inflammation begins with (a) coagulation, platelet aggregation, and fibrin clot formation; (b) inflammatory events then occur through neutrophil and macrophage infiltration and phagocytosis of debris, apoptotic cells, and pathogens; anti-inflammatory events occur through inhibition of destructive inflammatory process and proliferation promotion. (2) In the proliferation phase there occurs (a) angiogenesis; (b) re-epithelisation (epithelial cell mitosis and transformation of fibroblasts into myofibroblasts), and granulation tissue formation (EMC composed of collagen, glycoprotein, proteoglycan, fibroblasts, and keratinocytes, under the modulation of MMP-9). (3) Maturation and remodelling are marked by (a) EMC reorganisation: cell apoptosis and angiogenesis regression; and (b) type III collagen being replaced by type I (Yolanda *et al.*, 2014).

Within hours of an injury occurring, neutrophils are enlisted and help to resolve tissue damage by releasing cytokines and proteases as well as other substance that is contained within cytoplasmic granules (Mayadas *et al.*, 2014). The generation of reactive oxygen species (ROS), takes place and antimicrobial proteases are produced including defensins, lysozyme, lactoferrin and cathepsins. These antimicrobial proteases are able to destroy any microorganisms that are pathogenic or potentially pathogenic. As well as acting as a protection, they also release enzymes including elastases and collagenases that assist with tissue renewal and repair by supporting devitalised tissue digestion (Kolaczowska and Kubes, 2013).

Membrane metalloproteinases (MMPs) of a variety of types are produced by neutrophils. The principal subtypes MMP-8, MMP-9 and MMP-2 cleave collagen (MMP-8 splits fibrillar collagen and MMP-9 cleaves, amongst others, collagen IV). These types of MMPS play an important role in extracellular matrix degradation. Metalloproteinase tissue inhibitors are a molecular class that are produced by cells on the skin and restrain the MMPs' actions. Without the regulation of the proteases and the inhibitors, the result could be an impaired formation of granulation tissue (Wilgus *et al.*, 2013). Therefore, any migration of uncontrolled neutrophils causes activation of cells resulting in excessive proteases and ROS being produced. This then causes additional damage to tissues and unwanted extracellular matrix degradation which can lead to reduced tissue resistance, long-lasting inflammation with collagen deposition that is defective, delayed re-epithelialisation as well as limited healing and recovery (de Oliveira *et al.*, 2016). There is also a release of cytokines, for example, the inflammatory response is triggered by IL-6 and TNF- α , which is then increased by additional cells and neutrophils, like macrophages, being activated. Though these are incredibly important for the activation of repair cells, they can also cause harmful effects when intensified release takes place (Eming *et al.*, 2014). When the skin is healthy and intact, the cell-type present that is most abundant are macrophages and they perform homeostatic and sentinel functions. When there is a skin lesion present, the wound triggers monocytes to move from their position within the blood circulation through vessels to the wound site. The resident and infiltrating macrophages are triggered by signals and will then, determined by the distinctive functional phenotypes, develop into subpopulations (Murray and Wynn, 2011). Macrophages

have been known to demonstrate a proinflammatory phenotype termed “classically activated” or M1, in response to bacterial components. These M1 macrophages clean the debris and dead cells, defend the host, produce proinflammatory mediators (IL-12, IL-1, IL-6, inducible nitric oxide synthase (iNOS) and TNF- α) and perform phagocytosis. Macrophages can also assume a variety of “alternatively activated” or M2 phenotypes. In addition, chemokines will recruit more leukocytes (Galván-Peña and O’Neill, 2014). The IL-13, IL-4 and other cytokines will lead to M2 subset macrophages being formed. These assist by regulating the inflammation using mediators including IL-1 receptor antagonist, IL-1 type II receptor, transforming vasopressin endothelial growth factor (VEGF) and TGF- β to promote extracellular matrix synthesis, angiogenesis and fibroblast proliferation (Novak and Koh, 2013).

The next stage, known as the proliferative phase, is then initiated by the cells involved entering apoptosis as the resolution of inflammation takes place. This phase (proliferative) can be separated into four essential stages, these are re-epithelisation (successful wound closure), angiogenesis (the formation of new blood vessels), granulation (tissue formation) and finally, collagen deposition. The proliferative phase is recognisable by concentrated cellular activity that aims to repair connective tissue as well as to aid in the formation of epithelium and granulation tissue (Landén *et al.*, 2016).

The first of the four essential stages, re-epithelialisation, is when keratinocytes move away from the wound and the release of growth factors stimulates epithelial attachments that are responsible for an increase in epithelial hyperplasia and mitoses (Pastar *et al.*, 2014). In order to degrade and proliferate the provisional matrix and produce MMPs, fibroblasts migrate to it. The fibroblasts will also produce hyaluronic acid, collagen, glycosaminoglycans, fibronectin for the formulation of granulation tissues and proteoglycans. These will fill the wounded area and encourage wound repair by supporting the adhesion and migration of cells as well as their differentiation and growth (Levinson, 2013). AGE formation is very important when it comes to chronic hyperglycaemia. This is because AGEs have properties that are pro-inflammatory and pro-oxidant and, through cell surface receptor-mediated

interactions, they induce oxidant stress within cells and protein cross-linking (C. Sharma *et al.*, 2015).

In order for the new tissue to form properly in terms of oxygenation and nutrition, angiogenesis is vital. Growth factors including basic fibroblast growth factor (bFGF), platelet-derived growth factor (PDGF) and VEGF initiate the development of new blood vessels. Then, to dissolve the basal lamina, proteolytic enzymes are secreted. Following this, the angiogenic stimulus encourages endothelial cells to leave the blood vessels in order to multiply and go to the stimulus source. They will also assist in supplying oxygen for cell function maintenance (DiPietro, 2013).

The production of collagen is activated from the beginning of the formation of granulation tissue through the production and deposition steps as well as the steps of digestion and reorganisation. At first, collagen fibres are not in an organised form, as they are shadowing a fibronectin model. In an effort to order and organise the fibres, they are subjected to digestion. This is through the action of enzymes that are produced by macrophages, fibroblasts and neutrophils (Landén *et al.*, 2016). Then new, more organised, fibres are created and deposited following connective tissue which is adjacent, and this will initiate the next phase, remodelling (Ganeshkumar *et al.*, 2012). The remodelling phase takes place when granulation tissue formation is complete. Cytokine expression, amplified mechanical stress and tissue development help to encourage fibroblasts to separate into myofibroblasts. The myofibroblasts express smooth muscle actin and have a contractile function that prefers the movement of the cells from the edge of the lesion to the centre for contraction of the wound (Penn *et al.*, 2012). Collagen I is then produced in order to replace the rapidly produced collagen III in the extracellular matrix. Collagen I takes longer to deposit but has an increased tensile strength (Ganeshkumar *et al.*, 2012). Larger fibres and a greater number of fibrils characterise the new collagen. The very high number of cross-links that are present result in larger fibre diameter and increased tensile strength developed by the scar (Siviero, 2013).

There are multiple factors that can play a role in delaying the process of healing a wound including diabetes, arterial or venous insufficiency, renal disease, local

pressure effects, old age and trauma. Other local factors that can impair the healing of wounds include ischaemia, tissue hypoxia, exudates, foreign bodies, inflammatory process regulation disruptions, maceration of tissue, systemic factors such as a compromised immune system or a compromised nutritional status and infection (Eming *et al.*, 2014). The rise in the number of chronic wounds being seen is contributed to by the rise in the number of non-communicable diseases including obesity, vascular disease and diabetes. There is a significant global problem with chronic wounds including venous, pressure ulcers and diabetic, and the considerable management costs that come with these. The United States has seen a \$25 billion estimated annual figure being spent to manage the chronic wounds of the over 6 million people who are suffering from them (King *et al.*, 2014). The NHS of the UK managed over 2 million patients with a wound during 2012 – 2013, which is the same as 4.5% of the adult population within the UK (Guest *et al.*, 2015).

Diabetic foot ulcers are suffered by a considerable percentage of diabetic patients (15%), and may lead to amputation of the lower-leg (Eming *et al.*, 2014). Wound care currently focuses on recognising any factors that can aggravate the wound and remove these in order to, hopefully, lower the inflammation and encourage the healing process to continue (Velnar *et al.*, 2009). It is not unusual for these treatments to not only be inefficient but they can also take a long period of time and are often expensive. More than half of chronic wounds are unmanageable by the conventional methods of treatment (Mustoe *et al.*, 2006). Although the formation of scar tissue and fibrosis are very damaging and come with many consequences, there are currently no effective ways to treat prevent them (Mustoe *et al.*, 2006). Despite this, the global market for products that are aimed at advanced wound care, specifically promoting the healing of chronic wounds and reducing scarring, is over \$20 billion annually (Sen *et al.*, 2009).

1.13.1 The impact of diabetes on wound healing

When AGEs are present in the wounds of diabetic patients, they result in continued chronic inflammation. This result in the wound is unable to progress to the next stage of healing (matrix deposition and remodelling) and thereby prevents healing from taking place (Serra *et al.*, 2017). Small blood vessel damage and immune suppression

can also be present in diabetic patients and this can result in inadequate tissue oxygenation. All of this together can cause wounds to become chronic because of more ROS being created, amplified apoptosis of lymphocytes and immune deficiency (Arya *et al.*, 2013).

Many physiologic factors (~100) contribute to wound healing deficiencies in diabetic individuals (Figure 1.8). These include reduced or impaired growth factor production (Galkowska *et al.*, 2006), angiogenic response (Falanga, 2005), macrophage function (Maruyama *et al.*, 2007), collagen accumulation, epidermal barrier function, quantity of granulation tissue (Falanga, 2005), keratinocyte and fibroblast migration and proliferation, number of epidermal nerves (Gibran *et al.*, 2002), bone healing, and the balance between the accumulation of extracellular matrix (ECM) components and their remodelling by MMPs (Lobmann *et al.*, 2002). The wound healing process in response to injury involves activation of keratinocytes, fibroblasts, endothelial cells, macrophages, and platelets. Activation of these candidates is coordinated by the release of growth factors and cytokines to maintain healing.

Biopsies obtained from the epidermis of patients have identified pathogenic markers that are associated with delayed wound healing. For example, overexpression of c-myc and nuclear localisation of β -catenin (Stojadinovic *et al.*, 2005) coupled with a decrease in, and abnormal localisation of, estimated glomerular filtration rate (eGFR), stimulation of the glucocorticoid pathway and inhibition of keratinocyte migration (Stojadinovic *et al.*, 2005; Brem *et al.*, 2007). At the non-healing edge (callus) of diabetic foot ulcers (DFUs), keratinocytes exhibit hyperproliferation, partial differentiation and absence of migration (Stojadinovic *et al.*, 2005; Brem *et al.*, 2007). Fibroblasts show changes in phenotypic characteristics and the inhibition of migration and proliferation.

In contrast, in an adjacent non-ulcerated area, cells become physiologically impaired but still display the normal phenotype appearance. However, the ability of keratinocytes to respond to growth factors or cellular therapy is still unchanged. Microarray analyses of patient biopsies have confirmed that the transcription profiles of epithelial cells from the callus and adjacent non-ulcerated skin are distinct and well-recognised (Brem *et al.*, 2007).

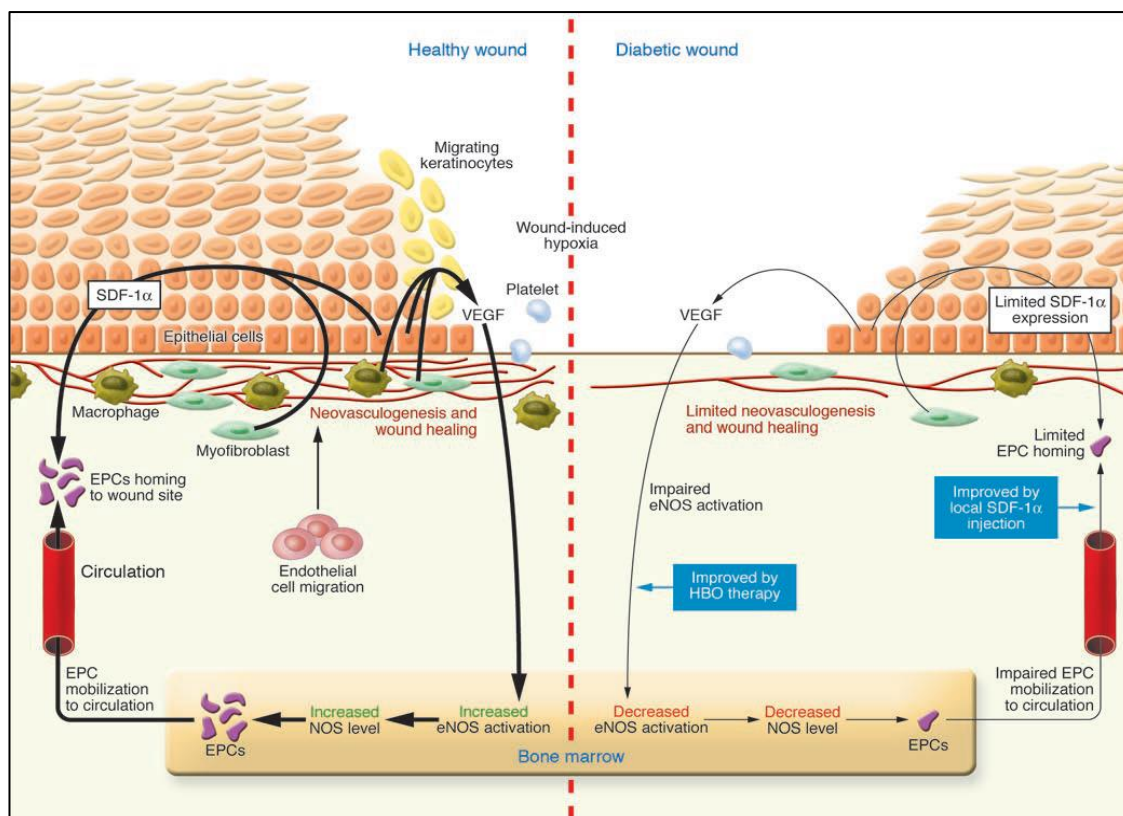


Figure 1.8: Comparison of wound healing in healthy and diabetic people.

In healthy individuals (left), the acute wound healing process is regulated by cytokines and chemokines released by keratinocytes, fibroblasts, endothelial cells, macrophages, and platelets. During wound healing and under hypoxic conditions, VEGF is released by macrophages, fibroblasts, and epithelial cells inducing the phosphorylation and activation of eNOS in the bone marrow. This results in an increase in NO levels, which triggers the mobilisation of bone marrow endothelial progenitor cells (EPCs) to the circulation. The chemokine Stromal-derived factor-1 alpha (SDF-1 α) promotes the homing of these EPCs to the site of injury to be involved in neovascularization. Impaired causing a limitation of EPC mobilization from the bone marrow into the circulation. A decrease in SDF-1 α expression in epithelial cells and myofibroblasts in the diabetic wound prevents EPC homing to wounds and therefore limits wound healing. Hyperoxia in wound tissue (via hyperbaric oxygen therapy) activates many NOS isoforms, elevates NO levels, and promotes EPC mobilisation to the circulation. However, the local administration of SDF-1 α triggers the homing of these cells to the wound site (Brem *et al.*, 2007).

Debridement is the medical removal of hyperkeratotic, infected, and nonviable tissue from a wound. It accelerates wound healing via a multitude of mechanisms (Saap and Falanga, 2002). Pathological diagnosis is essential to confirm the elimination of the hyperkeratotic epithelium and to determine the efficacy of debridement (Figure 1.9). DFU debridement should be carried out regularly until the callus or hyperkeratotic tissue has disappeared in the periphery of the wound and to ensure no scar or infection is present at the base of the wound.

There are many pathological factors that affect tissue repair in diabetes mellitus (Cunha, 2000) such as atherosclerosis, development of major vascular stenosis or occlusion, and renal failure. Atherosclerosis can lead to an embolism in proximal vessels that leads to a decrease in the blood flow and, ultimately, insufficient oxygen delivery and causes toe damage. In this case, angioplasty or vascular bypass should be performed to accelerate wound healing. The atherosclerosis complications are different from the manifestations in non-diabetic patients. Because the arteries are inflexible due to calcification, the ankle-brachial (AB) index becomes difficult to assess. However, a transcutaneous monitor can be used to ensure that there is enough local oxygen delivery for wound healing to accelerate. Also, diabetic patients may develop a thickened perivascular basement membrane that may contribute to the altered delivery of micronutrients and increase vascular permeability (Shimomura and Spiro, 1987). Diabetic people are more prone to the development of neuropathy and infectious diseases due to immunosuppression. Moreover, in diabetes and venous stasis disease, oedema impairs wound healing. The thickness of the basement membrane also slows the leukocyte migration. This ECM deposition may gather inflammatory cells increasing the tendency for infection (Shimomura and Spiro, 1987).

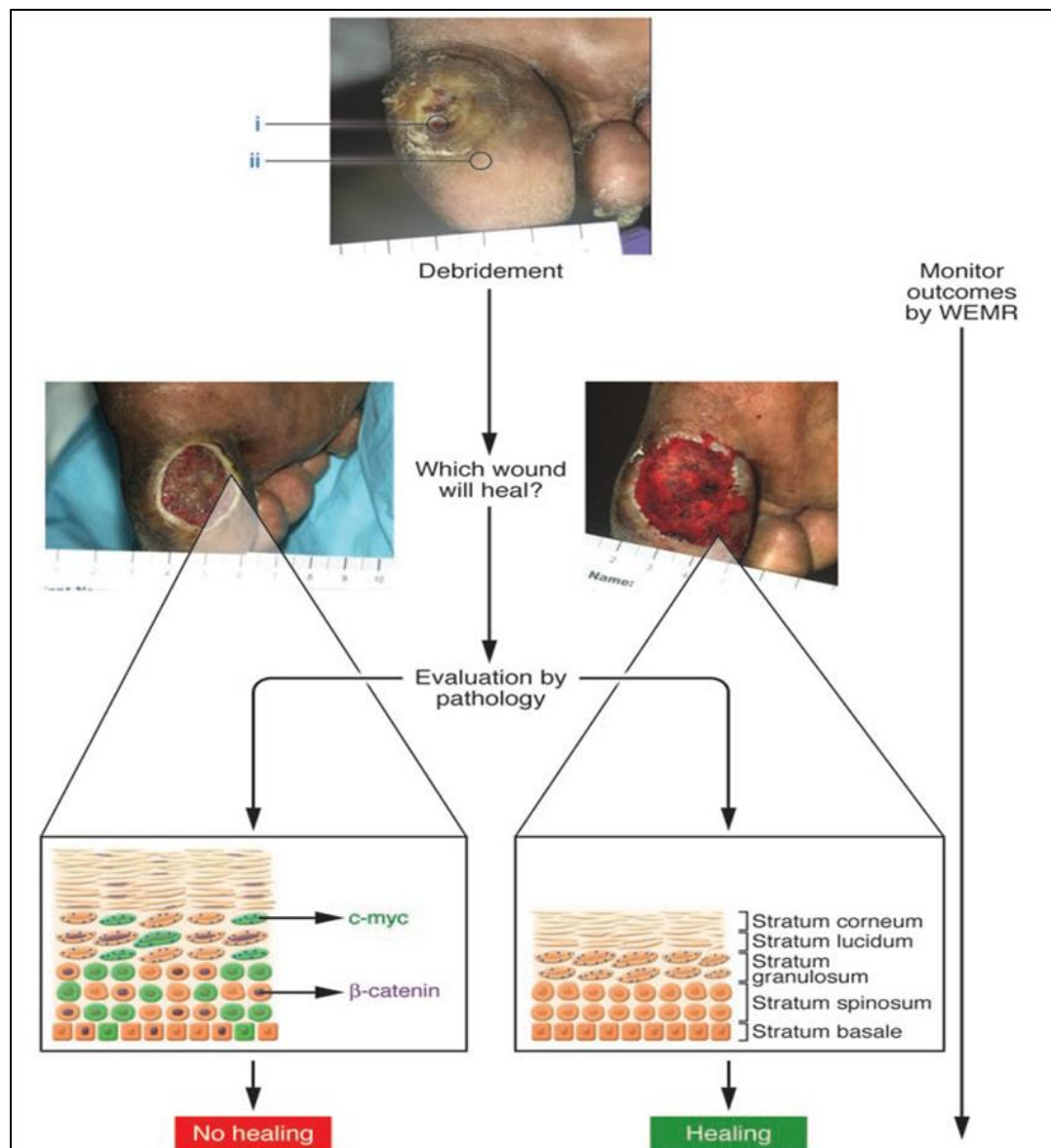


Figure 1.9: Molecular basis of debridement.

A typical diabetic patient foot ulcer is shown at the top. (i) Callus containing ulcerogenic cells expressing molecular markers, which are indicative of impaired wound healing. (ii) Cells presenting normal phenotypical characteristics but are physiologically impaired, though they can be stimulated to heal. After debridement, cells express c-myc (green) and nuclear β -catenin (purple) indicating the presence of ulcerogenic cells, which handicap wound healing, thus additional debridement becomes required. Weak/slow healing is also demarcated by a thicker epidermis and the presence of a nuclei-containing cornified layer (lower left lower diagram). If the debridement is successful (lower right lower diagram), no staining for c-myc or β -catenin is detected and there is no formation of ulcerogenic cells (Brem *et al.*, 2007).

1.14 Recognising and measuring AGEs

Recognised as being complex molecules, AGEs are generally difficult to detect within serum and tissue (Morais *et al.*, 2013; Lobo Júnior *et al.*, 2017). The measurement of

AGEs continues to be restricted to investigative laboratories as there remains a lack of a universally accepted method for AGE measurement (Lobo Júnior *et al.*, 2017; Villa *et al.*, 2017). There have been various methods used to observe the quantitative and qualitative levels of AGEs. Arguably, the main method that allows for fluorescent AGE detection both *in vivo* and *in vitro* is fluorescence spectroscopy (Villa *et al.*, 2017). Measuring the fluorescence of AGEs is a common method as it is quick and relatively simple to repeat data through incubating the reducing sugar and protein to then allowing investigation of its manifestation in diabetes mellitus (de Vos *et al.*, 2016). The limitations of this technique are that only AGE trend indicators are recognised as opposed to the actual structural AGEs themselves (de Vos *et al.*, 2016; Raposeiras-Roubín *et al.*, 2013) Matrix-assisted laser desorption ionisation time-of-flight mass spectrometry (MALDI-TOF-MS) has been used with success in order to observe AGEs (Uribarri, 2017). The method is cost-effective and fast with benefits including very little sample work-up, excellent sensitivity, soft ionisation and high resolution. In order to measure protein glycation products both *in vivo* and *in vitro*, the technique MALDI-TOF-MS peptide mapping is used (Uribarri, 2017; Ahmed and Thornalley, 2007). Throughout the duration of glycation research, separation assay methods are used, an example of this being SDS-PAGE (Xie *et al.*, 2011; Kishabongo *et al.*, 2015) Using this method identifies oligomerisation of glycated protein with ease and is a technique that is frequently used. It is a financially practical and effective method. Enzyme-linked immunosorbent assay (ELISA) is an immunochemical technique that uses monoclonal and polyclonal antibodies that are particular to structures of defined AGEs giving the benefit of being very sensitive to AGEs and allowing quantitative estimation to occur (Elosta *et al.*, 2012).

1.15 Using medicinal plants for diabetes

Naturally, derived products from plants to fungus, shells and minerals are the oldest practice of medicine. Even today, the majority of frequently used medications are derived from herbs with around one-quarter of prescription drugs containing one or more active ingredient derived from herbs, or even a compound that is synthetic but plant-mimicking (Saad and Said, 2011). Since ancient times, medicines that have been derived from plants, organic matter and minerals have been used to treat diabetes and other chronic disorders. Around 150 species are currently available commercially for

use as medicine around the world (out of 21,000 plants), according to the WHO (Raman *et al.*, 2012). A number of recent studies have indicated that a combination of antioxidant nutrients, antiglycation and complementary medicine is understood as a simple and safe accompaniment to the traditional medications and it is hoped to inhibit and focus on the complications relating to diabetes (Aljohi *et al.*, 2016). An example is tomato paste, which demonstrates effective inhibitory effects against glycation (Kiho *et al.*, 2004) as well as autoxidative reactions (Cervantes-Laurean *et al.*, 2006). Other plant medicines that contain polyphenolic molecules have demonstrated their ability to inhibit the production of AGEs, such as garcinol originating from *Garcinia indica* (amagishi, 2011), crisilineol originating from *Thymus vulgaris* (Roby *et al.*, 2013) and soy sauces (Mashilipa *et al.*, 2011). There has also been a variety of antioxidant compounds identified to have *in vitro* antiglycation properties, including green tea extract, which has a large number of flavonoids or tannins (Panche *et al.*, 2016) and garlic (*Allium sativum*) which has high amounts of S-allyl cysteine (Ourouadi *et al.*, 2016). This is similar to curcumin which has been isolated from turmeric (*Curcuma longa*) (Qader *et al.*, 2011). There has also been a large number of natural compounds that have been shown to inhibit AGEs, including epigallocatechin-3-gallate (Lee *et al.*, 2013), caffeic acid, chlorogenic acid (Agunloye and Oboh, 2018), hesperidin and capsaicin (Fattori *et al.*, 2016a).

1.15.1 The origins and medicinal properties of garlic

Believed to come from Central Asia origins, garlic (*Allium sativum*) belongs to the *Alliaceae* plant family. Garlic has been used for centuries as a functional food, folklore medicine and flavouring agent (Ourouadi *et al.*, 2016). Similar to many other plants, an effective defence system is present in garlic that is composed of several different components that aid in boosting the immune system of humans. When garlic is injured, it produces allicin enzymatically in an effort to safeguard itself from fungi and insects (Ghani, 2010; Ourouadi *et al.*, 2016). Due to the beneficial effects that garlic has, it is consumed both as it is and in the form of a supplement in numerous cultures (Ourouadi *et al.*, 2016). Garlic has been known to be used medicinally for reducing triglycerides and serum cholesterol, inhibiting the formation of platelets and lowering blood pressure (Samakradhamrongthai, 2017). The healing properties that are present in

garlic are largely produced by the bioactive components present (Santhosha *et al.*, 2013).

1.15.1.1 Garlic – a closer look into the key compounds

Garlic is part of the *Liliaceae* family. The beneficial effects are produced by the larger sulphur compound concentration present, which is also responsible for the strong taste and flavour that is characteristic to garlic. Garlic is made up of a large percentage of water (65%) as well as over a quarter (28%) carbohydrate (fructans), 2.3% organosulphur compounds, 2% proteins (alliinase), 1.5% fibre and 1.2% free amino acid (arginine). The therapeutic properties and the strong smell of garlic are caused by an active substance called allicin (diallyl thiosulfate) (Santhosha *et al.*, 2013; Macpherson *et al.*, 2005). The substances within garlic that are biologically active can be separated into two units (Yongkun Ma *et al.*, 2011). Group 1 is the sulphur compounds and group 2 is the sulphur-free active substances. Group 1, for example, alliin, ajoene and allicin, are vital flavour compounds. Alliin is an active substance that is biologically ineffective and sensorily inactive until cell damage occurs when it forms allicin, the effective garlic essential oil. Allicin is what gives garlic the characteristic strong smell and its important antibiotic properties. It is possible to modify the off-odour of garlic using certain processing methods, for example; steaming, roasting, using soaked water to cook it in, autoclaving, hydrostatic pressure treatment and fermentation (Sharma and Prasad, 2006). There is no allicin found in the plant when it is intact, only when garlic bulbs are crushed do the enzyme reactions between a precursor molecule, alliinase (enzyme) and alliin (non-protein amino acid) take place. Although these are all present within intact garlic, compartments separate them (Arzanlou and Bohlooli, 2010). Recent research has been focussed on the allicin of garlic, specifically on compounds containing sulphur and the benefits of this (Omar and Al-Wabel, 2010). The organosulphur compounds can be separated into water-soluble and oil-soluble constituents. Water-soluble organosulphur components include S-allyl cysteine (SAC) (Figure 1.10) and N-acetylcysteine (NAC) (Figure 1.11) (Santhosha *et al.*, 2013) and oil-soluble organosulphur components include DAS (diallyl sulfide), DADS (diallyl disulfide) and DATS (diallyl trisulfide). NAC has a –SH residue donor and a nucleophile (Nishikawa-Ogawa *et al.*, 2005). Deriving from

gamma-glutamyl-S-allyl-L-cysteine, SAC is a major compound which is primarily seen in the garlic extracts from alcoholic and aqueous bases (Kodera *et al.*, 2017). A study that was conducted by Yin and Cheng focused on the antimicrobial and antioxidant protection of NAC, DADS, S-ethyl cysteine (SEC) and DAS for 5 inoculated pathogenic bacteria. They found that DADS and DAS both showed antimicrobial and antioxidant protection whereas NAC and SEC may stabilise the protein structure or redox status directly (Yin and Cheng, 2003). In a study of alloxan diabetic rats, it was found that S-allyl cysteine sulfoxide (SACS), which is an amino acid present in garlic that contains sulphur and is the originator of garlic oil and allicin, demonstrated antidiabetic effects (Ourouadi *et al.*, 2016). A typical antidiabetic treatment combined with garlic has exhibited an ability to improve antihyperlipidemic activity as well as glycaemic control indicating that garlic could be a useful and suitable addition for patients managing hyperlipidaemia and diabetes (Ashraf *et al.*, 2011). It has also been found that garlic alcohol extract decreased uric acid, urea, triglycerides, cholesterol, serum glucose, Aspartate amino transferase (ALT) and Alanine amino transferase (AST), and when comparing treated diabetic rats with control diabetic rates there was an increase in serum insulin levels seen in the former (Eidi *et al.*, 2006).

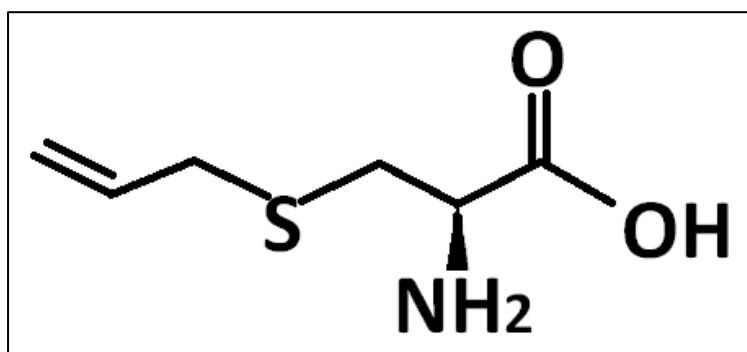


Figure 1.10: S-allyl cysteine chemical structure.
Molecular Formula: C₆H₁₁NO₂S and Molecular Weight: 161.224

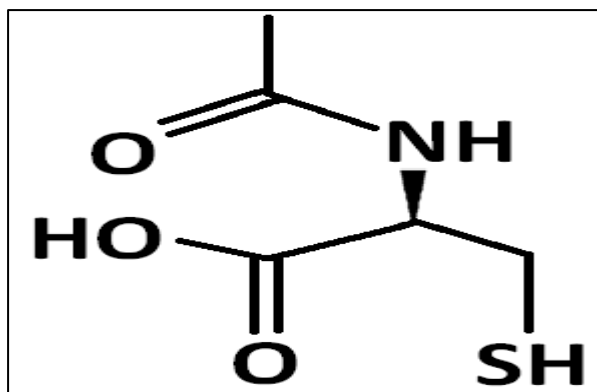


Figure 1.11: N-acetylcysteine chemical structure.

Molecular Formula: C₅H₉NO₃S and Molecular Weight: 163.195

1.15.1.2 Use and properties of aged garlic extract

In the last decade, there has been an increase in the popularity of garlic and the number of garlic products that are available in international markets. Many consumers have become influenced by commercially available products as a way to increase their daily intake of garlic by avoiding the strong smell that fresh garlic possesses (Cardelle-Cobas *et al.*, 2010). The development of garlic extraction has been based around its traditional uses. The chosen solution used for extracting often diluted alcohol or purified water is used to soak sliced or whole cloves of garlic for a varying period of time. The solution is separated, and the extract is then concentrated and ready for use. The produced extract contains mostly water-soluble compounds but also a small number of oil-soluble constituents (Mane *et al.*, 2011; Cardelle-Cobas *et al.*, 2010). An extract that is created using a method slightly different from the other garlic products is aged garlic extract. No heat is required when creating this, instead, slices of raw garlic are soaked in a 15 - 20% solution of aqueous ethanol for at most 20 months at room temperature. Under reduced pressure, the extract is then filtered as well as concentrated at a low temperature. The extract has a low number of oil-soluble compounds but a high number of water-soluble compounds. The process of aged garlic extract increases the concentration of antioxidants and converts alliin and other unstable compounds into stable substances that promote health such as S-allylmercaptocysteine (SAMC) and SAC (Ahmed *et al.*, 2012). Aged garlic extract has anti-glycation effects, which are thought to be a result of the antioxidant compound SAC, which can prevent glycooxidation and autoxidative reactions that play a role in

the formation of AGEs. The amino groups in SAC could also prevent the formation of reducing sugars, dicarbonyl intermediates and Amadori products due to a reaction with, and blocking of, carbonyl groups thereby stopping them from carrying out AGEs' conversion (Ahmad *et al.*, 2007). Aged garlic extract is believed to be an excellent natural oxidant that may be able to protect the macromolecules that are essential for the survival of cells, limit the oxygen effects and inhibit the free radical processes (Goffin, 2012). There has also been particular attention to AGEs due to studies showing an effective antioxidant with the capacity for free radical scavenging (Soloviev *et al.*, 2002). Due to its ability to be detected and its quantitative increase in the blood, SAC is the sole reliable marker that is used in studies concerning garlic consumption by humans (Steiner and Li, 2001). SAC may be used to compare a number of sources or for garlic preparation standardisation as it is found in many preparations. The sole product that is standardised for SAC is AGEs (Cardelle-Cobas *et al.*, 2010). Various toxicological studies have been able to confirm the safety of use and consumption of aged garlic extract (Amagase *et al.*, 2001).

1.15.1.3 Recommended daily garlic intake

The amount of garlic consumed on a daily basis has not been standardised, however, there are multiple suggestions from various sources. The German Commission E Monograph (GKEM) suggested that consuming around 4 grams or 1 to 2 cloves of garlic that are intact each day may result in benefits to health (Amagase *et al.*, 2001). However, there is no scientific evidence that backs up this claim. A recent study involving dehydrated garlic powder estimated a dose each day of around 900mg. When we consider aged garlic extracts, the daily intake is between 1.7g and 2g per day and this has been successfully used in humans to lower plasma cholesterol (Steiner and Li, 2001). There have been several studies involving aged garlic extract that have found a dose each day of between 1.8g and 10g has an enhancing effect on the immune response and which does not cause any toxic or severe side effects (Abdullah, 1989). It has been noted that even in clinical studies administering high doses of the extract, there have been no severe or toxic side effects reported (Rahman, 2007).

1.16 Using synthetic compounds for diabetic complications

Synthetic mimic compounds A, B and C were kindly supplied by Dr Alan Jones from the Chemistry Department at Manchester Metropolitan University, UK. These compounds are small molecules inhibitor – mimic of SAC and NAC. Compound A [(R) S-Benzyl-L-cysteine] and its molecular formula is C₁₀H₁₃NO₂S. It is more fat-soluble compound. Compound B [L-cysteine methyl ester hydrochloride] and its molecular formula is C₄H₁₀ClNO₂S. It is more water-soluble compound. Compound C [(R)-S-triphenylmethyl cysteine] and its molecular formula is C₂₂H₂₁NO₂S. It is much more fat-soluble compound than compound A (Figure 1. 12).

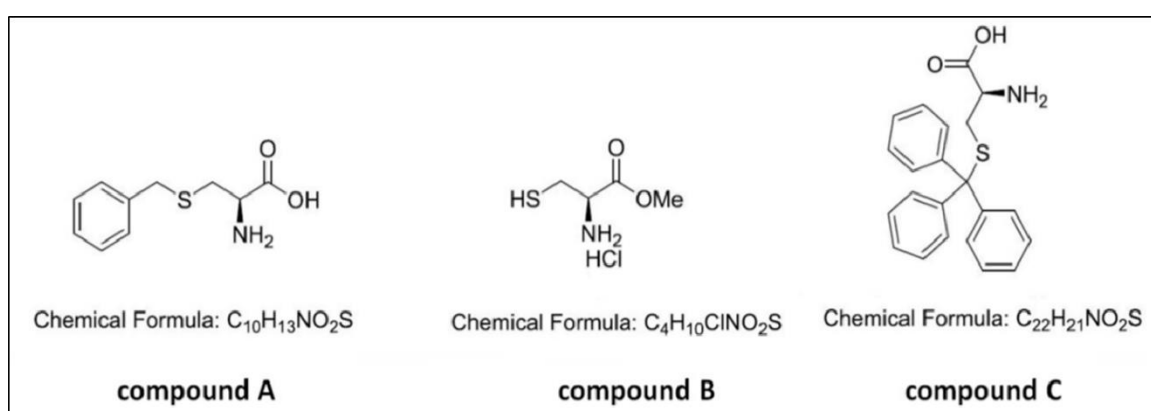


Figure 1.12: Structure of mimic compound A, B and C.

1.17 The role of mesenchymal stem cells

Conventionally, the term mesenchymal stem cell, or MSCs, describes a collection of cells known as multipotent stromal cells (Waterman and Betancourt, 2011) that have the ability to differentiate into a variety of cell types. Mesenchymal stem cells have been known by various names before MSCs including “bone marrow stromal” or “osteogenic” stem cells (Caplan, 1991), another later example being “stromal progenitor” stem cells (Bianco *et al.*, 2008). However, those within the scientific community have expressed concerns regarding whether or not the MSCs are actually stem cells at all. This is due to there being little or no evidence to show that these cells are capable of self-renewing *in vivo* as stem cells are known to do (Dominici *et al.*, 2009). In a 2005 statement from the International Society for Cellular Therapy it was said that, as a term, mesenchymal stem cell should be used only in cases where the cells are in alignment with the stem cell criteria and instead the term multipotent

mesenchymal stromal cells should be used to describe fibroblast-like plastic-adherent cells, regardless of the tissue they are isolated from. However, MSCs can continue, as they have been, to be used to describe both cell types/populations. Although this statement has been made, little has changed in the use of the term. The mesenchymal stem cell is a commonly used term and, in addition to this, the European consortium Genostem stated that there is evidence of MSCs being true stem cells as they have self-renewal capabilities, something that was reported during a systematic analysis of bone marrow-derived MSCs (Charbord *et al.*, 2011). The feature that is most characteristic of these cells is the ability to differentiate into adipocytes, osteoblasts and chondroblasts *in vitro*. In fact, this differentiation ability *in vitro* is frequently used to identify MSCs (Keating, 2012).

MSCs are multipotent progenitor cells that are capable of self-renewing and are able to differentiate themselves into several cell types (under appropriate stimuli) (Sollazzo *et al.*, 2011). The mesenchymal stem cells are able to differentiate into a range of cell types comprising fat cells, cartilage cells and bone cells (Mittal, 2011). It is possible to isolate MSCs from both adult or embryonic tissues including adipose and bone marrow (Hima Bindu and Srilatha, 2011). In fact, these cells and similar are also isolated from, amongst other tissues, the placenta (Igura *et al.*, 2004), blood (Zvaifler *et al.*, 2000), umbilical cord blood (Erices *et al.*, 2000) and trabecular bone (Sottile *et al.*, 2002). An incredible property that MSCs have is the ability to institute repair when tissue injury is present. They do this by either increasing the number of endogenous cells that are capable of repairing tissue and influencing the immune response by the creation of a milieu (Ankeny *et al.*, 2004) or by becoming tissue-specific cell phenotypes (Tadokoro *et al.*, 2009). Recent studies have been more focused on the ability that MSCs possess to repair, without significant differentiation or engraftment, the tissues rather than studying the cell differentiation itself and this has resulted in concepts relating to the therapeutic effects of human adipose mesenchymal stem cells (hADMSCs). This new concept depends on the MSC's capability to answer to the needs of damaged tissue in an immediate and specific manner as well as the ability secretes a mixture that is rich in soluble factors (Ma, 2010).

1.17.1 The use of MSCs as a mean to deliver drugs

Delivery of drugs into the systems is traditionally carried out by applying the substance to the mucous membranes or skin, injection or oral administration. These are the conventional systems and most of them distribute the drug to the blood flow proportionally by using the systemic circulation of blood. This also means that the medication is carried through the entire body indiscriminately as opposed to tackling just the diseased tissues. This non-specific distribution of the substance then causes the patient to experience side effects (Branco and Schneider, 2009). In order to improve the method of drug delivery and increase efficiency, the potential of using delivery vehicles is being explored. To use a delivery vehicle means to encapsulate the drug in a specific material that will release the medicine in a way that is controlled, allowing the dosage to be optimised for a certain time period (Goldberg *et al.*, 2007; Lee and Yuk, 2007). The abilities of MSCs to move to the inflammation sites, influencing immune responses and slow inflammatory responses as well as prevent tissue damage and assist in repairing tissue damage are unique to MSCs and all make them an appealing option for use as a therapy to assist in the treatment of inflammatory-related diseases (Newman *et al.*, 2009). On top of this, MSCs have shown that they are also capable of increasing neurogenic factors, mitogenic factors, angiogenesis and anti-apoptotic factors (Quittet *et al.*, 2015) in addition to being able to, when facilitated by micro and nanovesicles, accept and release medicines using endocytosis (Baglio *et al.*, 2012).

The novel idea of utilising stem cells to deliver drugs within the body has been recently researched, with results showing that MSCs are able to effectively accept and release treatments (Andrews, 2015). The concept of using these cells as a drug delivery system has been proven by many preclinical studies. Tumour can be regarded as a kind of wounds that never heal and continuously generate various inflammatory cytokines (Li *et al.*, 2019). Indeed, MSCs that are either *de novo* mobilized or exogenously administered have been found to migrate to tumour cells and adjacent tissue sites (Clavreul *et al.*, 2017). In view of this property, Chulpanova *et al.* (2018) reported that MSCs have the characteristics of tumor tendency and avoidance of immune clearance; thus, it is promising that MSCs are utilized as vectors for the delivery of antitumor treatments. Additionally, BM-MSCs have been used for clinical trials to

treat damaged tissues of neurological diseases, spinal infarction, and myocardial infarction which difficult to heal by normal tissue regeneration (Squillaro *et al.*, 2016; Lukomska *et al.*, 2019). However, the clinical studies have concentrated on unmodified human mesenchymal stem cells. For the cells to be additionally modified may assist in the amount of therapeutics that the cells generate, or encourage therapeutics not usually found within the naive cells to be produced. It is possible to modify MSCs using non-genetic and genetic techniques, including pre-differentiation of the cells in growth factor-containing media. A clinical study has used adipose-derived insulin-producing MSCs as a treatment for type 1 diabetes (Bose *et al.*, 2018; Takahashi *et al.*, 2019).

The use of MSCs as a delivery vehicle in therapeutic and diagnostic situations is an attractive option as they are readily available, safe, can travel to the specific tumorigenesis and injury sites and have a small immunogenicity profile (Prasad *et al.*, 2011). However, there are studies to be carried out and challenges to master before the use of MSCs clinically to deliver drugs within the body. One such challenge is how to effectively load the drug on the cell. The cells need to be altered to manufacture high levels of the agent or loaded with enough drugs to produce healing effects without having a negative impact of the viability of the cell or the necessary properties needed for effective delivery of the drugs, for example, the migration potential of the cell. Studies carried out on animals have shown it is possible to generate modified and still therapeutically effective MSCs, and it will be down to the human clinical trials to determine if these outcomes can be effectively translated. Another necessary challenge is to develop a method for the drug to be released effectively. This would require mechanisms that start the release from the MSCs in order to enter or access the target cell. Overall, the use of MSCs as a drug delivery system is a promising prospect. The use of these cells in this way will become widespread only if an effective loading and release of drugs at the right times and locations can be developed and ensured (Todd *et al.*, 2011).

1.17.2 The role MSCs play in healing wounds

Skin plays a vitally important role for our bodies; from actively synthesising vitamin D, preventing dehydration, providing a protective barrier, being a site for active immune surveillance and being a thermoregulatory and sensory organ (Lee *et al.*, 2006). Epidermis and dermis make up the skin. Distinct layers are present in the epidermis, and these layers mirror the sequential differentiation of keratinocytes while they move to the outer cornified layers from the basal layer as terminal differentiation sets in and they lose the capability of proliferation. Once they are in the outermost layers, they will be shed (Wikramanayake *et al.*, 2014). Healing of wounds that are present on the skin surface is an intensely coordinated effort with an organised succession of processes taking place in order to effectively restore the tissue with the desired functions and integrity. It is when these processes are interrupted that a non-healing, or chronic, wound can develop (Eming *et al.*, 2014). A chronic wound is one that has persisted for a minimum period of three months, and commonly classified as being diabetic, pressure ulcer or vascular (Pang *et al.*, 2017; Hu *et al.*, 2018).

There are multiple chronic wound therapies that have been developed, although the success rates have been varied (Eming *et al.*, 2014). One type of therapy that has caught interest and shown promise for use in enhancing tissue regeneration is using stem cells. Using MSCs as a wound treatment results in the increased formation of granulation tissue, increased angiogenesis and it speeds up the rate of wound closure. However, it is not the MSCs replacing the damaged cells by differentiating that causes the positive outcomes, it is instead the MSCs ability to produce therapeutic properties agent by the secretion of soluble factors. This secretion actually helps to regulate the cells' responses to a cutaneous wound (Hocking and Gibran, 2010; Hocking, 2012). Angiogenesis is promoted, cell death reduced and the formation of scars at the area of the injury reduced with the MSCs cytokine and growth factor secretion (Ankrum and Karp, 2010). On top of this, immunosuppressive factors are released by MSCs and these aid in preventing the increase of immune cells including natural killer cells, B-cells and T-cells (Matthay *et al.*, 2010). Administering exogenous MSCs to wounds helps to speed up the closure of the wound, increase angiogenesis and increase the formation of granulation tissue (Hocking and Gibran, 2010). It is also suggested, by a further study, that the secretions from MSCs are able to produce such results due to

their ability to regulate the responses to an injury by the main cell types that are present within the wound, which are keratinocytes, endothelial cells, macrophages and dermal fibroblasts (Hocking and Gibran, 2010). In another study, topical allogeneic MSCs were used to treat full-thickness wounds that resulted in less inflammation and enhanced healing. These results were likely to be due to the immunosuppressive factors within the wound that were released and prevented the increase of immune cells (Kim *et al.*, 2013). A recent study found that MSCs used on bioengineering scaffolds encouraged an enhancement of re-epithelialisation. This is characterised by the enhanced formation of blood vessels, a reappearance of hair follicles, multi-layered epidermis and sebaceous glands (Formigli *et al.*, 2015). In a study on animals, adipose MSCs were used on an acellular dermal matrix and this resulted in improved angiogenesis, enhanced healing of the wound and they played a role in the newly-formed vasculature (Huang *et al.*, 2012).

It appears as though MSCs are an effective therapy when it comes to wound healing as well as the healing of scars, despite the warnings about their source or identity (Hu *et al.*, 2018). Bone marrow mesenchymal stem cells (BMSCs) *in vitro* could have limits in terms of long-term potential for differentiation and growth (Barry and Murphy, 2004). Due to this, it is vital to identify other MSC sources in humans that can be used for therapies to heal wounds. Various MSCs including dermal, adipose-derived stromal cells, MSCs from the umbilical cord and from the amniotic fluid have all been involved within the preclinical investigations into the healing of wounds (Böttcher-Haberzeth *et al.*, 2014). The dermal MSCs and adipose-derived stromal cells (ASCs) can be harvested using procedures that are minimally invasive and the cells are abundant within skin and fat. The use of these cells presents an ethical alternative to other more controversial harvest sites, which makes them a great alternative. The use of dermal MSCs and ASCs show promise as, when compared with BMSCs, they exhibit the similar immunogenicity, differentiation potential and biological characteristics (Driskell *et al.*, 2011). In studies based on wound healing, adipose-derived stem cells (ASCs) display promising outcomes *in vitro* (Collawn *et al.*, 2012) and, in animals, *in vivo* (Kato *et al.*, 2017) and they are being tested in clinical trials for their ability to help heal ulcers and burn wounds. A high level of success has been seen with the healing of chronic radiation wounds using human ASCs

taken from the debridement of the burned artificial dermis (Akita *et al.*, 2010). It was shown in a study that the paracrine factors' secretion from Amniotic fluid MSCs (AF-MSCs) was related to cell survival and proliferation was enhanced by hypoxia (Jun *et al.*, 2014). In addition to this, hypoxic conditioned medium taken from human amniotic fluid MSCs (AF-MSC-hypo CM) improved the *in vitro* migration of dermal fibroblasts and enhanced the *in vivo* wound healing by the PI3K/AKT and TGF- β /SMAD2 pathways. It has been shown that murine full-thickness wound margins injected with human MSCs resulted in reduced tissue fibrosis and accelerated wound closure. The TSG-6 released by MSCs was found to suppress TNF- α -mediated inflammation as well as switching the synthesis of TGF- β 3 and TGF- β 1 from promoting scars to instead being anti-fibrogenic. This reduces the differentiation of myofibroblasts and suppresses excessive collagen deposition, similar to what is seen in foetal wound healing (Qi *et al.*, 2014). These clinical studies are very promising and show that using MSCs as a base for therapies is both potentially effective and safe, with no suggestion that the use of one MSCs tissue of origin is more advantageous in wound healing than another of a different origin (Maxson *et al.*, 2012).

As opposed to a direct structural contribution, paracrine signalling of trophic mediators (Garg *et al.*, 2014) by releasing stromal cell-derived factor-1, keratinocyte growth factor, VEGF, epidermal growth factor, matrix metalloproteinase-9 and insulin-like growth factor, MSCs are able to promote the formation of new vessels, recruit endogenous progenitor cells and direct the differentiation, extracellular matrix formation and proliferation of cells during the repair of wounds (Rustad *et al.*, 2012; Garg *et al.*, 2014). The secretion MSCs produces prostaglandin E2 that also helps to regulate inflammation and fibrosis while also promoting the healing of tissues as well as reducing scarring (Hu *et al.*, 2014). Myeloid cells such as macrophages (Oh *et al.*, 2014), granulocytes (Chen *et al.*, 2014) and monocytes (Chiossone *et al.*, 2016) display proinflammatory activity which is suppressed by MSCs. An MSC-conditioned medium acts as a chemo-attractant when it comes to macrophages, through producing macrophage inflammatory protein-1 α and β (Wu *et al.*, 2010). The MSCs also alter a macrophage's phenotype so it is more of an anti-inflammatory M2 phenotype which is characterised by an upregulation of interleukin-12 and other similar anti-inflammatory cytokines as well as TNF- α and an increase in phagocytic ability

(Maggini *et al.*, 2010). MSCs also show bactericidal properties as they secrete an antimicrobial substance as well as increase phagocytosis by immune cells and enhance bacteria killing (Mei *et al.*, 2010) (Figure 1.13).

The therapeutic benefits of MSCs are mostly a result of their capability of secreting cytokines that are pro-regenerative, which makes them a potentially successful option for chronic wound treatment (Garg *et al.*, 2014). There are currently studies and tests being carried out using stem cells obtained from various sources to discover their abilities in the regeneration of tissue and in wound healing. These clinical and preclinical trials have proven that therapy using stem cells is a safe and tolerable option (Kirana *et al.*, 2012), and have also shown the therapies to have positive results. 96 critical limb ischemia patients were studied by Prochazka *et al.* demonstrating that using autologous MSCs as a treatment can reduce the number of amputations to major limbs seen within the follow-up of 120 days compared with the standard treatment (Li *et al.*, 2014; Procházka *et al.*, 2010). In addition to this, MSCs aid in the rate of wound closure and therefore enhance healing of the wound (Rodriguez-Menocal *et al.*, 2015). MSCs derived from human bone marrow have been shown to increase the rate of wound closure by encouraging keratinocyte and fibroblast migration *in vitro* (Walter *et al.*, 2010). Similarly, MSCs derived from murine bone marrow increase the migration of dermal fibroblasts which accelerate the closure of a wound (Smith *et al.*, 2010). Another study demonstrated that skin fibroblasts that are cultured with media-conditioned MSCs derived from human umbilical cord blood (UCB-MSCs) showed a significant elevation in the ability to migrate (Jinfeng *et al.*, 2016).

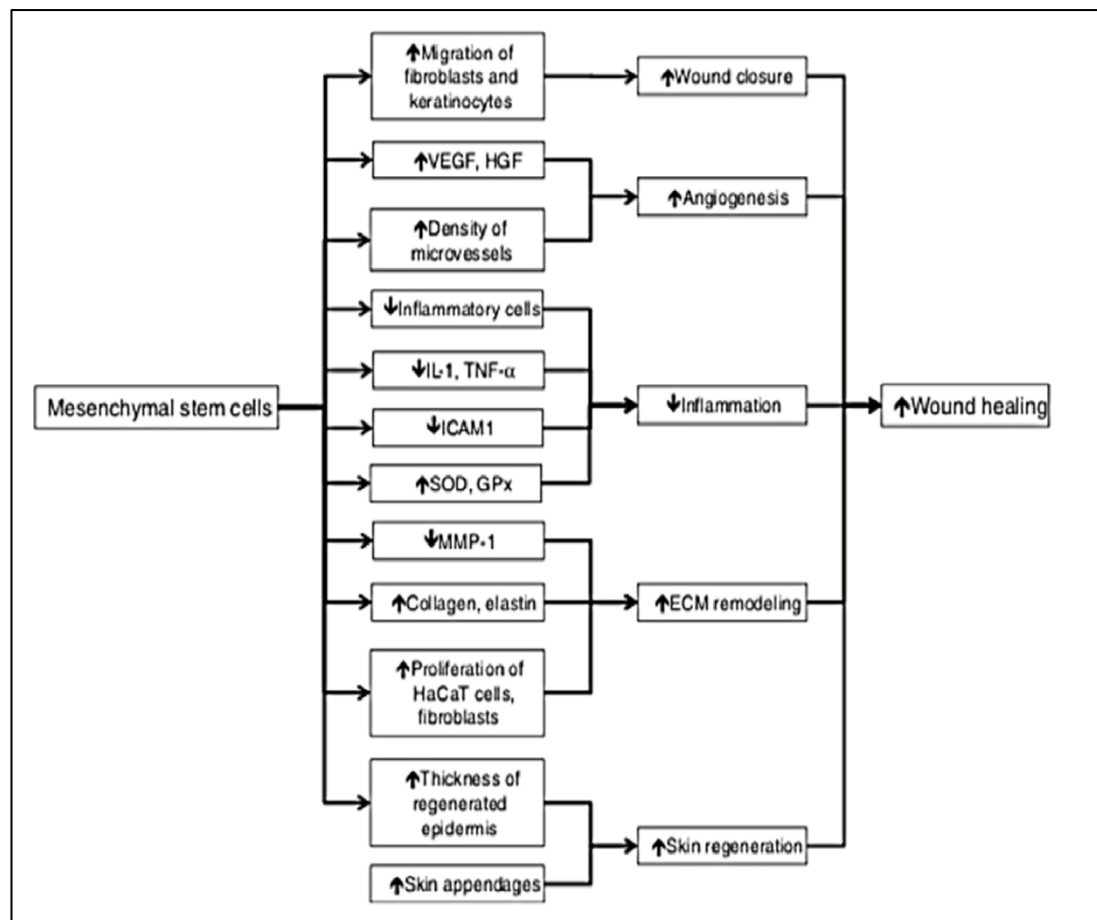


Figure 1.13: The involvement of MSCs in healing cutaneous wounds.

The mesenchymal stem cells help to enhance healing in many ways, from encouraging the migration of fibroblasts and keratinocytes, increasing the density of microvessels, enhancing the thickness of regenerated epidermis as well as decreasing the number of inflammatory cells. Each factor that is influenced by MSCs plays a role in an aspect of healing including; increased angiogenesis, enhanced wound closure, reduced inflammation, enhanced skin regeneration and the regulation of ECM remodelling. Paracrine signalling helps to mediate these effects (Lee *et al.*, 2016).

1.17.3 Ability of MSCs to express pro-angiogenic factors

Angiogenesis is enhanced by MSC during the process of wound healing. Using MSCs derived from the human umbilical cord to treat rat wounds showed an increase in VEGF, microcirculation in the cutaneous wound and microvessel density (Liu *et al.*, 2014). A study using stem cells derived from rat adipose cells that were implanted into wounds of rats showed MSCs had the ability to contribute to the vasculogenesis of wound healing by differentiation directly into vascular endothelial cells (Nie *et al.*, 2011). This same result has also been seen in similar studies and trials (Lu *et al.*, 2008). The same MSCs were also responsible for secreting greater levels of hepatocyte growth factor and pro-angiogenic cytokine VEGF (Nie *et al.*, 2011). Another study

indicated that injected MSCs from murine bone marrow lowered the resistance of the arteriolar vasculature and, in murine skin that is recuperating from ischaemia, there were enhancements seen in the functional capillary density. The important finding of that particular study was that the MSCs had the ability to express pro-angiogenic cytokines including VEGF.

1.17.4 The impact of MSCs on immune modulation

Successful healing of wounds requires inflammation to be resolved, and poor healing is often the result of chronic inflammation (Xu *et al.*, 2012). The wounds' inflammatory response is regulated by the MSCs, which supports the healing process. MSCs derived from human umbilical cord transplanted into cutaneous rat wounds, resulted in a significantly reduced amount number of inflammatory cells as well as pro-inflammatory cytokines such as TNF- α and interleukin (Liu *et al.*, 2014). The wounds also demonstrated a quicker recovery time along with a faster rate of healing. A study showed that MSCs derived from murine bone marrow co-cultured with human dermal fibroblasts reduced intercellular adhesion molecule 1 mRNA levels. It is thought that intercellular adhesion molecule 1 mediates the binding of leukocytes to dermal fibroblasts, which indicates a role within inflammation. A reduction of the expression of this by fibroblasts could aid in resolving inflammation throughout the wound repair process (Couture *et al.*, 2009). Jeon *et al.* studied the activity of antioxidants seen in fibroblasts that had been exposed to MSCs conditioned media derived from the human umbilical cord, which demonstrated that MSCs promoted glutathione peroxidase and superoxide dismutase synthesis. The ability to detoxify is significant at wound sites as superoxide detoxification helps to promote the proper healing of the wound (Schäfer and Werner, 2008). In addition to this, the detoxification of hydrogen peroxide is also an important factor for the VEGF upregulation within skin wounds, indicating pro-angiogenic effects (Jeon *et al.*, 2010).

The extracellular matrix remodelling by MSCs has shown that they are able to enhance ECM events within the healing of wounds (Ojeh and Navsaria, 2014). The expression of MMP-1 is inhibited by conditioned MSCs from human umbilical cord blood, which indicates that the stem cells suppress destruction of the collagenous matrix, play a role

in the regeneration of fibroblasts as well as preserve the matrix (Jeon *et al.*, 2010). Within the study there was also an increase in collagen product and fibroblast elastin, adding to the wound healing enhancement factors. MSCs derived from human adipose cells were used alongside the wound healing assay *in vitro* and showed a significant increase in human adult keratinocyte (HaCaT) cell proliferation as well as dermal fibroblasts, and an enhancement in the overall healing of the wound (Lee *et al.*, 2012). The dermal fibroblasts' ability to contract collagen lattices was enhanced by the MSCs, which indicates that MSCs are able to induce the transformation of fibroblasts into myofibroblasts.

1.17.5 Skin regeneration improvements with the application of MSCs

The redevelopment of normal skin function and architecture is essential for optimal wound healing. There have been several studies that have shown MSCs are able to produce this level of regeneration (Ojeh and Navsaria, 2014). A study carried out by Luo *et al.* (2010) observed the impact of MSCs derived from human umbilical cord blood on mice suffering from severe combined immunodeficiency. The study found that the wounds healed at a significantly enhanced rate, the epidermis regenerated more thickly, the cell number in the regenerated skin was increased, the healing tissue was produced with increased regular fibre alignment and an increased number of dermal ridges were seen. In addition to this, the wound also developed normal skin appendages including sweat glands and hair follicles. These positive results showed that MSCs may enhance the quality of wound healing, enhance the physiology of the skin that is regenerated and accelerate the rate of healing too. A skin model of *in vitro* human keratinocyte-MSCs was used in another study to show that the MSC-cultured keratinocytes create epidermis that is well differentiated and multi-layered (Ojeh and Navsaria, 2014). The study also indicated that MSCs have the ability to control the production of ECM by the expression of collagen. The accelerations of wound closure, enhanced re-epithelialisation, increased angiogenesis, moderation of inflammation, regulation of extracellular matrix remodelling and the promotion of granulation tissue formation, on MSCs administration has displayed many benefits on the healing of cutaneous wounds and the regeneration of skin. Paracrine signalling seems to mediate these beneficial effects (Lee *et al.*, 2012).

1.18 Uses method of analysis with chromatography

There are several types of chromatography techniques including thin layer chromatography, gas chromatography, supercritical fluid chromatography and, the focus of this section, high performance liquid chromatography (HPLC). The HPLC method is most often used to separate and determine pesticide residues in foods and other mixtures (Torres *et al.*, 1996). The analysis of a sample is carried out by separating the analytes using a sample mixture known as the mobile phase. The analytes interact within the HPLC column when high pressure is applied and the solution separates between the mobile phase and stationary phase. The solution separation that occurs varies depending on how the sample components interact and their affinity for the stationary and mobile phases. The separation will first occur with the component that has the least affinity for the chromatographic packing material, or stationary phase (Snyder *et al.*, 2012).

The general structure of the HPLC method includes a mobile phase reservoir, a high-pressure pump, injector system, stationary phase column, the detector and a data acquisition system (Figure 1.14). It is also possible to carry out reverse-phase HPLC using a specialised instrument, such as an Agilent Technologies integrated Agilent HP Series 1100 Liquid Chromatography equipment. This needs to be fitted with the necessary degasser, auto-injector, and a single channel as well as a 230nm tunable ultraviolet absorbance detector, in order to be effective. A sample is introduced to the HPLC analysis system using the injector, and this can be done automatically or by injection valves. The use of automated devices for injection is common, particularly in sophisticated systems that are used for the analysis of 100 samples or fewer. The core of any HPLC system is the column which is filled with chromatic packing material such as silica or polymer. This material is what is referred to as the stationary phase. The stationary phase material has regularly- shaped and -sized particles, and is necessary to effect separation. It is vital to the analysis as the particles help to retain neutral, ionic, polar and non-polar molecules within the column. The common chromatic packing material is silica, which offers great polar selectivity and has dominant areas for analyte interactions in the form of active adsorption sites of silanol (Si-O-H). Analyte detection is carried out by using a low detection level such as UV, fluorescence, mass spectrometry or diode array and a suitable detector. The most

extensively used low detection level in HPLC analysis is UV as it is cost-effective, and some compounds within the samples are able to absorb one or more wavelengths of light in the UV range. Conventionally, a UV detector can measure absorbance at just one wavelength, whereas a diode array detector (DAD) is able to measure absorbance at multiple wavelengths. A DAD is able to show the spectrum of sample components, providing more means of identification than when using one UV wavelength alone. When using UV, the absorption intensity by each component is recorded via an electronic signal that is generated for the chromatogram. The data system is then used to structure and show the collected data such as the peak area and retention time. The software optimises the development of the method by increasing the validation of accuracy and precision. The data software can also be used to make predictions as well as decisions to improve separation and the conditions of the analysis (Snyder *et al.*, 2012).

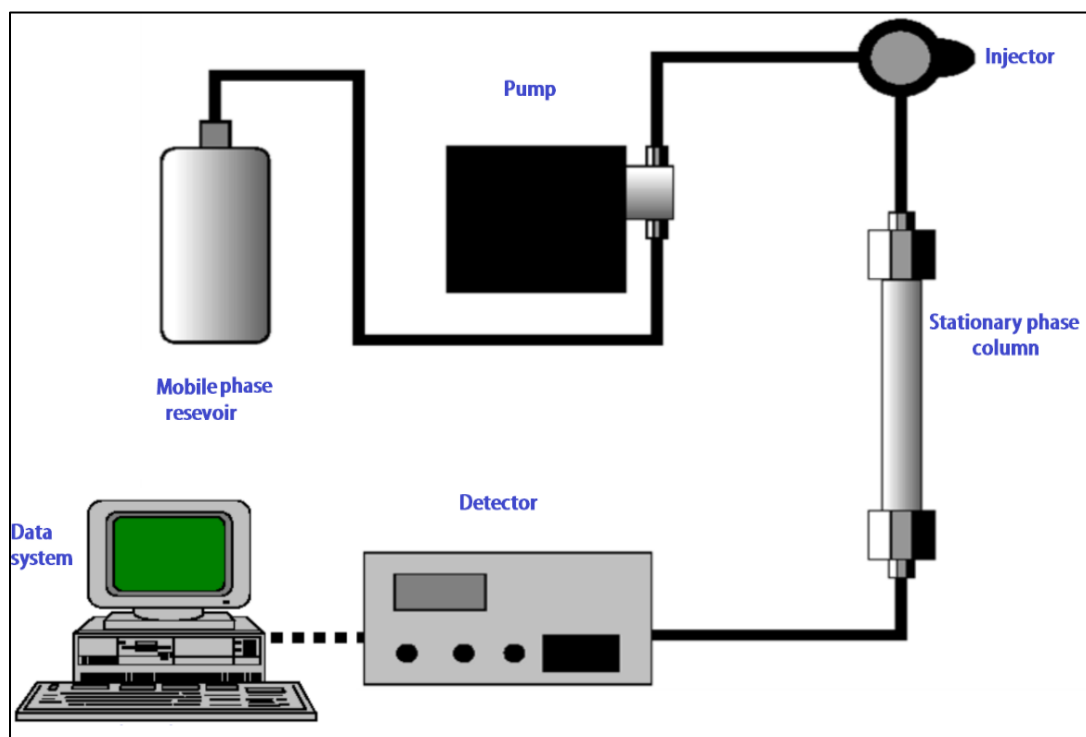


Figure 1.14: Diagram of the general structure of an HPLC system

1.18.1 Selection and developing of the chromatography method

There are multiple considerations to take into account when beginning method development. The analytical method is used to determine the target component within the sample so it is important to think about the analysis objective, the sample nature and the HPLC equipment that is available. The best-suited detector for the specific analysis also needs to be determined, for example, consideration of which component needs to be measured and whether a single detection method or qualitative analysis will be required (Snyder *et al.*, 2012). The chromatographic separation should start the method development process as it requires the selection of HPLC method and deciding the most suitable experimental conditions. There are many approaches to the method that are used, especially in modern analysis. Many now choose reverse-phase HPLC as the preferred method and this is increasingly being considered to be the best technique because of its reduced run-time and high resolution. Reverse-phase HPLC also offers the possibility of manipulating the conditions to reproduce retention time (Majors and Przybyciel, 2002). This tends to depend on the composition of the sample itself when deciding which chromatography technique is best suited. There are important factors that can affect the analysis, for example, column temperature which can influence on retention time, selectivity and peak separation, but the column temperature can cause problems too (Dolan, 2002). It is not just temperature that can have an impact on the separation and analysis efficiency, the size of the particles, length and mobile phase flow rate can also have an impact (Wang *et al.*, 2003; Snyder *et al.*, 2012).

1.19 Aims and objectives

The aims and objectives of this study were:

- To investigate and compare the ability of SAC/NAC (The key component of aged garlic extract) and synthesised compounds A, B and C mimics of SAC and NAC to inhibit the formation of methylglyoxal-derived AGE cross-links *in vitro*.
- To develop an HPLC method for the separation and quantification of NAC to test the effectiveness of drug loaded hADMSCs on wound healing *in vitro*.
- To examine the effect of SAC/NAC and compound A as well as SAC/NAC- and compound A-primed MSCs CM on angiogenesis *in vitro*

Chapter 2 – Materials and methods

2.1 Materials

- Acetic acid (Fisher Scientific International, Loughborough, UK)
- Acetonitrile (Fisher, St Louis, MO, USA)
- Acrodisc® 32mm syringe filter with 0.2 µm membrane (Pall Corporation, UK)
- Acrylamide/Bis solution (BIO-RAD, Hertfordshire, UK)
- Advanced glycation endproducts ELISA Kit (Human) (OKEH00348) (Aviva Systems Biology, San Diego, USA)
- Affinity Pak™ Detoxi-Gel™ endotoxin removing gel column (Thermo Scientific, USA)
- Ammonium persulphate, APS (Sigma-Aldrich, Heidelberg, UK)
- Antibiotics: Penicillin-Streptomycin solution containing L-glutamine (PSG) in 0.9% NaCl (Sigma-Aldrich, Heidelberg, UK)
- Anti-MG AGEs antibody, Rabbit polyclonal to AGEs antibody (Abcam, Cambridge, UK)
- Anti-Tubulin antibody, Mouse monoclonal to tubulin antibody (Abcam, Cambridge, UK)
- Bio-Rad protein assay Kit (Bio-Rad Laboratories, Hertfordshire, UK)
- Bovine aortic endothelial cells, secondary cell line (Cell and Molecular Biology Research Laboratory, Manchester Metropolitan University, UK)
- Bovine serum albumin, BSA (Sigma-Aldrich, Hertfordshire, UK)
- Bromophenol blue (Serva, Feinbiochemica, Heidelberg, Germany)
- Coomassie Brilliant Blue (BDH, UK)
- Cryotubes (Scientific Laboratory Supplies, UK)
- Cryovials (Nunc Corporation, Roskilde, Denmark)
- Deionised water (Local store, Manchester, UK)
- Detoxi-gel endotoxin removal columns (Thermo Scientific, USA)
- D-glucose (Sigma-Aldrich, Heidelberg, UK)
- Dialysis membrane (Medical International, UK)
- Dialysis tubes (Visking, UK)

- Digital multi-channel pipettes (Eppendorf, Germany)
- Dimethyl sulfoxide (DMSO) (Sigma-Aldrich, Heidelberg, UK)
- Dulbecco's Modified Eagle Medium (Sigma-Aldrich, Heidelberg, UK)
- Eppendorf tubes (Scientific Laboratory Supplies, UK)
- Ethanol (Fisher Scientific International, Loughborough, UK)
- E-toxic kit for endotoxin measurement (Sigma-Aldrich, Heidelberg, UK)
- Fibroblast growth factor-basic (FGF-2) (R & D Systems, USA)
- Foetal bovine serum (FBS) (Sigma-Aldrich, Heidelberg, UK)
- Glycerol (Sigma-Aldrich, Heidelberg, UK)
- Glycine (Sigma-Aldrich, Heidelberg, UK)
- Hydrochloric acid (Sigma-Aldrich, Heidelberg, UK)
- Isopropanol (Sigma-Aldrich, Heidelberg, UK)
- Liquid nitrogen (BOC Cryospeed Thermolyne, Surrey, UK)
- Lysozyme from chicken egg white (Sigma-Aldrich, Heidelberg, UK)
- Matrigel™ basement membrane reduced (Becton Dickinson, San Jose, UK)
- 2-Mercaptoethanol (Sigma-Aldrich, Heidelberg, UK)
- Methanol (Fisher Scientific International, Loughborough, UK)
- Methylene blue stain (Sigma-Aldrich, Heidelberg, UK)
- Methylglyoxal, MG (Sigma-Aldrich, Heidelberg, UK)
- N-acetyl-L-cysteine, NAC (Wakunaga Pharmaceutical Company, Japan)
- Nitrocellulose membrane (Scientific Laboratory Supplies, UK)
- N, N, N', N'-tetramethylethylenediamine (TEMED) (Sigma-Aldrich, Heidelberg, UK)
- Phosphate buffered saline, PBS (Lonza, USA)
- Pipette tips (Sarstedt AG & Co, Germany)
- Polyclonal Goat Anti-rabbit Immunoglobulin/Horseradish peroxidase, HRP (Dako, Glostrup, Denmark)
- Protein assay Kit (Bio-Rad Laboratories, Germany)
- Protein molecular weight marker for SDS – PAGE (Sigma-Aldrich, Heidelberg)
- Rabbit anti-Mouse (Murine) IgG (Dako, Glostrup, UK)
- Radioimmunoprecipitation assay buffer (Sigma-Aldrich, Heidelberg, UK)

- S-allyl cysteine, SAC (Wakunaga Pharmaceutical Company, Japan)
- Silver stain kit (BIO-RAD, California, USA)
- Six-well plates, polystyrene, flat bottom, sterile (Corning Life Sciences, USA, supplied by Fisher Scientific, UK)
- Skimmed milk powder (Local store, Manchester, UK)
- Sodium azide (Sigma-Aldrich, Heidelberg, UK)
- Sodium chloride, NaCl (Sigma-Aldrich, Heidelberg, UK)
- Sodium dodecyl sulfate, SDS (BDH, Poole, UK)
- Sodium phosphate dibasic (Sigma-Aldrich, Heidelberg, UK)
- Sodium phosphate monobasic (Sigma-Aldrich, Heidelberg, UK)
- Sterile bijoux (SLS, Nottingham, UK)
- Sterile needle (BD Plastipak, UK)
- Sterile universal containers (SLS, Nottingham, UK)
- Tissue culture flasks (T-25, and T-75) (Scientific Laboratory Supplies, UK)
- Tris (hydroxymethyl) methylamine (Fisher Scientific, UK)
- Trypan blue dye (Sigma, Heidelberg, UK)
- Trypsin 10X (Sigma-Aldrich, Heidelberg, UK)
- Tween- 20 (TBST) (Sigma-Aldrich, Heidelberg, UK)

2.2 Equipment

- Autoclaves (Lab Impex Research, UK)
- Automated Cell Counter TC10™ (Bio-Rad, California, USA)
- Autovortex mixer SA1 (Stuart Scientific Co, UK)
- Blotter (Semi-Phor, Hoefer Scientific Instrument, London, UK)
- Centrifuge (Eppendorf and Laborzentrifugen 3K10, Sigma, Hertfordshire, UK)
- ChemiDoc™ Touch Imaging System (Bio-Rad Laboratories Ltd, UK)
- CO₂ incubator (Lab Impax Research, London, UK)
- Electrophoresis unit Mini-Protean® 3 (Bio-Rad, California, USA)
- ELISA plate reader model 354 (Thermo Life Sciences, UK)
- Freezer -80°C (Juan Quality System, London, UK)

- Fridge (Scientific Laboratory Supplies, UK)
- Haemocytometer chamber (Weber Scientific International Ltd, UK)
- High performance liquid chromatography (HPLC) column (Zorbax Columns, PN, USA)
- Ice maker (Borolab Ltd, Abingdon, UK)
- Image J software analyser (free online software)
- Incubator model E4C (Phillip Harris, UK)
- Laminar flow hood tissue culture grade (Walker Safety Cabinets Ltd, London, UK)
- LTE IP 30 incubator (Scientific Laboratory Supplier, UK)
- Magnetic stirrer hotplate (Stuart Scientific Co, Abingdon, UK)
- Microplate reader, 96-well (Spectramax, Finland)
- Microscope (Nikon TMS)
- MiniRocker-Shaker, PMR30, (Grant-Bio, Cambridge, UK)
- PH meter AGB-75 (Medical Scientific Instruments, England)
- Pipettes 0.5-10, 2-20,100-200,100-1000 μ l (Scientific Laboratory Supplies Ltd, UK)
- Power supply PS-251-2 (Sigma-Aldrich, Heidelberg, UK)
- Sigma laboratory centrifuge 3K10 for cell culture use (Howe, Germany)
- Single threshold coulter counter (Beckman Coulter, UK)
- Spectrophotometer, Biochrom WPA Biowave II (Pharmaxia Biotech, Cambridge, UK)
- Trans-blot SD semi-dry transfer (Bio-Rad, California, USA)
- Water bath (Grant Instruments Ltd, UK)

2.3 Buffer solutions

- Ammonium persulphate (10%): 100mg APS was dissolved in 1ml of dH₂O. The solution was prepared and used fresh
- Blocking buffer (1%): 1g BSA was dissolved in 100ml of Tris-buffered-saline and Tween-20 (TBST). The pH was adjusted to 7.4 and the buffer was stored at 4°C for one week

- Destaining buffer: 250ml Methanol was dissolved in 70ml of acetic acid and the volume was made up to 1L with dH₂O. The buffer was stored at room temperature
- Electrophoresis buffer: 12.02g Tris-base, 4g SDS and 57.68g glycine were dissolved in 2 L of dH₂O. The buffer was stored at room temperature
- Milk (5%): 5.0g Skimmed milk powder was dissolved in 100ml of TBST buffer. The pH was adjusted to 7.4 and the solution was stored at 4°C for one week
- Radioimmunoprecipitation assay (RIPA) buffer: 50mM Tris-HCl, 0.25% (w/v) SDS, 1% Triton X-100, 0.15M NaCl, 1mM EDTA, 1% (w/v) sodium deoxycholate, 2.5mM sodium pyrophosphate, 1mM sodium orthovanadate, 1mM β-glycerophosphate, 1μg/ml pepstatin and 0.5mM PMSF, pH 7.2. The solution was stored at -20°C
- Reconstitution of FGF-2: Sterile phosphate-buffered saline was added to the vial in order to prepare a working stock solution (≥ 100g/ml). The carrier-free protein was immediately used upon reconstitution to avoid loss of activity
- Sample buffer: 1.5g Tris-base, 20ml glycerol, 4g SDS, 10ml 2-mercaptoethanol and 0.004g of bromophenol blue was dissolved in 100ml of dH₂O filtered and stored at -20°C. Prior to use, the pH was adjusted to 6.8
- Separation buffer: 45.5g Tris-base and 1g of SDS were dissolved in dH₂O. The pH was adjusted to 8.8 with HCl and made to the final volume of 250ml. The buffer was stored at room temperature
- Sodium phosphate buffer (0.1M, pH 7.4): the acid component of the buffer (sodium dihydrogen phosphate) and the basic component (sodium hydroxide) were weighed out in a certain ratio according to the Henderson Hasselbalch equation. The desired volume was then accordingly adjusted with dH₂O and the solution was mixed. The pH of the buffer was adjusted to 7.4. Sodium azide was added to the mixture to prevent any bacterial growth. The buffer was stored at 4°C

- Stacking buffer: 15g Tris-base and 1g of SDS were dissolved in dH₂O. The pH was adjusted to 6.8 with HCl and volume adjusted to 250ml. The buffer was stored at room temperature
- Staining buffer: 2.5g Coomassie brilliant blue was dissolved in 500ml methanol and 100ml acetic acid. The volume was made up to 1L with dH₂O and then filtered. The staining solution was stored at room temperature
- Towbin buffer: 1.51g Tris-base, 7.2g glycine, 0.167g SDS were dissolved in 400ml of dH₂O and 75ml methanol. The pH adjusted to 8.3 and volume adjusted to 50ml with dH₂O. The buffer was kept at room temperature
- Tracking dye buffer: 1mg Bromophenol blue was added to 0.1ml of glycerin and mixed with 0.9ml dH₂O
- Tris-buffered saline and Tween-20 (TBS-Tween) buffer: 2.422g Tris-base, 16.36g NaCl, and 2ml Tween 20 mixed and made up to 2L with dH₂O. The pH was adjusted to 7.4 with HCl and the buffer was kept at room temperature
- Treatment buffer: SDS (0.1g), and 0.1ml of 2-mercaptoethanol were added to 1 ml of stacking buffer (pH 6.8) and 2ml of glycerine and the volume was made up to 10ml with dH₂O

2.4 Methods

2.4.1 Methods for *in vitro* protein glycation

2.4.1.1 Preparation of AGEs

This methodology was described by Mashilipa et al. (2011). Briefly, BSA or lysozyme was incubated with 0.1M MG in sodium phosphate buffer (0.1M, pH 7.4) at 37°C for different time intervals (1 and 3 days). The prospective inhibitors SAC and NAC (provided by the Wakunaga Pharmaceutical Company, Japan), and mimic compounds A, B and C (chemically synthesised small molecule inhibitors which mimic of SAC/NAC, kindly supplied by Dr Alan Jones, Chemistry Dept., Manchester Metropolitan University, UK), were introduced into the incubation mixture simultaneously. BSA or lysozyme was incubated alone under the same

conditions as negative controls. All experiments were carried out in triplicate and repeated at least twice. The results represent one of the experiments.

2.4.1.2 Measurement of cross-linked AGEs using SDS – PAGE

Sodium dodecyl sulphate-polyacrylamide gel electrophoresis (SDS-PAGE) was used to determine the degree of cross-linking of glycated proteins. The Mini-Protean®³ apparatus (Bio-Rad, UK) was used to cast vertical slab gels and run SDS-PAGE. The cross-linking efficiency was assessed using 12% SDS-PAGE according to the method of Laemmli (Laemmli, 1970). The glass plate sandwiches were assembled with gaskets and clips in place. The acrylamide gel was prepared by mixing 3.3ml 40% bis-acrylamide with 4.8 ml dH₂O and 2.5ml separating buffer in a universal tube. 100µl 10% APS solution was added followed by 10µl TEMED solution. The 5ml of the resolving gel solution was added to the sandwich and a few drops of isopropanol were added on top of the gel, which was left to polymerise for 30 minutes. Isopropanol was washed off after the gel polymerised and rinsed with plenty of dH₂O (Table 2.1).

Table 2.1: Preparation of separating gel

Material	Volume
ddH ₂ O	4.2ml
40% Acrylamide	3.3ml
Separating buffer	2.5ml
10% APS	100µl
TEMED	10µl

The stacking gel solution was prepared in a fresh universal tube by combining 1.45ml 40% bis-acrylamide with 6.1ml dH₂O, and 2.5ml stacking buffer. 100µl APS was added followed by 10µl TEMED solution, 3ml of the stacking gel solution was added onto the top of the resolving gel. Combs was quickly inserted and allowed to polymerise for up to 30 minutes. The stacking gel was left to

polymerise for a minimum of 30 minutes. Slowly the combs, clamps, and gaskets were then removed taking care not to damage the wells, and the gel plates inserted into the electrophoresis chamber (Table 2.2).

Table 2.2: Preparation of stacking gel

Material	Volume
ddH ₂ O	6.1ml
40% Acrylamide	1.4ml
Stacking buffer	2.5ml
10% APS	100 μ l
TEMED	10 μ l

The chamber was subsequently filled with electrode buffer. A total of 500ml electrode buffer was used to fill the tank. 1 μ l of glycosylated protein was mixed with 9 μ l of treatment buffer and blocked at 100°C for 10 minutes. Protein marker was loaded into the first well of each gel and 3 μ l tracking dye loaded in the rest of the wells. Then, 10 μ l of the appropriate sample was loaded to the rest of the wells. Electrophoresis was carried out at 65V until the blue band reached the separating gel (approximately after 45 minutes). Then the voltage was increased to 200V and run for further approximately 60 minutes. After running, the gels were stained with Coomassie Brilliant Blue staining or silver staining to detect the proteins.

2.4.1.3 Coomassie Brilliant Blue staining

After electrophoresis, the running buffer was discarded, and the gels were removed from the gel cassette sandwiches. Gels were stained for two hours in a staining buffer containing 0.25% (w/v) Coomassie blue R, 10% (v/v) acetic acid and 50% (v/v) methanol. After two hours of staining, gels were de-stained in a de-staining buffer, containing 25% (v/v) methanol and 7% (v/v) acetic acid. The de-

staining buffer was changed several times with fresh de-staining solution until the gel was clear.

2.4.1.4 Silver stain

Following SDS-PAGE, silver staining was carried out according to the manufacturer's recommendations using the silver stain kit from Bio-Rad. Briefly, the gel was fixed with gentle agitation in a solution of 40% (v/v) methanol, 10% (v/v) acetic acid and 50% dH₂O (v/v) fixative enhancer concentrate for 30 minutes minimum. Pour the fixative and add 10% (v/v) Oxidizer with 90% dH₂O (v/v) for 5 minutes. After decanting the oxidiser solution, the gel was rinsed in 400ml deionised dH₂O for 15 minutes with three changes of water after every 10 minutes. Then, the gels were incubated in 10% silver reagent for 20 minutes and rinsed quickly with water for a maximum of 30 seconds. The gel was then stained in the staining and developing solution for 30 seconds or until a brown or smoky precipitate appeared. The solution was quickly poured off and fresh developer added until the desired intensity was obtained. The staining reaction was stopped by placing the gel in a 5% (v/v) solution of acetic acid. This was followed by rinsing the gel in deionised dH₂O for 5 minutes.

2.4.1.5 Preparation of bovine serum albumin-derived advanced glycation end products (BSA-AGEs)

Bovine serum albumin (10mg/ml) was incubated with 0.5M glucose in 0.1M sodium phosphate buffer containing 3mM sodium azide, pH 7.4 at 37°C for four weeks. The glycated albumin was subsequently extensively dialysed with dH₂O at 4°C. Endotoxin was removed by using Detoxi-Gel resin columns according to the method described below. The formation of BSA-AGEs was assessed by their characteristic fluorescence emission spectra at 420nm after excitation at 350nm using a luminescence spectrometer. Prior to the addition to cell cultures, BSA-AGEs were dissolved in DMEM and were filtered through a sterile 0.2µm filter.

2.4.1.6 Endotoxin removal from BSA-AGEs

Endotoxins were removed from the dialysed BSA-AGE samples using the Detoxi-Gel endotoxin removing gel. The Detoxi-Gel resin column underwent regeneration through wash cycles with five resin-bed volumes using 1% sodium deoxycholate and basal media. BSA-AGEs were added to and were allowed to run into, the column. The flow of the column was stopped when the AGE sample filled the resin-bed from top to bottom. Following this, incubation was carried out for 2 hr at room temperature prior to samples being collected. In an attempt to achieve greater efficiency with a gravity-flow column, the samples emerged from the column after the void volume was collected.

2.4.1.7 Determination of endotoxin content in BSA-AGE solutions

Bovine serum albumin-derived advanced glycation end product samples were analysed to detect the remaining Endotoxin content using an E-toxic kit (Sigma, UK). Samples, water and endotoxin standards (100µl) were added to the endotoxin-free glass test tubes. Subsequently, E-toxic working solution (100µl) was added to each tube by inserting a pipette to just above the contents, and the lysate was then allowed to flow down the side of the tube. The tubes were mixed gently and covered with Parafilm and incubated for 1 hour at 37°C. Following incubation, the tubes were gently inverted 180 degrees and observed for evidence of gelation. The formation of a hard gel was considered to be a positive test. All other results including soft gels, turbidity, and increased viscosity or clear liquid were considered to be negative. Notably, the amount of endotoxin level (EU/ml) was calculated using the following formula:

Endotoxin (EU/ml) = $1 / (\text{Highest dilution of sample found positive} \times \text{Lowest concentration of Endotoxin standard found positive})$

2.4.1.8 Glycated protein dialysis

To remove unbound sugars (glucose or MG) before the protein assay, glycated proteins were subjected to extensive dialysis against dH₂O by making a tight knot at one end of the tubing. Protein samples were delivered into the dialysis tubing

and then the other end of the tube was closed carefully. The dialysis bag was placed into a 2litre beaker containing dH₂O. A few drops of chloroform were added to prevent any contamination. Dialysis was carried out by stirring the samples at 4°C with 4 - 5 changes over two days until equilibrium was reached. At the end of dialysis, the dialysed samples were transferred into clean tubes and stored at -20°C until used.

2.4.1.9 Imaging SDS-PAGE gels

The gels were photographed using a ChemiDoc™ Touch Imaging System (Bio-Rad, UK). All the bands were compared within the same gel. Integrated Density (I.D) was measured to analyse the one-dimensional electrophoretic gels and computed using the following formula:

Integrated Density = N x (mean – background)

Where N is the number of pixels in the selection and the background is the modal grey value (most common pixel value) after smoothing the histogram. Sufficient background was included in the selection to avoid errors.

2.4.1.10 Percentage inhibition of cross-linked AGEs

This was calculated using the following formula:

$$100(\text{I.D without inhibitor} - \text{I.D with inhibitor}) / \text{I.D without inhibitor}.$$

2.4.1.11 Measurements of fluorescent AGEs

The formation of AGEs was assessed by their characteristic fluorescence emission spectra at 460nm after excitation at 350nm using a fluorescence plate reader (Thermo Life Sciences, UK) operating at room temperature. Glycated samples were thawed at 4°C and each sample was diluted in 1.8ml of dH₂O to give a solution with a final concentration of 1mg/ml. Fluorescent measurements were carried out on a plate reader. Fluorescence intensity standards were used to the manufacturer's protocol. Sodium phosphate buffer was used to calibrate the instrument and monitor its performance. A water blank was used to zero the

instrument. Fluorescence of AGE was expressed in arbitrary units (AU) per mg of protein.

2.4.1.12 Measurement of cross-linked AGE by Western blotting

The glycated proteins (AGEs) were separated using 12% SDS-PAGE, and the proteins were transferred to a nitrocellulose membrane (NCM) according to the method described previously (Towbin *et al.*, 1979). After blotting, the membrane was blocked for 1 hour in blocking buffer (1% BSA, w/v) on a shaker at room temperature. Then, the membrane was incubated with primary antibody (rabbit anti-AGE antibody, at 1:1000 dilution in 1% BSA, w/v) on a shaker at 4°C overnight. The following day, the membrane was washed five times with TBST buffer on a shaker at room temperature for 10 minutes per wash. The membrane was then incubated with a secondary antibody [Polyclonal Goat anti-Rabbit IgG-horseradish peroxidase (HRP)] diluted in 5% (w/v) milk solution (1:2000) and incubated for 1 hour on a shaker at room temperature. After one hour, the secondary antibody was discarded, and the membrane was washed five times for 10 minutes each wash in new changes of TBST buffer. The glycated proteins were then detected by using the enhanced chemiluminescence (ECL) solution and photographed using a ChemiDoc™ Touch Imaging System for image analysis.

2.4.1.13 Measurement of AGEs using ELISA

For rapid detection and quantification of AGEs, enzyme-linked immunosorbent assay (ELISA) was performed using an Aviva Systems Biology AGE ELISA kit (Human). Briefly, a series of BSA-AGE standards were prepared as showed in table 2.3. Glycated-BSA samples were diluted to 10µg/ml in sample diluent. To each well of a 96-well plate, 100µl sample and the standards were incubated in duplicate for 2 hours at 37°C. After incubation, the samples and the standards were discarded and the wells were washed with 300µl of 1× washing buffer. Then 100µl of 1× Biotinylated AGEs detector antibody was added to each well and incubated at 37°C for 60 minutes. After that, the liquids from each well were discarded, and the wells washed three times with 300µl of 1× washing buffer. A 100µl of 1× Avidin-HRP conjugate was added to each well and incubated for 1 hour at 37°C.

After that, the wells were washed 5 times with 300µl of 1× washing buffer, then 90µl of TMB substrate solution added and incubated at 37°C for up to 30 minutes. The enzymatic reaction was stopped by adding 50µl of stop solution to the wells, and the absorbance at 450nm measured using a microplate reader (Lin *et al.*, 2002). Table 2.3 shows the volume of the standard to dilute the buffer.

Table 2.3: Volume of the standard to dilute and sample diluent buffer required to establish the standard curve

Standard Number	Standard to Dilute	Volume of Standard to Dilute (µl)	Volume of Sample Diluent Buffer (µl)	Total Volume (µl)	Final Concentration
1	50,000 pg/ml Reconstituted AGE standard	600	0	600	50,000 pg/ml
2	50,000 pg/ml	300	300	600	25,000 pg/ml
3	25,000 pg/ml	300	300	600	12,500 pg/ml
4	12,500 pg/ml	300	300	600	6,250 pg/ml
5	6,250 pg/ml	300	300	600	3,125 pg/ml
6	3,125 pg/ml	300	300	600	1,650 pg/ml
7	1,560 pg/ml	300	300	600	780 pg/ml
8	NA	0	300	300	0

2.4.2 Methods for cell culture techniques

All cell culture experiments were carried out in a sterile environment and performed in a Class II microbiological safety cabinet (Labcaire SC-R Recirculating Class II, North Somerset, UK). Ethanol [70% volume/volume (v/v) in dH₂O] was used for cleaning all surface before commencing work. Only sterile

plastics were used, and all media were pre-warmed by placing them in a 37 °C water bath for 30 minutes before use. All cell incubations were performed in a Nuaire DH Autoflow CO₂ Air-Jacketed Incubator (Triple Red Laboratory Technology, Buckinghamshire, UK). Liquid, media and supernatants were discarded using an aspirator (IBS Integra Biosciences Vacusafe Comfort, Chur, Switzerland). All solutions used for cell culture were prepared with H₂O from an Elgastat option 4 water purifier (Elga Ltd., High Wycombe, UK).

2.4.2.1 Preparation of cell culture medium for BAECs

Pre-warmed sterile FBS was de-complemented at 65 – 70°C for approximately 45 min and other reagents were mixed as described below (Table 2.4).

Table 2.4: Preparation of cell culture medium supplemented with 0.1 – 15% of FBS

Reagents	0.1% FBS	0.5% FBS	2.5% FBS	10% FBS
DMEM	98.9ml	98.5ml	96.5ml	89ml
FBS	0.1ml	0.5ml	2.5ml	10ml
PSG	1ml	1ml	1ml	1ml

2.4.2.2 Cell culture techniques for BAECs

Bovine aortic endothelial cells were obtained from Dr Sabina Matou (Manchester Metropolitan University) and previously characterised as EC by the presence of the Von Willebrand factor. They were seeded into T-75 flasks and cultured in DMEM medium composed of 10% (v/v) FBS, 2mM L-glutamine and 1% antibiotics (100U/ml penicillin and 100µg/ml streptomycin). The culture flasks were maintained at 37°C in a dH₂O humidified atmosphere of 95% air and 5% CO₂-incubator. Following confluence, the cells were subcultured at 1:3 split and cultured in fresh flasks or frozen in liquid nitrogen for later use. Passage numbers between 4 – 12 were used for the experiments.

2.4.2.3 Sub-culture of BAECs

Bovine aortic endothelial cells ($1.5 \times 10^5 - 5 \times 10^5$) were seeded in T-75 flasks with 12ml of growth medium (10% FBS DMEM, v/v) and incubated in a dH₂O humidified atmosphere of 95% air and 5% CO₂-incubator for 24 hours. The growth medium was changed every three days. Upon reaching confluence, the growth medium was discarded from the T-75 flask. Then, the cells were washed with 10ml of sterile, warm PBS three times and incubated with 5ml of 1× trypsin solution for 5 minutes at 37°C. When the cells were detached (with a brief check under the phase contrast microscope), 5ml of growth medium was immediately added to the flask to stop the trypsinisation. The cell suspension was centrifuged at 200 5 minutes at room temperature. After discarding the supernatant, the cell pellet was re-suspended in 1 ml fresh growth medium, and then split at a ratio of 1:3 before being seeded in fresh T-75 flasks, which corresponded to a new passage.

2.4.2.4 Preparation of freezing medium

The freezing medium was composed of 90% FBS and 10% dimethyl sulfoxide (DMSO), a cryo-protector agent. Briefly, 1ml of DMSO in 9ml of FBS were mixed and kept at -20°C until use. The fresh freezing medium was prepared or defrosted shortly before use.

2.4.2.5 Freezing of cells

The trypsinised cells taken from the flask were centrifuged at 300×g for 5 minutes; the supernatant was then removed, and the cell pellet was re-suspended in 250 µL of complete medium with the addition of 750 µL of 10% (v/v) DMSO (freezing medium). One ml of the medium containing approximately 2.5×10^6 of cells was kept in a 1.5ml cryovial labelled with the cell passage, number and date. Cryovials containing cells were kept at -20°C for 30 minutes. then the cryovial was transferred into a -80°C freezer overnight. After 24 hours, the cryovial was transferred to liquid nitrogen (-190°C) and the location was recorded.

2.4.2.6 Thawing of cells

A cryo-tube containing the frozen BAECs were taken out from liquid nitrogen and decontaminated by spraying with 70% (v/v) ethanol. During the thawing process, the cells were defrosted at 37°C under sterile conditions until liquid but still cold to prevent any cell toxicity effect of the DMSO. The cells were re-suspended in 1 ml of warm, fresh complete medium. Subsequently, the cells were seeded in a T-25 flask and incubated at 37°C in a humidified atmosphere of 95% air and 5% CO₂ incubator.

2.4.2.7 Cell counting

A TC10™ automated cell counter (Bio-Rad, UK) was used for counting the cells. From sub-culturing of BAECs, 20µl of 1ml cell suspension was added into an Eppendorf tube containing 20µl of trypan blue dye. The sample was then loaded onto a dual-chamber slide. The slide was inserted into the TC10 cell counter and the counting of the cells automatically started. As a final point, the total cell count was obtained from the screen.

2.4.2.8 Protein extraction

BAECs (2×10^5 /ml) were seeded in complete medium in a 6-well plate (Corning Life Sciences, USA) (2ml /well), together with various concentrations of MG (300µM), alone and together with the SAC/NAC, and compound A (0.001µg/ml, 0.01µg/ml, 0.05µg/ml, 0.1µg/ml, 0.5µg/ml, 1µg/ml and 2µg/ml) and incubated at 37°C in a humidified atmosphere of 95% air and 5% CO₂ incubator. After 3 days incubation, the medium was discarded, and the cells were washed with cold PBS three times. Ice-cold RIPA buffer (300µl) was added to lyse the cells. The plate was put on ice for one minute, and the cells were scraped using a cell scraper. The cell lysate was collected and transferred into a 0.5ml microcentrifuge tube and incubated on ice for 20 minutes. Then, protein samples were stored at -20°C for later use.

2.4.2.9 Protein estimation

The protein concentration was determined using protein assay (Bio-Rad Laboratories, Germany). Briefly, 10 μ l of protein sample was added and completed with 90 μ l of dH₂O in a bijou. After that, 2ml of Bio-Rad protein assay (1:4 dilution) was added in each bijou. A standard curve was prepared by BSA at 1mg/ml as a standard protein and measured by the absorbance at 595nm. The data outlining the reading of each protein sample and the standard curve required for protein estimation are shown in Table 2.5.

Table 2.5: The volume of BSA, dH₂O and Bio-Rad solution required to establish the standard curve

BSA Standard (μ g)	BSA volume added (1μ g/ μ l)	Volume of dH ₂ O (μ l)	Volume of diluted Bio-Rad reagent (ml)
0	0	100	2
5	5	95	2
10	10	90	2
20	20	80	2
40	40	60	2

2.4.2.10 Cell migration – wound healing assay

Thermanox plastic coverslips (Nunc™) were placed into each well of a 24-well plate. Approximately, 6×10^4 BAECs /ml were added to each well in complete growth medium (15% FBS) and incubated for 24 – 48 hours. When confluence was attained, the medium was then replaced with DMEM containing 0.1% (v/v) FBS and the cells were then incubated for a further 24 – 48 hours. After removing the medium, cells were pre-incubated with Mitomycin C (10 μ g/ml) for 3hrs to arrest the proliferation phase. Coverslips containing cells were washed with warm PBS (3 – 4 times) and the wound was made using a sterile razor blade to produce straight-edged cuts. The wounded cell monolayer was washed with warm sterile

PBS three times in order to remove cellular debris and dislodged cells, then placed in a fresh 24-well plate containing serum- poor medium (SPM) (0.1% (v/v) FBS). Different concentrations of glucose, BSA-AGEs, SAC/NAC and compound A were applied respectively and incubated for a further 24 hours. Untreated cells in SPM were used as controls. Cells treated with FGF-2 (25ng/ml) were used as positive controls. After 24 hours of incubation, the coverslips were rinsed 3 times in PBS, fixed in 100% ethanol for 5 mins, then the ethanol was removed, and subsequently, the wells allowed to dry at room temperature. The cells were stained with methylene blue for 1 minute before being washed with dH₂O and left to dry at room temperature. Finally, the cells were examined under the microscope and pictures were taken using phase contrast microscopy (10× magnification) for 5 random areas of each coverslip. The picture analysis was performed using Image-J software.

2.4.2.11 Matrigel™ tube formation assay

A tube formation assay was performed in order to assess the ability of BAECs to form vascular structures, which are important in new vessel formation. One day, prior to performing the assay, a matrigel matrix was incubated on ice overnight. On the day of the assay, a 96-well plate was coated with 50µl of growth factor-reduced Matrigel™ and incubated at 37°C for 1 hour. BAECs (8×10³cells) were mixed respectively in 50µl of medium ± different concentrations of inhibitor (glucose, BSA-AGEs, SAC/NAC and compound A), and 500µl of growth medium (15% FBS, v/v) were added in order to cover each cell/matrigel spot. Cells containing FGF-2 (25ng/ml) were used as positive controls. After 7 hours incubation, 4% (v/v) paraformaldehyde (PFA) was added to fix the endothelial tube-like structures in the well. Under an optical microscope (10 × magnification), closed areas surrounded by endothelial tube-like structures were counted in 3 - 5 areas from each well.

2.4.2.12 Preparation of cell growth medium for human adipose-derived mesenchymal stem cells (hADMSCs)

Human adipose-derived mesenchymal stem cells (hADMSCs) were kindly

provided by Professor Giulio Alessandri and Professor Valentina Cocce (Istituto Neurologico "Carlo Besta"). Resume the cells from liquid nitrogen and put the cells in a T-25 flask containing 5 ml stem cell growth media (SCM) and incubated for 4 hours. Then, the medium was changed with the fresh growth medium. Cells were grown in SCM composed of 80% Iscove's modified Dulbecco's medium (IMDM; Sigma-Aldrich) containing 5% foetal bovine serum (FBS; Sigma-Aldrich), 10% NeuroCult medium (Stem Cell Technologies) and 10% endothelial basal medium (EBM; Lonza) in a humidified incubator with 5% CO₂ at 37°C.

2.4.2.13 Subculture of stem cells MSCs

When cells reached confluency, MSCs was performed using Trypsin-EDTA (0.25% Trypsin, 0.02% EDTA; Sigma-Aldrich) for 5 minutes at 37°C in the incubator. Once the cells were detached, 5ml of growth medium was added to inactivate the enzyme reaction and then the Trypsin-EDTA solution with the cell suspension was transferred into a centrifuge tube. The flask was rinsed out with 3 – 5ml of PBS and that was transferred into the same centrifuge tube (Jouan CR422). This minimised cell loss. The cell suspension was then centrifuged at 300×g for 5 minutes. The supernatant was discarded leaving behind 200 – 500µl supernatant to re-suspend the cells and then split at a ratio of 1:3 before seeded in fresh T-75 flasks, which corresponded to a new passage.

2.4.2.14 Cytotoxicity of the compounds on hADMSCs

The toxicity of SAC/NAC and compound A on hADMSCs was determined in a 24-hour alamarBlue assay (cytotoxicity test; Life Technologies). Briefly, 96-well plates containing cells in growth medium were set up. Sub-confluent cultures (2×10^5 /ml) of hADMSCs were exposed to different concentrations of SAC/NAC (0.0076 – 500µg/ml) and compound A (0.12 – 250µg/ml) and the final volume was made up to 100µl in each well. After a 24-hour incubation, 20µl/well of Cell Titer-Blue® Reagent was added. The cells were incubated for a further 4 hours. then, fluorescence emission spectra were recorded at 560nm after excitation at 590nm.

2.4.3 High performance liquid chromatography (HPLC) analysis

The flow rate was 1.0 ml/min (using LC-FC-B) with an injection volume of 1 μ l. The fluorimeter was operated at an excitation wavelength of 330nm and an emission wavelength of 380nm. The stationary phase (Eclipsex DB. C18, 4.6mm \times 25cm, particle size: 3 μ m) used in the study was obtained from HiChrom Limited (Reading, UK). The column was fitted with a guard cartridge (ACE 3 C18) and maintained at an isothermal temperature of 22 $^{\circ}$ C with an Agilent HP Series 1100 column oven with a programmable controller (Agilent Technologies, Wokingham, UK). Detection of the analyte was performed using a suitable detector. In this study, a diode array detector (DAD), which can measure the absorbance at several wavelengths, was used (λ ex = 330nm and λ em = 376nm).

2.4.3.1 Preparation of the mobile phase

The mobile phase for HPLC analysis was prepared from the organic solvent of water-acetonitrile (50:50, v/v) and was adjusted to a pH of 3.75 through the addition of 0.1ml of acetic and phosphoric acids. The N-(1-pyrenyl) maleimide (NPM) derivatives were eluted from the column isocratically at a flow-rate of 0.45ml/min. The water used for the preparation of the mobile phase was supplied from an Elga Purelab Option deioniser model LA613.

2.4.3.2 Preparation of calibration solution

For calibration studies, a calibration standard stock solution of NAC (500 μ g/ml) was weighed accurately into a 10.0ml clear glass volumetric flask and diluted to volume with dH₂O to give a solution containing the components at 1mg/ml. This solution was then further diluted with dH₂O to prepare the diluted calibration standard working solutions (500, 400, 300, 200 and 100 μ g/ml) of each analyte in a volume of μ l.

2.4.3.3 Sample preparation and derivatisation

Conditioned medium from hADMSCs was derivatised with NPM, which reacts with free sulfhydryl groups to form fluorescent derivatives. Acetonitrile (250 μ l)

and 500 μ l of 1.5mM NPM solution in acetonitrile were added to diluted samples (250 μ l). The resulting solution was mixed and then incubated at room temperature for 5 min. At the conclusion of the incubation period, 10 μ l of 50% (v/v) acetic acid was added to stop the reaction. Filtration through a 0.2 μ m acrodisc was performed and the derivatised samples were injected onto a 3 μ m C18 column in a reversed-phase HPLC system (Figure 2.1).

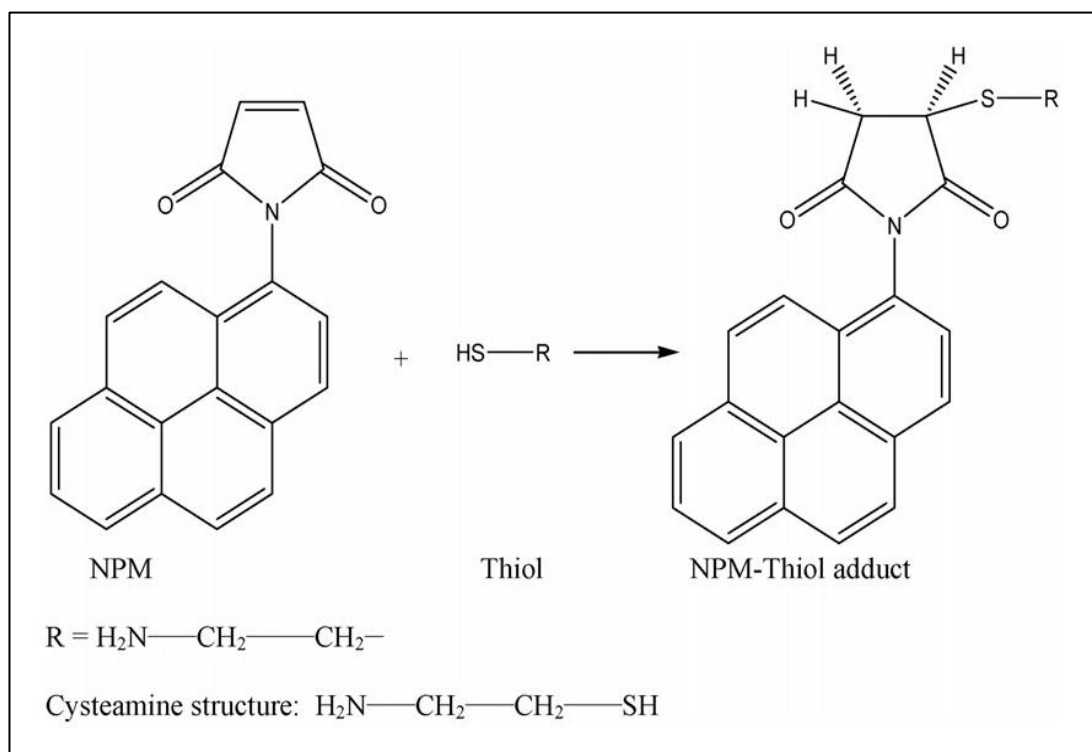


Figure 2.1: Reaction of NPM with thiols to form fluorescent adducts.
(Ogony *et al.*, 2006).

2.5 Statistical analysis

Data was reported as the mean \pm standard deviation (SD). Students t-test was performed to test the statistical significance. Values were considered significant with a p-value below 0.005. All the values (mean, SD and p-value) were calculated using Microsoft[®] Excel 2016. Statistical significance between groups was tested by *t*-tests and one-way analysis of variance (one-way ANOVA). The analysis was performed by the statistical package IBM SPSS Statistics for Windows, version 22.0 (IBM).

Chapter 3 – Results

3.1 AGE formation of lysozyme induced by MG

3.1.1 Lysozyme glycation by MG after 24 hours

After 1 day of incubation, glycation of lysozyme by MG produced cross-linked AGEs and the formation of dimers with an approximate molecular weight of 28.7 kDa, as indicated by the protein marker ladder shown in Figure 3.1, lane 1. Compare to lysozyme control (Figure 3.1, lane 2), the effect of MG on cross-linked AGE formation is clearly visible by their ability to reduce electrophoretic mobility in a dose-dependent manner (Figure 3.1, lanes 3-6).

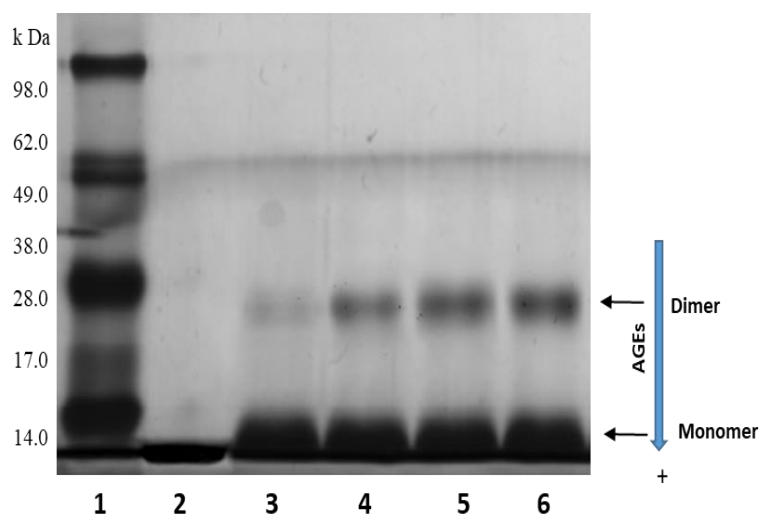


Figure 3.1: SDS-PAGE gel showing lysozyme glycation by MG after 24 hours.

Gel showing lysozyme (10mg/ml) with or without MG. Molecular Weight Marker (lane 1), lysozyme incubated alone (lane 2) or in the presence of MG, 40mM (lane 3), 60mM (lane 4), 80mM (lane 5) and 100mM (lane 6), respectively. The gel shows evidence of dimer formation caused by protein cross-linking in 0.1M sodium phosphate buffer the pH 7.4 at 37 °C for 24 hours. The cross-linked AGEs were analysed using SDS-PAGE and stained with silver stain. The results shown here are representative of three independent experiments.

Image analysis of the gel was performed, and the results based on the integrated density of each band are presented in Figure 3.2. MG (40 - 100mM). After 1 day of incubation with MG, the formation of cross-linked AGEs was evident and occurred in a dose-dependent manner. Glycation of 10mg/ml lysozyme by MG at 60mM caused significant ($p < 0.05$) production of AGE dimers while at 80 - 100mM caused significant ($p < 0.01$) production of AGE dimers compared to the lysozyme control.

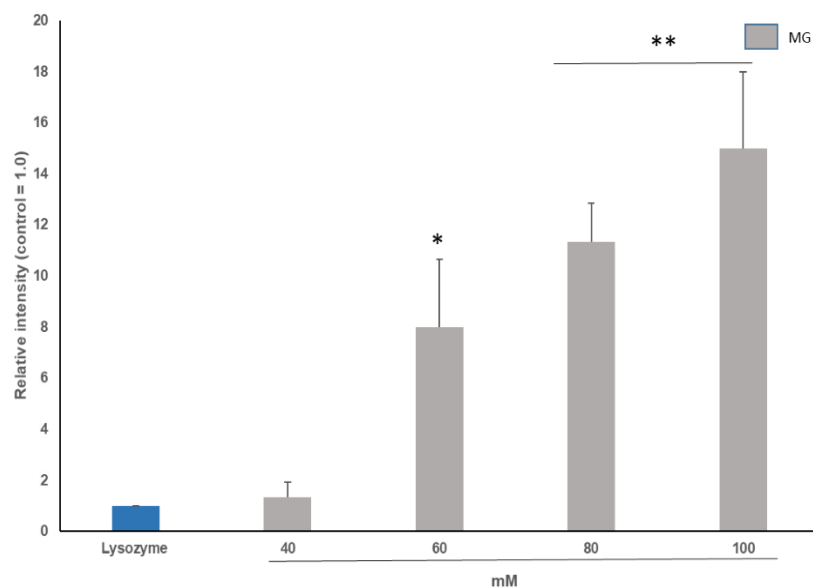


Figure 3.2: Lysozyme glycated by different concentrations of MG after 24 hours.

Bar chart showing evidence of dimer formation with an increased band density of lysozyme glycated by MG (40 - 100mM) compared to control (=1.0). Each value represents the mean \pm SD (n = 3), * $p < 0.05$ and ** $p < 0.01$.

3.1.2 Lysozyme glycation by MG after 72 hours

After three days of incubation, glycation of lysozyme by MG produced cross-linked AGEs and the formation of dimers and trimer bands as indicated by comparison with the protein marker ladder shown in Figure 3.3, lane 1. Compare to lysozyme control (Figure 3.3, lane 2), glycated lysozyme (Figure 3.3, lanes 3 - 6) showed reduced electrophoretic mobility with an increased intensity of the dimer bands of approximate molecular weight of 28.7 kDa at a concentration of 100mM in a dose-dependent manner.

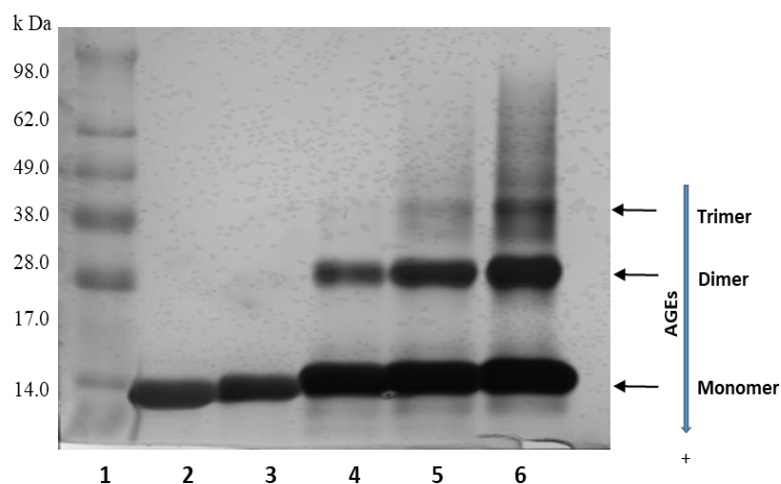


Figure 3.3: SDS-PAGE gel showing lysozyme glycation by MG after 72 hours.

Gel showing lysozyme (10mg/ml) with or without MG. Molecular Weight Marker (lane 1), lysozyme incubated alone (lane 2) or in the presence of MG, 40mM (lane 3), 60mM (lane 4), 80mM (lane 5) and 100mM (lane 6), respectively, and showing evidence of dimer and trimer formation caused by protein cross-linking in 0.1M sodium phosphate buffer pH 7.4 at 37 °C for 72 hours. The cross-linked AGEs were analysed using SDS-PAGE and stained with silver stain. The results shown here are representative of three independent experiments.

Figure 3.4 shows that glycation of 10mg/ml lysozyme by MG (60 - 80mM) caused a significant ($p < 0.01$) production of AGEs compared to the lysozyme control. In addition, at a concentration of 100mM, there was significant ($p < 0.001$) inhibition of dimers cross-linked AGE formation. The cross-linked AGE production was more than 14-fold greater when lysozyme was incubated with 100mM MG as compared to 40mM MG.

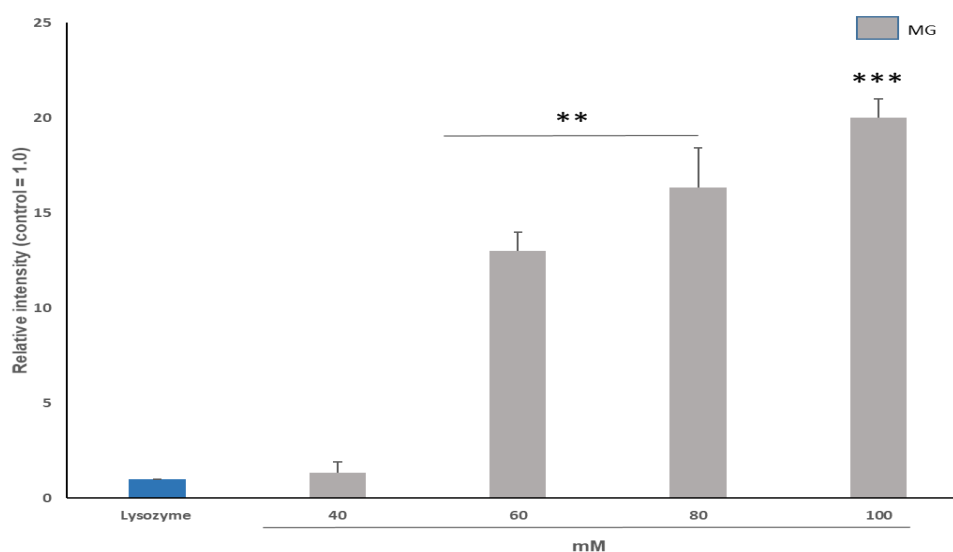


Figure 3.4: Lysozyme glycated by MG after 72 hours.

Bar chart showing evidence of dimer formation with an increased band density of lysozyme glycated by MG (40 - 100mM) compared to control (=1.0). Each value represents the mean \pm SD (n = 3), ** $p < 0.01$ and *** $p < 0.001$.

3.2 Detection of AGEs

3.2.1 Detection of AGEs by fluorescence

Fluorescence modifications were investigated as an index of alterations in protein structure and conformation. The effect of MG (0 – 10mM) on fluorescent AGE production over 72 hours of lysozyme glycation was determined from the specific fluorescence intensity. Lysozyme alone was used as the reference compound at a concentration of 10mg/ml. In contrast with the control, the fluorescent intensity of lysozyme incubated with MG showed a significant increase ($p < 0.05$). The results show that AGE production increased in a dose-dependent manner. The effect determined for lysozyme incubated for 3 days with 10mM MG was more than twenty-fold greater as compared to control and two-fold greater than the effect observed with 1mM MG (Figure 3.5).

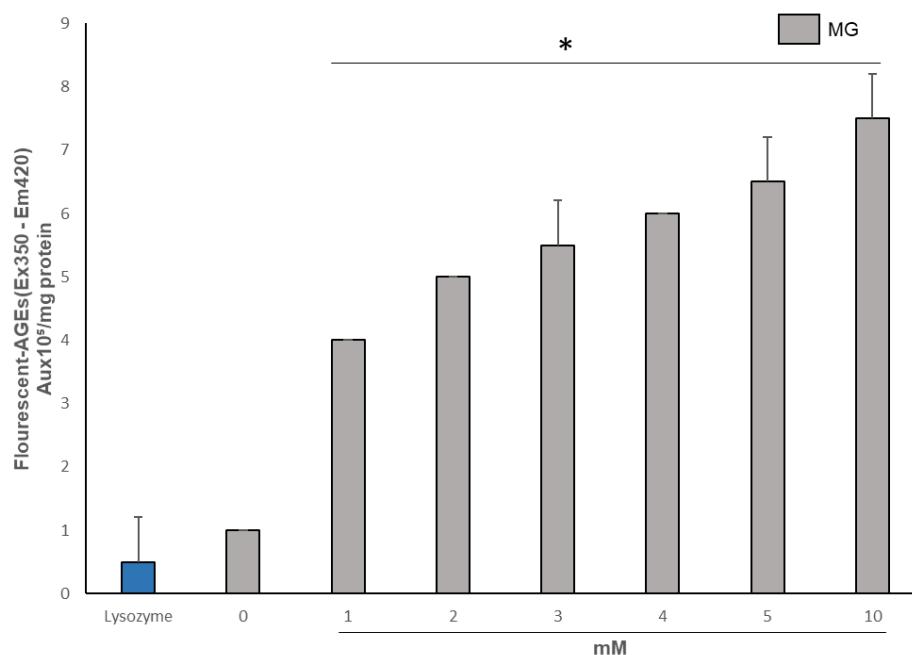


Figure 3.5: Effect of MG on fluorescent AGE formation.

Lysozyme (10mg/ml) was incubated with or without of MG (0 -10mM) in 0.1M sodium phosphate buffer pH 7.4 at 37°C for 72hours. Each value represents the mean \pm SD (n = 3), *p<0.05.

3.2.2 Detection of AGEs by SDS-PAGE-silver stain

3.2.2.1 The effect of SAC on MG-derived AGE formation

Glycation of lysozyme by MG produces cross-linked AGEs and the formation of dimers bands as indicated by comparison with the protein ladder. Glycated lysozyme (Figure 3.6, lane 3) was used as the control and clearly showed reduced electrophoretic mobility with higher molecular weight compared with native lysozyme (Figure 3.6, lane 2). The molecular weight of glycated lysozyme was approximately twice that of the original lysozyme as determined by protein molecular ladder (Figure 3.6, lane 1). SAC inhibited AGE formation causing a reduction in the intensity of the dimerised lysozyme band of approximate molecular weight of 28.7 kDa (Figure 3.6, lanes 4 – 10).

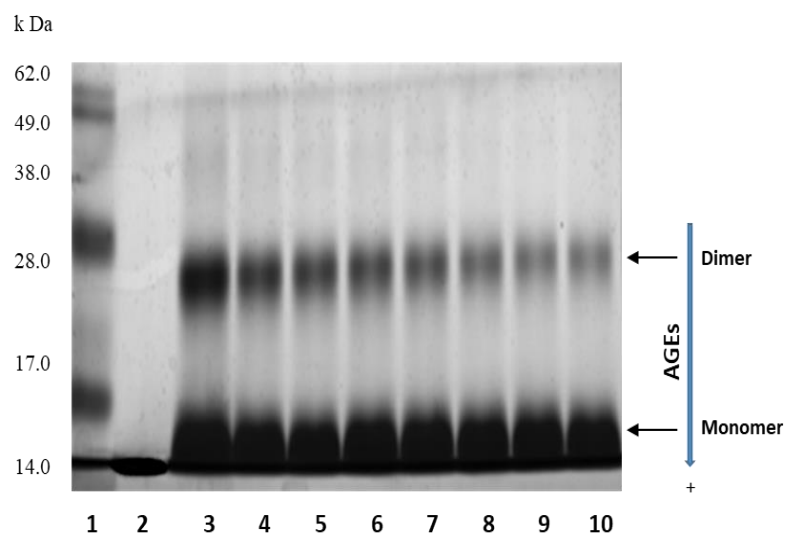


Figure 3.6: SDS-PAGE gel showing the effect of SAC on MG-derived AGE formation.

Gel showing lysozyme (10mg/ml) with or without SAC. Molecular Weight Marker (lane 1), lysozyme incubated alone (lane 2), in the presence of 100mM MG (lane 3) or MG in the presence of SAC, 0.001µg/ml (lane 4), 0.01µg/ml (lane 5), 0.05µg/ml (lane 6), 0.1µg/ml (lane 7), 0.5µg/ml (lane 8), 1µg/ml (lane 9) and 2µg/ml (lane 10), respectively. The gel shows evidence of dimer formation caused by protein cross-linking in 0.1M sodium phosphate buffer pH 7.4 at 37 °C for 72 hours. The cross-linked AGEs were analysed using SDS-PAGE and stained with silver stain. The results shown here are representative of three independent experiments.

Image analysis of the gel was performed and the results based on the integrated density of each band are presented in Figure 3.7. The percentage inhibition of SAC compared to the control was used to evaluate the protective effect of SAC on MG-derived cross-linked AGEs *in vitro*. In comparison to the control, SAC showed significant ($p < 0.05$) inhibition on cross-linked AGE formation *in vitro* only at concentration of 0.01µg/ml while at 0.05 - 0.1µg/ml ($p < 0.01$). In addition, SAC at a concentration of 0.5 - 2µg/ml, showed highly significantly ($p < 0.001$) inhibition of cross-linked AGE formation. This inhibitory effect occurred in a dose-dependent manner with a maximum inhibition of 79% in samples containing 2µg/ml of SAC.

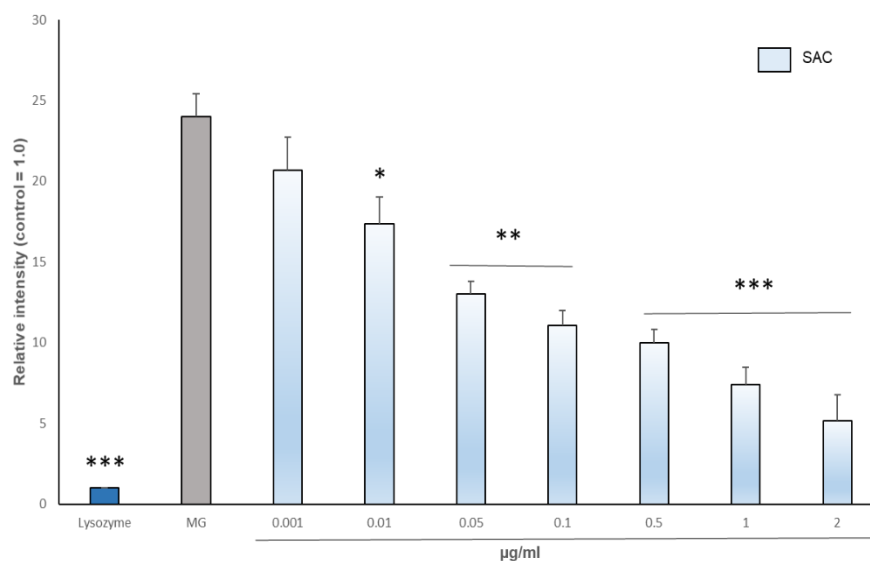


Figure 3.7: The effect of SAC on MG-derived AGE formation.

Bar chart showing decreased band density of dimer formation of lysozyme glycosylated by MG in the presence of SAC compared to control (=1.0). Each value represents the mean \pm SD (n = 3) of three independent experiments, * p <0.05, ** p <0.01 and *** p <0.001.

3.2.2.2 The effect of NAC on MG-derived AGE formation

Figure 3.8 shows the effect of NAC on the formation of cross-linked AGEs. Lysozyme incubated in the presence of MG produced cross-linked AGE, as is apparent from the analysis of this gel, to cause the formation of dimers. Glycated lysozyme (Figure 3.8, lane 3) was used as the control and clearly showed reduced electrophoretic mobility with higher molecular weight compared with native lysozyme (Figure 3.8, lane 2). The molecular weight of glycated lysozyme was approximately twice that of the original lysozyme as determined by comparison with the protein marker ladder (Figure 3.8, lane 1). Like SAC, inhibition of dimer formation by NAC showed a reduction in the intensity of the dimerised lysozyme band of approximate molecular weight of 28.7 kDa (Figure 3.8, lanes 4 - 10).

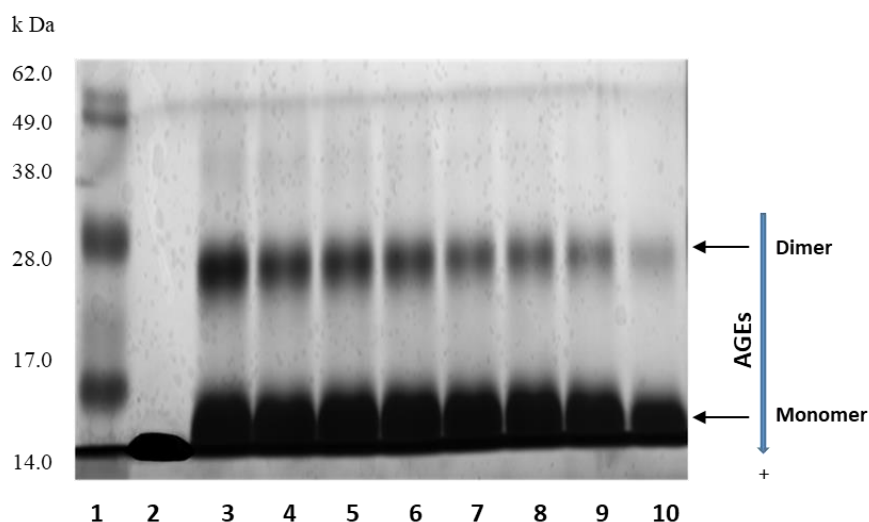


Figure 3.8: SDS-PAGE gel showing the effect of NAC on MG-derived AGE formation.

Gel showing lysozyme (10mg/ml) with or without NAC. Molecular Weight Marker (lane 1), lysozyme incubated alone (lane 2), in the presence of 100mM MG (lane 3) or MG in the presence of NAC, 0.001µg/ml (lane 4), 0.01µg/ml (lane 5), 0.05µg/ml (lane 6), 0.1µg/ml (lane 7), 0.5µg/ml (lane 8), 1µg/ml (lane 9) and 2µg/ml (lane 10), respectively. The gel shows evidence of dimer formation caused by protein cross-linking in 0.1M sodium phosphate buffer pH 7.4 at 37 °C for 72 hours. The cross-linked AGEs were analysed using SDS-PAGE and stained with silver stain. The results shown here are representative of three independent experiments.

The results obtained from the preliminary analysis of the effect of NAC on cross-linked AGE formation are presented in Figure 3.9. The percentage inhibition compared to the control was used to evaluate the effect of NAC on MG-derived cross-linked AGEs *in vitro*. In comparison to the control, NAC showed significant ($p < 0.01$) inhibition of cross-linked AGE formation between the concentrations of 0.1, 0.5, 1 and 2µg/ml. The percentage inhibition was 43%, 49%, 59% and 65%, respectively and this inhibitory effect occurs in a dose-dependent manner.

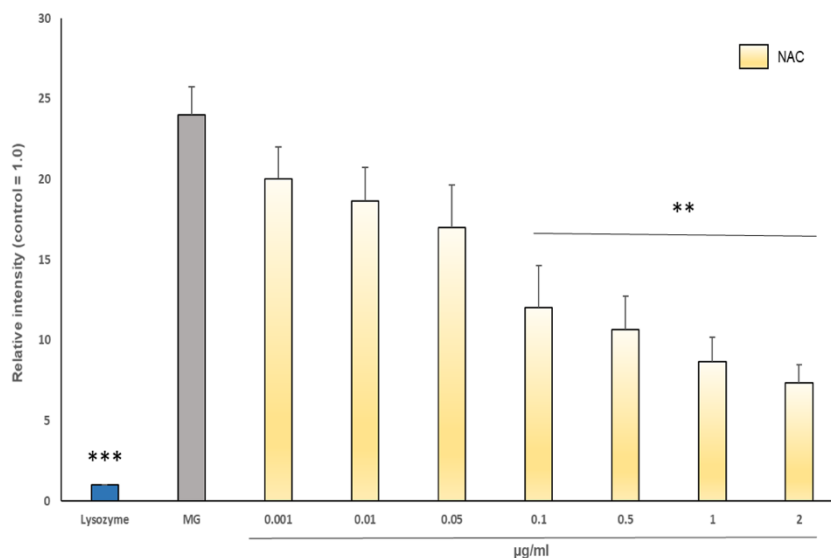


Figure 3.9: The effect of NAC on MG-derived AGE formation.

Bar chart showing decreased band density of dimer formation of lysozyme glycated by MG in the presence of NAC compared to control (=1.0). Each value represents the mean \pm SD (n= 3) from three independent experiments, **p<0.01 and ***p<0.001.

3.2.2.3 The effect of SAC/NAC on MG-derived AGE formation

The synergetic effect of both SAC and NAC (SAC/NAC) was also tested to determine their role in the inhibition of cross-linked AGEs. Incubation of lysozyme with MG produced cross-linked AGEs and the formation of dimers and trimers band. The glycated lysozyme (Figure 3.10, lane 3) was used as the control and clearly showed reduced electrophoretic mobility with a higher molecular weight as compared to native lysozyme (Figure 3.10, lane 2). The molecular weight of glycated lysozyme was approximately twice that of the original lysozyme, as determined by comparison with the protein marker ladder (Figure 3.10, lane 1). SAC (Figure 3.10, lanes 4 and 7), NAC (Figure 3.10, lanes 5 and 8) and SAC/NAC (Figure 3.10, lanes 6 and 9) inhibited AGE formation causing a reduction in the intensity of the dimerised lysozyme band of approximate molecular weight of 28.7 kDa.

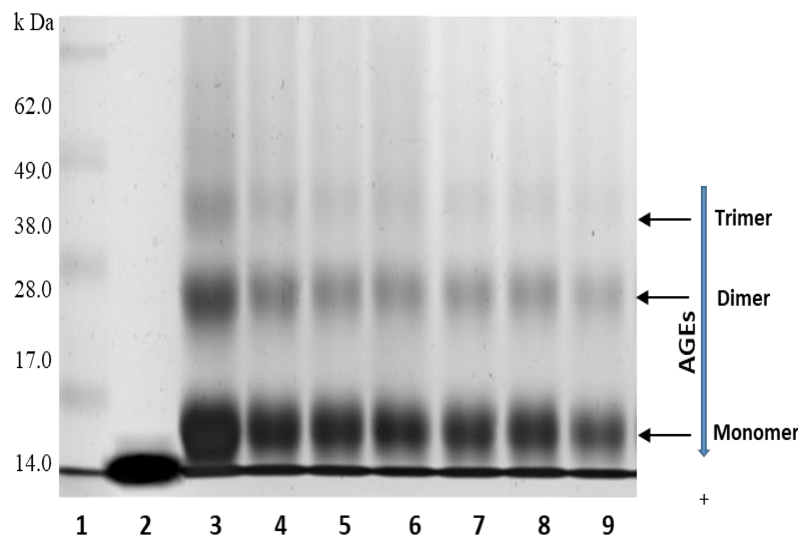


Figure 3.10: SDS-PAGE gel showing the effect of SAC/NAC on the formation of cross-linked AGEs.

Gel showing lysozyme (10mg/ml) with or without SAC, NAC and SAC/NAC. Molecular Weight Marker (lane 1), lysozyme incubated alone (lane 2), in the presence of 100mM MG (lane 3) or MG in the presence of 0.25µg/ml of SAC, NAC and SAC/NAC (lanes 4 - 6), respectively and 0.5µg/ml of SAC, NAC and SAC/NAC (lanes 7 - 9), respectively. The gel shows evidence of dimer and trimer formation caused by protein cross-linking in 0.1M sodium phosphate buffer pH 7.4 at 37 °C for 72 hours. The cross-linked AGEs were analysed using SDS-PAGE and stained with silver stain. The results shown here are representative of three independent experiments.

The percentage inhibition compared to the control was used to evaluate the effect of these inhibitors on AGE formation *in vitro*. The effects of different concentrations of SAC, NAC and SAC/NAC on AGE formation were compared with each other. The results showed that SAC, NAC at a concentration of 0.25 - 0.5µg/ml significantly ($P < 0.01$) inhibited AGE formation and the maximum percentage inhibitions for both inhibitors were 65%. Therefore, the inhibitory effects of SAC/NAC significantly inhibited AGE formation at the concentration of 0.25µg/ml ($P < 0.01$) and 0.5µg/ml ($P < 0.001$). This inhibitory effect occurred in a dose-dependent manner with a maximum inhibition of 76% that was higher than those of SAC and NAC at a concentration of 0.5µg/ml (Figure 3.11).

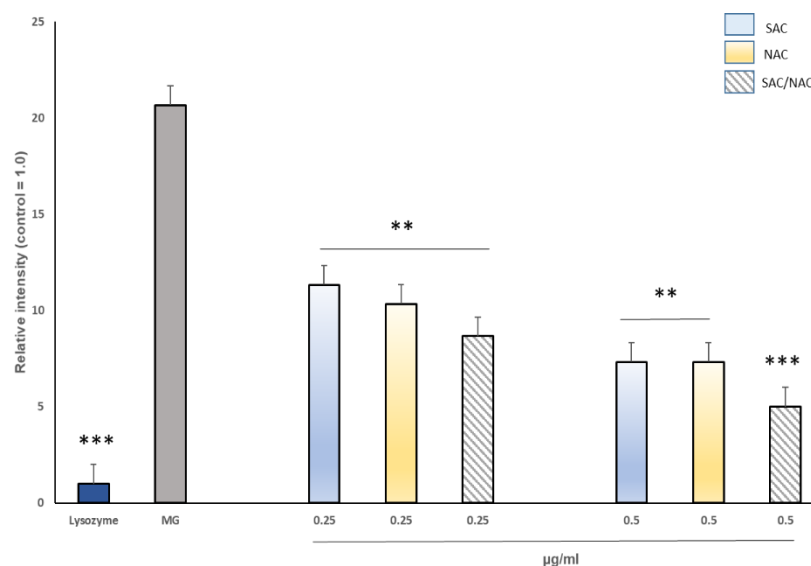


Figure 3.11: The effect of SAC/NAC on the formation of cross-linked AGEs.

Bar chart showing decreased band density of dimer formation of lysozyme glycosylated by MG in the presence of SAC, NAC and SAC/NAC compared to control (=1.0). Each value represents the mean \pm SD (n = 3). **p<0.01 and ***p<0.001.

3.2.2.4 Comparison between mimic compounds A, B and C on MG-derived AGE formation

The effect of three mimic compounds A, B and C were also tested to determine their role in the inhibition of cross-linked AGEs. Incubation of lysozyme with MG generated cross-linked AGEs that caused the formation of dimer bands with an approximate molecular weight of 28.7 kDa. The glycosylated lysozyme (Figure 3.12, lane 3) was used as the control and clearly showed reduced electrophoretic mobility with a higher molecular weight as compared to native lysozyme (Figure 3.12, lane 2). The molecular weight of glycosylated lysozyme was approximately double that of the original lysozyme, as determined by comparison with the protein marker ladder (Figure 3.12, lane 1). Compound A (Figure 3.12, lanes 4, 7 and 10), compound B (Figure 3.12, lanes 5, 8 and 11) and compound C (Figure 3.12, lanes 6, 9 and 12) inhibited AGE formation causing a reduction in the intensity of the dimerised lysozyme band.

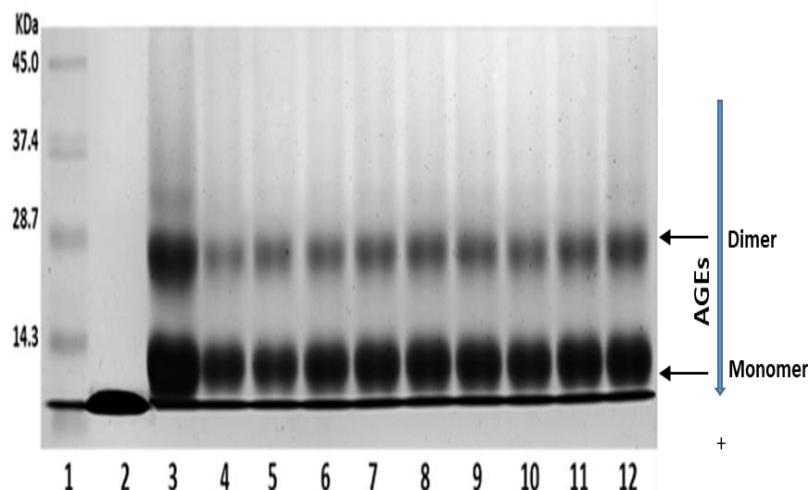


Figure 3.12: SDS-PAGE gel showing the effect of compounds A, B and C on MG-induced cross-linked AGE formation.

Gel showing lysozyme (10mg/ml) with or without compounds A, B and C. Molecular Weight Marker (lane 1), lysozyme incubated alone (lane 2), in the presence of 100mM MG (lane 3) or MG in the presence of 10µg/ml of compound A, B and C (lanes 4 - 6), 5µg/ml of compound A, B and C (lanes 7 - 9) and 0.5µg/ml of compound A, B and C (lanes 10 - 12), respectively. The gel shows evidence of dimer formation caused by protein cross-linking in 0.1M sodium phosphate buffer pH 7.4 at 37 °C for 72 hours. The cross-linked AGEs were analysed using SDS-PAGE and stained with silver stain. The results shown here are representative of three independent experiments.

Figure 3.13 compares the effects of three concentrations of these inhibitors on AGE formation. The percentage inhibition compared to the control was used to evaluate the effect of compounds A, B and C on MG-derived cross-linked AGEs *in vitro*. The results show that all the inhibitors were effective in reducing MG-derived cross-linked AGEs *in vitro*. Compound A produced a significant ($p < 0.01$) inhibition on AGE formation at 0.5µg/ml while at concentrations of between 5-10µg/ml, the inhibition was more significantly ($p < 0.001$). The percentage inhibitions were 64% and 77%, respectively. Compounds B and C showed significant inhibition ($p < 0.01$) of AGE formation at all concentrations. The maximum percentage inhibitions of compound B were 65% and for compound C 58%. Therefore, the inhibitory effect of all inhibitors occurred in a dose-dependent manner. At all concentrations tested, compound A showed a stronger inhibitory effect than compounds B and C on the *in vitro* formation of cross-linked AGEs. Therefore, compound A was used in future experiments.

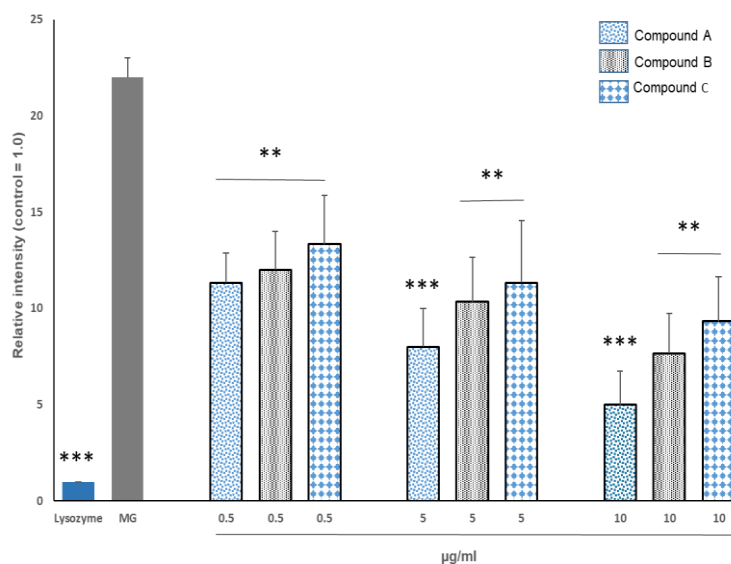


Figure 3.13: The effect of compounds A, B and C on MG-induced cross-linked AGE formation. Bar chart showing decreased band density of the dimer formation of lysozyme glycated by MG in the presence of compounds A, B and C compared to control (=1.0). Each value represents the mean \pm SD (n = 3), **p<0.01 and ***p<0.001.

3.2.2.5 The effect of compound A on MG-induced AGE formation

Lysozyme (10mg/ml) was incubated with 0.1M MG and compound A (0.01 - 2µg/ml) for 72 hours, the glycated lysozyme was tested by SDS-PAGE-silver stain to determine their role in the inhibition of cross-linked AGEs. Incubation of lysozyme in the presence of MG produced cross-linked AGEs that present as dimers and trimers. Glycated lysozyme with MG (Figure 3.14, lane 3) was used as the control and clearly showed reduced electrophoretic mobility with the higher molecular weight as compared to native lysozyme (Figure 3.14, lane 2). The molecular weight of glycated lysozyme was approximately twice that of the original lysozyme as determined by comparison with the protein marker ladder (Figure 3.14, lane 1). The inhibition of dimer formation by compound A showed a reduction in the intensity of the dimerised lysozyme band of approximate molecular weight of 28.7 kDa (Figure 3.14, lanes 4 – 9).

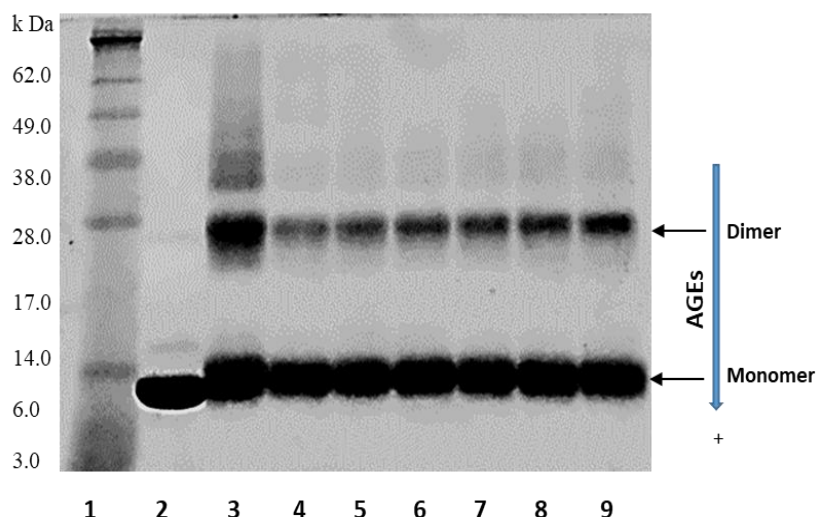


Figure 3.14: SDS-PAGE gel showing the effect of compound A on MG-induced cross-linked AGE formation.

Gel showing lysozyme (10mg/ml) with or without compound A. Molecular Weight Marker (lane 1), lysozyme incubated alone (lane 2), in the presence of 0.1M MG (lane 3) or MG in the presence of compound A, 2 μ g/ml (lane 4), 1 μ g/ml (lane 5), 0.5 μ g/ml (lane 6), 0.1 μ g/ml (lane 7), 0.05 μ g/ml (lane 8) and 0.01 μ g/ml (lane 9), respectively. The gel shows evidence of dimer formation caused by protein cross-linking in 0.1M sodium phosphate buffer pH 7.4 at 37 °C for 72 hours. The cross-linked AGEs were analysed using SDS-PAGE and stained with silver stain. The results shown here are representative of three independent experiments.

The results obtained from the preliminary analysis of the effect of compound A on cross-linked AGE formation *in vitro* are presented in Figure 3.15. The percentage inhibition compared to control was used to evaluate the effect of this inhibitor on AGE formation *in vitro*. The effect of different concentrations of compound A on AGE formation was compared with each other and with the control. Compound A showed significant ($p < 0.05$) inhibition on AGE formation at concentrations of between 0.01-0.05 μ g/ml while at 0.1 - 2 μ g/ml the significance was ($p < 0.01$) with maximum percentage inhibitions of 79%. This inhibitory effect occurred in a dose-dependent manner with a maximum inhibition of 77% in the sample containing 2 μ g/ml.

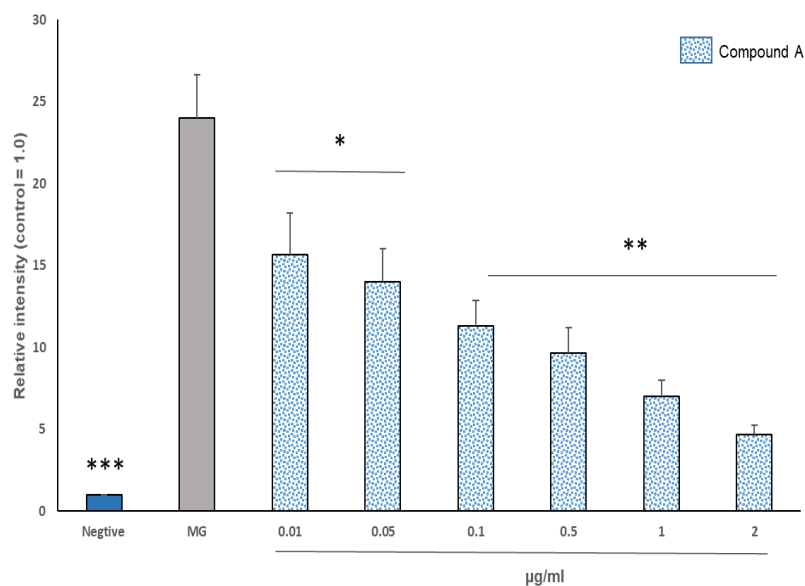


Figure 3.15: The effect of compound A on MG-induced cross-linked AGE formation.

Bar chart showing decreased band density of dimer formation of lysozyme glycosylated by MG in the presence of compound A compared to control (=1.0). Each value represents the mean \pm SD (n = 3), *p<0.05, **p<0.01 and ***p<0.001.

3.2.2.6 The effect of SAC/NAC and compound A on MG-induced cross-linked AGE formation

This experiment was designed to compare in parallel the effects of SAC/NAC and compound A on the cross-linked AGE formation *in vitro*. Incubation of lysozyme (10mg/ml) with 0.1M MG produced cross-linked AGEs that cause the formation of dimers, trimers and tetramers bands. The glycosylated lysozyme (Figure 3.16, lane 3) was used as the control and clearly showed reduced electrophoretic mobility with a higher molecular weight as compared with native lysozyme (Figure 3.16, lane 2). The molecular weight of glycosylated lysozyme was approximately twice that of the original lysozyme as determined by comparison with the protein marker ladder (Figure 3.16, lane 1). Silver staining showed the presence of both SAC/NAC (Figure 3.16, lanes 4, 6, 8, 10 and 12) and compound A (Figure 3.16, lanes 5, 7, 9, 11 and 13) inhibited AGE formation causing a reduction in the intensity of the dimerised lysozyme band of approximate molecular weight of 28.7 kDa.

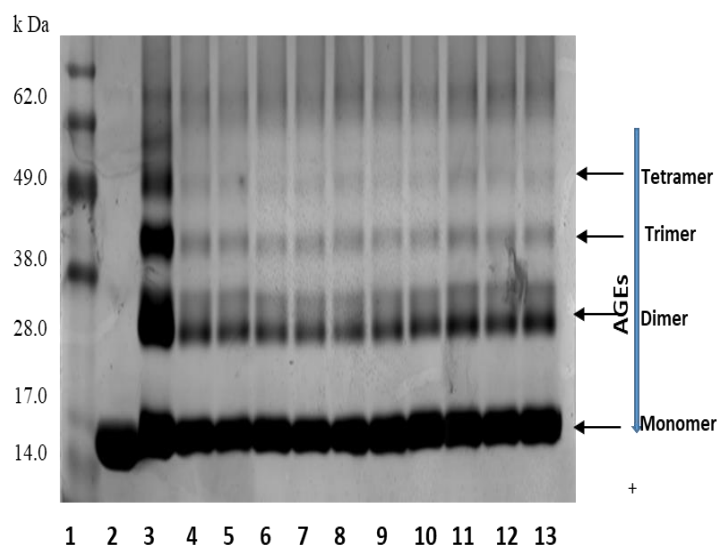


Figure 3.16: SDS-PAGE gel showing the effect of SAC/NAC and compound A on MG-induced cross-linked AGE formation.

Gel showing lysozyme (10mg/ml) with or without SAC/NAC and compound A (0.01-1µg/ml). Molecular Weight Marker (lane 1), lysozyme incubated alone (lane 2), in the presence of 0.1M MG (lane 3) or MG in the presence of SAC/NAC and compound A, 1µg/ml (lane 4 - 5), 0.5µg/ml (lane 6 - 7), 0.1µg/ml (lane 8 -9), 0.05µg/ml (lane 10 - 11) and 0.01µg/ml (lane 12 - 13), respectively. The gel shows evidence of dimer, trimer and tetramer formation caused by protein cross-linking in 0.1M sodium phosphate buffer pH 7.4 at 37 °C for 72 hours. The cross-linked AGEs were analysed using SDS-PAGE and stained with silver stain. The results shown here are representative of three independent experiments.

The results obtained from the preliminary analysis of the percentage inhibition of different concentrations of SAC/NAC and compound A on cross-linked AGE formation are shown in Figure 3.17. The effects of different concentrations of SAC/NAC and compound A on AGE formation were compared with each other and with the control. The results showed that both inhibitors significantly ($p < 0.05$) inhibited AGE formation at the concentration of 0.05µg/ml while highly significant ($p < 0.01$) inhibition at concentrations of between (0.1 - 1µg/ml) with maximum percentage inhibition were 61% and 65%, respectively. Thus, the inhibitory effect of SAC/NAC and compound A occurred in a dose-dependent manner.

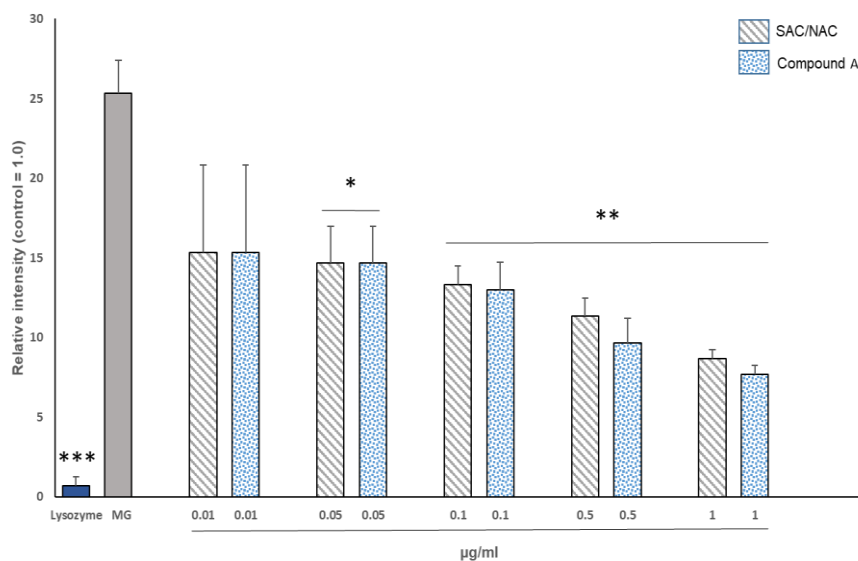


Figure 3.17: The effect of SAC/NAC and compound A on MG-induced cross-linked AGE formation.

Bar chart showing decreased band density of dimer formation of lysozyme glycosylated by MG in presence of SAC/NAC and compound A compared to control (=1.0). Each value represents the mean \pm SD (n=3), *p<0.05, **p<0.01 and ***p<0.001.

3.2.2.7 Effect of SAC/NAC-primed hADMSCs CM on MG-induced cross-linked AGE formation

Lysozyme (10mg/ml) was incubated with 0.1M MG in the presence of 500µg/ml SAC/NAC-loaded hADMSCs CM for four days and the conditioned medium released from hADMSCs was collected for each day and replaced with fresh medium. The collected medium (days 1 - 4) were tested by SDS-PAGE-silver stain to determine its role on the inhibition of cross-linked AGEs. Incubation of MG with lysozyme produced sufficient cross-linked AGEs that cause the formation of dimers bands. The glycosylated lysozyme (Figure 3.18, lane 3) was used as the control and clearly showed reduced electrophoretic mobility with a higher molecular weight as compared to native lysozyme (Figure 3.18, lane 2). The molecular weight of glycosylated lysozyme was approximately twice that of the original lysozyme as determined by comparison with the protein marker ladder (Figure 3.18, lane 1). SAC/NAC-primed hADMSCs CM; day 1 (Figure 3.18, lane 4), day 2 (Figure 3.18, lane 5), day 3 (Figure 3.18, lane 6) and day 4 (Figure 3.18, lane 7). These inhibited AGE formation causing a reduction in the intensity of the dimerised lysozyme band with an approximate molecular weight of 28.7 kDa.

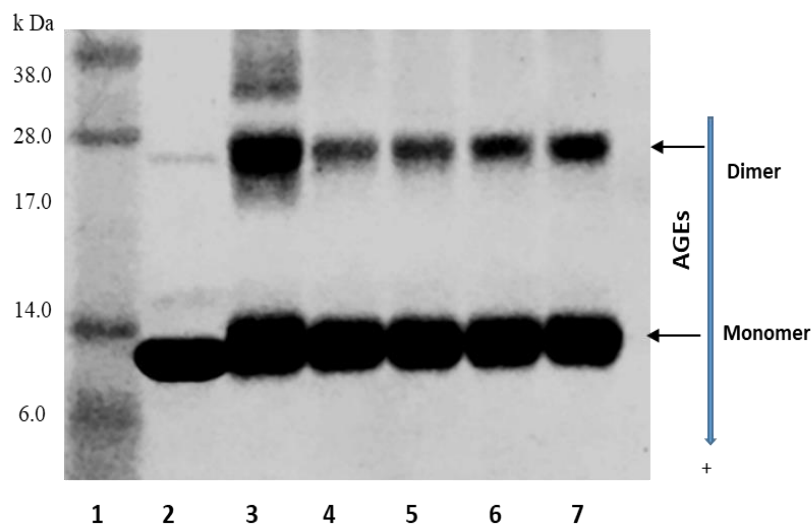


Figure 3.18: SDS-PAGE gel showing the effect of SAC/NAC-primed hADMSCs CM on MG-induced cross-linked AGE formation.

Gel showing lysozyme (10mg/ml) with or without SAC/NAC-primed hADMSCs CM. Molecular Weight Marker (lane 1), lysozyme incubated alone (lane 2), in the presence of 0.1M MG (lane 3) or MG in the presence of SAC/NAC-loaded hADMSCs CM, day 1 (lane 4), day 2 (lane 5), day 3 (lane 6) and day 4 (lane 7), respectively. The gel shows evidence of dimer formation caused by protein cross-linking in 0.1M sodium phosphate buffer pH 7.4 at 37 °C. The cross-linked AGEs were analysed using SDS-PAGE and stained with silver stain. The results shown here are representative of three independent experiments.

Figure 3.19 compares the results obtained from the effect of four days of the collected medium of this inhibitor of AGE formation. At days (1 - 3), SAC/NAC-primed hADMSCs CM showed significant ($p < 0.05$) inhibition of AGE formation in a dose-dependent manner. The percentage inhibitions were 41%, 28% and 17%, respectively.

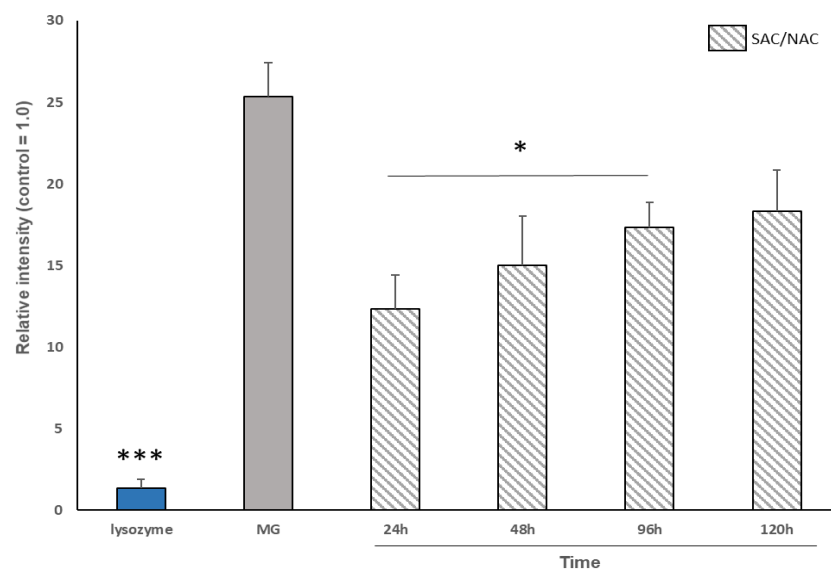


Figure 3.19: The effect of SAC/NAC-primed hADMSCs CM on MG-induced cross-linked AGE formation.

Bar chart showing decreased band density of dimer formation of lysozyme glycosylated by MG in presence of SAC/NAC-primed hADMSCs CM compared to control (=1.0). Each value represents the mean \pm SD (n = 3), * p <0.05 and *** p <0.001.

3.2.2.8 Effect of compound A-primed hADMSCs CM on MG-induced cross-linked AGE formation

Lysozyme (10mg/ml) was incubated with 0.1M MG in the presence of 250 μ g/ml compound A-loaded hADMSCs CM for four days and the conditioned medium released from hADMSCs was collected for each day and replaced with fresh medium. The collected medium (days 1 - 4) were tested by SDS-PAGE-silver stain to determine its role on the inhibition of cross-linked AGEs. Incubation of MG with lysozyme produced sufficient cross-linked AGEs to cause the formation of dimers bands (Figure 3.20, lane 3) was used as the control and clearly showed reduced electrophoretic mobility with a higher molecular weight as compared to native lysozyme (Figure 3.20, lane 2). The molecular weight of glycosylated lysozyme was approximately twice that of the original lysozyme as determined by comparison with the protein marker ladder (Figure 3.20, lane 1). These were compound A-primed hADMSCs CM for; day 1 (Figure 3.20, lane 4), day 2 (Figure 3.20, lane 5), day 3 (Figure 3.20, lane 6) and day 4 (Figure 3.20, lane 7) and they inhibited AGE formation causing a reduction in the intensity of the dimerised lysozyme band with an approximate molecular weight of 28.7 kDa.

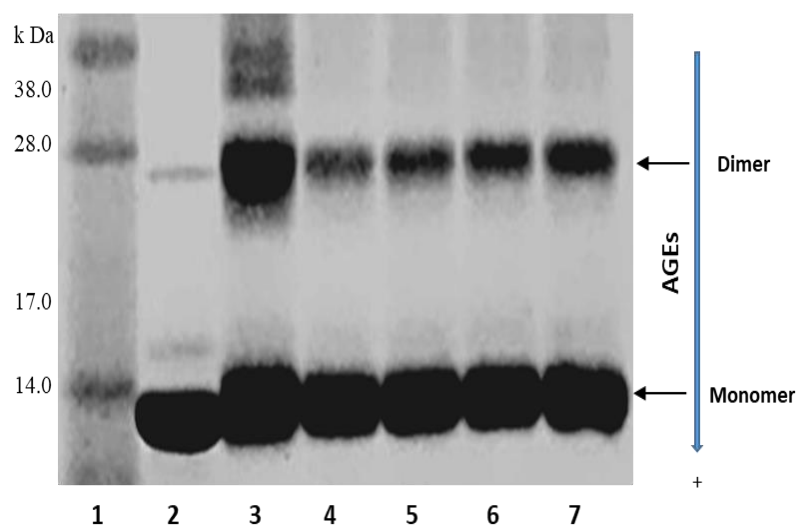


Figure 3.20: SDS-PAGE gel showing the effect of compound A-primed hADMSCs CM on MG-induced cross-linked AGE formation.

Gel showing lysozyme (10mg/ml) with or without compound A-primed hADMSCs CM. Molecular Weight Marker (lane 1), lysozyme incubated alone (lane 2), 0.1M MG (lane 3) or MG in the presence of compound A-loaded hADMSCs CM, day 1 (lane 4), day 2 (lane 5), day 3 (lane 6) and day 4 (lane 7), respectively. The gel shows evidence of dimer formation caused by protein cross-linking in 0.1M sodium phosphate buffer pH 7.4 at 37°C. The cross-linked AGEs were analysed using SDS-PAGE and stained with silver stain. The results shown here are representative of three independent experiments.

The percentage of inhibition compared to controls was used to evaluate the protective effect of four days of the collected medium of this inhibitor on AGE formation. Figure 3.21 compares the effect of different collected media of compound A on AGE formation. Like SAC/NAC, compound A-primed hADMSCs CM at days (1 - 3) showed significant ($p < 0.05$) inhibition of AGE dimer formation in a dose-dependent manner. The percentage inhibitions were 47%, 37% and 26%, respectively.

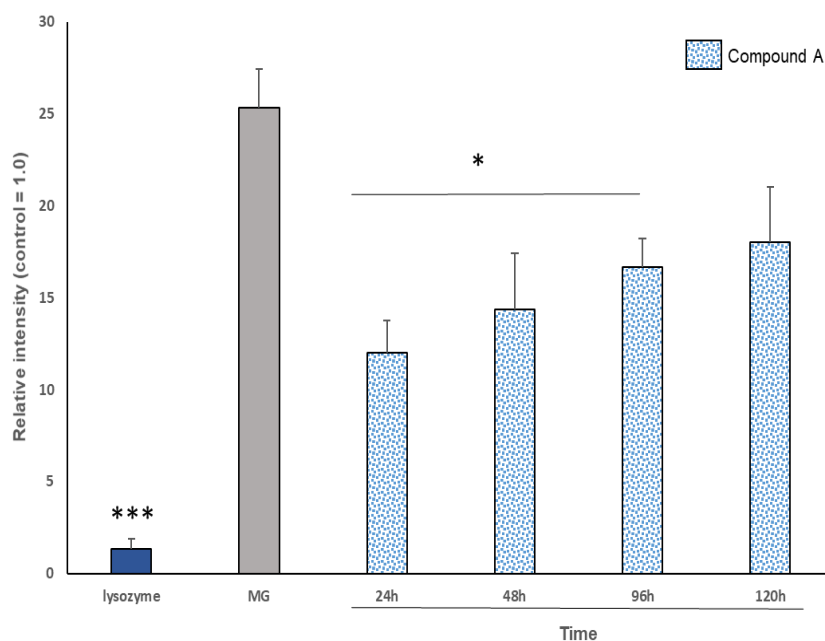


Figure 3.21: The effect of compound A-primed hADMSCs CM on MG-induced cross-linked AGE formation.

Bar chart showing decreased band density of dimer formation of lysozyme glycosylated by MG in the presence of compound A CM compared to control (=1.0). Each value represents the mean \pm SD (n=3), * p <0.05 and *** p <0.001.

3.2.2.9 Effect of SAC/NAC- and compound A- loaded hADMSCs CM on MG-induced cross-linked AGE formation.

Figure 3.22 compares the effect of SAC/NAC- and compound A-primed hADMSCs CM (days 1 - 4) on AGE formation. Incubation of 0.1M MG with (10mg/ml) lysozyme produced sufficient cross-linked AGEs to cause the formation of dimers and trimerise. Glycated lysozyme (Figure 3.22, lane 3) was used as the control and clearly showed reduced electrophoretic mobility with a higher molecular weight as compared to native lysozyme (Figure 3.22, lane 2). The molecular weight of glycated lysozyme was approximately twice that of the original lysozyme as determined by comparison with the protein marker ladder (Figure 3.22, lane 1). Like the individual effect of each SAC/NAC- and compound A-primed hADMSCs CM, both of SAC/NAC- and compound A-primed hADMSCs CM exhibited the inhibitory effects on AGE formation after 4 days' incubation in conditioned media. SAC/NAC- (Figure 3.22, lanes 4, 6, 8 and 10) and compound A- primed hADMSCs CM (Figure 3.22, lanes 5, 7, 9 and 11) inhibited AGE formation causing a reduction in the intensity of the dimerised lysozyme bands with an approximate molecular weight of 28.7 kDa.

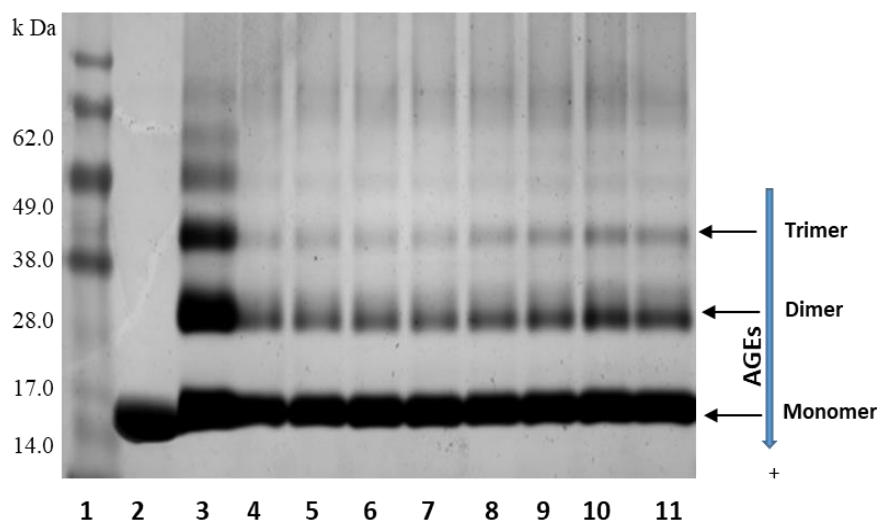


Figure 3.22: SDS-PAGE gel showing the effect of SAC/NAC- and compound A-primed hADMSCs CM on MG-induced cross-linked AGE formation.

Gel showing lysozyme (10mg/ml) with or without SAC/NAC- and compound A-primed hADMSCs CM. Molecular Weight Marker (lane 1), lysozyme incubated alone (lane 2), in the presence of 0.1M MG (lane 3) or MG in the presence of SAC/NAC- and compound A- primed hADMSCs CM, day 1 (lane 4 - 5), day 2 (lane 6 - 7), day 3 (lane 8 - 9) and day 4 (lane 10 - 11), respectively. The gel shows evidence of dimer and trimer formation caused by protein cross-linking in 0.1M sodium phosphate buffer of pH 7.4 at 37 °C. The cross-linked AGEs were analysed using SDS-PAGE and stained with silver stain. The results shown here are representative of three independent experiments.

As a result, the effects of SAC/NAC- and compound A-loaded hADMSCs CM occurred in a dose-dependent manner. SAC/NAC- and compound A-loaded hADMSCs CM showed a significant ($p < 0.05$) inhibition at days 1-3 in a dose-dependent manner. The maximum percentage of inhibitions were 40% and 44%, respectively. On the other hand, no significant inhibition was found at day 4. The inhibition was dose-dependent (Figure 3.23).

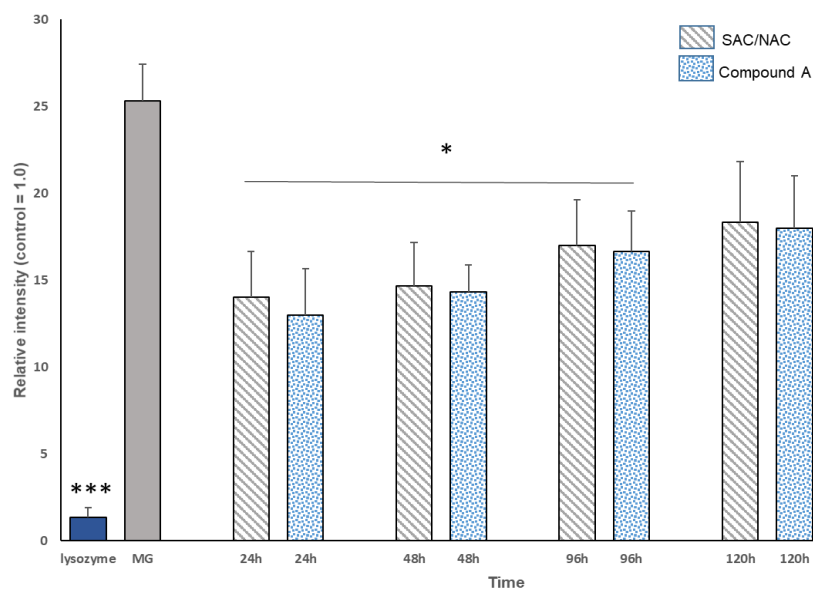


Figure 3.23: The effect of SAC/NAC- and compound A-primed hADMSCs CM on MG-induced cross-linked AGE formation.

Bar chart showing decreased band density of dimer formation of lysozyme glycated by MG in presence of SAC/NAC- and compound A- primed hADMSCs CM compared to control (=1.0). Each value represents the mean \pm SD (n = 3), * p <0.05, *** p <0.001.

3.2.3 Detection of AGEs by Western blot

3.2.3.1 Protein determination

The protein contents of different samples were determined using the Bradford method in order to compare the concentrations of MG obtained from the cell samples. Protein standard curves using albumin protein with a known concentration of BSA is a frequently used protein standard. A calibration curve was plotted from serial dilutions of BSA corresponding to protein concentrations of 0 – 60 μ g/ml. A protein concentration for each cell sample was read from the calibration curve and expressed relative to the BSA standard in μ g of protein. The BSA standard curve showed a linear correlation between the protein concentration and the absorbance at 595nm using a spectrophotometer (Figure 3.24).

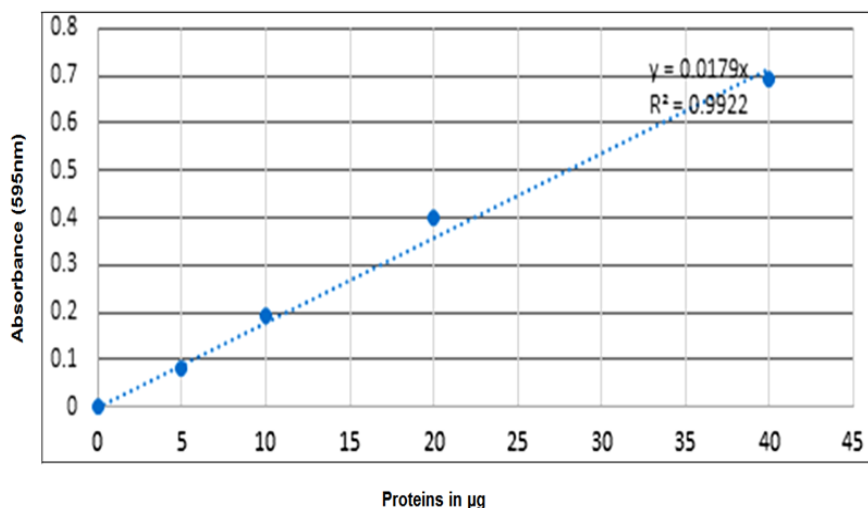


Figure 3.24: Calibration graph of protein estimation for Western blot analysis.

3.2.3.2 The effect of MG on BAEC glycation after 24 hours.

In order to validate the inhibitory effect of SAC/NAC and compound A on AGE formation, the immunological characterisation was performed by Western blotting analysis using an anti-MG antibody. This experiment was performed to optimise the incubation time corresponding to the MG glycation effects on BAECs for 24 hours was assessed by Western blot analysis. Glycated bands were measured at 72.0 kDa (upon the anti-MG-AGE antibody) (Figure 3.25A, lane 1), untreated BEACs were used as controls (Figure 3.25A, lane 2) or in presence of (1 - 300 μM) MG (Figure 3.25A, lanes 3 - 8), respectively. Tubulin was used as a loading control (Figure 3.25B).

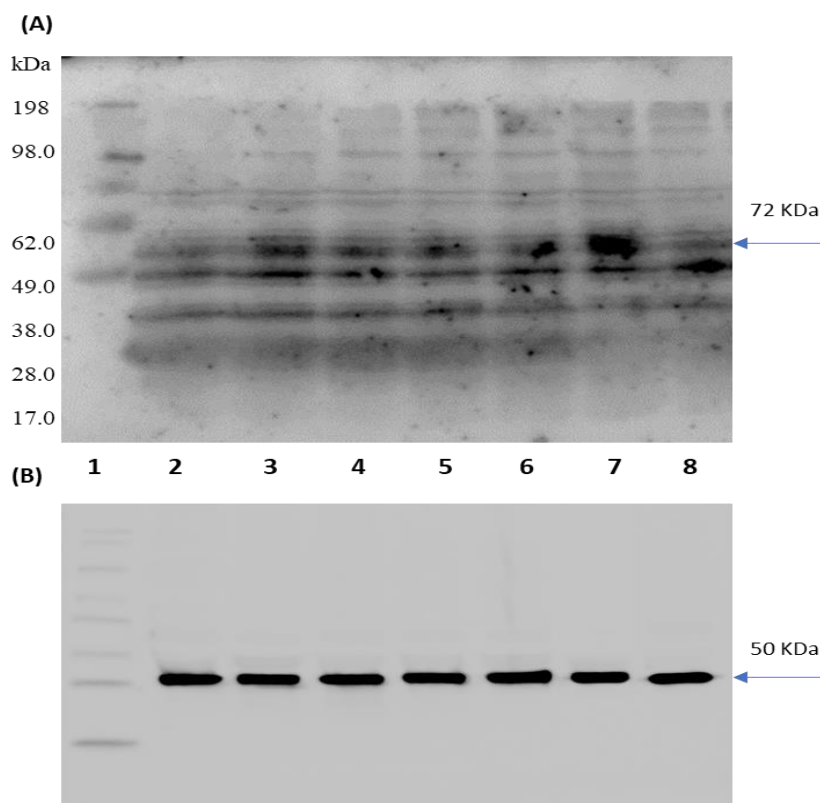


Figure 3.25: SDS-PAGE gel showing the effect of MG on BAEC glycation after 24 hours. Representative Western blot of proteins from BAECs incubated with MG. (A) Molecular Weight Marker (lane 1), untreated BEACs control (lane 2) or in presence of MG 1 μM (lane 3), 10 μM (lane 4), 50 μM (lane 5), 100 μM (lane 6), 200 μM (lane 7) and 300 μM (lane 8), respectively. (B) Tubulin. The samples were separated by SDS-PAGE and the gels were transferred to nitrocellulose membranes and protein detected using an anti-MG AGE antibody. The results are a representative example of three independent experiments.

The relative density of protein expression was analysed using Image-J. After 24 hours of incubation, there were no clear bands and there is some evidence of partial glycation. However, Band intensity of protein cross-linking showed a non-significant increase as compared to control (Figure 3.26).

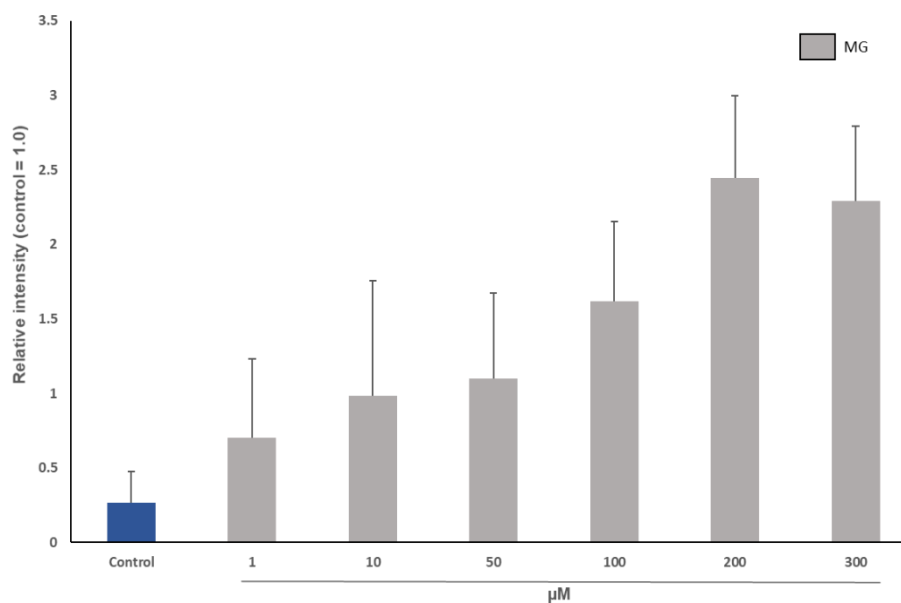


Figure 3.26: The effect of MG on BAEC glycation after 24 hours.

Bar chart showing the relative protein glycated by MG (72.0 kDa) (control = 1.0) from Figure 3.25. The experiment was repeated at least three times.

3.2.3.3 The effect of MG on BAEC glycation after 72 hours.

BAEC were incubated with MG for 72 hours and the relative density of protein expression was analysed using the free software Image J. After 3 days' incubation, MG produced sufficient cross-linked AGEs at an approximate molecular weight of 72.0 kDa with respect to anti- MG AGE antibody (Figure 3.27A, lane 1). However, incubation of BAECs with different concentrations of MG caused the formation of AGEs and an increased band intensity at concentrations in a dose-dependent manner (Figure 3.27, lanes 3-8) compared to untreated cells (Figure 3.27, lane 2). This suggests that the incubation time was good and that carbonyl groups were bound to the protein. Tubulin was used as a loading control (Figure 3.27B).

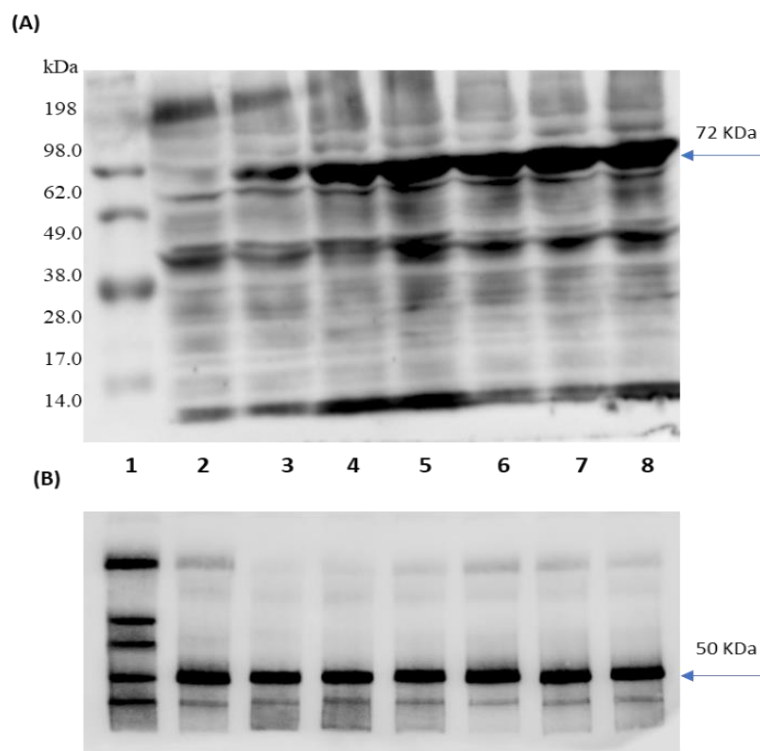


Figure 3.27: SDS-PAGE gel showing the effect of MG on BAEC glycation after 72 hours.

Representative Western blot of protein from BAECs incubated with MG. (A) Molecular Weight Marker (lane 1), untreated BAECs (lane 2) or in presence of MG 1 μM (lane 3), 10 μM (lane 4), 50 μM (lane 5), 100 μM (lane 6), 200 μM (lane 7) and 300 μM (lane 8), respectively. (B) Tubulin. The samples were separated by SDS-PAGE and the gels were transferred to nitrocellulose membranes and protein detected using an anti-MG AGE antibody. The results are a representative example of three independent experiments.

As can be seen in Figure 3.28, the results show that after three days, Incubation of BAECs with MG at concentrations of between 10 - 100 μM caused significant ($p < 0.05$) production of AGE formation compared to the control and was more significant ($p < 0.01$) at concentrations of 200 - 300 μM. The cross-linked AGE production was more than 16-fold greater when BAECs were incubated with 300 μM MG compared to control and 14 -fold greater when 100 μM MG was used. Therefore, 300 μM MG and 3 days' incubated were applied to the rest of the experiments.

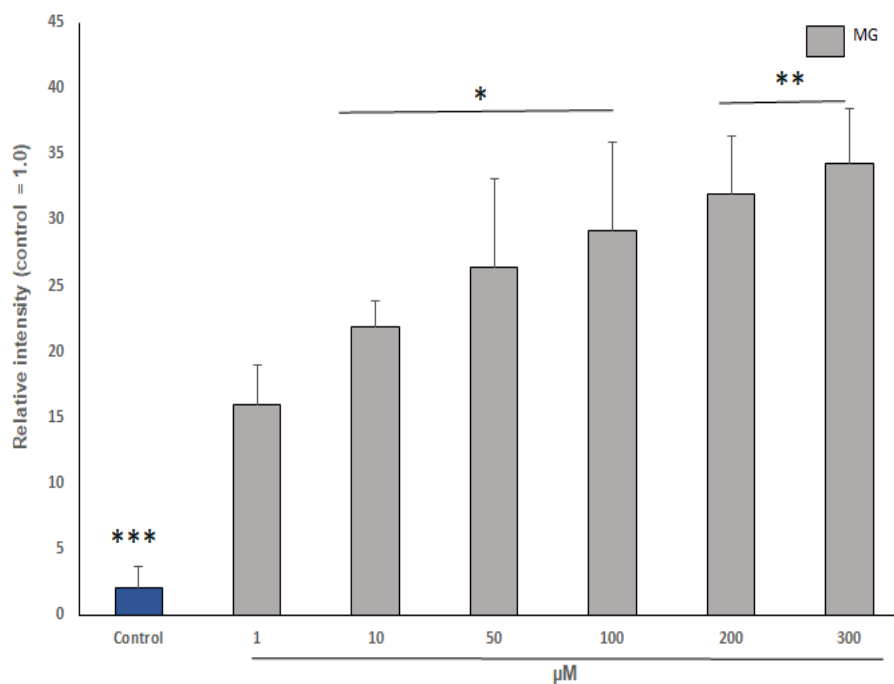


Figure 3.28: The effect of MG on BAEC glycation after 72 hours.

Bar chart showing the relative protein glycated by MG (72.0 kDa) (control = 1.0) from Figure 3.27. The experiment was repeated at least three times. * $P < 0.05$, ** $p < 0.01$ and *** $p < 0.01$.

3.2.3.4 The effect of MG on BAEC glycation after 120 hours.

BAEC were incubated with MG for 120 hours and the relative density of protein expression was analysed using free software Image J. Glycation was measured as indexed by the presence of the 72.0 kDa with respect to anti- MG AGE antibody (Figure 3.29A, lane 1), untreated BEACs were used as controls (Figure 3.29A, lane 2) or in presence of MG (1 - 300µM) (Figure 3.29A, lane 3-8), respectively. Tubulin was used as a loading control (Figure 3.29B).

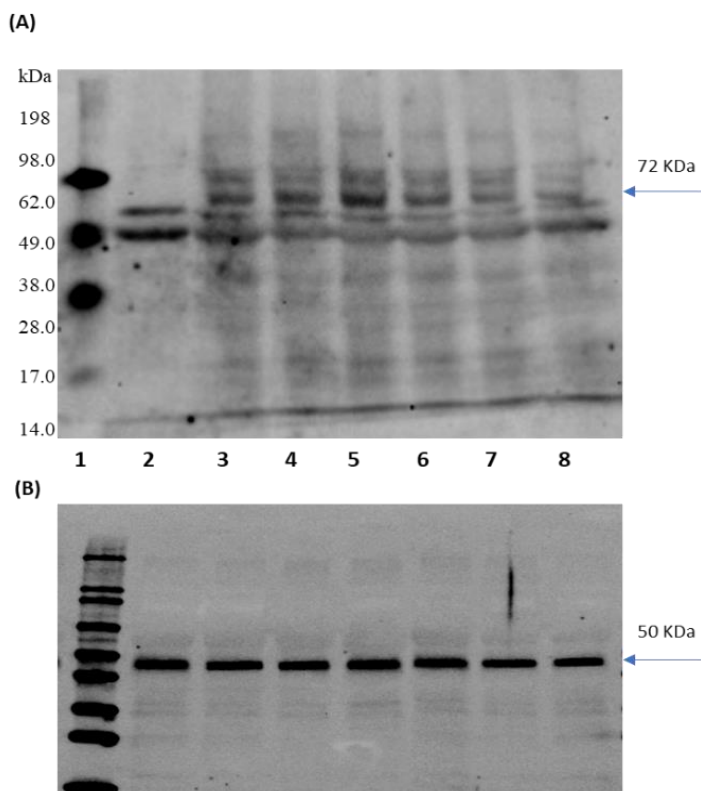


Figure 3.29: SDS-PAGE gel showing the effect of MG on BAEC glycation after 120 hours. Representative Western blot of protein from BAECs incubated with MG. (A) Molecular Weight Marker (lane 1), untreated BEAC (lane 2) or in present of MG, 1 μ M (lane 3), 10 μ M (lane 4), 50 μ M (lane 5), 100 μ M (lane 6), 200 μ M (lane 7) and 300 μ M (lane 8), respectively. (B) Tubulin. The samples were separated by SDS-PAGE and the gels were transferred to nitrocellulose membranes and protein detected using an anti-MG antibody. The results are a representative example of three independent experiments.

After 5 days' incubation, the results show that decreased band intensity in most of the samples due to the hydrolysis of the AGEs, suggesting that the incubation time was too long (Figure 3.30).

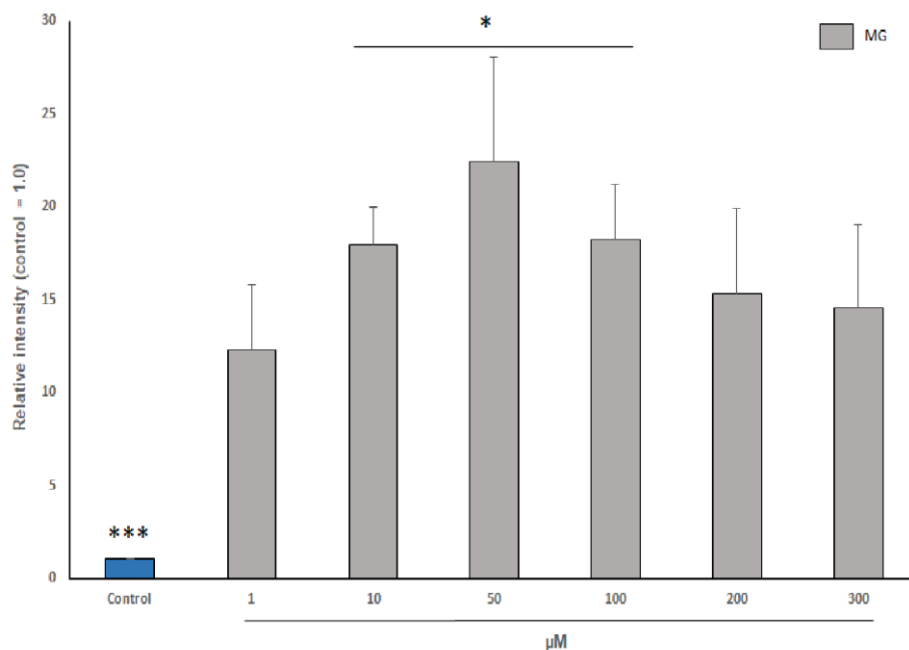


Figure 3.30: The effect of MG on BAEC glycation after 120 hours.

Bar chart showing the relative protein glycation by MG (72.0 kDa) (control = 1.0) from Figure 3.29. The experiment was repeated at least three times, * $P < 0.05$ and *** $P < 0.001$.

3.2.3.5 The effect of SAC/NAC on BAEC glycation.

BAECs were incubated with SAC/NAC and the relative density of protein expression was analysed using free software Image J. Glycation was measured as indexed by the presence of the 72.0 kDa with respect to anti- MG AGE antibody (Figure 3.31A, lane 1), untreated BEACs were used as controls (Figure 3.31A, lane 2), 300 μ M MG (Figure 3.31A, lane 3) or MG in the presence of SAC/NAC (Figure 3.31A, lanes 4 - 9), respectively. Tubulin was used as a loading control (Figure 3.31B).

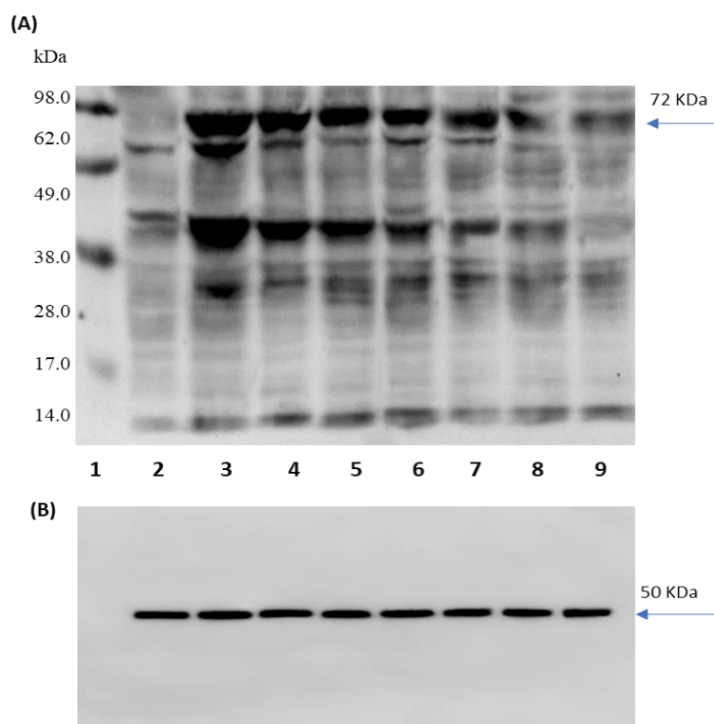


Figure 3.31: SDS-PAGE gel showing the effect of SAC/NAC on BAEC glycation.

Representative Western blot of protein from BAECs incubated with MG and SAC/NAC for 3 days. (A) Molecular Weight Marker (lane 1), untreated BEACs negative control (lane 2), treated BEACs with 300 μ M MG positive control (lane 3) or MG in present of SAC/NAC, 0.01 μ g/ml (lane 4), 0.05 μ g/ml (lane 5), 0.1 μ g/ml (lane 6), 0.5 μ g/ml (lane 7), 1 μ g/ml (lane 8) and 2 μ g/ml (lane 9), (B) Tubulin. The samples were separated by SDS-PAGE and the gels were transferred to nitrocellulose membranes and protein detected using an anti-MG antibody. The results are a representative example of three independent experiments.

As can be seen in Figure 3.32, SAC/NAC inhibited AGEs formation *in vitro* in a dose-dependent manner. The intensity of each band was calculated and the percentage of inhibition of each band was assessed by comparing it with the value of the control. Following 3 days' incubation, SAC/NAC significantly ($p < 0.05$) inhibited AGE formation between the concentrations of 0.1, 0.5 and 1 μ g/ml. The percentages of inhibition were 24%, 35% and 46%, respectively. At 2 μ g/ml, SAC/NAC inhibited AGE formation even more significantly ($p < 0.01$) and the percentage inhibition was 66%.

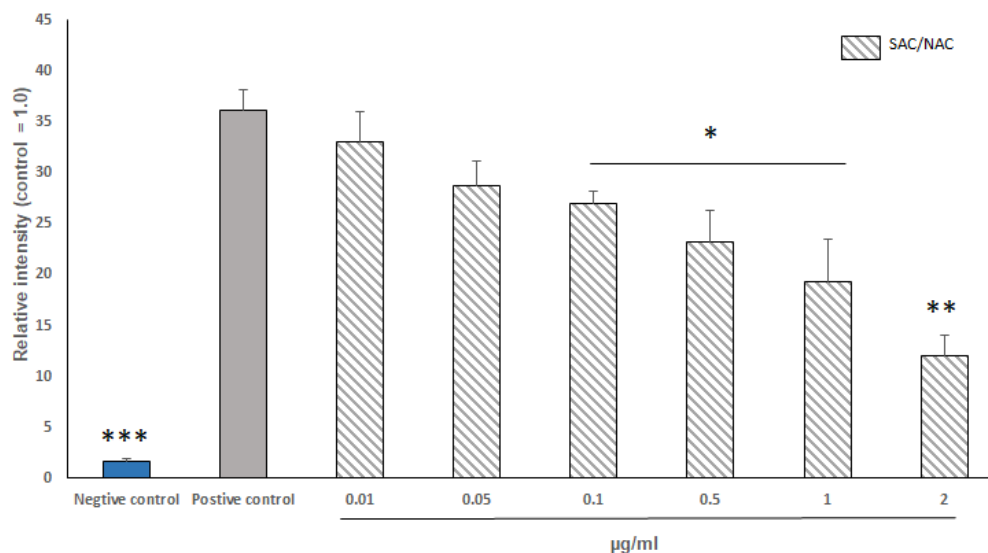


Figure 3.32: The effect of SAC/NAC on BAEC glycation.

Bar chart showing the relative protein glycated by MG (72.0 kDa) (control = 1.0) from Figure 3.31. The experiment was repeated at least three times, * $P < 0.05$, ** $p < 0.01$ and *** $p < 0.001$.

3.2.3.6 The effect of compound A on BAEC glycation.

BAECs were incubated with compound A and the relative density of protein expression was analysed using free software Image J. Glycation was measured as indexed by the presence of the 72.0 kDa with respect to anti- MG AGE antibody (Figure 3.33A, lane 1), untreated BEACs were used as controls (Figure 3.33A, lane 2), 300µM MG (Figure 3.33A, lane 3) or MG in the presence of compound A (Figure 3.33A, lanes 4 - 9), respectively. Tubulin was used as a loading control (Figure 3.33B).

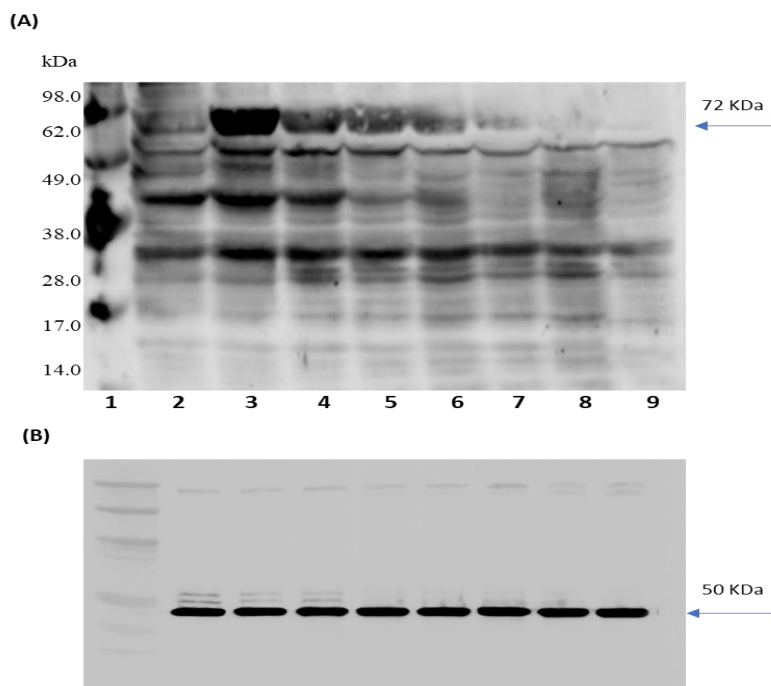


Figure 3.33: SDS-PAGE gel showing the effect of compound A on BAEC glycation.

Representative Western blot of protein from BAECs incubated with MG and compound A for 3 days. (A) Molecular Weight Marker (lane 1), untreated BEACs negative control (lane 2), treated BEACs with 300 μM MG positive control (lane 3) or MG in present of mimic compound A, 0.01 μg/ml (lane 4), 0.05 μg/ml (lane 5), 0.1 μg/ml (lane 6), 0.5 μg/ml (lane 7), 1 μg/ml (lane 8) and 2 μg/ml (lane 9), respectively. (B) Tubulin. The samples were separated by SDS-PAGE and the gels were transferred to nitrocellulose membranes and protein detected using an anti-MG antibody. The results are a representative example of three independent experiments.

Figure 3.34 shows that compound A effectively inhibited AGEs formation *in vitro*. The intensity of each band was calculated and the percentage of inhibition of each band was assessed by comparing it with the value of the control. Results show that compound A significantly ($p < 0.01$) inhibited AGE formation between the concentrations 0.1 and 0.5 μg/ml. The percentages of inhibition were 64% and 76%, respectively. Further analysis showed that a more significant ($p < 0.001$) inhibition was detected at 1 - 2 μg/ml where the percentage of inhibition were 89% and 93%, respectively and the inhibition was dose-dependent.

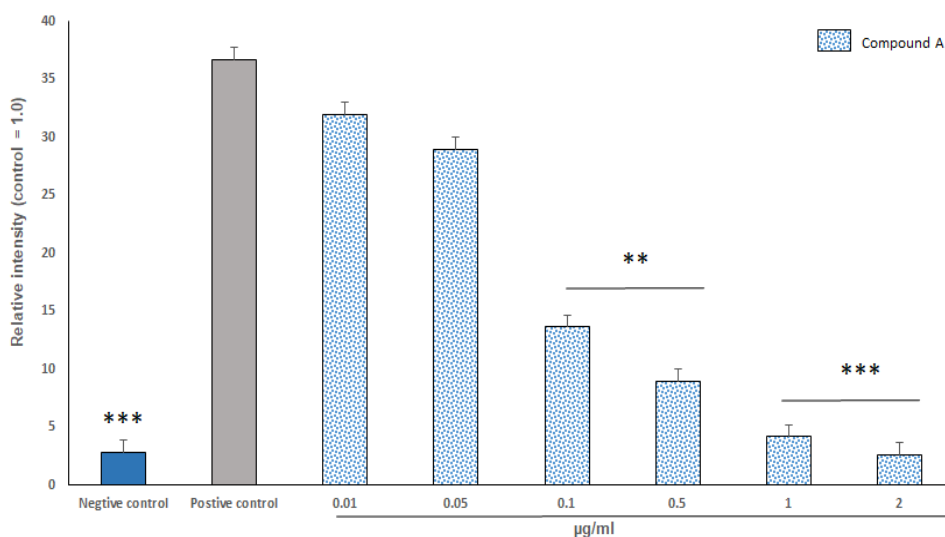


Figure 3.34: The effect of compound A on BAEC glycation.

Bar chart showing the relative protein glycated by MG (72.0 kDa) (control = 1.0) from Figure 3.33. The experiment was repeated at least three times, ** $p < 0.01$ and *** $p < 0.001$.

3.2.3.7 The effect SAC/NAC and compound A on BAEC glycation.

BAEC were incubated with MG in the presence of SAC/NAC and compound A and the relative density of protein expression was analysed using free software Image J. Glycation was measured as indexed by the presence of the 72.0 kDa with respect to anti- MG AGE antibody (Figure 3.35A, lane 1), untreated BEACs were used as controls (Figure 3.35A, lane 2), 300µM MG (Figure 3.35A, lane 3) or MG in the presence of SAC/NAC and compound A (Figure 3.35A, lanes 4 - 13), respectively. Tubulin was used as a loading control (Figure 3.35B).

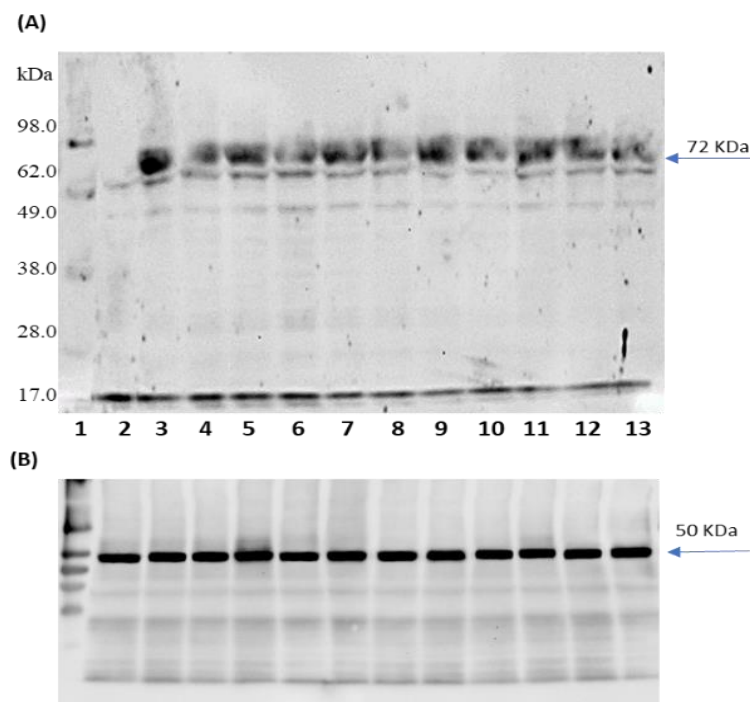


Figure 3.35: SDS-PAGE gel showing the effect of SAC/NAC and compound A on BAEC glycation.

Representative Western blot of protein from BAECs incubated with MG in the presence of SAC/NAC and compound A for 3 days. (A) Molecular Weight Marker (lane 1), untreated BEACs negative control (lane 2), treated BEACs with 300 μ M MG positive control (lane 3) or MG in present of SAC/NAC and compound A, 0.01 μ g/ml (lane 4 - 5), 0.05 μ g/ml (lane 6 - 7), 0.1 μ g/ml (lane 8 - 9), 0.5 μ g/ml (lane 10 - 11) and 1 μ g/ml (lane 12 -13), respectively. (B) Tubulin. The samples were separated by SDS-PAGE and the gels were transferred to nitrocellulose membranes and protein detected using an anti-MG antibody. The results are a representative example of three independent experiments.

The results obtained from the preliminary analysis of the effect of SAC/NAC and compound A on AGE formation are shown in Figure 3.36. All inhibitors showed variable reducing power as demonstrated by their effectiveness in reducing AGE formation. The intensity of each band was calculated and the percentage of inhibition was detected by comparing it with the control value. SAC/NAC at concentrations between 0.05-0.1 μ g/ml significantly ($p < 0.05$) inhibited AGE formation and the percentage inhibitions were 23% and 33%, respectively. At 0.5 μ g/ml, the inhibition was more significant ($p < 0.01$) and the percentage inhibition increased to 49%. In addition, 1 μ g/ml of SAC/NAC inhibited AGE formation by 60% ($p < 0.001$). Compound A at 0.05 μ g/ml significantly ($p < 0.05$) inhibited AGE formation by 29% while between 0.1 - 0.5 μ g/ml, the inhibition was more significant ($p < 0.01$) and the percentages inhibition increased to 37% and 50%, respectively. At a concentration of

1 μ g/ml, the percentage inhibition was 60% ($p < 0.001$). Thus, the results clearly indicate that increasing concentrations of both inhibitors have a higher reducing power.

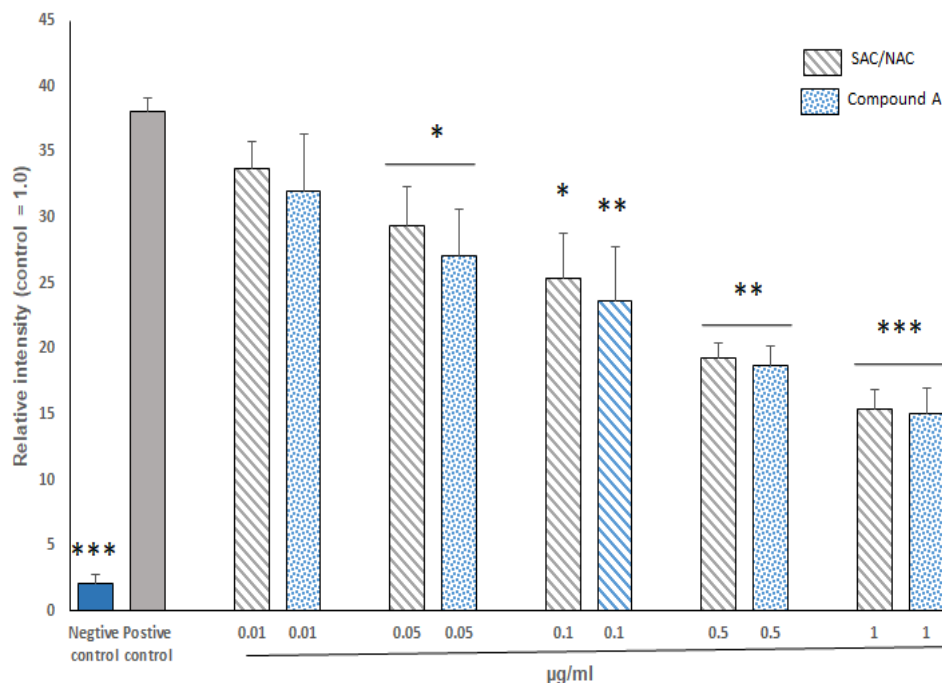


Figure 3.36: The effect of SAC/NAC and compound A on BAEC glycation.

Bar chart showing the relative protein glycated by MG (72.0 kDa) (control = 1.0) from Figure 3.35. The experiment was repeated at least three times, * $P < 0.05$, ** $p < 0.01$ and *** $p < 0.001$.

3.2.3.8 The effect of SAC/NAC- and compound A-loaded hADMSCs CM on BAEC glycation.

MSCs were incubated with MG and 500 μ g/ml of SAC/NAC-primed hADMSCs CM or with MG and 250 μ g/ml of compound A-primed hADMSCs CM for four days. The released conditioned medium for each day was collected and replaced by fresh medium. BAECs were incubated with MG and conditioned medium and the relative density of protein expression was analysed using free software Image J. Glycation was measured as indexed by the presence of the 72.0 kDa with respect to anti- MG AGE antibody (Figure 3.37A, lane 1), untreated BEACs were used as controls (Figure 3.37A, lane 2), 300 μ M MG (Figure 3.37A, lane 3) or MG in the presence of SAC/NAC- and compound A- loaded hADMSCs CM (Figure 3.37A, lanes 4 - 11), respectively. Tubulin was used as a loading control (Figure 3.37B).

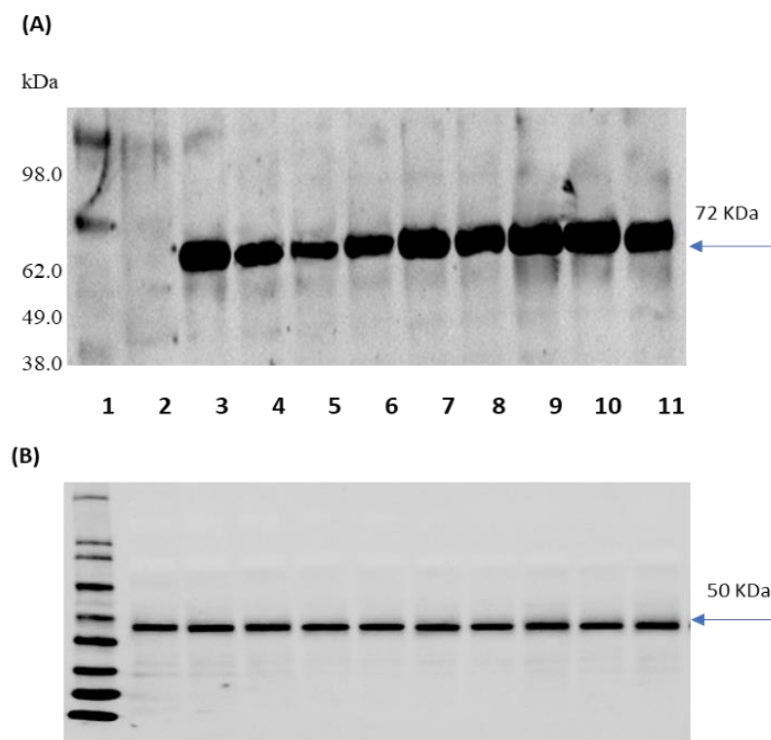


Figure 3.37: SDS-PAGE gel showing the effect of SAC/NAC- and compound A- loaded hADMSCs CM on BAEC glycation.

Representative Western blot of protein from BAECs incubated with MG and SAC/NAC- and compound A-loaded hADMSCs CM (day 1 - 4). Molecular Weight Marker (lane 1), untreated BEACs negative control (lane 2), treated BEACs with 300 μM MG positive control (lane 3) or MG in present of SAC/NAC- and compound A-loaded hADMSCs CM, day 1 (lanes 4 - 5), day 2 (Lanes 6 - 7), day 3 (Lanes 8 - 9) and day 4 (lanes 10 - 11), respectively. (B) Tubulin. The samples were separated by SDS-PAGE and the gels were transferred to nitrocellulose membranes and protein detected using an anti-MG antibody. The results are a representative example of three independent experiments.

Figure 3.38 shows the effect of CM on BAECs. The percentage inhibition compared to control was used to evaluate the inhibitory effect of both inhibitors on AGE formation. The results show that SAC/NAC- and compound A- CM significantly ($p < 0.05$) inhibited the formation of AGE at days 1 and 2. The maximum percentage of AGE inhibition was 44% and 45%, respectively. On the other hand, CM containing inhibitors did not show any inhibition of AGE formation at days 3 and 4.

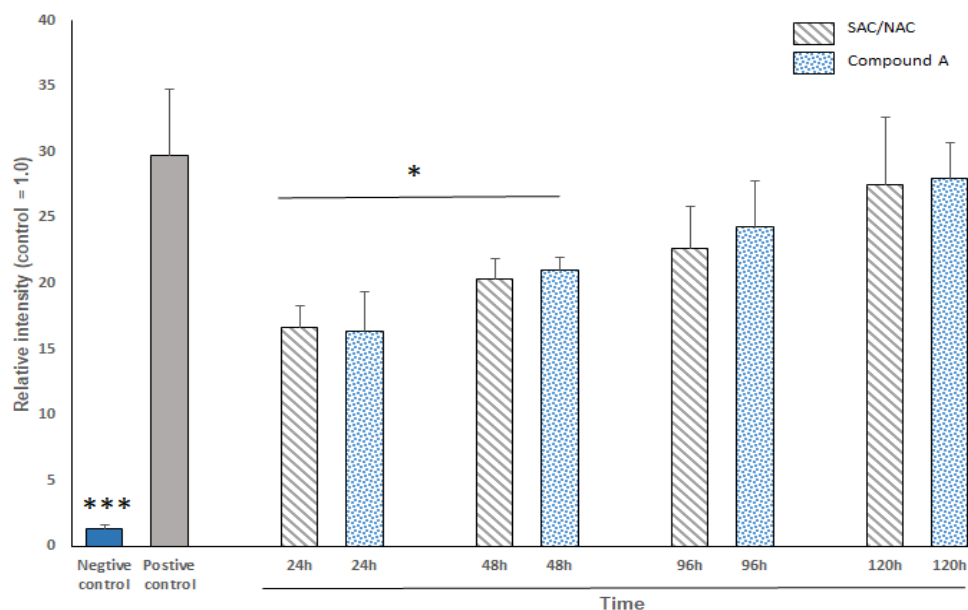


Figure 3.38: The effect of SAC/NAC and compound A loaded hADMSCs CM on BAEC glycation.

Bar chart showing the relative protein glycation by MG (72.0 kDa) (control = 1.0) from Figure 3.37. The experiment was repeated at least three times, * $P < 0.05$ and *** $p < 0.001$.

3.2.4 Detection of AGEs by ELISA

3.2.4.1 Standardisation of ELISA for measurement of AGE

A universal standard calibrator to identify AGE was available using an AGE ELISA kit (Human). The standard curve was generated by plotting the mean replicate relative OD₄₅₀ of each standard serial dilution point vs. the respective standard protein concentrations from 0-50ng/ml. The absorbance of samples was read from the calibration curve and expressed relative to a BSA-AGE standard in AGE ng of protein. Each sample was analysed in triplicate on the plate. The standard curve of BSA-AGE showed a linear correlation between the glycation protein concentration and the absorbance at 450nm (Figure 3.39).

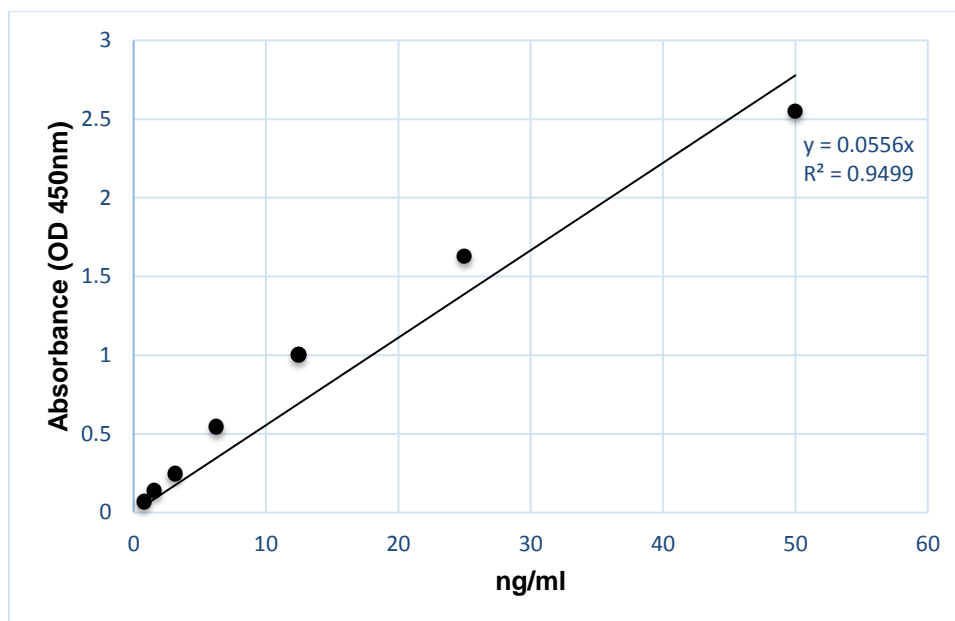


Figure 3.39: Standard curve of BSA-AGE.

3.2.4.2 The effect of SAC/NAC and compound A on AGE levels

A sandwich ELISA technique was used to detect AGE levels *in vitro* using a polyclonal anti-AGEs antibody in an attempt to validate the inhibitory effect of SAC/NAC and compound A on AGE formation. After 3 days' incubation, the concentration of AGE in BAEC was measured from untreated cells (negative control), cells treated with 300 μ M MG (positive control) or MG treated with SAC/NAC (Figure 3.40, A) and compound A (Figure 3.40, B). The results showed that the effect of SAC/NAC significantly ($p < 0.05$) inhibited AGEs' formation at concentrations of between 0.1-2 μ g/ml, while compound A also showed significant inhibition ($p < 0.05$) at concentrations between 0.05 - 2 μ g/ml. Therefore, AGE levels (U) in control cells ($2.31 \pm 0.07U$) was significantly higher than in samples containing inhibitors and inhibition of AGEs occurred in a dose-dependent manner (Figure 3.40).

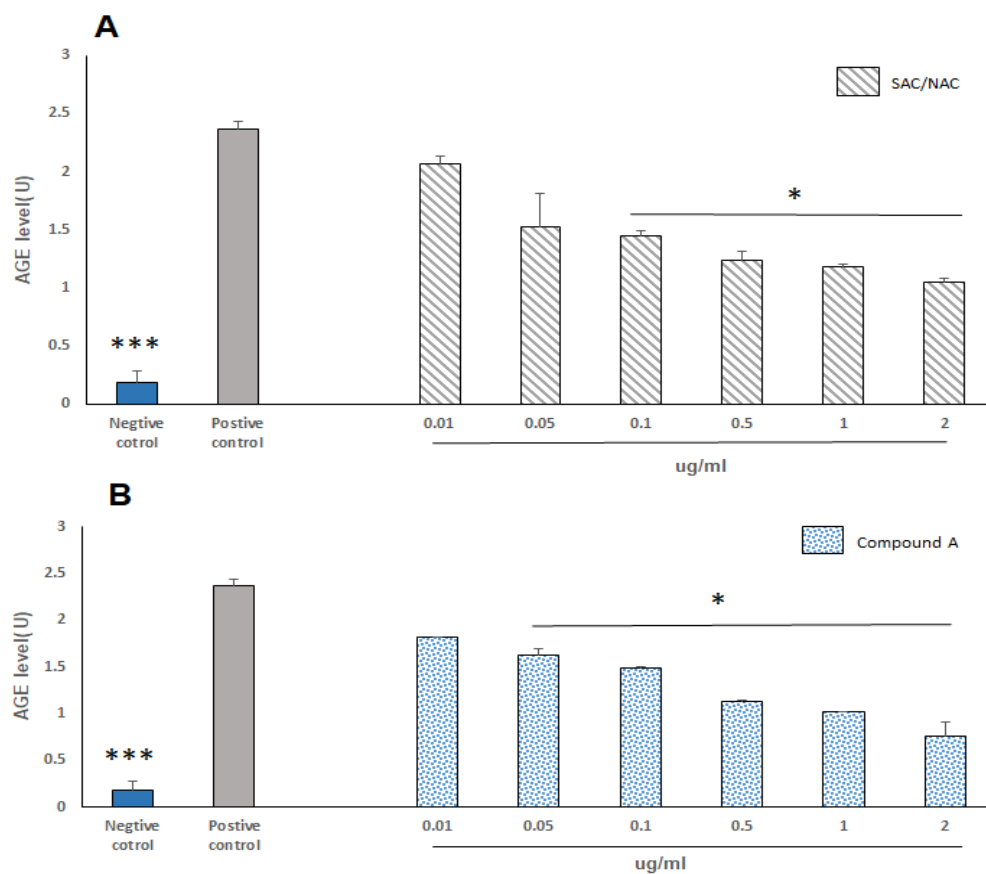


Figure 3.40: Interaction of SAC/NAC and compound A on MG induced AGEs' production. BAECs were incubated with 300 μ M MG and with or without (A) 0.01 - 2 μ g/ml SAC/NAC and (B) 0.01 - 2 μ g/ml compound A for 3 days. The bar graph shows the inhibition effect of both inhibitors on AGEs. The AGE levels, in 0.1ml of BSA-AGE diluted to 1 μ g/ml, were defined as 1 unit (U). The bar chart was made from the average of two independent experiments, * $P < 0.05$ and *** $p < 0.001$.

3.3 Cytotoxicity study of SAC/NAC using CellTiter-Blue® Cell Viability Assay

This study tested the toxicity of the SAC/NAC and compound A solution on hADMSCs. The results showed the maximum doses of SAC/NAC (Figure 3.41A) and compound A (Figure 3.41B), that did not affect cell viability, were 500 and 250 μ g/ml, respectively using the alamarBlue assay. Based on these results, maximum concentrations of SAC/NAC (500 μ g/ml) and compound A (250 μ g/ml), were employed in the current study. The effects of different concentrations of both SAC/NAC and compound A on hADMSCs viability are presented in Figure 3.41. The results showed that no significant inhibition of hADMSCs viability was found with

the inhibitors at all the concentrations. However, the inhibitors seemingly produced no cytotoxic effect.

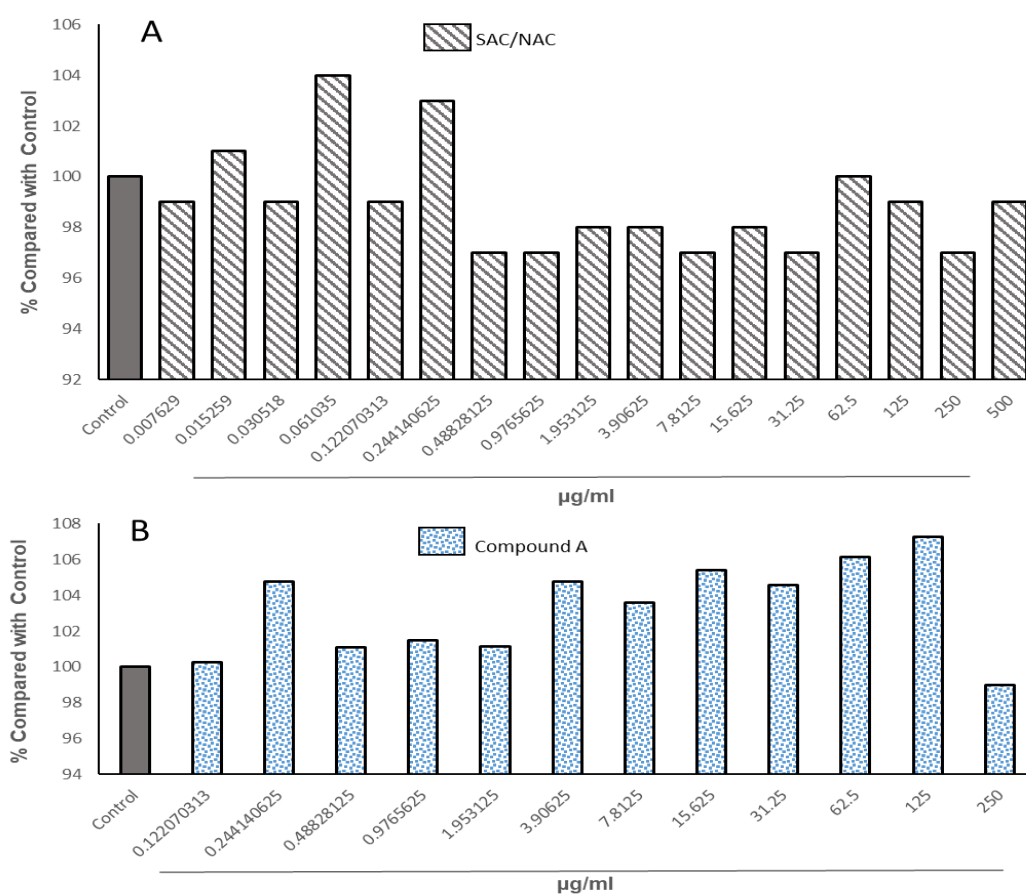


Figure 3.41: The effect of SAC/NAC and compound A on hADMSCs viability using the alamrBlue assay.

hADMSCs (2×10^5 /ml) were seeded in 96-well plates and incubated with (A) SAC/NAC (0.0076 – 500 µg/ml) and (B) compound A (0.122 - 250 µg/ml). After 24 hours of incubation, the cell suspension (100 µl) was mixed with 20 µl/well of CellTiter-Blue® Reagent and incubated for 4 hours before recording the fluorescence. Emission spectra were recorded at 560nm after excitation at 590nm using a Labsystems Fluoroskan Ascent plate reader. This experiment was done twice.

3.4 Cell Angiogenesis Assay

3.4.1 Effect of glucose on BAEC migration

Since cell migration is an essential process for angiogenesis (Griffioen and Molema, 2000), it was believed necessary to evaluate the effects of increased glucose levels on BAEC migration *in vitro* using a denudation injury model. To determine the effects of different concentrations of glucose treatment on cell migration (Figure 3.42), representative photomicrographs of the migration of untreated cells (1), cells treated with FGF-2 (2) or 15 - 100mM glucose (3 - 7) were evaluated. Due to the cell proliferation assay was not performed, images were only show the cell migration experiment. Pictures taken at time 0 and then after 24 hours to capture the differences in the number of cells which had migrated. In comparison to controls, the migration of cells in glucose concentrations of between 25 - 50mM were decreased significantly ($p < 0.05$) with the distance reduced ranging between 8.0 ± 2.0 and 6.0 ± 1.5 mm. The migration of wounded cells in the presence of glucose at concentrations of between 75 - 100mM were significantly decreased ($p < 0.01$) with the maximum distance reduced to 3.0 ± 2.0 mm. The inhibition was in a dose-dependent manner (Figure 3.43).

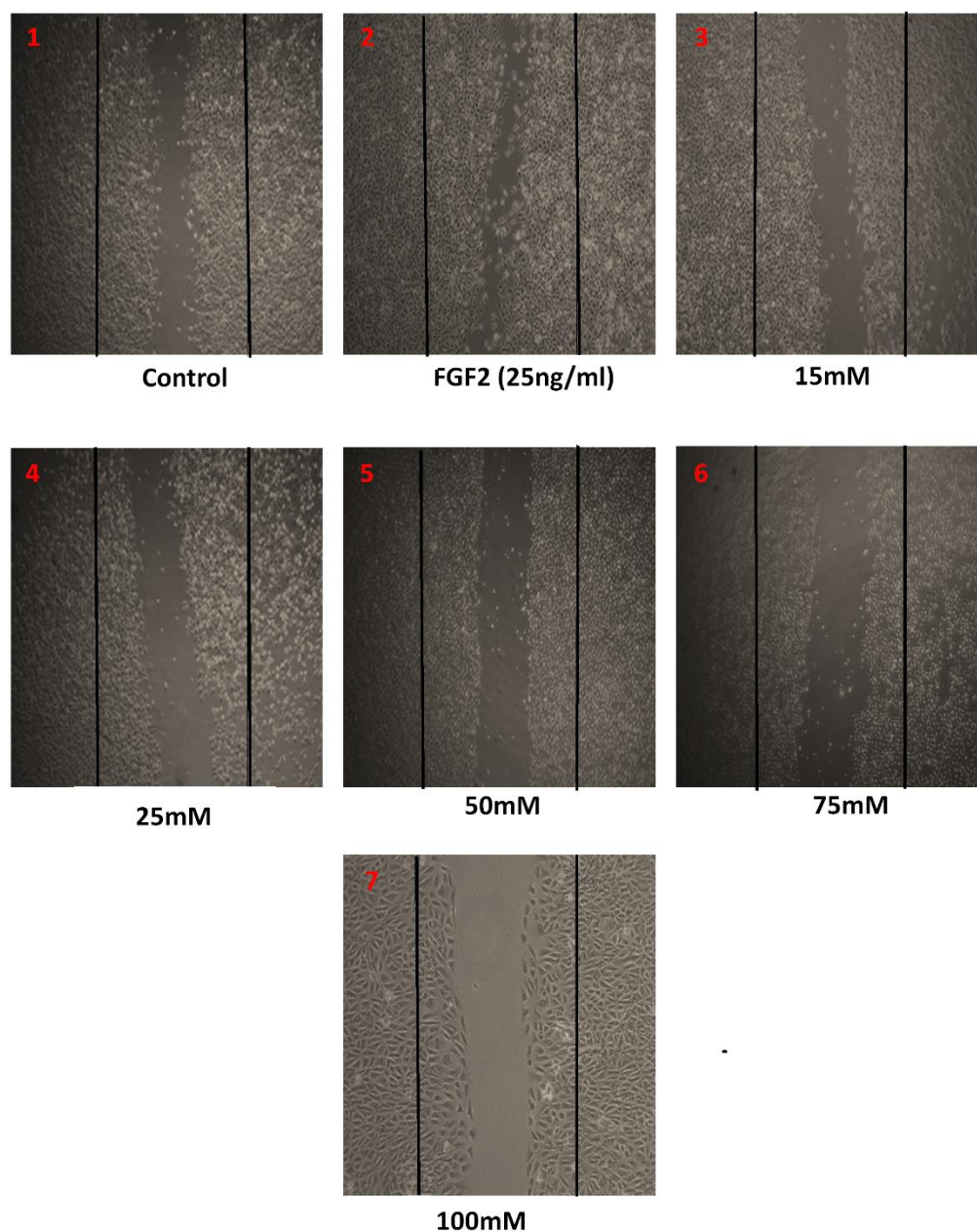


Figure 3.42: Photomicrographic showing the effect of glucose on BAEC wound healing. Photomicrographs 24 hours following wounding showing the effect of glucose on BAEC ($1 \times 10^6/\text{ml}$) migration were taken using phase contrast microscopy (magnification $\times 100$). Untreated cells cultured in 2.5% FBS (1), FGF-2 (25ng/ml) used as a positive control (2) or areas (3 – 7) show cells exposed to different concentrations of glucose (15 - 100mM). The number of migrated cells in the denuded area was counted in 5 random areas per slide and averaged accordingly. This panel is representative of at least two independent experiments.

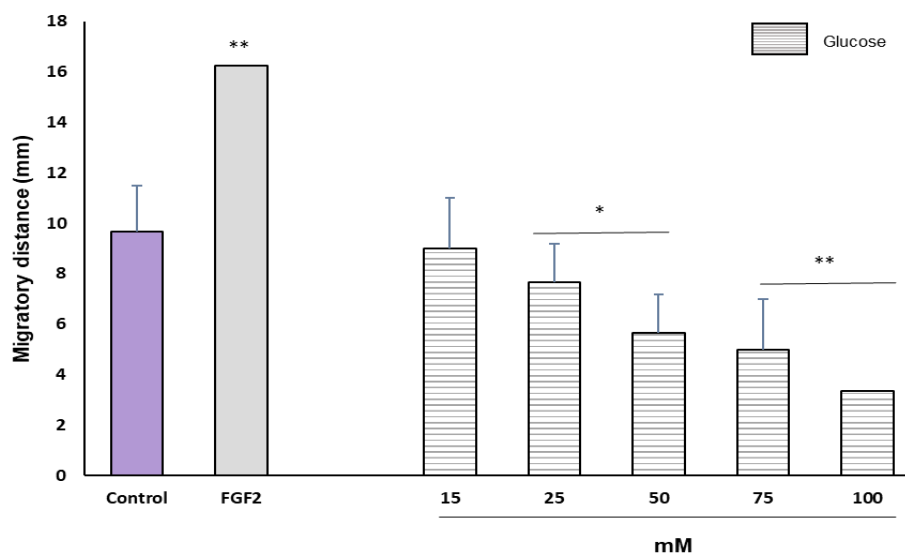


Figure 3.43: Effect of glucose on BAEC wound healing.

Bar graph showing the effect of different concentrations of glucose on BAEC migration. The number of migrated cells in the denuded area was counted in 5 random areas per slide and averaged accordingly. The results are presented as mean \pm S.D. (n=3), *P<0.05 and ** P<0.01, significantly different from control.

3.4.2 Effect of glucose on tube formation

As BAEC migration processes to the formation of microvascular tubes *in vitro*, assays for the tube-like structure of endothelial cells have been developed and used to study this crucial step of angiogenesis. The cells take only several hours to associate with each other and form micro-tubes. To test the effects of glucose on tube formation, an *in vitro* Matrigel assay was used (Figure 3.44). Representative photomicrographs show tube formation in untreated cells without FBS (1), untreated cells cultured in 2.5% FBS (2), cells treated with FGF-2 (3) or with 15 - 100mM glucose (4 - 8) are shown. Compared to untreated cells (negative control), FGF-2 was used as a positive control. Pictures were taken after 7 hours to capture the differences in the number of tubes formed. As shown in Figure 3.45, the capillary tube formation of BAECs was markedly and dose-dependently inhibited by the addition of glucose. BAECs exposed to glucose at concentrations of 25mM showed significant ($p<0.05$) inhibition of BAECs' closed areas with a percentage inhibition of 69% compared with control. Significant inhibition was shown at concentrations of between (50 - 100mM) with the percentage inhibition ranging from 81% - 93% compared with control ($p<0.01$). This inhibition occurred in a concentration-dependent manner. These results suggest that

high glucose-treated cells failed to form networks and showed impaired tube formation.

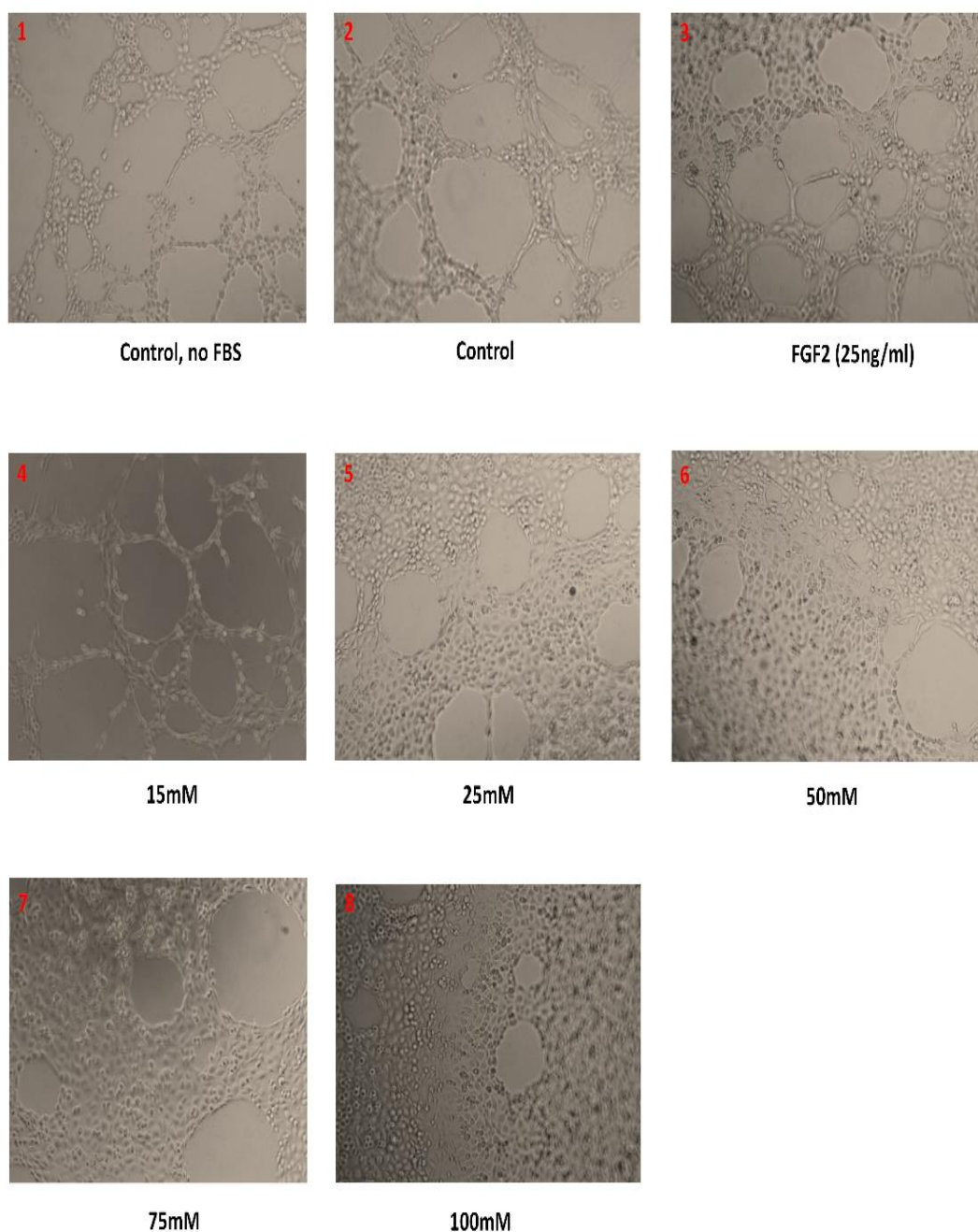


Figure 3.44: Photomicrographic showing the effect of glucose on BAEC tube formation. Photomicrographs showing the effect of glucose on BAEC (1×10^6 /ml) tube formation in Matrigel. Negative control (untreated cells) without FBS (1), untreated cells cultured in 2.5% FBS (2), FGF-2 (25ng/ml) used as a positive control (3) or areas (4 – 8) show cells exposed to different concentrations of glucose (15 - 100mM). After 7 hours, tubes had formed and the number of closed areas was counted from 5 random fields of 3 wells of a 96-well plate (magnification $\times 100$). This panel is a representative example of at least two independent experiments.

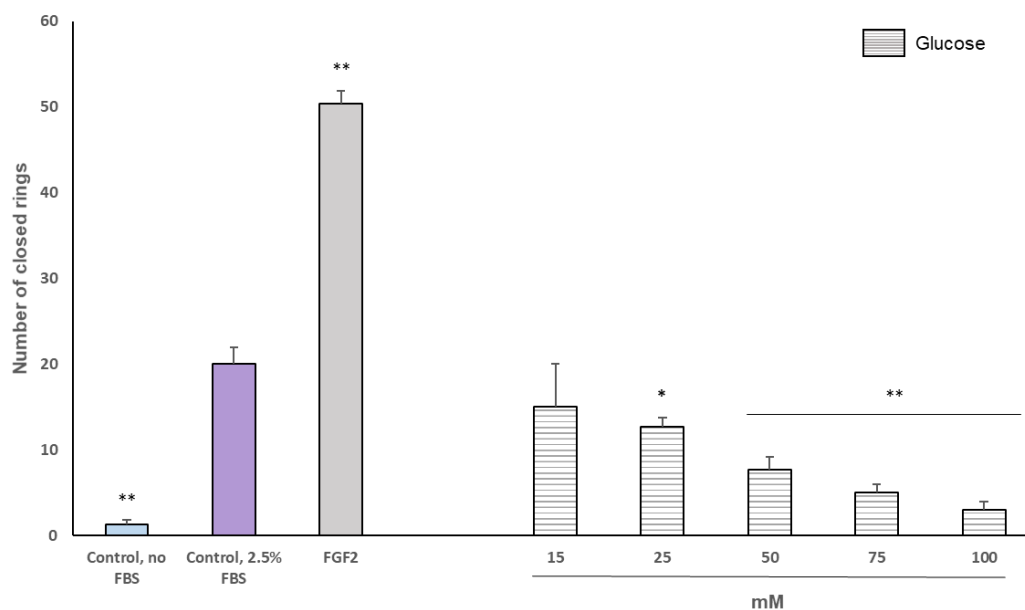


Figure 3.45: Effect of glucose on BAEC tube formation.

Bar graph showing the effect of different concentrations of glucose on BAEC tube formation. The results are presented as mean \pm S.D. (n=3), * $P < 0.05$ and ** $P < 0.01$, significantly different from control.

3.4.3 Effect of SAC/NAC in the presence of glucose on BAEC wound healing

As mentioned previously, glucose at high concentrations inhibited BAEC migration. This experiment was designed to determine whether SAC/NAC altered the effects of 75mM glucose on the migration of BAECs (Figure 3.46). Representative photomicrographs of the migration of untreated cells cultured in 2.5% FBS (1), cells treated with FGF-2 (2), 75mM glucose (3) or 0.01 - 2 μ g/ml SAC/NAC combined with 75mM glucose (4 - 9) are shown. Images were taken at time 0 and then after 24 hours to capture the differences in the number of cells which had migrated. In comparison to controls, the results showed the addition of SAC/NAC significantly inhibited cell migration at all concentrations ($p < 0.05$) with the maximum distance reduced to 3.0 ± 0.5 mm. The results suggested that SAC/NAC did not protect against the anti-migratory effect of glucose and the inhibition was dose-dependent (Figure 3. 47).

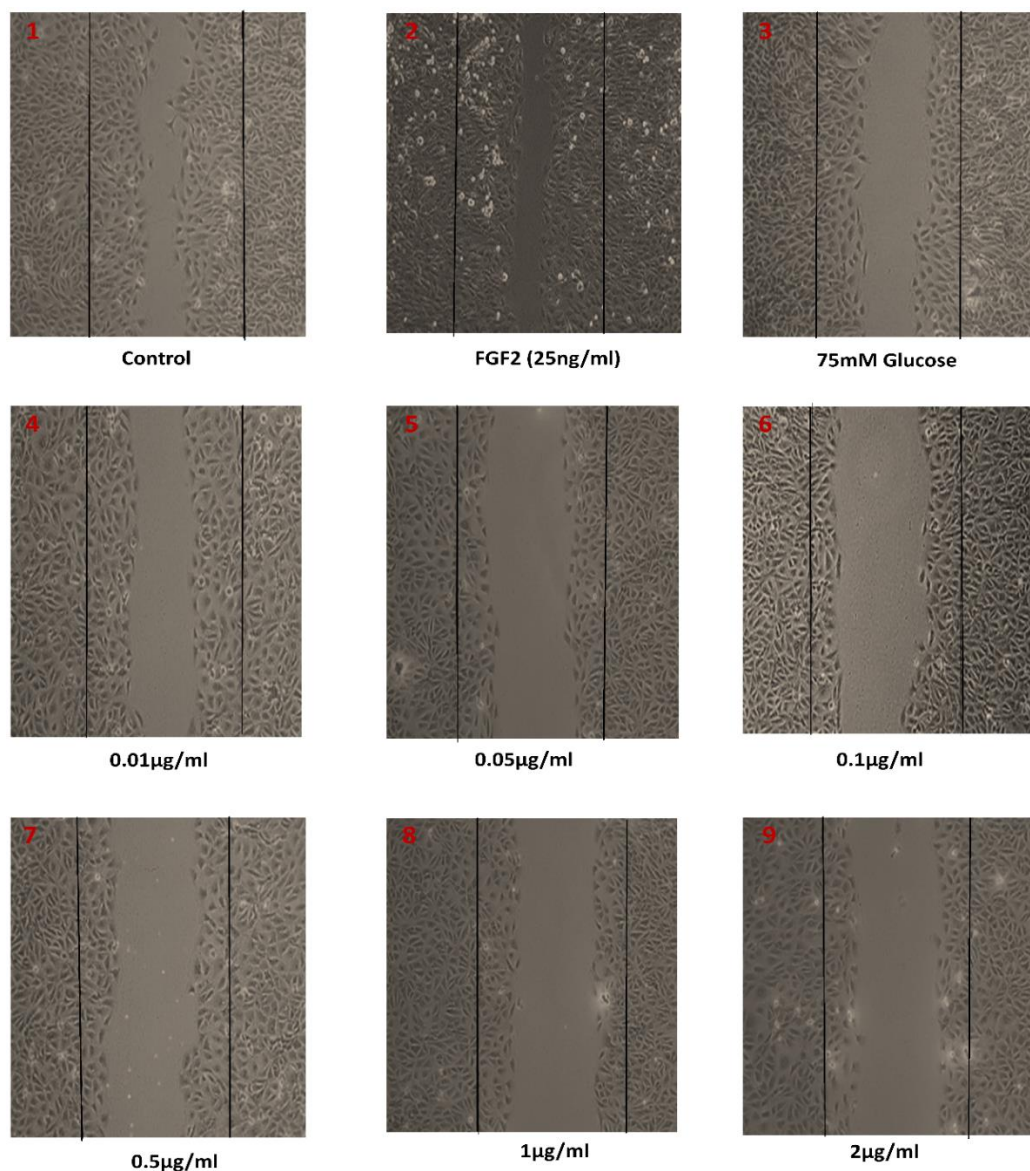


Figure 3.46: Photomicrographic showing the effect of SAC/NAC in the presence of glucose on BAEC wound healing.

Photomicrographs 24 hours following wounding showing the effect of SAC/NAC with 75mM of glucose on BAEC (1×10^6 /ml) migration were taken using phase contrast microscopy (magnification $\times 100$). Untreated cells cultured in 2.5% FBS (1), FGF-2 (25ng/ml) used as a positive control (2), 75mM glucose (3) or areas (4 – 9) show cells exposed to different concentrations of SAC/NAC (0.01 - 2µg/ml) with 75mM glucose. The number of migrated cells in the denuded area was counted in 5 random areas per slide and averaged accordingly. This panel is representative of at least two independent experiments.

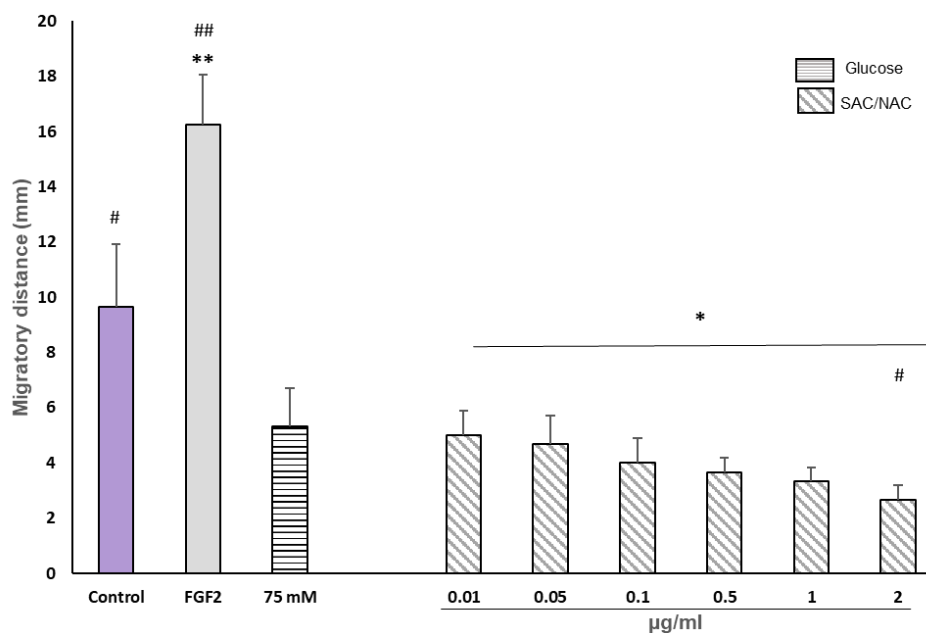


Figure 3.47: Effect of SAC/NAC in the presence of glucose on BAEC wound healing.

Bar graph showing the effect of different concentrations of SAC/NAC with 75mM of glucose on BAEC migration. All treatments were compared with the control (2.5% FBS). The number of migrated cells in the denuded area was counted in 5 random areas per slide and averaged accordingly. The results are presented as mean \pm S.D. (n=3), * $P < 0.05$ and ** $P < 0.01$, significantly different from control. # $P < 0.05$ and ## $P < 0.01$, significantly different from glucose (75mM).

3.4.4 Effect of SAC/NAC in the presence of glucose on BAEC tube formation

To determine whether SAC/NAC altered the effects of 75mM glucose on endothelial cells capillary tube formation (Figure 3.48), representative photomicrographs are shown of the tube formation in untreated cells without FBS (1), untreated cells cultured in 2.5% FBS (2), cells treated with FGF-2 (3), 75mM glucose (4) or 0.01-2 μ g/ml SAC/NAC combined with 75mM glucose (5 - 10) are shown. Compared to the untreated cells (negative control), FGF-2 was used as a positive control. Pictures were taken after 7 hours to capture the differences in the number of tubes formed. As shown in Figure 3.49, in comparison to controls, the addition of SAC/NAC significantly inhibited tube formation at all concentrations with the percentage inhibition ranging from 86% - 97% compared with control ($p < 0.01$). The results indicated that SAC/NAC has no protective effect on the tube formation and the inhibition was dose-dependent.

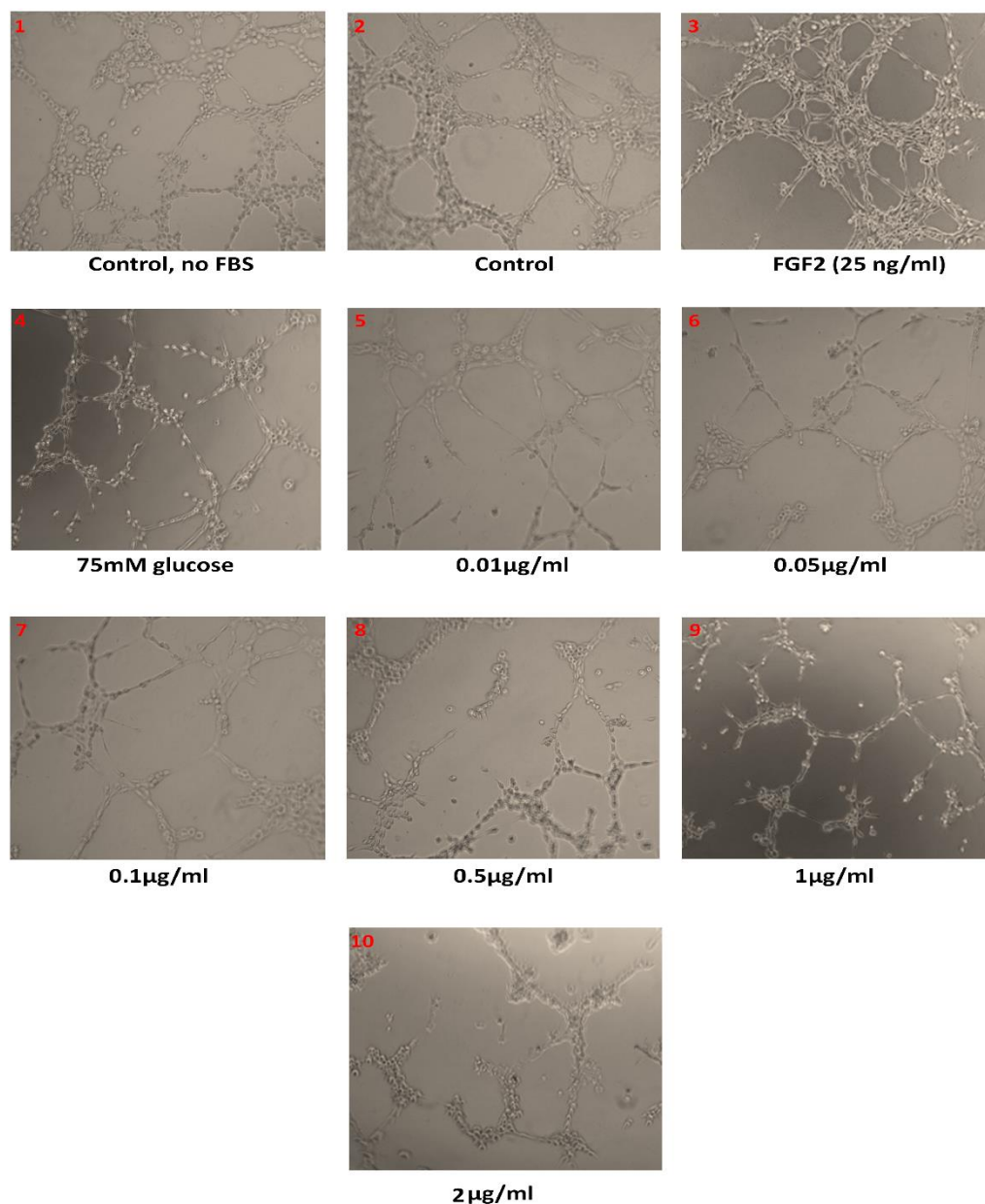


Figure 3.48: Photomicrographic showing the effect of SAC/NAC in the presence of glucose on BAEC tube formation.

Photomicrographs showing the effect of SAC/NAC with 75mM of glucose on BAEC (1×10^6 /ml) tube formation in Matrigel (magnification $\times 100$). Negative control (untreated cells) without FBS (1), untreated cells cultured in 2.5% FBS (2), FGF-2 (25ng/ml) used as a positive control (3), 75mM glucose (4) or areas (5 – 10) show cells exposed to different concentrations of SAC/NAC (0.01 - 2µg/ml) with 75mM glucose. After 7 hours, tubes had formed and the number of closed areas was counted from 5 random fields of 3 wells of a 96-well plate. This panel is a representative example of at least two independent experiments.

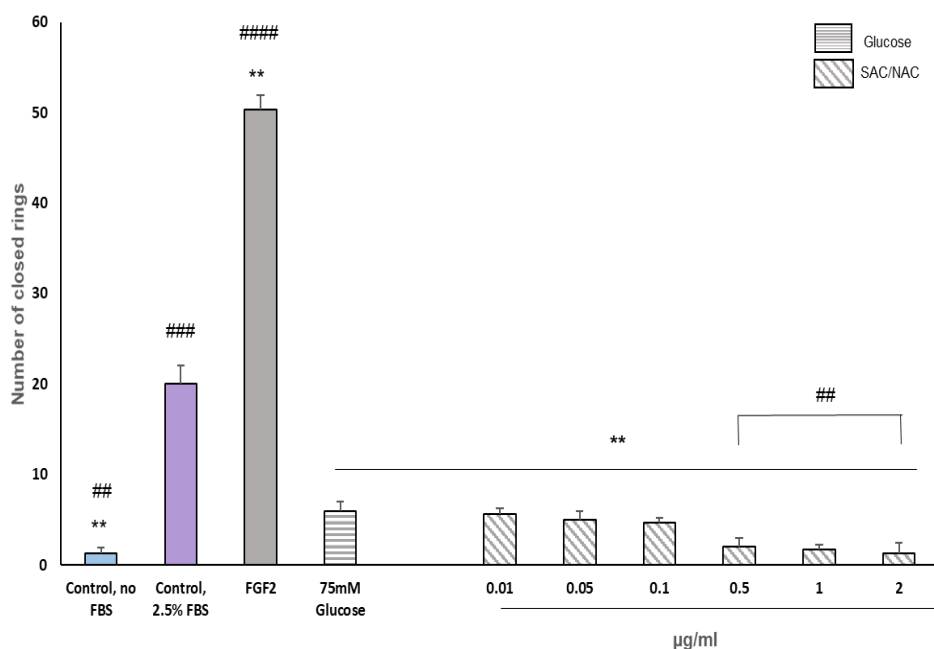


Figure 3.49: Effect of SAC/NAC in the presence of glucose on BAEC tube formation.

Bar graph showing the effect of different concentrations of SAC/NAC with 75mM of glucose on BAEC tube formation. The results are presented as mean \pm S.D. (n=3), ** $P < 0.01$, significantly different from control. # $P < 0.01$, ### $P < 0.001$ and #### $P < 0.0001$, significantly different from 75mM glucose.

3.4.5 Effect of compound A in the presence of glucose on BAEC wound healing

Figure 3.50 shows representative photomicrographs of the migration of untreated cells cultured in 2.5% FBS (1) or cells treated with FGF-2 (2), 75mM glucose (3) or 0.01 - 2µg/ml compound A combined with 75mM glucose (4 - 9) are shown. The images were taken at time 0 and then after 24 hours to capture the differences in a number of cells that had migrated. In comparison to controls, the results showed the addition of compound A at concentrations of between 0.01 - 0.5µg/ml significantly ($p < 0.05$) inhibited the cell migration while at the concentration of 1 - 2µg/ml, there were more significant inhibition ($p < 0.01$) with the maximum distance being reduced to 2.0 ± 0.9 mm. The results suggested compound A did not protect against the anti-migratory effect of glucose and the inhibition was dose-dependent (Figure 3.51).

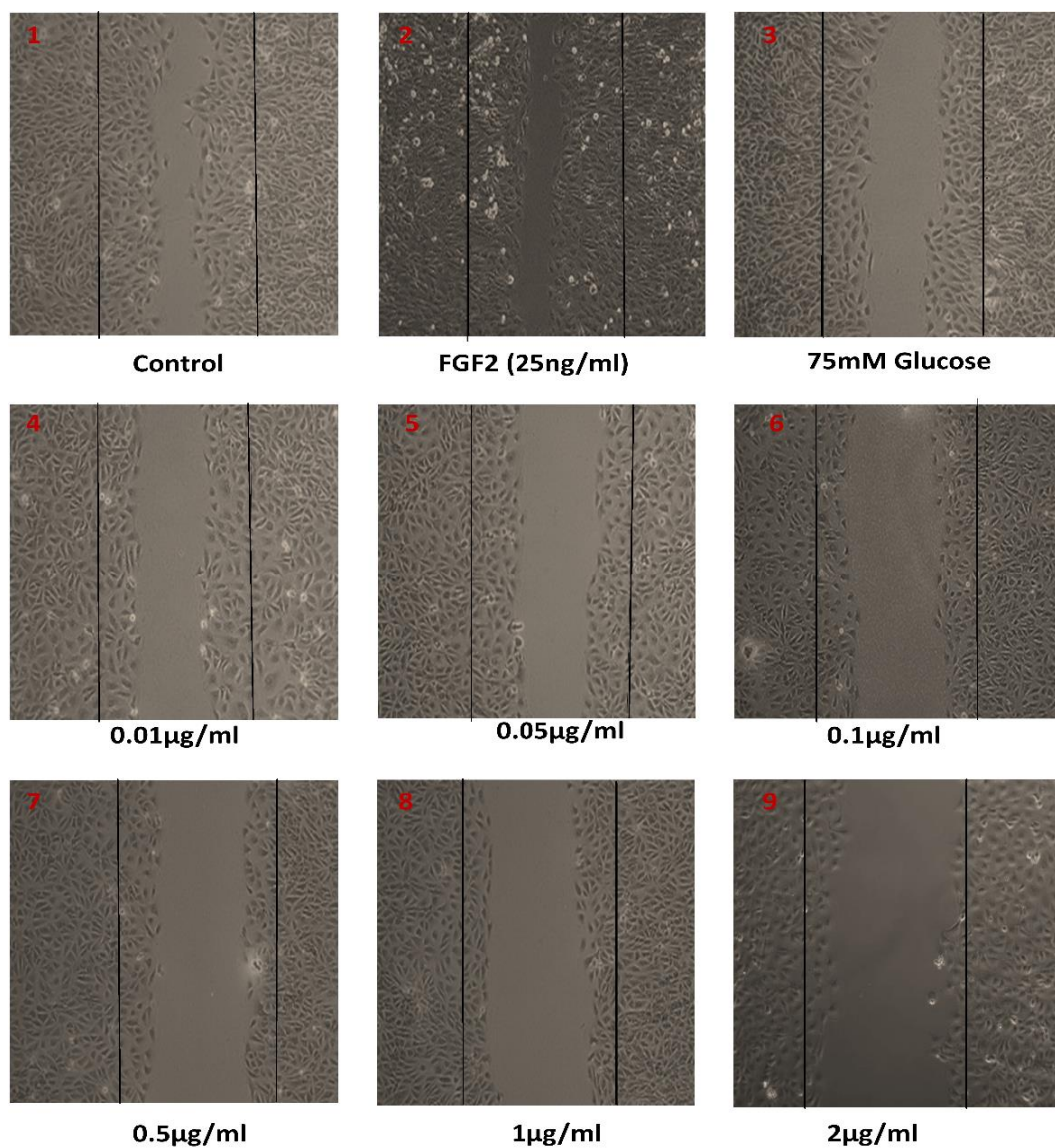


Figure 3.50: Photomicrographic showing the effect of compound A in the presence of glucose on BAEC wound healing.

Photomicrographs 24 hours following wounding showing the effect of compound A with 75mM of glucose on BAEC (1×10^6 /ml) migration were taken using phase contrast microscopy (magnification $\times 100$). Untreated cells cultured in 2.5% FBS (1), FGF-2 (25ng/ml) used as a positive control (2), 75mM glucose (3) or areas (4 - 9) shows cells exposed to different concentrations of compound A (0.01 - 2µg/ml) with 75mM glucose. The number of migrated cells in the denuded area was counted in 5 random areas per slide and averaged accordingly. This panel is representative of at least two independent experiments.

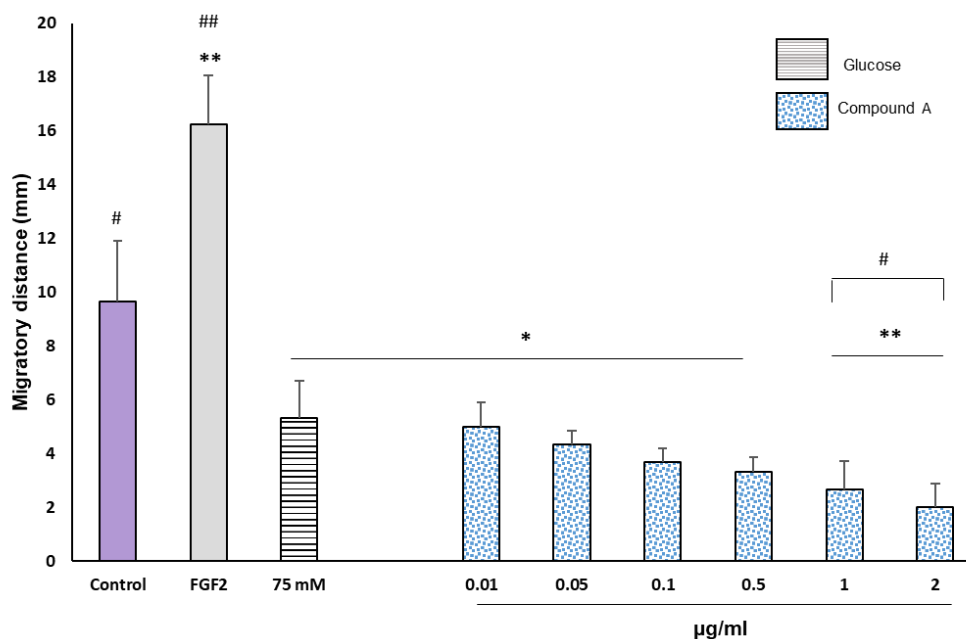


Figure 3.51: Effect of compound A in the presence of glucose on BAEC wound healing. Bar graph showing the effect of different concentrations of compound A with 75mM of glucose on BAEC migration. All treatments were compared against the positive control (2.5% FBS). The number of migrated cells in the denuded area was counted in 5 random areas per slide and accordingly averaged. The results are presented as mean \pm S.D. (n=3), * $P < 0.05$ and ** $P < 0.01$, significantly different from control. # $P < 0.05$, and ## $P < 0.01$, significantly different from 75mM glucose.

3.4.6 Effect of compound A in the presence of glucose on BAEC tube formation

Using the Matrigel assay, the influence of mimic compound A treated with high glucose (75mM) on BAEC tube formation was also investigated (Figure 3.52). Representative photomicrographs of the tube formation in untreated cells without FBS (1), untreated cells cultured in 2.5% FBS (2), cells treated with FGF-2 (3), 75mM glucose (4) or 0.01 - 2 μ g/ml compound A combined with 75mM glucose (5 - 10) are shown. Compared to the untreated cells (negative control), FGF-2 was used as a positive control. Images were taken after 7 hours to capture the differences in the number of tubes formed. In comparison to controls, the addition of compound A significantly ($p < 0.01$) inhibited tube formation at concentrations (0.01 - 2 μ g/ml) with the maximum percentage inhibition of 98%. The results indicated that compound A has no protective effect on the tube formation and the inhibition was dose-dependent (Figure 3.53).

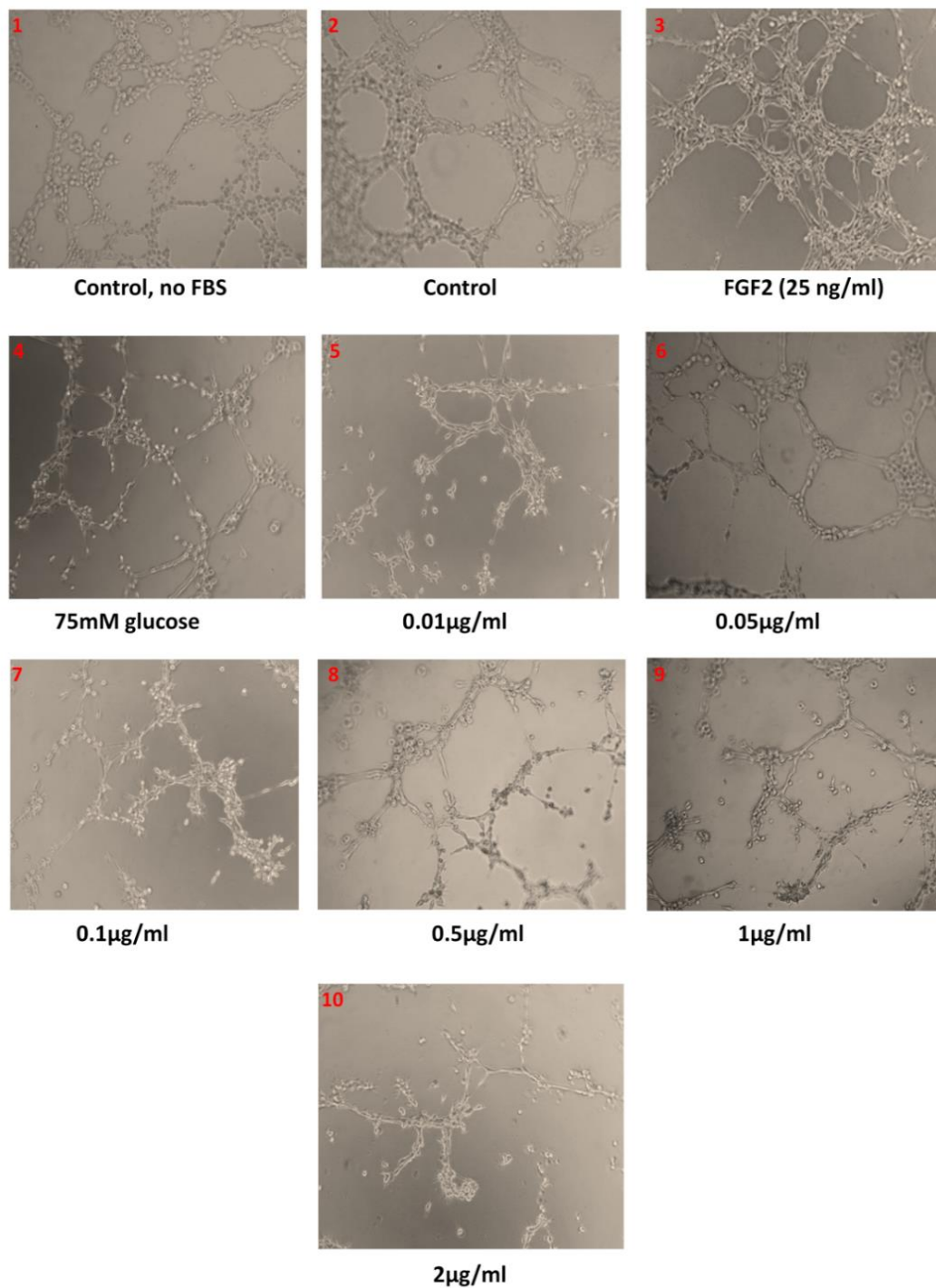


Figure 3.52: Photomicrographic showing the effect of compound A in the presence of glucose on BAEC tube formation.

Photomicrographs showing the effect of compound A with 75mM of glucose on BAEC (1×10^6 /ml) tube formation in Matrigel (magnification $\times 100$). Negative control (untreated cells) without FBS (1), untreated cells cultured in 2.5% FBS (2), FGF-2 (25ng/ml) used as a positive control (3), 75mM glucose (4) or areas (5 - 10) shows cells exposed to different concentrations of compound A (0.01 - 2µg/ml) with 75mM glucose. After 7 hours, tubes had formed and the number of closed areas was counted from 5 random fields of 3 wells of a 96-well plate. This panel is a representative example of at least two independent experiments.

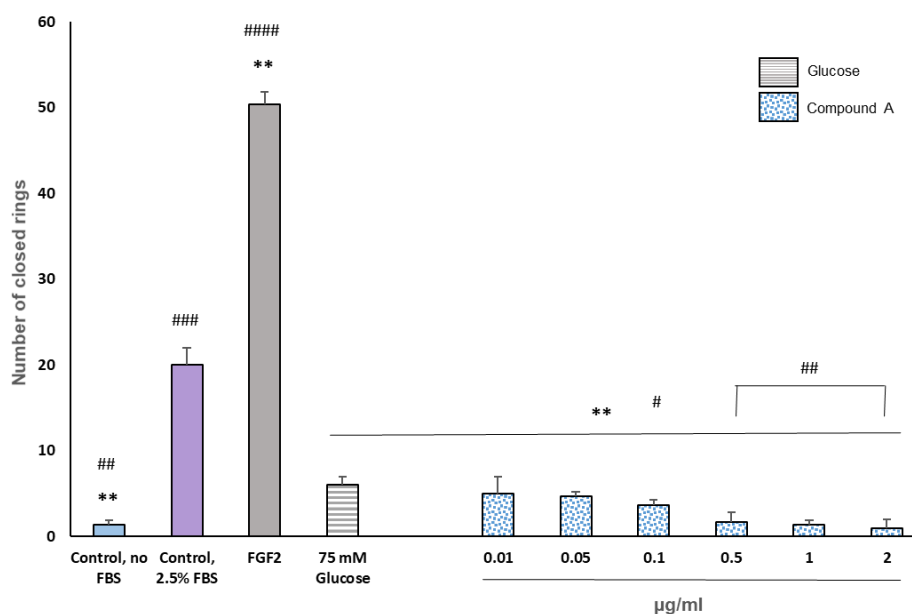


Figure 3.53: Effect of compound A in the presence of glucose on BAEC tube formation.

Bar graph showing the effect of compound A with 75mM of glucose on BAEC tube formation. The results are presented as mean \pm S.D. (n=3), ** $P < 0.01$, significantly different from control. ### $P < 0.001$, #### $P < 0.0001$, significantly different from 75mM glucose.

3.4.7 Effect of BSA-AGEs on BAEC wound healing

This study was designed to determine the effect of BSA-AGEs on endothelial cells. Following 24 hours of incubation (Figure 3.54), representative photomicrographs were taken of the migration of untreated cells cultured in 2.5% FBS (1), cells treated with FGF-2 (2) or 15 - 50 $\mu\text{g/ml}$ BSA-AGEs (3 - 6) are shown. Images were taken at time 0 and then after 24 hours to capture the differences in the number of cells which had migrated. In comparison to controls, BSA-AGEs markedly ($p < 0.05$) decreased cell migration across the middle line at concentrations of between 15 - 35 $\mu\text{g/ml}$ with the distance migrated being reduced to between of 8.0 ± 2.0 - 6.0 ± 3.0 mm. The distance migrated showed a more significant reduction to 3.0 ± 0.9 mm ($p < 0.01$) when the cells were treated with 50 $\mu\text{g/ml}$ BSA-AGEs and the inhibition was dose-dependent (Figure 3.55).

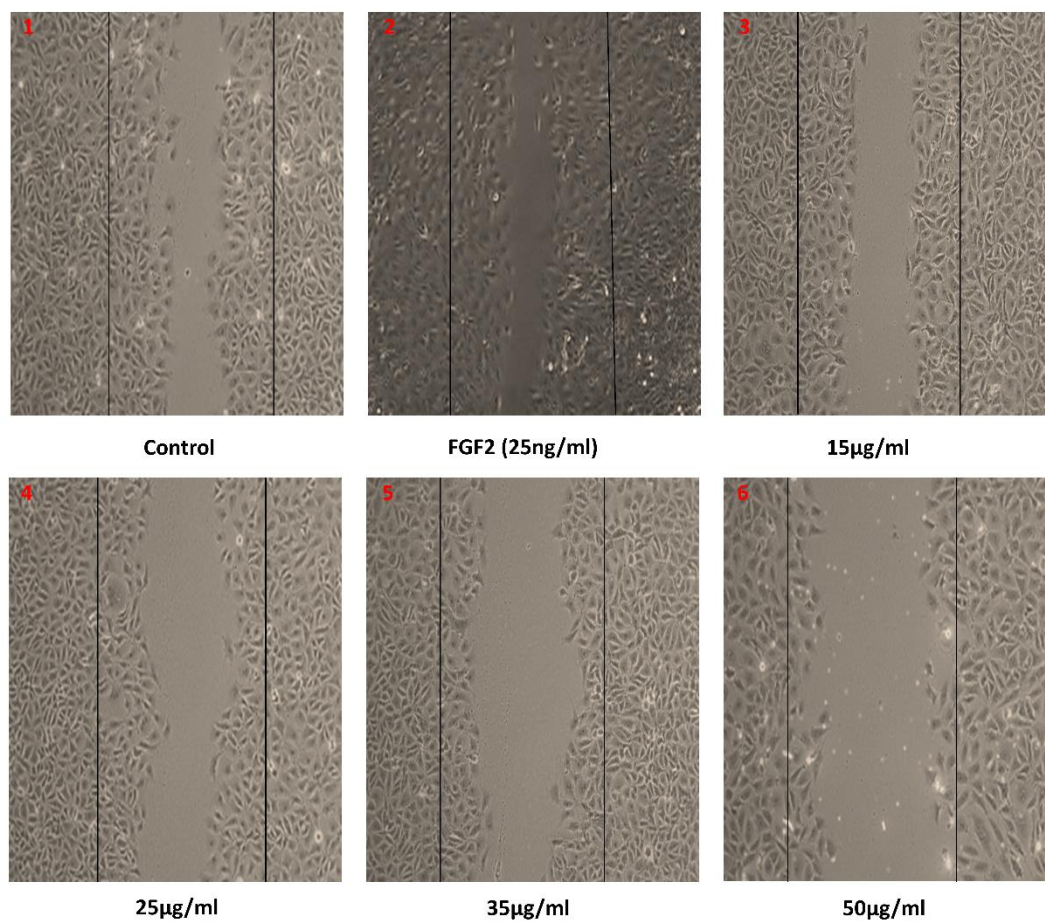


Figure 3.54: Photomicrographic showing the effect of BSA-AGEs on BAEC wound healing. Photomicrographs 24 hours following wounding showing the effect of different concentrations of BSA-AGEs on BAEC ($1 \times 10^6/\text{ml}$) cell migration were taken using phase contrast microscopy (magnification $\times 100$). Untreated cells cultured in 2.5% FBS (1), FGF-2 (25ng/ml) used as a positive control (2) or areas (3 – 6) show cells exposed to different concentrations of BSA-AGEs (15 - 50µg/ml). The number of migrated cells in the denuded area was counted in 5 random areas per slide and averaged accordingly. This panel is representative of at least two independent experiments.

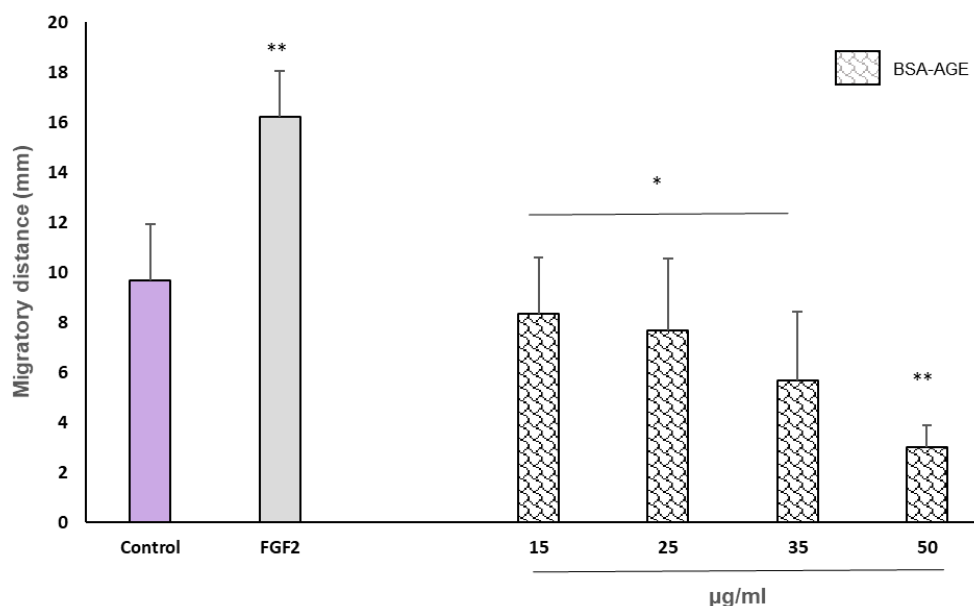


Figure 3.55: Effect of BSA-AGEs on BAEC wound healing.

Bar graph showing the effect of different concentrations of BSA-AGEs on BAEC migration. The number of migrated cells in the denuded area was counted in 5 random areas per slide and averaged accordingly. The results are presented as mean \pm S.D. (n=3), * $P < 0.05$ and ** $P < 0.01$, significantly different from controls.

3.4.8 Effect of BSA-AGEs on BAEC tube formation

Using the Matrigel assay, the effect of BSA-AGEs on BAEC tube formation was also investigated (Figure 3.56). Representative photomicrographs of the tube formation in untreated cells without FBS (1), untreated cells cultured in 2.5% FBS (2), cells treated with FGF-2 (3) or 15 - 50 μ g BSA-AGEs (4 - 7) are shown. Compared to the untreated cells (negative control), FGF-2 was used as a positive control. Images were taken after 7 hours to capture the differences in a number of tubes formed. The results showed that AGEs suppressed tube formation of endothelial cells effectively ($p < 0.01$) at a concentration of 25 μ g/ml with percentage inhibition of 69% while the inhibition was significantly greater ($p < 0.001$) at concentrations of between 35 - 50 μ g/ml with percentage inhibition ranging of between 75% - 79%. Thus, the results demonstrated the suppressive effect of BSA-AGEs on BAEC tube formation in a dose-dependent manner (Figure 3.57).

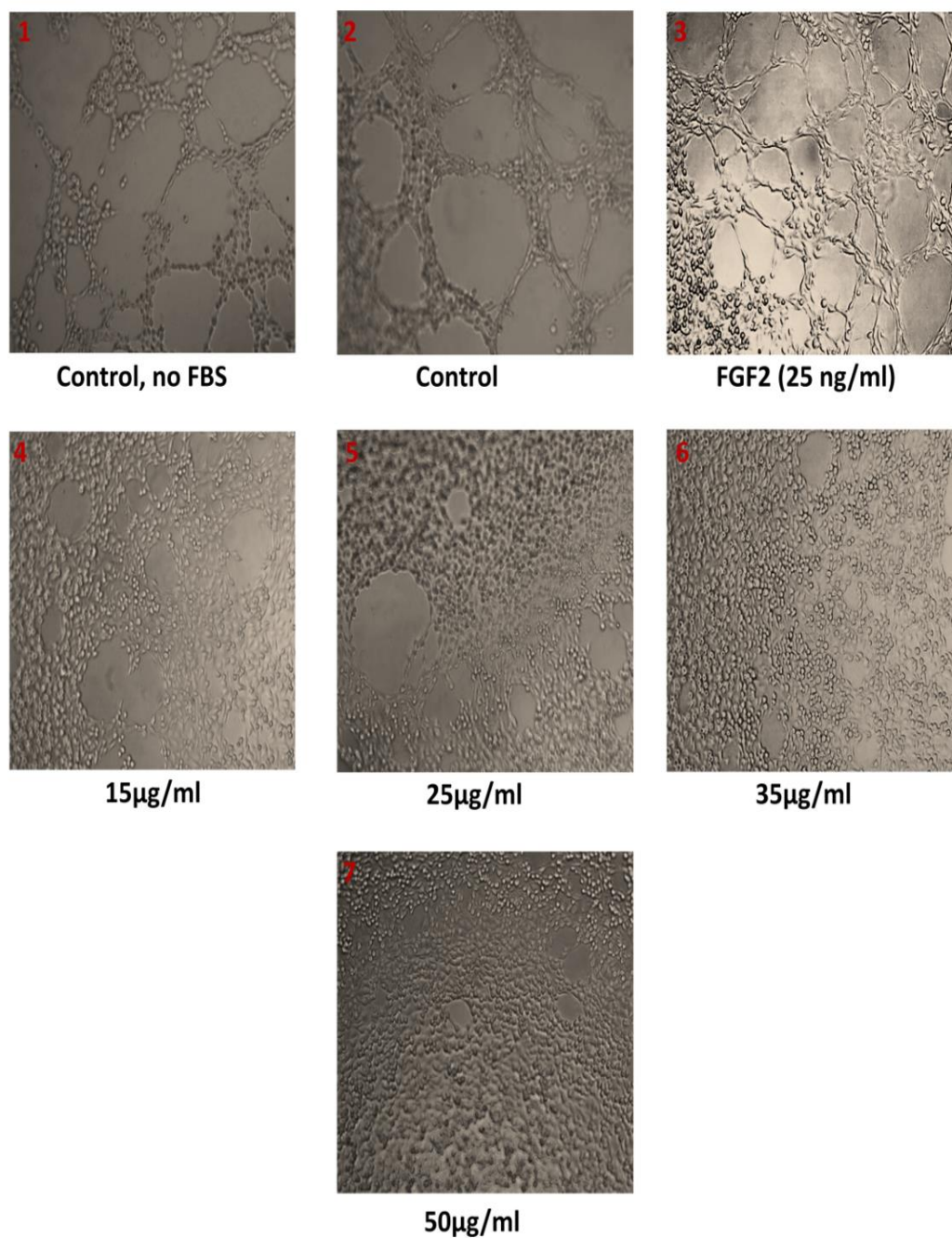


Figure 3.56: Photomicrographic showing the effect of BSA-AGEs on BAEC tube formation. Photomicrographs showing the effect of different concentrations of BSA-AGEs on BAEC (1×10^6 /ml) tube formation in Matrigel (magnification $\times 100$). Negative control (untreated cells) without FBS (1), untreated cells cultured in 2.5% FBS (2), FGF-2 (25ng/ml) used as a positive control (3) or areas (4 – 7) show cells exposed to different concentrations of BSA-AGEs (15 - 50µg/ml). After 7 hours, tubes had formed and the number of closed areas was counted from 5 random fields of 3 wells of a 96-well plate. This panel is a representative example of at least two independent experiments.

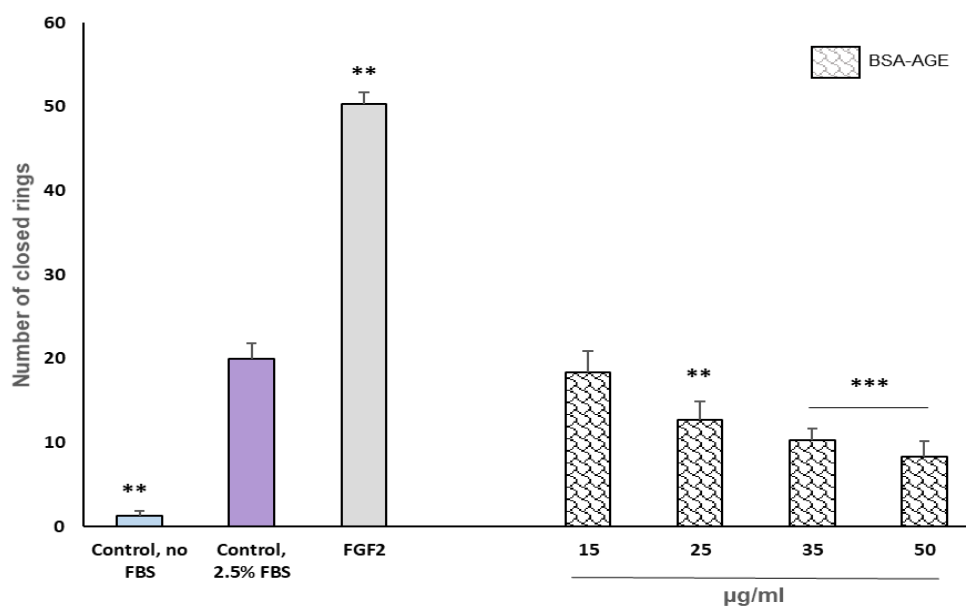


Figure 3.57: Effect of BSA-AGEs on BAEC tube formation.

Bar graph showing the effect of different concentrations of BSA-AGEs on BAEC tube formation. The results are presented as mean \pm S.D. (n=3), ** $P < 0.01$ and *** $P < 0.001$, significantly different from controls.

3.4.9 Effect of SAC/NAC in the presence of BSA-AGEs on BAEC wound healing

Since AGEs at high concentrations were shown as a potent inhibitor of BAEC migration, it was interesting to test whether SAC/NAC is able to reverse the effects of a high concentration of BSA-AGEs (50 $\mu\text{g/ml}$) on the migration of BAECs (Figure 3.58). Representative photomicrographs of the migration of untreated cells cultured in 2.5% FBS (1), cells treated with FGF-2 (2), 50 $\mu\text{g/ml}$ BSA-AGEs (3) or 0.01 - 2 $\mu\text{g/ml}$ SAC/NAC combined with 50 $\mu\text{g/ml}$ BSA-AGEs (4 - 9) are shown. Images were taken at time 0 and then after 24 hours to capture the differences in the number of cells that had migrated. The addition of SAC/NAC not only suppressed the inhibitory effect of BSA-AGEs on BAEC migration but significantly induced cell migration at concentrations of 1 $\mu\text{g/ml}$ ($p < 0.05$) and 2 $\mu\text{g/ml}$ ($p < 0.01$). At the same time, the maximum distance migrated increased to $16.0 \pm 2.0\text{mm}$. The results suggested that the migration of endothelial cells was promoted in a dose-dependent manner (Figure 3.59).

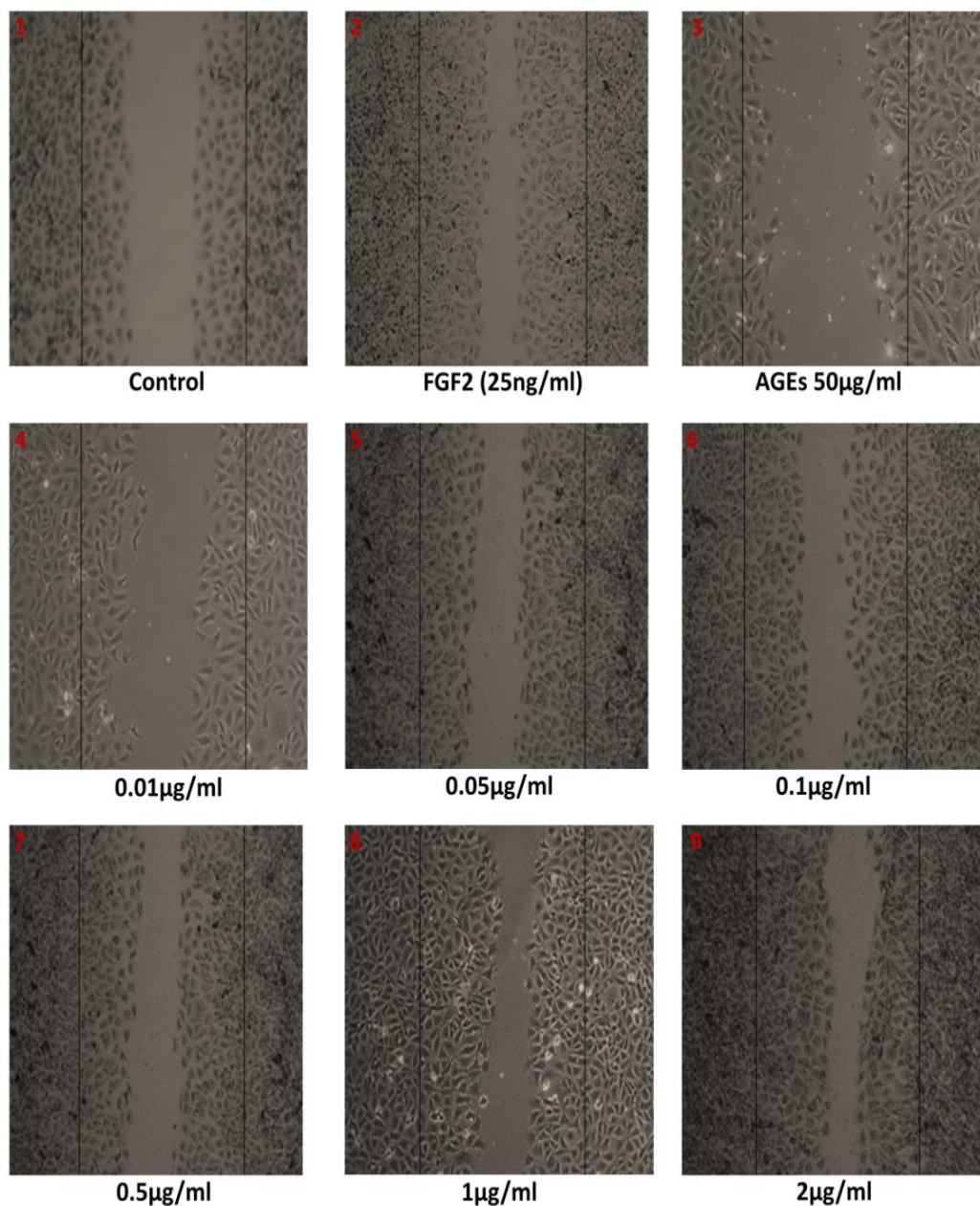


Figure 3.58: Photomicrographic showing the effect of SAC/NAC in presence of BSA-AGEs on BAEC wound healing.

Photomicrographs 24 hours following wounding showing the effect of different concentrations of SAC/NAC with BSA-AGEs on BAEC (1×10^6 /ml) migration were taken using phase contrast microscopy (magnification $\times 100$). Untreated cells cultured in 2.5% FBS (1), FGF-2 (25ng/ml) used as a positive control (2), 50µg/ml BSA-AGEs (3) or areas (4 – 9) show cells exposed to different concentrations of SAC/NAC (0.01 - 2µg/ml) with 50µg/ml BSA-AGEs. The number of migrated cells in the denuded area was counted in 5 random areas per slide and averaged accordingly. This panel is representative of at least two independent experiments.

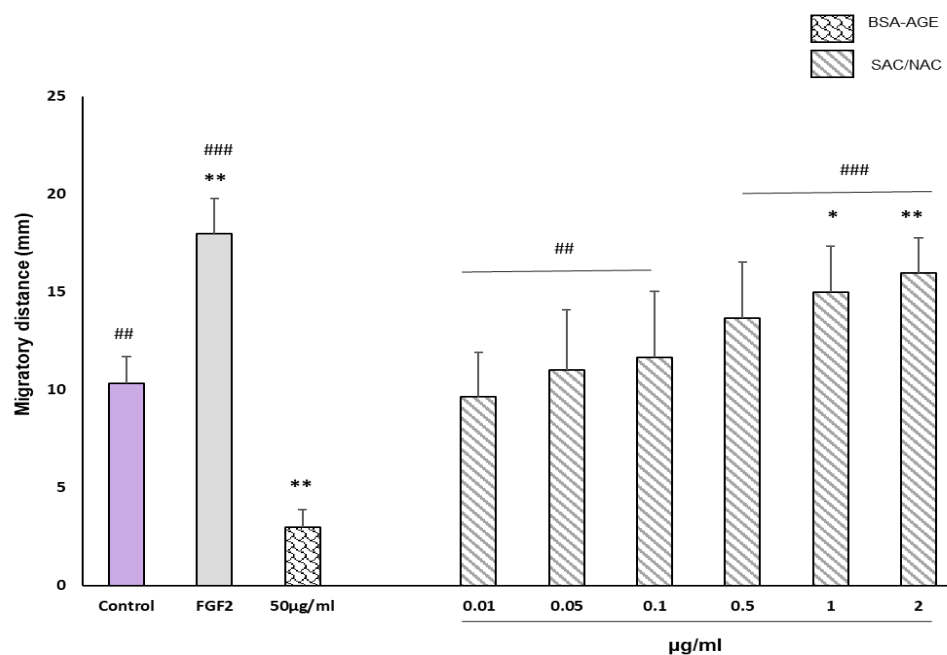


Figure 3.59: Effect of SAC/NAC in the presence of BSA-AGEs on BAEC wound healing. Bar graph showing the effect of different concentrations of SAC/NAC with 50µg/ml BSA-AGEs on BAEC migration. The number of migrated cells in the denuded area was counted in 5 random areas per slide and averaged accordingly. The results are presented as mean \pm S.D. (n=3), * P <0.05 and ** P <0.01, significantly different from control. ## P <0.01 and ### P <0.001, significantly different from BSA-AGEs (50µg/ml).

3.4.10 Effect of SAC/NAC in the presence of BSA-AGEs on BAEC tube formation

As shown in the previous results, AGEs at high concentrations of 35-50µg/ml were shown to be a potent inhibitor of BAEC tube formation (Figure 3.56). Therefore, experiments were performed to check whether SAC/NAC was able to reverse the effects of a high concentration of BSA-AGEs (50µg/ml) on tube formation (Figure 3.60). Representative photomicrographs of the tube formation in untreated cells without FBS (1), untreated cells cultured in 2.5% FBS (2), cells treated with FGF-2 (3), 50µg/ml BSA-AGEs (4) or 0.01 - 2µg/ml SAC/NAC combined to 50µg/ml BSA-AGEs (5 - 10) are shown. Compared to the untreated cells (negative control), FGF-2 was used as a positive control. Images were taken after 7 hours to capture the differences in the number of tubes formed. The results showed that addition of SAC/NAC suppressed the inhibitory effect of BSA-AGEs on BAEC tube formation and significantly induced tube formation at concentrations of between 1 - 2µg/ml in a dose-dependent manner (p <0.05) with percentage inhibition ranging from 37.0% - 36.0% compared to the control (Figure 3.61).

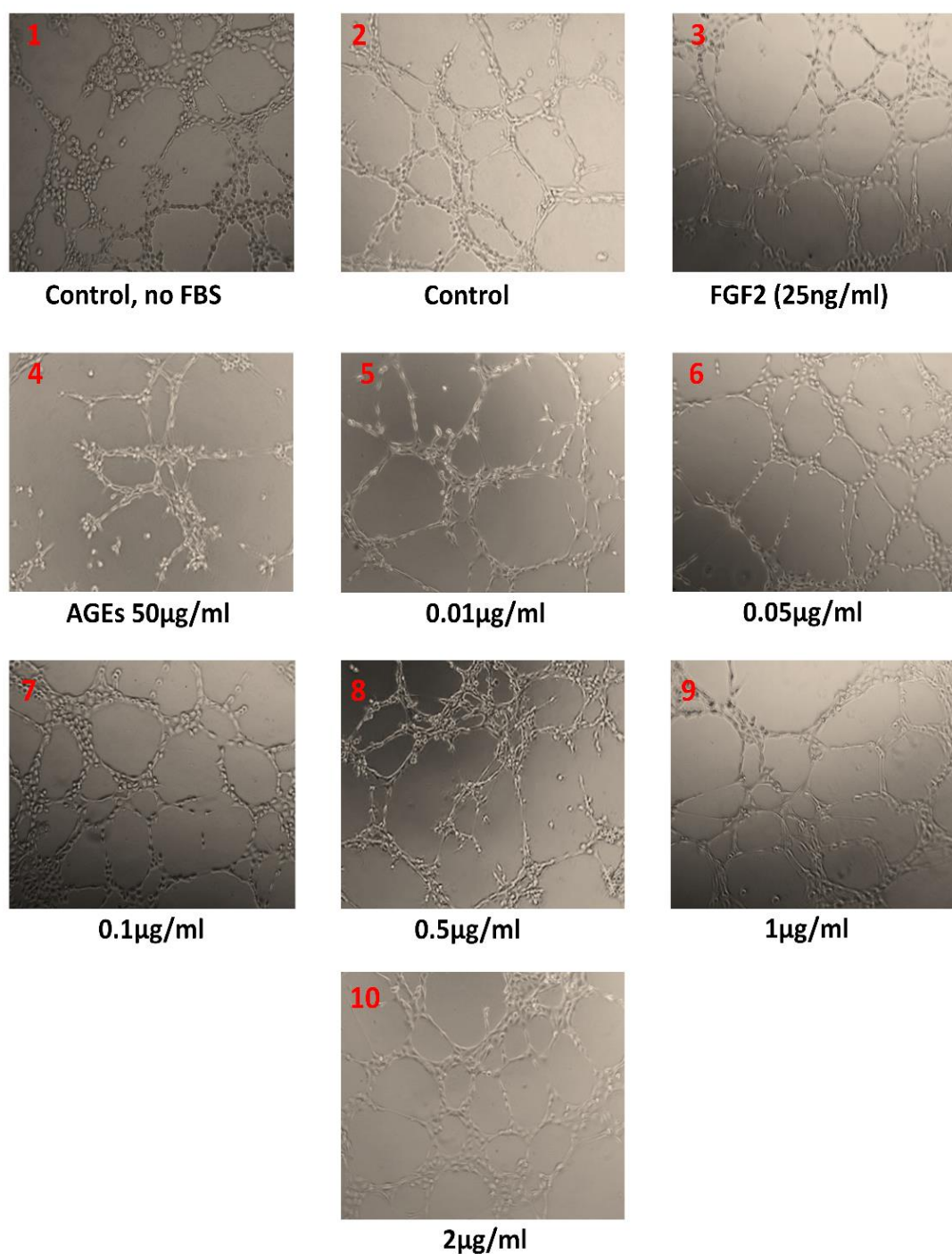


Figure 3.60: Photomicrographic showing the effect of SAC/NAC in the presence of BSA-AGEs on BAEC tube formation.

Photomicrographs showing the effect of different concentrations of SAC/NAC with 50µg/ml BSA-AGEs on BAEC (1×10^6 /ml) tube formation in Matrigel (magnification $\times 100$). Negative control (untreated cells) without FBS (1), untreated cells cultured in 2.5% FBS (2), FGF-2 (25ng/ml) used as a positive control (3), 50µg/ml BSA-AGEs (4) or areas (5 – 10) show cells exposed to different concentration of SAC/NAC (0.01 - 2µg/ml) with 50µg/ml BSA-AGEs. After 7 hours, tubes had formed and the number of closed areas was counted from 5 random fields of 3 wells of a 96-well plate. This panel is a representative example of at least two independent experiments.

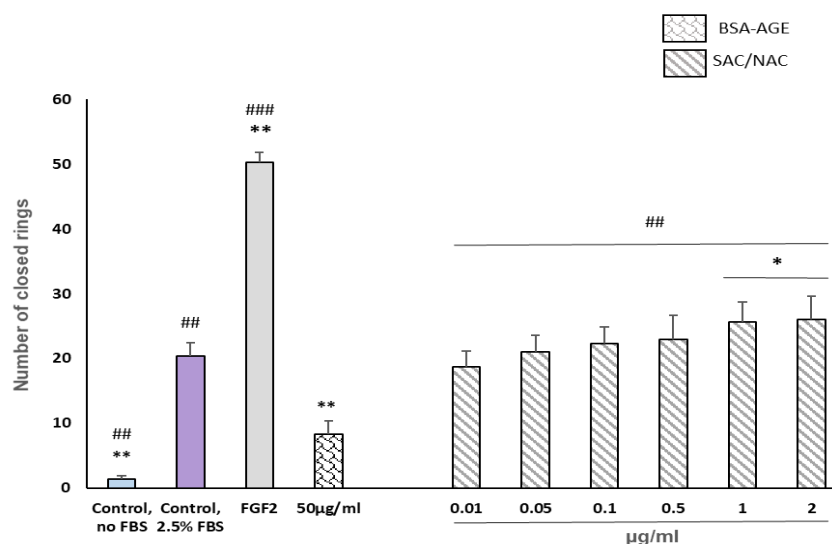


Figure 3.61: Effect of SAC/NAC in the presence of BSA-AGEs on BAEC tube formation.

Bar graph showing the effect of different concentrations of SAC/NAC with 50µg/ml BSA-AGE on BAEC tube formation. All treatments were compared to the control (2.5% FBS). The results are presented as mean \pm S.D. (n=3), * P <0.05 and ** P <0.01, significantly different from control. ## P <0.01 and ### P <0.001, significantly different from BSA-AGEs (50µg/ml).

3.4.11 Effect of compound A in the presence of BSA-AGEs on BAEC wound healing

Figure 3.62 shows representative photomicrographs of the migration of untreated cells cultured in 2.5% FBS (1), cells treated with FGF-2 (2), 50µg/ml BSA-AGEs (3) or 0.01 - 2µg/ml compound A combined with 50µg/ml BSA-AGEs (4 - 9) are shown. Images were taken at time 0 and then after 24 hours to capture the differences in the number of cells that had migrated. In comparison to controls, the presence of compound A significantly (P <0.01) induced cells migration at concentrations of between 0.5 - 2µg/ml. Consistently, BAECs treated with compound A showed a similar effect as SAC/NAC in promoting cell migration, with the maximum distance migrated being 17.0 ± 2.0 mm. The results suggested that the migration of endothelial cells was promoted in a dose-dependent manner (Figure 3.63).

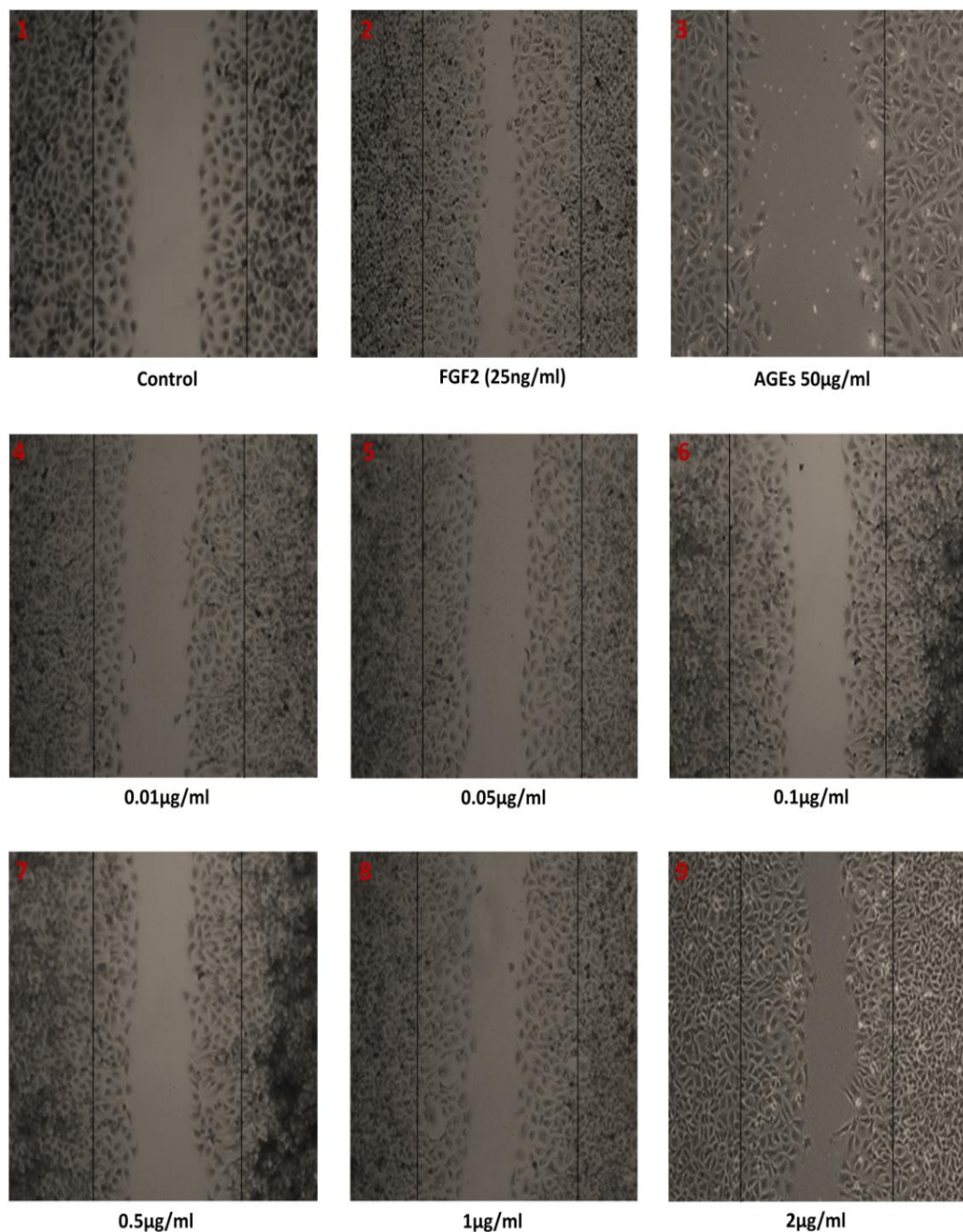


Figure 3.62: Photomicrographic showing the effect of compound A in the presence of BSA-AGEs on BAEC wound healing.

Photomicrographs 24 hours following wounding showing the effect of different concentrations of compound A with BSA-AGEs on BAEC (1×10^6 /ml) migration were taken using phase contrast microscopy (magnification $\times 100$). Untreated cells cultured in 2.5% FBS (1), FGF-2 (25ng/ml) used as a positive control (2), 50µg/ml BSA-AGEs (3) or areas (4 – 9) show cells exposed to different concentration of compound A (0.01 - 2µg/ml) with 50µg/ml BSA-AGEs. The number of migrated cells in the denuded area was counted in 5 random areas per slide and averaged accordingly. This panel is representative of at least two independent experiments.

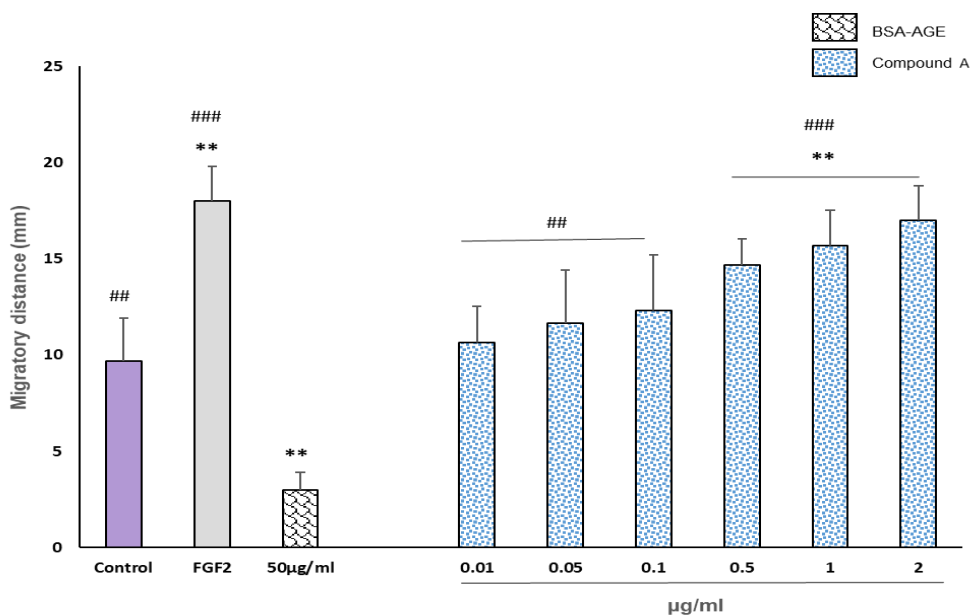


Figure 3.63: Effect of compound A in the presence of BSA-AGEs on BAEC wound healing.

Bar graph showing the effect of different concentrations of compound A with 50µg/ml BSA-AGEs on BAEC migration. The number of migrated cells in the denuded area was counted in 5 random areas per slide and averaged accordingly. The results are presented as mean \pm S.D. (n=3), ** P <0.01, significantly different from control. ## P <0.01 and ### P <0.001, significantly different from BSA-AGEs (50µg/ml).

3.4.12 Effect of compound A in the presence of BSA-AGEs on BAEC tube formation

This study was designed to determine whether compound A was able to reverse the effects of a high concentration of BSA-AGEs (50µg/ml) on tube formation (Figure 3.64). Representative photomicrographs of tube formation in untreated cells without FBS (1), untreated cells cultured in 2.5% FBS (2), cells treated with FGF-2 (3), 50µg/ml BSA-AGEs (4) or 0.01 - 2µg/ml compound A combined to 50µg/ml BSA-AGEs (5 - 10) are shown. Compared to the untreated cells (negative control), FGF-2 used as a positive control to prove the cells' ability to respond. Images were taken after 7 hours to capture the differences in the number of tubes formed. The results showed that addition of compound A protect against the inhibitory effect of BSA-AGEs on BAEC tube formation and significantly induced tube formation at concentrations of between 0.5 - 2µg/ml (p <0.05) with the percentage inhibition ranging between 41 - 32%. The results suggested that compound A promoted tube formation in a dose-dependent manner compared to controls (Figure 3.65).

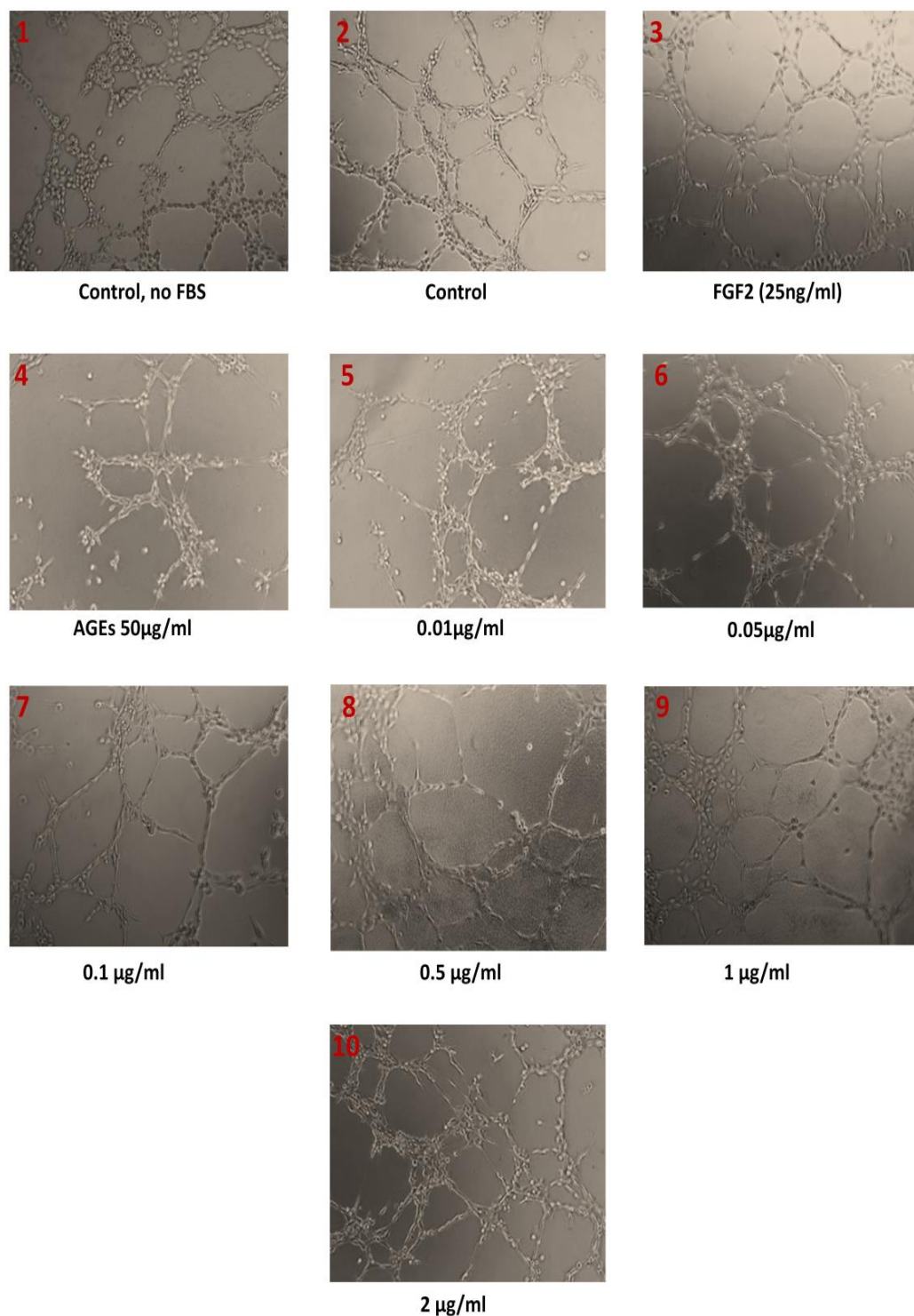


Figure 3.64: Photomicrographic showing the effect of compound A in the presence of BSA-AGEs on BAEC tube formation.

Photomicrographs showing the effect of different concentrations of compound A with BSA-AGEs on BAEC (1×10^6 /ml) tube formation in Matrigel (magnification $\times 100$). Negative control (untreated cells) without FBS (1), untreated cells cultured in 2.5% FBS (2), FGF-2 (25ng/ml) used as a positive control (3), 50µg/ml BSA-AGEs (4) or areas (5 – 10) show cells exposed to different concentration of compound A (0.01 - 2µg/ml) with 50µg/ml BSA-AGEs. After 7 hours, tubes had formed and the number of closed areas was counted from 5 random fields of 3 wells of a 96-well plate. This panel is a representative example of at least two independent experiments.

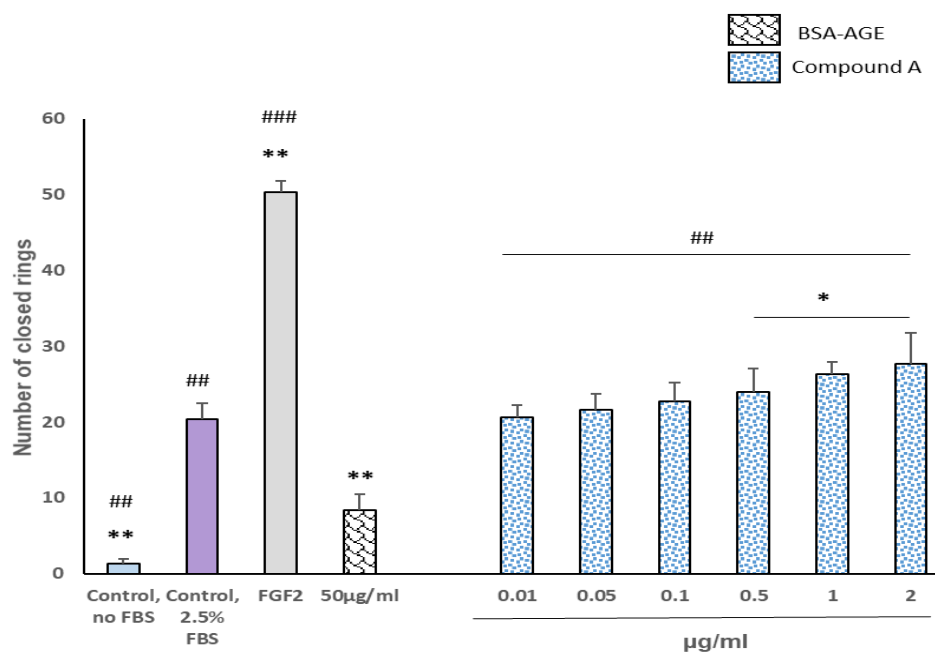


Figure 3.65: Effect of compound A in the presence of BSA-AGEs on BAEC tube formation. Bar graph showing the effect of different concentrations of compound A with 50µg/ml BSA-AGEs on BAEC tube formation. The results are presented as mean \pm S.D. (n=3), * P <0.05 and ** P <0.01, significantly different from control. ## P <0.01 and ### P <0.001, significantly different from BSA-AGEs (50µg/ml).

3.4.13 Effect of SAC/NAC on BAEC wound healing

To examine the inhibitory effect of SAC/NAC on BAEC migration, a wound healing assay was performed (Figure 3.66). Representative photomicrographs show the migration of untreated cells cultured in 2.5% FBS (1), cells treated with FGF-2 (2) or 0.01 - 2µg/ml SAC/NAC (3 - 8) are shown. Images were taken at time 0 and then after 24 hours to capture the differences in the number of cells that had migrated. In comparison to the controls, migration of the cells exposed to 0.05µg/ml of SAC/NAC showed significant (p <0.05) inhibition and the distance migrated was 8.0 ± 2.0 mm. SAC/NAC at concentrations of between 0.1 - 2µg/ml significantly suppressed the cell migration (p <0.01) where the maximum migrated distance was only 4.0 ± 1.0 mm. These results suggest that SAC/NAC inhibited cell migration in a dose-dependent manner (Figure 3.67).

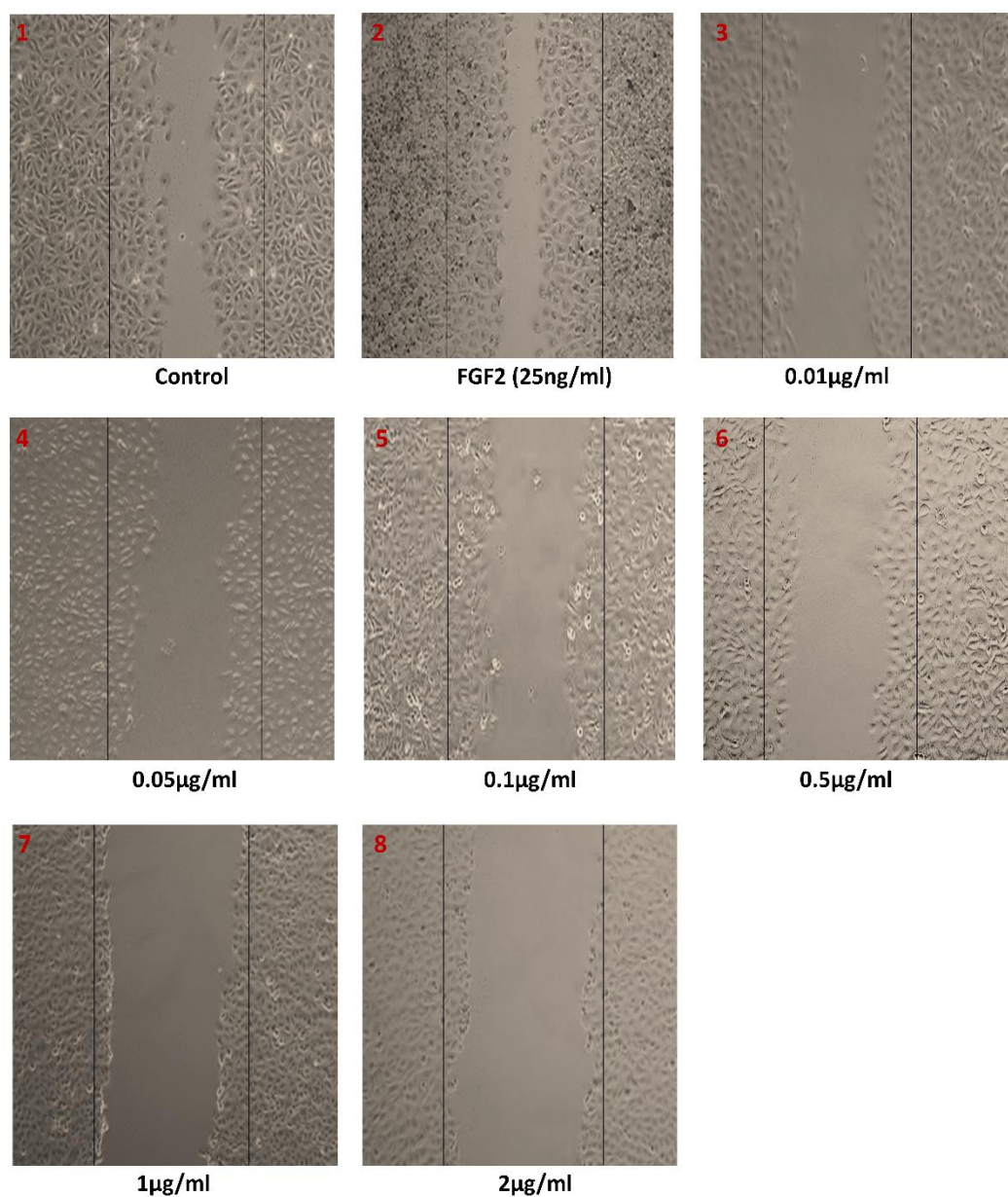


Figure 3.66: Photomicrographic showing the effect of SAC/NAC on BAEC wound healing. Photomicrographs 24 hours following wounding showing the effect of SAC/NAC on BAEC (1×10^6 /ml) migration were taken using phase contrast microscopy (magnification $\times 100$). Untreated cells cultured in 2.5% FBS (1), FGF-2 (25ng/ml) used as a positive control (2), or areas (3 – 8) show cells exposed to different concentrations of SAC/NAC (0.01 - 2µg/ml). The number of migrated cells in the denuded area was counted in 5 random areas per slide and averaged accordingly. This panel is representative of at least two independent experiments.

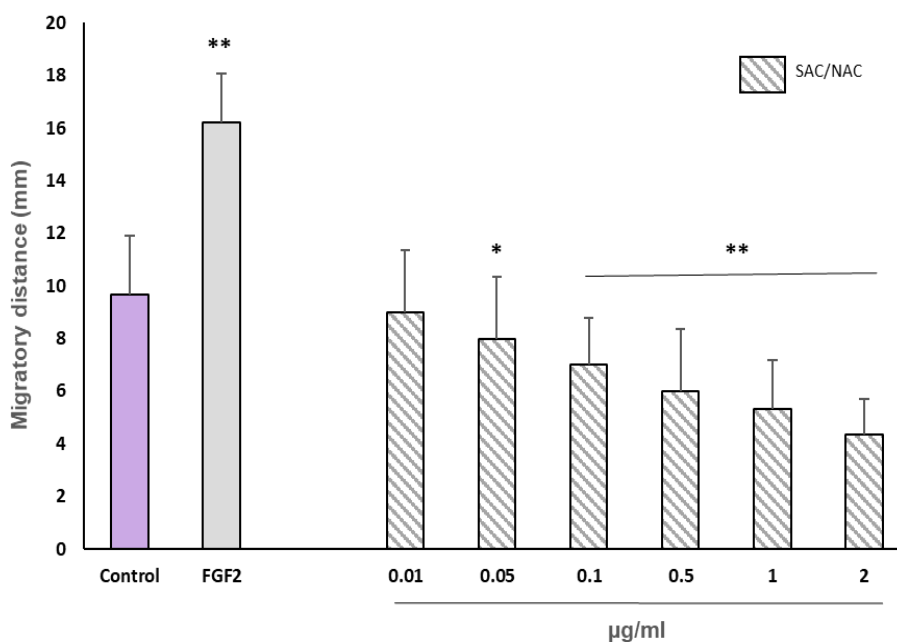


Figure 3.67: Effect of SAC/NAC on BAEC wound healing.

Bar graph showing the effect of different concentrations of SAC/NAC on BAEC migration. The number of migrated cells in the denuded area was counted in 5 random areas per slide and averaged accordingly. The results are presented as mean \pm S.D. (n=3), * P <0.01 and ** P <0.01, significantly different from control.

3.4.14 Effect of SAC/NAC on BAEC tube formation

Using the Matrigel assay system, the influence of SAC/NAC on BAEC tube formation was investigated, and the results are highlighted in Figure 3.68. Representative photomicrographs of the tube formation in untreated cells without FBS (1), untreated cells cultured in 2.5% FBS (2), cells treated with FGF-2 (3) or 0.01 - 2 µg/ml SAC/NAC (4 - 9) are shown. Compared to the untreated cells (negative control), FGF-2 used as a positive control to improve the cells ability to respond. Images were taken after 7 hours to capture the differences in the number of tubes formed. The results showed that tube formation was significantly inhibited (p <0.05), as seen by the reduction in tubule-like structures. Thus, the cells were unable to migrate to form new capillary structures in the presence of SAC/NAC at concentration of 0.01 µg/ml with inhibition of 82% and the results showed more significant inhibition (p <0.01) was seen at a concentrations of between 0.05 - 2 µg/ml with inhibition ranges between 84% - 59%. The results indicated that SAC/NAC inhibited tube formation and the inhibition was dose-dependent (Figure 3.69).

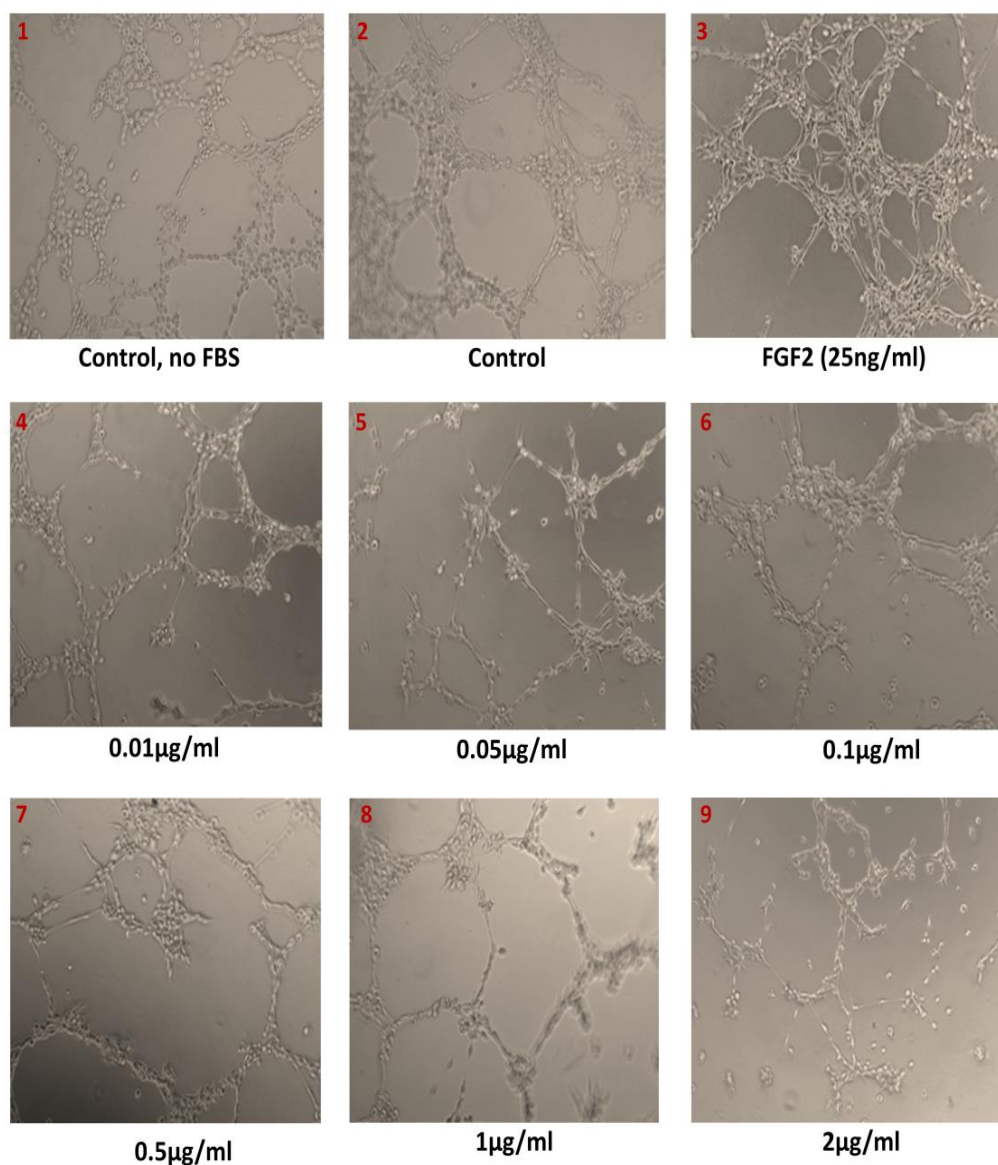


Figure 3.68: Photomicrographic showing the effect of SAC/NAC on BAEC tube formation. Photomicrographs showing the effect of SAC/NAC on BAEC (1×10^6 /ml) tube formation in Matrigel (magnification $\times 100$). Negative control (untreated cells) without FBS (1), untreated cells cultured in 2.5% FBS (2), FGF-2 (25ng/ml) used as a positive control (3) or areas (4 – 9) show cells exposed to different concentrations of SAC/NAC (0.01 - 2µg/ml). After 7 hours, tubes had formed and the number of closed areas was counted from 5 random fields of 3 wells of a 96-well plate. This panel is a representative example of at least two independent experiments.

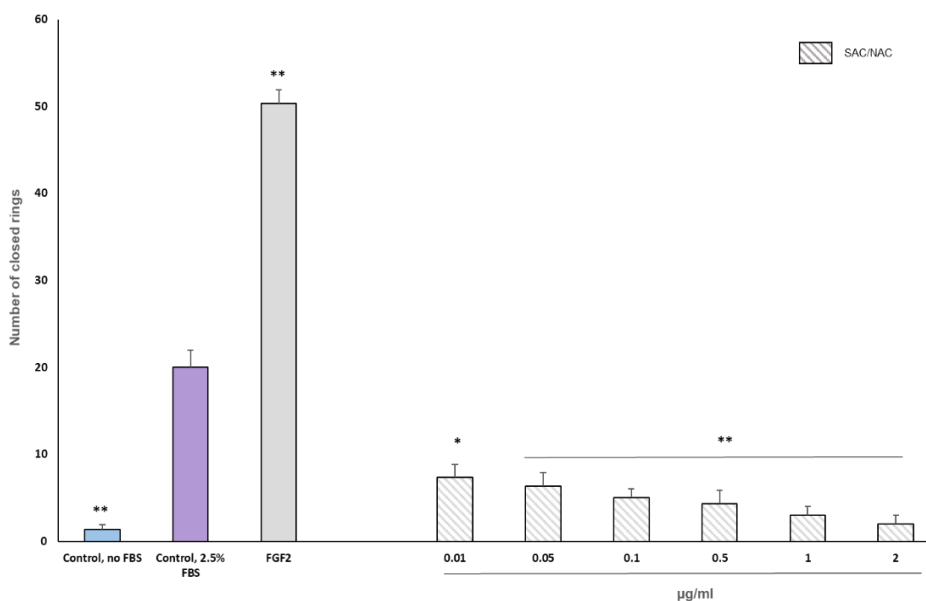


Figure 3.69: Effect of SAC/NAC on BAEC tube formation.

Bar graph showing the effect of different concentrations of SAC/NAC on BAEC tube formation. The results are presented as mean \pm S.D. (n=3), * P <0.05 and ** P <0.01 significantly different from control.

3.4.15 Effect of compound A on BAEC wound healing

As shown in Figure 3.70, there are representative photomicrographs of the migration of untreated cells cultured in 2.5% FBS (1), cells treated with FGF-2 (2) or 0.01 - 2µg/ml compound A (3 - 8) are shown. Images were taken at time 0 and then after 24 hours to capture the differences in the number of cells that had migrated. Migration of the cells exposed to 0.05µg/ml of compound A showed significant (p <0.05) inhibition, while the migration of cells exposed in compound A at concentrations of between 0.1 - 2µg/ml were decreased (p <0.01) and the maximum migrated distance was only 4.0 ± 2.0 mm, respectively. Compound A inhibited wound healing in BAECs in a dose-dependent manner (Figure 3.71).

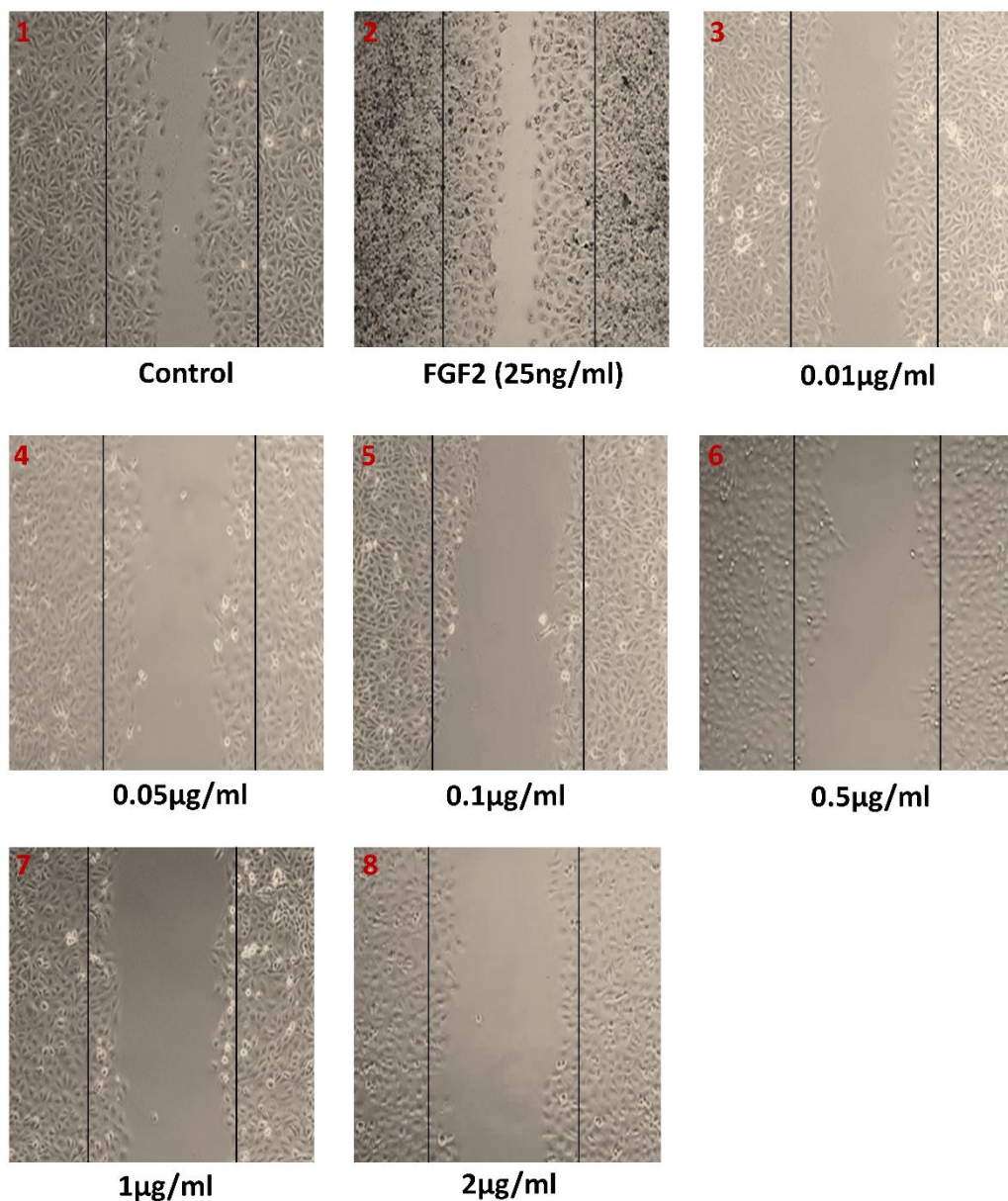


Figure 3.70: Photomicrographic showing the effect of compound A on BAEC wound healing. Photomicrographs 24 hours following wounding showing the effect of compound A on BAEC (1×10^6 /ml) migration were taken using phase contrast microscopy (magnification $\times 100$). Untreated cells cultured in 2.5% FBS (1), FGF-2 (25ng/ml) used as a positive control (2), or areas (3 – 8) show cells exposed to different concentrations of compound A (0.01 - 2µg/ml). The number of migrated cells in the denuded area was counted in 5 random areas per slide and averaged accordingly. This panel is representative of at least two independent experiments.

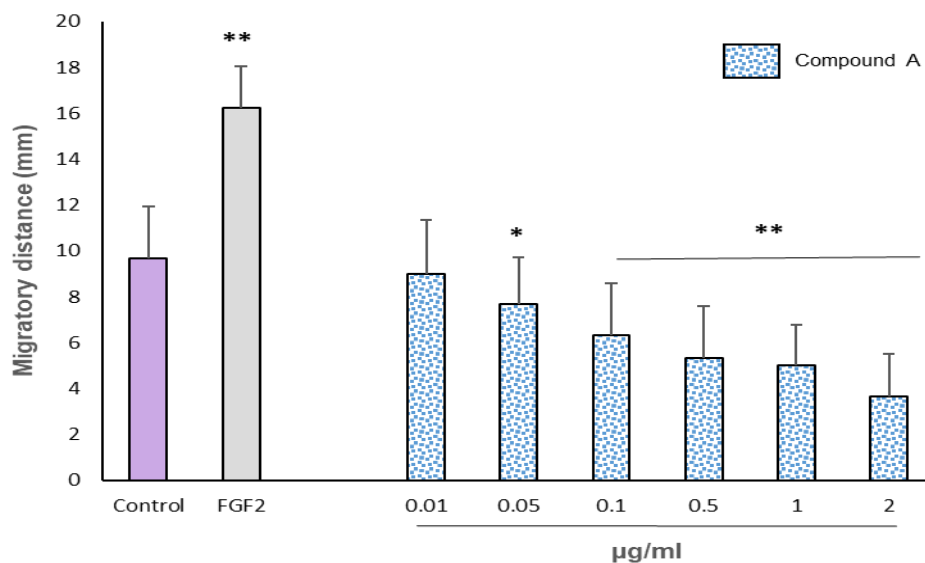


Figure 3.71: Effect of compound A on BAEC wound healing.

Bar graph showing the effect of different concentrations of compound A on BAEC migration. The number of migrated cells in the denuded area was counted in 5 random areas per slide and averaged accordingly. The results are presented as mean \pm S.D. (n=3), * P <0.05, and ** P <0.01, significantly different from control.

3.4.16 Effect of compound A on BAEC tube formation

Using the Matrigel assay system, the influence of compound A on endothelial cells tube formation was investigated (Figure 3.72). Representative photomicrographs of the tube formation in untreated cells without FBS (1), untreated cells cultured in 2.5% FBS (2), cells treated with FGF-2 (3) or 0.01 - 2µg/ml compound A (4 - 9) are shown. Compared to the untreated cells (negative control), FGF-2 used as a positive control to prove the cells' ability to respond. Images were taken after 7 hours to capture the differences in the number of tubes formed. The results showed that compound A significantly (p <0.01) reduced the tube formation as seen by the reduction in tube-like structures. Thus, the cells were unable to migrate to form new capillary structures in the presence of compound A at concentrations of between 0.01 - 0.1µg/ml. In addition, the results showed more significant (p <0.001) in the reduction of the tube formation at concentrations of between 0.5 - 2µg/ml, with 90% as the maximum percentage inhibition. The inhibition was dose-dependent (Figure 3.73).

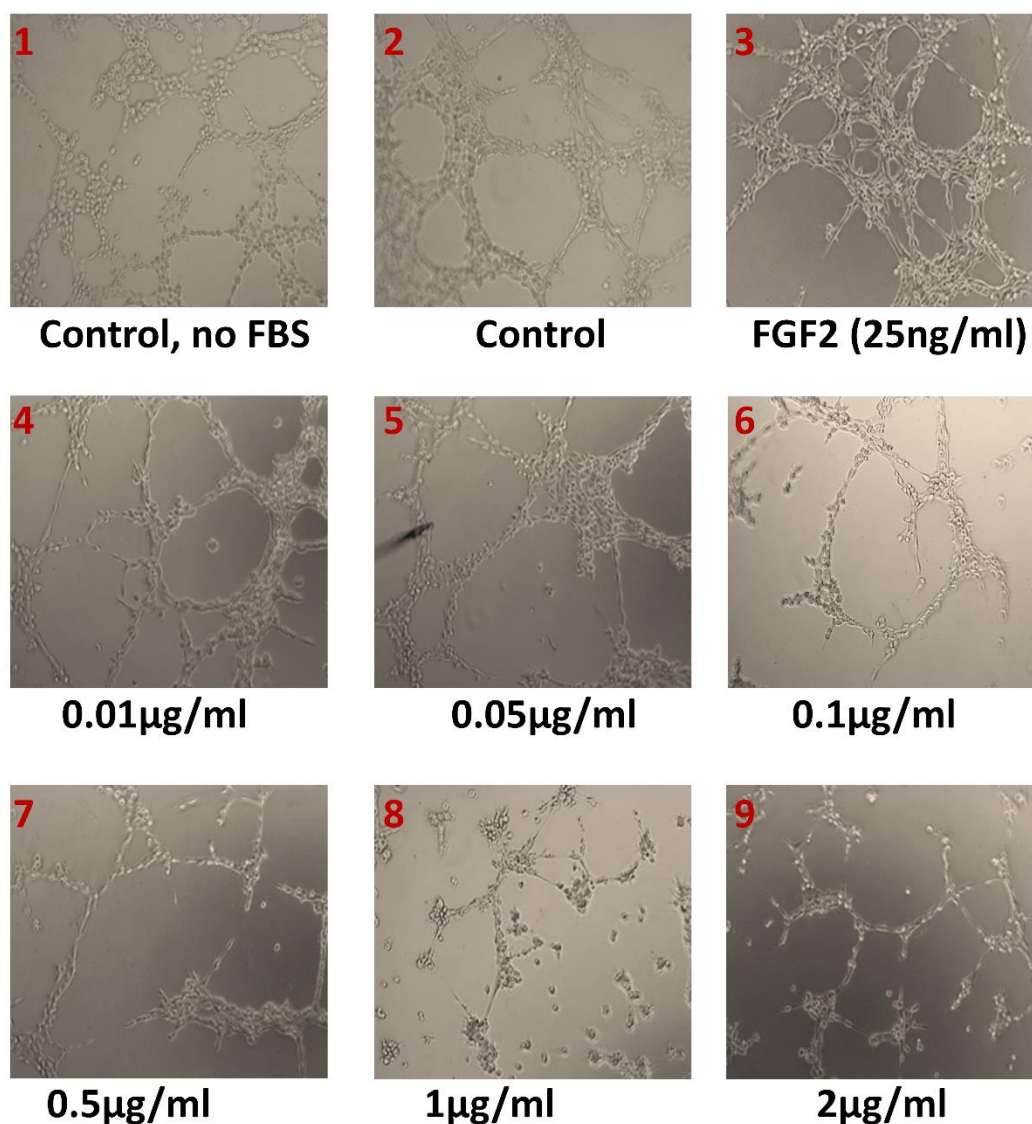


Figure 3.72: Photomicrographic showing the effect of compound A on BAEC tube formation. Photomicrographs showing the effect of compound A on BAEC (1×10^6 /ml) tube formation in Matrigel (magnification $\times 100$). Negative control (untreated cells) without FBS (1), untreated cells cultured in 2.5% FBS (2), FGF-2 (25ng/ml) used as a positive control (3) or areas (4 – 9) show cells exposed to different concentrations of compound A (0.01 - 2µg/ml). After 7 hours, tubes had formed and the number of closed areas was counted from 5 random fields of 3 wells of a 96-well plate. This panel is a representative example of at least two independent experiments.

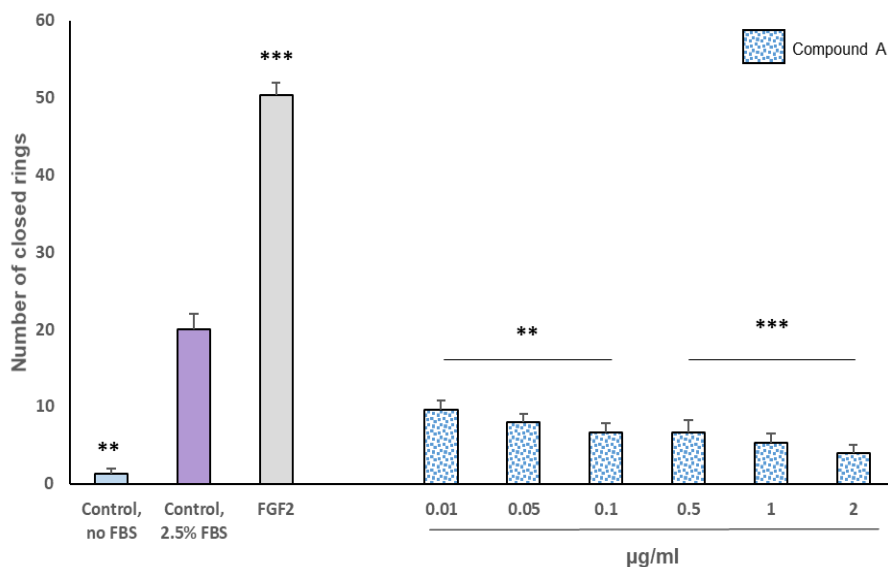


Figure 3.73: Effect of compound A on BAEC tube formation.

Bar graph showing the effect of different concentrations of compound A on BAECs tube formation. The results are presented as mean \pm S.D. (n=3), ** P <0.01 and *** P <0.001, significantly different from control.

3.4.17 Effect of SAC/NAC-loaded hADMSCs CM on BEAC wound healing

This study designed to evaluate the therapeutic effect of SAC/NAC-loaded hADMSCs CM on BAEC wound healing (Figure 3.74). Representative photomicrographs show the migration of treated cells cultured in SCM (1), 2µg/ml SAC/NAC cultured in SCM (2), cells treated with CM- day 1 alone used as control (3), cells treated with CM- day 2 alone used as control (4), 500µg/ml SAC/NAC-loaded hADMSCs CM- day 1 (5) or day 2 (6) are shown. Images were taken at time 0 and then after 24 hours to capture the differences in the number of cells that had migrated. The results show that 500µg/ml SAC/NAC-primed hADMSCs CM- days 1 and 2 significantly (p < 0.05) induced the cell migration compared to control with distance migrated increasing to 27.0 ± 2.0 mm and 25.0 ± 1.0 mm, respectively. In addition, compared to 2µg/ml SAC/NAC treatment with SCM, 500µg/ml SAC/NAC-primed hADMSCs CM- days 1 and 2 significantly (p < 0.05) increased tube formation (Figure 3.75).

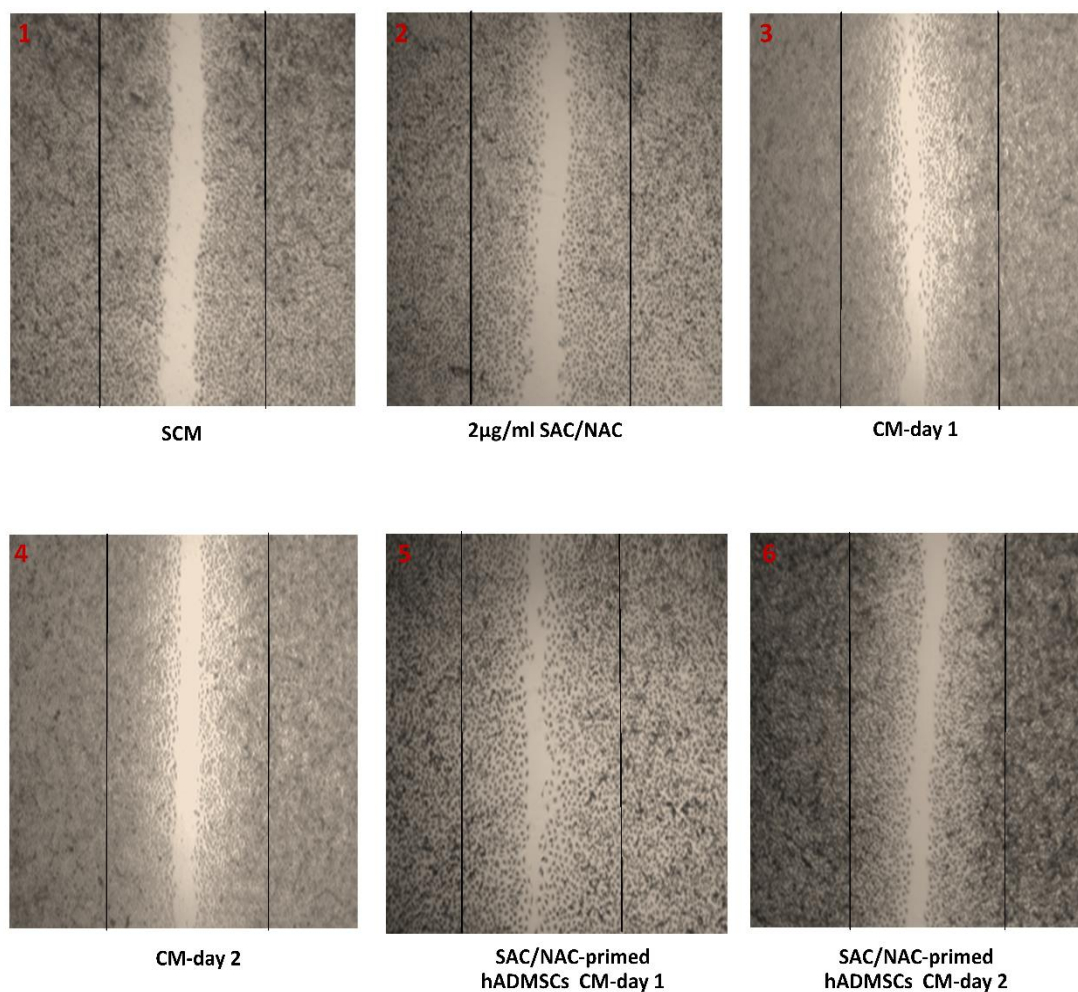


Figure 3.74: Photomicrographic showing the effect of SAC/NAC-loaded hADMSCs CM on BAEC wound healing.

Photomicrographs 24 hours following wounding showing the effect of SAC/NAC-loaded hADMSCs CM (24 - 48 h) on BAEC ($1 \times 10^6/\text{ml}$) migration were taken using phase contrast microscopy (magnification $\times 100$). Untreated cells cultured in SCM (1), $2\mu\text{g/ml}$ SAC/NAC cultured in SCM (2), CM-day 1 (3), CM-day 2 (4), SAC/NAC-loaded hADMSCs CM-day 1 (5) or day 2 (6). The number of migrated cells in the denuded area was counted in 5 random areas per slide and averaged accordingly. This panel is representative of at least two independent experiments. SCM= stem cells medium, CM-day 1= conditioned medium alone after 24h, CM-day 2= conditioned medium alone after 48h.

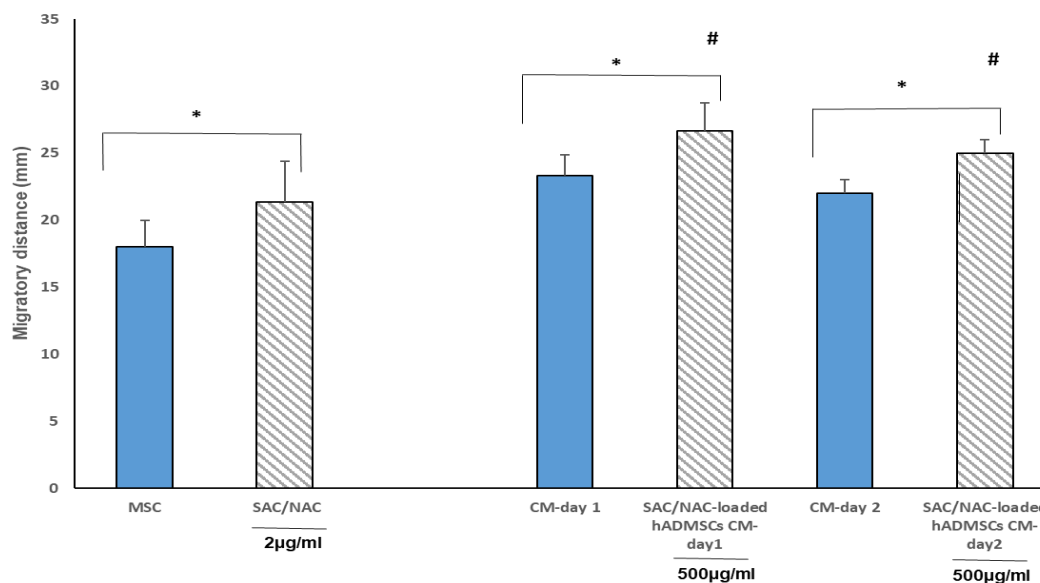


Figure 3.75: The effect of SAC/NAC-loaded hADMSCs CM on BAEC wound healing.

Bar graph showing the effect of SAC/NAC-loaded hADMSCs CM on BAEC migration. The number of migrated cells in the denuded area was counted in 5 random areas per slide and averaged accordingly. The results are presented as mean \pm S.D. (n=3), * P <0.05, significantly different from control. # P <0.05, significantly different from 2µg/ml SAC/NAC-treated cells.

3.4.18 Effect of SAC/NAC-loaded hADMSCs CM on BAEC tube formation

Using the Matrigel assay system, to evaluate the therapeutic effect of SAC/NAC-primed hADMSCs CM on endothelial cells tube formation was investigated (Figure 3.76). Representative photomicrographs show tube formation in cells cultured in SCM (1), 2µg/ml SAC/NAC cultured in SCM (2), cells treated with CM- day 1 alone used as control (3), cells treated with CM- day 2 alone used as control (4), 500µg/ml SAC/NAC-primed hADMSCs CM- day 1 (5) or day 2 (6) are shown. Images were taken after 7 hours to capture the differences in the number of tubes formed. The results showed that 500µg/ml SAC/NAC-loaded hADMSCs, CM- days 1 and 2 significantly (p <0.05) induced cell tube formation compared to control. In addition, compared to 2µg/ml SAC/NAC treatment with SCM, 500µg/ml SAC/NAC-primed hADMSCs CM significantly promotes tube formation at days 1 (p < 0.01) and 2 (p < 0.05) (Figure 3.77).

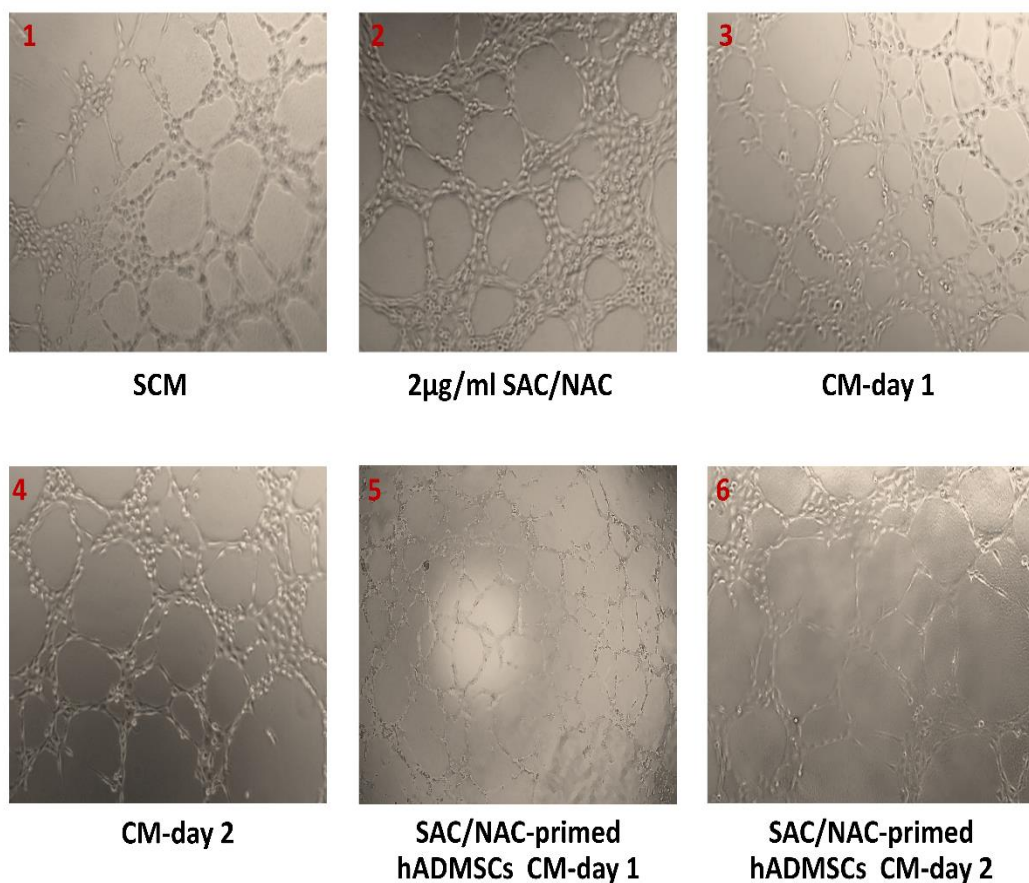


Figure 3.76: Photomicrographic showing the effect of SAC/NAC-loaded hADMSCs CM on BAEC tube formation.

Photomicrographs showing the effect of SAC/NAC-loaded hADMSCs CM (24 - 48 h) on BAEC (1×10^6 /ml) tube formation in Matrigel (magnification $\times 100$). Untreated cells cultured in SCM (1), 2µg/ml SAC/NAC cultured in SCM (2), CM-day 1 (3), CM-day 2 (4), SAC/NAC-loaded hADMSCs CM-day 1 (5) or day 2 (6). After 7 hours, tubes had formed and the number of closed areas was counted from 5 random fields of 3 wells of a 96-well plate. This panel is a representative example of at least two independent experiments. SCM= stem cells medium, CM-day 1= stem cells conditioned medium alone after 24h, CM- day 2= stem cells conditioned medium alone after 48h.

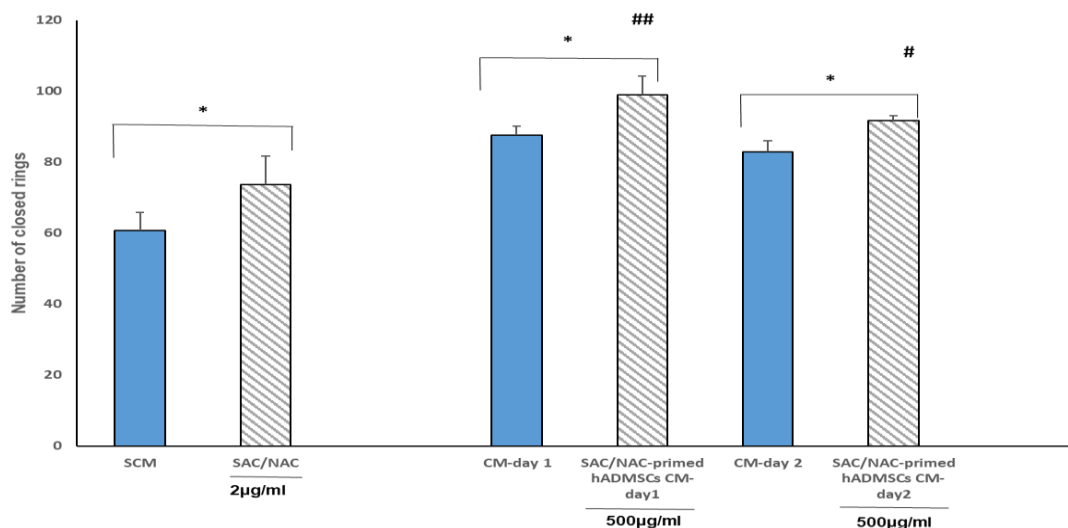


Figure 3.77: Effect of SAC/NAC-loaded hADMSCs CM on BAEC tube formation.

Bar graph showing the effect of SAC/NAC-loaded hADMSCs CM on BAEC tube formation. The results are presented as mean \pm S.D. (n=3), * P <0.05, significantly different from control. # P <0.05 and ## P <0.01, significantly different from 2µg/ml SAC/NAC-treated cells.

3.4.19 Effect of compound A-loaded hADMSCs CM on BAEC wound healing

To evaluate the therapeutic effect of compound A-primed hADMSCs CM on wound healing (Figure 3. 78). Representative photomicrographs are shown of the migration of cells cultured in SCM (1), 2µg/ml compound A cultured in SCM (2), cells treated with CM- day 1 alone used as control (3), cells treated with CM- day 2 alone used as control (4), 500µg/ml compound A-loaded hADMSCs CM- day 1 (5) or day 2 (6) are shown. Pictures were taken at time 0 and then after 24 hours to capture the differences in the number of cells migrated. The results show that 250µg/ml compound A-loaded hADMSCs CM significantly promoted cell migration at days 1 (p <0.01) and 2 (p <0.05) compared to control. In addition, compared to 2µg/ml compound A treatment with SCM, 250µg/ml compound A-primed hADMSCs CM- days 1 and 2 a significantly (p < 0.01) increased cell migration (Figure 3.79).

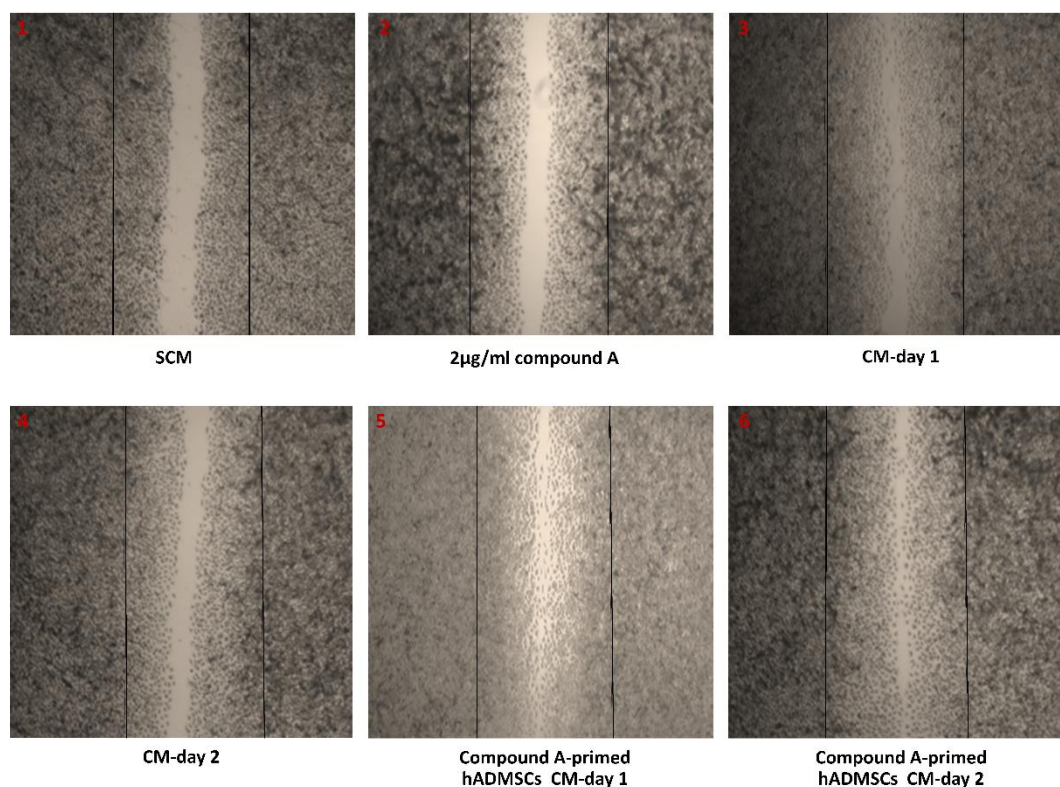


Figure 3.78: Photomicrographic showing the effect of compound A-loaded hADMSCs CM on BAEC wound healing.

Photomicrographs 24 hours following wounding showing the effect of compound A-loaded hADMSCs CM (24 - 48 h) on BAEC ($1 \times 10^6/\text{ml}$) migration were taken using phase contrast microscopy (magnification $\times 100$). Untreated cells cultured in SCM (1), 2µg/ml compound A (2), CM-day 1 (3), CM-day 2 (4), compound A-loaded hADMSCs CM-day 1 (5) or day 2 (6). The number of migrated cells in the denuded area was counted in 5 random areas per slide and averaged accordingly. This panel is representative of at least two independent experiments. SCM= stem cells medium, CM1-day 1= stem cells conditioned medium alone after 24h, CM2= stem cells conditioned medium alone after 48h.

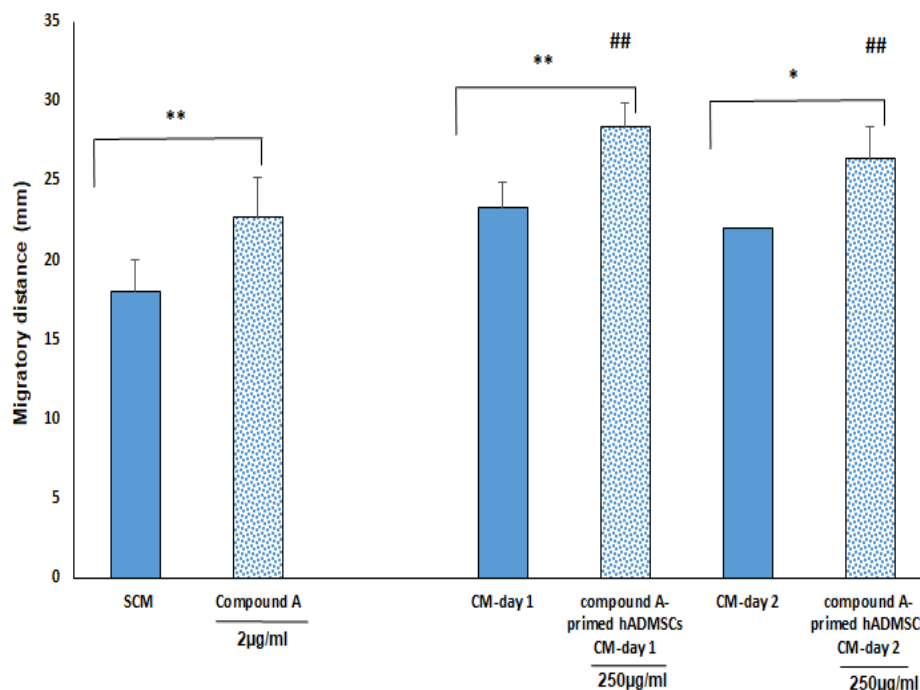


Figure 3.79: Effect of compound A-loaded hADMSCs CM on BAEC wound healing.

Bar graph showing the effect of compound A-loaded hADMSCs CM on BAEC migration. The results are presented as mean \pm S.D. (n=3), * P <0.05, ** P <0.01, significantly different from control. ## P <0.01, significantly different from 2µg/ml compound A-treated cells.

3.4.20 Effect of compound A-loaded hADMSCs CM on BAEC tube formation

To evaluate the therapeutic effect of compound A-primed hADMSCs CM on endothelial cells tube formation was investigated (Figure 3.80). Representative photomicrographs are shown of the tube formation in cells cultured with SCM (1), 2µg/ml compound A cultured with SCM (2), cells treated with CM- day 1 alone used as control (3), cells treated with CM- day 2 alone used as control (4), 500µg/ml compound A-primed hADMSCs CM- day 1 (5) or day 2 (6) are shown. Images were taken after 7 hours to capture the differences in the number of tubes formed. The results show that 250µg/ml compound A-primed hADMSCs CM- days 1 and 2 significantly (p <0.05) induced the cell tube formation compared to control. In addition, compare to 2µg/ml compound A treatment with SCM, 250µg/ml mimic compound A-primed hADMSCs CM- significantly (p <0.001) promotes tube formation at days 1 and 2 (Figure 3.81).

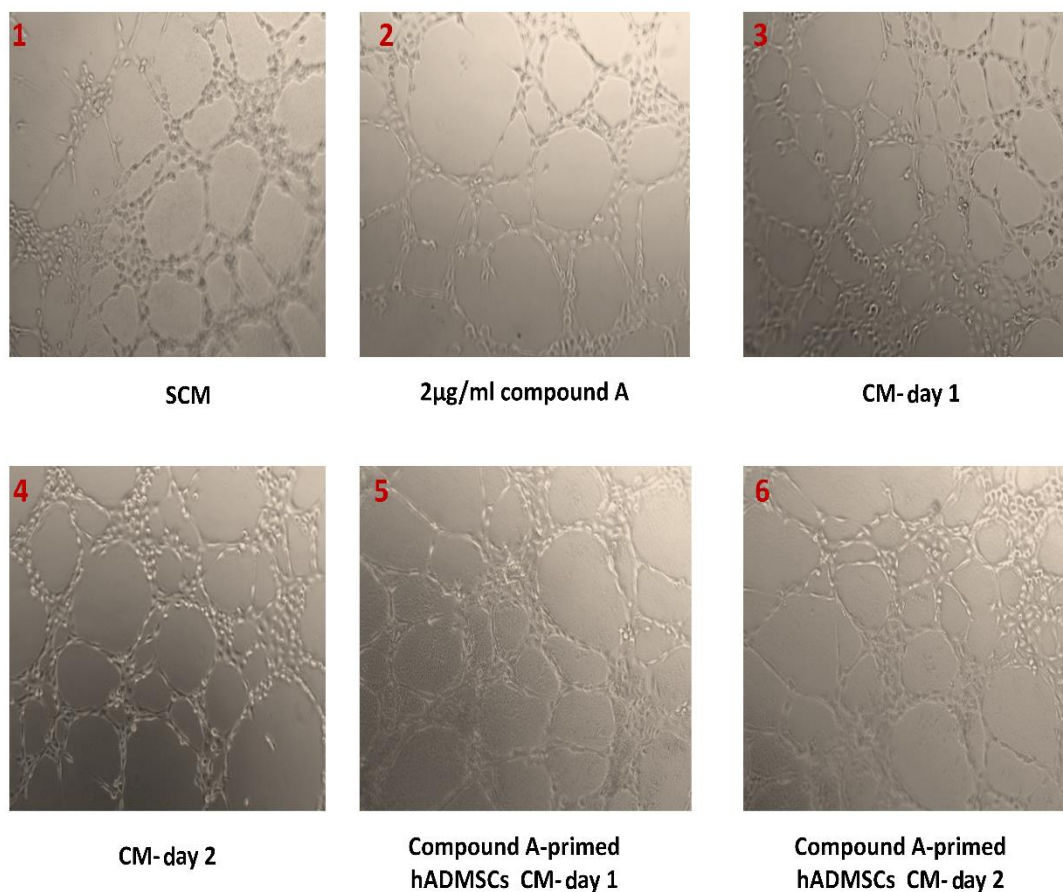


Figure 3.80: Photomicrographic showing the effect of compound A-loaded hADMSCs CM on BAEC tube formation.

Photomicrographs showing the effect of compound A-loaded hADMSCs CM (24 - 48 h) on BAEC ($1 \times 10^6/\text{ml}$) tube formation in Matrigel (magnification $\times 100$). Untreated cells cultured with SCM (1), $2\mu\text{g}/\text{ml}$ compound A cultured with SCM (2), CM-day 1 (3), CM-day 2 (4), compound A-loaded hADMSCs CM-day 1 (5) or day 2 (6). After 7 hours, tubes had formed and the number of closed areas was counted from 5 random fields of 3 wells of a 96-well plate. This panel is a representative example of at least two independent experiments. SCM= stem cells medium, CM1-day 1= stem cells conditioned medium alone after 24h, CM2-day 2= stem cells conditioned medium alone after 48h.

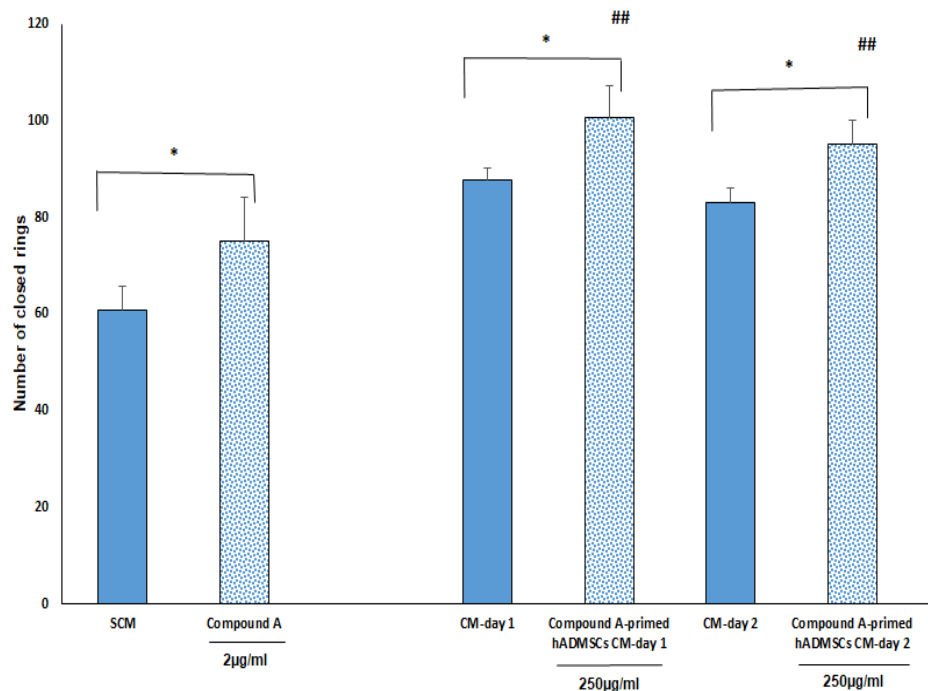


Figure 3.81: The effect of compound A-loaded hADMSCs CM on BAEC tube formation.

Bar graph showing the effect of compound A-loaded hADMSCs CM on BAEC tube formation. The results are presented as mean \pm S.D. (n=3), * P <0.05, significantly different from control. # P <0.05 and ## P <0.01, significantly different from 2µg/ml mimic compound A-treated cells.

3.5 Analysis of hADMSCs-loaded CM with high performance liquid chromatography (HPLC)

3.5.1 HPLC method development and optimisation

For quantification with increased sensitivity, NAC was studied using the application of HPLC. According to the literature review, there are no reported methods for the estimation of NAC-loaded hADMSCs CM by HPLC. Hence, it was necessary to develop an accurate and selective HPLC method for the determination of NAC-loaded hADMSCs CM. In this experiment, an HPLC method with post-column NPM derivatisation was used as the starting point. Initially, using an HPLC column (Hypersil Elite. C18, 3.0mm x 100cm, particle size: 3µm) packing material. The injection volume was 10µl and fluorimetric detection was with an excitation wavelength of 330nm and an emission wavelength of 380nm. The reaction appeared as broad peaks (Figure 3.82, A). Increasing the length of the column was not preferred, as an increase in retention time gave increased peak broadening and a lower column temperature would exhibit poor separation and peak shape problems. In this case, it was desirable to decrease the plate height equivalent of a theoretical plate by decreasing the particle size of the stationary phase, which leads to an increase of the

separation efficiency of the HPLC column and the column temperature was increased to 60°C to accelerate the degradation of the stationary phase. In addition, the injection volume was reduced to 1µl from 10µl to work with small volumes. Chromatographic separation of derivatised NAC was conducted on a C-18 column (4.6mm x 25cm, 3µm particle size) and NPM derivatives' detection wavelength was measured by a fluorescence detector (FID) ($\lambda_{ex} = 330 \text{ nm}$ and $\lambda_{em} = 376 \text{ nm}$) (Figure 3.82, B) (Lindsay, 1992).

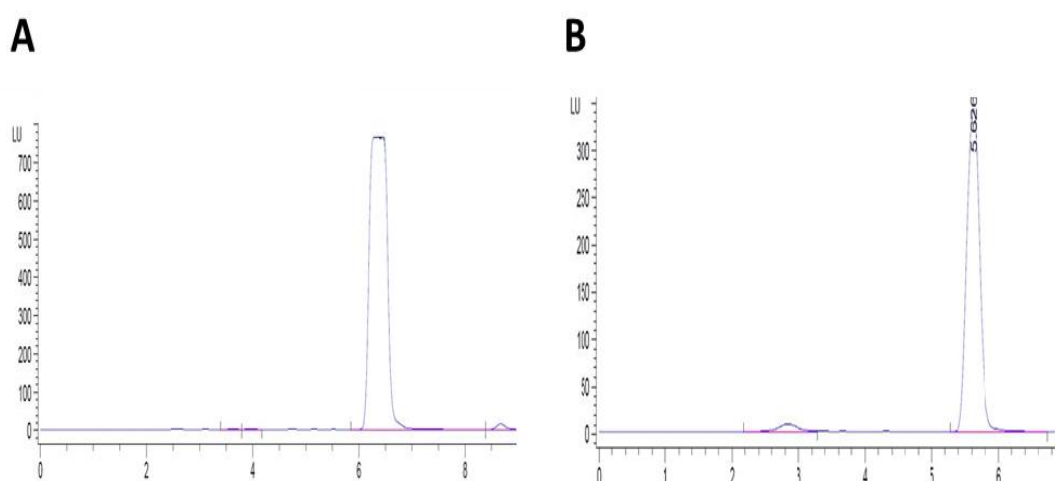


Figure 3.82: Chromatograms representing the specificity of the developed HPLC method. (A) Column used (Hypersil Elite. C18, 3.0mm x 100cm, particle size: 3µm), injection volume was 10µl and the column temperature was 25°C, (B) Column used (Eclipsex DB. C18, 4.6mm x 25cm, particle size: 3µm), injection volume of 1µl and the column temperature increased to 60°C. The NPM derivatives were measured by a fluorescence detector (FID) ($\lambda_{ex} = 330\text{nm}$ and $\lambda_{em} = 376\text{nm}$).

3.5.2 Calibration curves

As shown in Figure 3.83, a calibration curve was constructed by plotting integrated peak areas versus standard NAC concentrations (100, 200, 300, 400 and 500µg/ml). Linearity for NAC standards was obtained only between 100-300µg/ml ($r=0.9871$).

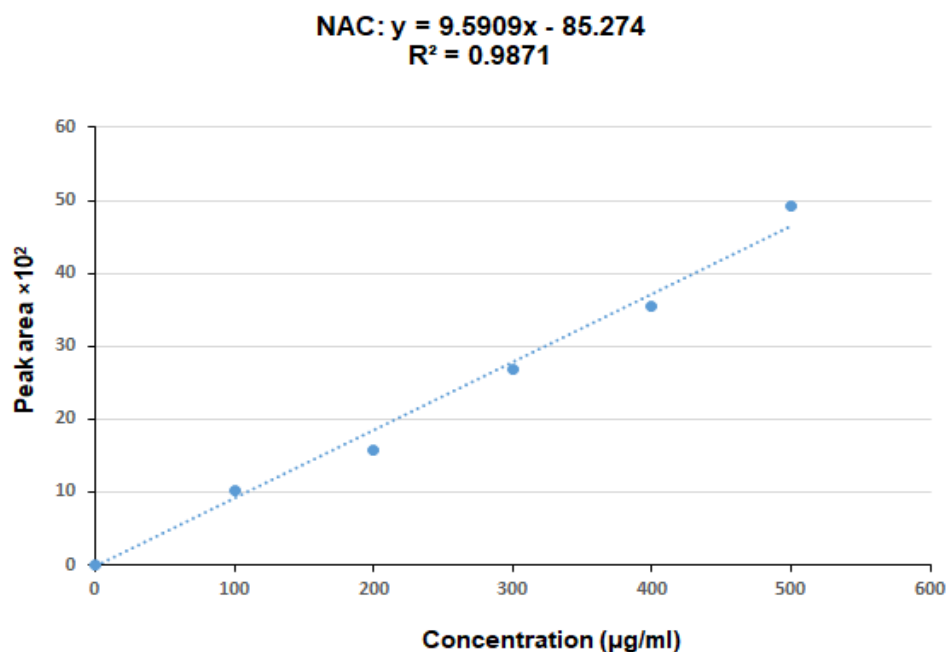


Figure 3.83: Calibration curves of NAC with water.

Column used (Eclipsex DB. C18, 4.6mm x 25cm, particle size: 3µm) with injection volume of 1µl and column temperature 60°C. NAC concentrations were measured by a fluorescence detector (FID) ($\lambda_{ex} = 330\text{nm}$ and $\lambda_{em} = 376\text{nm}$).

3.5.3 Detection of NAC by UV-DAD

The UV-DAD (photodiode array detection) spectra of aqueous solutions of NAC alone were recorded in the wavelength of Sig=230 and Ref=360nm. As compared to blank (Figure 3.84, A), the solution of NAC showed a peak at RT of 2.383min (Figure 3.84, B). Unfortunately, analysis of NAC without derivatisation did not permit a satisfactory separation and absorption at the ultraviolet wavelengths, nor did they exhibit fluorescence. Hence, NPM has been used as the fluorescent derivatising agent for many thiol compounds.

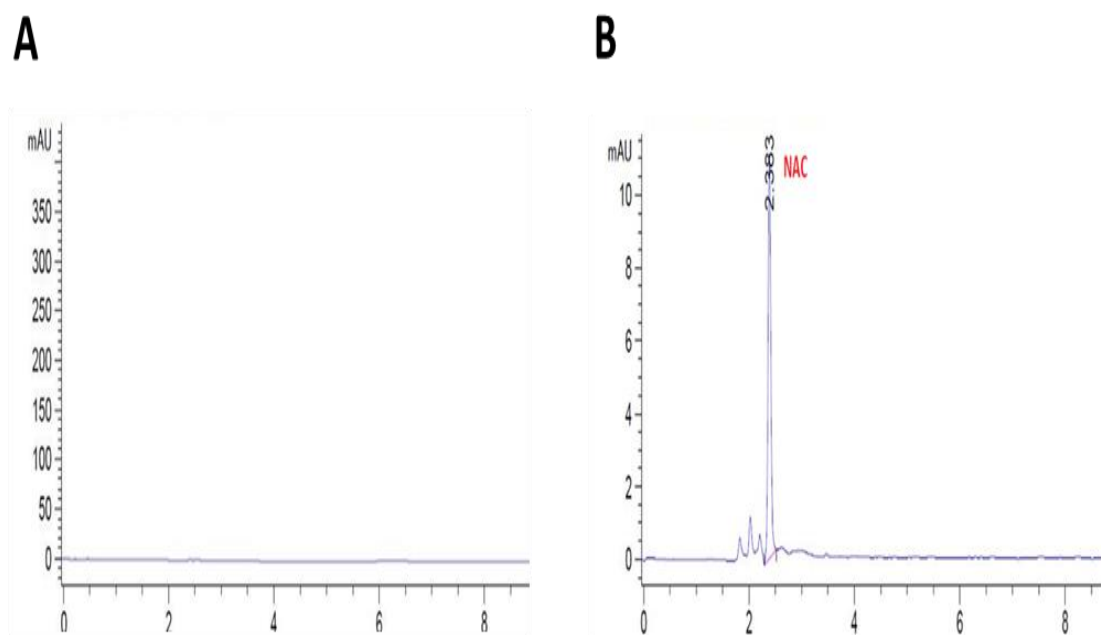


Figure 3.84: HPLC-DAD.

(A) Blank (no peaks), (B) 500µg/ml NAC alone at RT of 2.383min. The column used (Eclipsex DB. C18, 4.6mm x 25cm, particle size: 3µm) with an injection volume of 1µl and column temperature of 60°C. NAC concentrations were measured by photodiode array detection (UV-DAD) (Sig=230, Ref=360 nm).

3.5.4 HPLC analysis of NAC

In order to quantify the NAC released by SAC/NAC- loaded hADMSCs, this experiment tested NAC by FID (flame ionisation detection) ($\lambda_{ex} = 330 \text{ nm}$ and $\lambda_{em} = 376 \text{ nm}$) HPLC analysis. NAC was extracted using C18 solid phase extraction cartridges in cell media. These samples were then run through the HPLC to identify whether NAC was successfully extracted from the cell media and that there was a high enough recovery after the extraction process. In this study, SAC and mimic compound A were not analysed due to limited time and the unavailability of a detector for both of them. *In situ* derivatisation of biological samples with NPM produced, an NPM-NAC adduct which was rapidly separated by the HPLC system employed for this study. The chromatogram pictured in Figure 3.85 confirms that adequate separation of the NPM-NAC adduct from the hydrolysis peaks. When the analytical column was introduced into the system, the RT of NAC-NPM was approximately 6.34/6.393 min while NPM alone exhibited a peak at RT of 8.133/8.208min. After 24 hours, the 500µg/ml NAC standard showed that the average peak area at RT of 5.647 min was

135.1LU (Figure 3.85, A). CM alone release by hADMSCs showed only the NPM peak and the average peak area was 7.668LU (Figure 3.85, B). The average peak area for CM from 500 μ g/ml SAC/NAC-primed hADMSCs collected on days 1 and 2 from 3 tests at RT of 6.345 and 6.346min, respectively, were for both of them 110.1LU and NAC concentration was 149.75 and 124.21 μ g/ml, respectively (Figure 3.85, C and D). The results indicated that HPLC analysis could quantify NAC.

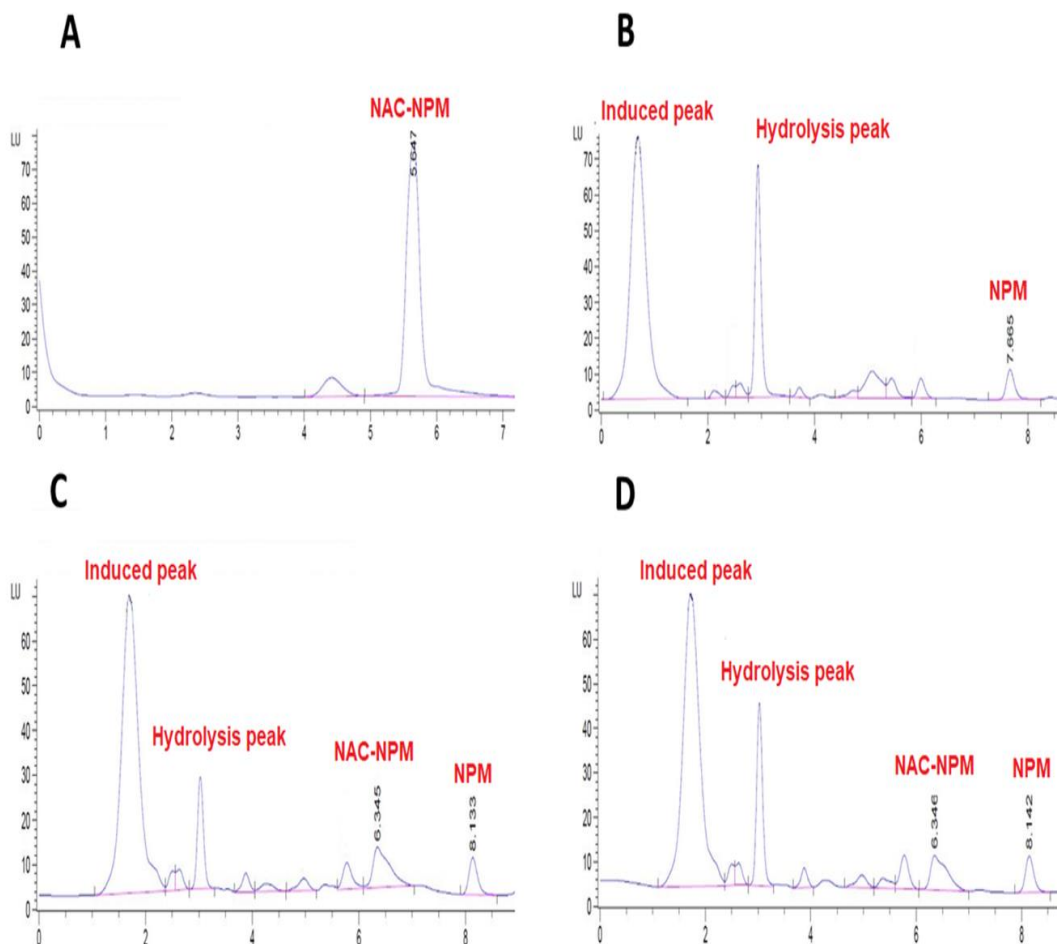


Figure 3.85: Chromatograms of derivative samples.

(A) Chromatogram of NAC 500 μ g/ml in water standard with NPM derivatives showing a NAC peak at RT of 5.647min, (B) Chromatogram of CM alone released by hADMSCs showing NMP peak at RT of 7.66min (no NAC-NPM peak), (C) Chromatogram of 500 μ g/ml SAC/NAC-primed hADMSCs CM after 24hours, showing NAC-NPM peak at RT of 6.345min and calculated NAC concentration was 149.75 μ g/ml and (D) Chromatogram of 500 μ g/ml SAC/NAC-primed hADMSCs CM after 48 hours, showing NAC-NPM peak at RT of 6.346min and the calculated NAC concentration was 124.21 μ g/ml. The column used (Eclipsex DB. C18, 4.6mm x 25cm, particle size: 3 μ m) with an injection volume of 1 μ l and the column temperature was 60 $^{\circ}$ C. The NAC-NPM derivatives were measured by a fluorescence detector (FID) (λ ex = 330nm and λ em = 376nm)

Chapter 4 - Discussion

4.1 Detection of AGEs

Advanced glycation end products can be generated from the amino residues of proteins, lipids and DNA through several different mechanisms. Such mechanisms include non-enzymatic glycation by glucose and reactions with metabolic intermediates and reactive dicarbonyl intermediates (MG and glyoxal). Consequently, these reactions not only alter the form and structure of the proteins but also lead to intramolecular and intermolecular cross-link production. The accumulation of cross-linked AGEs in biological compartments such as tissues and plasma plays a vital role in long-term complications associated with diabetes mellitus (Wu *et al.*, 2009; Genuth *et al.*, 2015).

Several studies have highlighted the benefits of using medicinal plants for inhibiting AGE formation, and may, therefore, provide protection to alleviate the development of such complications (Kaewkamson *et al.*, 2007; Wang *et al.*, 2009; Parveen *et al.*, 2017). In addition, these naturally derived chemicals also contribute to improved intercellular drug delivery, which is considered an important factor in attaining good therapeutic effects (Jeetah *et al.*, 2014). In this regard, extensive studies were carried out on garlic, which has a very long history of use as both a food and medicinal plant (Rivlin, 2001; Bozin *et al.*, 2008; Cardelle-Cobas *et al.*, 2010). Notably, garlic is available in different formulations, with one such preparation being aged garlic extract (Agarwal *et al.*, 2004; Cardelle-Cobas *et al.*, 2010; Arreola *et al.*, 2015).

In this study, protein glycation was established *in vitro* by incubation of proteins with a reducing sugar (MG) at physiological pH for various time intervals. Lysozyme is a popular protein for the detection of cross-linked AGE production, as oligomerisation occurs readily and is easily measurable by SDS-PAGE techniques. A number of researchers have examined the glycation of lysozyme *in vitro* (Kislinger *et al.*, 2004; Muthenna *et al.*, 2012; Adisakwattana *et al.*, 2012; Mariño *et al.*, 2017). Lysozyme consists of 6 lysines and 11 arginines per molecule, and modifications of these residues can be achieved by both glucose and MG. The results of SDS-PAGE illustrate that elevated cross-linked AGE formation is correlated with glucose concentration and the

period of incubation. This finding is consistent with a previous study which found that high AGE cross-link formation was correlated with increased glucose levels and incubation time (Mashilipa *et al.*, 2011).

Like other workers, this study has also demonstrated that exposure of proteins to MG reacts relatively rapidly with proteins and induces crosslinking to form AGEs. It was suggested that glycation by MG is increased disproportionately compared to the increase in glucose concentration in experimental and clinical diabetes (Ahmed, 2005). This may be attributed to the formation of MG from triosephosphate accumulation in vascular cells suffering cytosolic hyperglycaemia (Brownlee, 2001; Thornalley, 2008; Gaens *et al.*, 2013). Moreover, the other important features of MG are its ability to bind with sulphhydryl, amino, lysine and arginine functional groups in protein molecules (Richarme *et al.*, 2015). In this respect, MG-induced generation of AGEs has contributed to the progression and development of diabetic microvascular complications such as neuropathy, retinopathy and atherosclerosis (Chawla *et al.*, 2016) and the concentration of MG is elevated during diabetes (Kong *et al.*, 2014; Moraru *et al.*, 2018). Moreover, MG is recognised as a toxic agent (Lee and Park, 2017) and its toxicity is mainly associated with cell apoptosis (Di Loreto *et al.*, 2008) in a variety of cells, including endothelial cells, epithelial cells, human leukaemia cells, Schwann cells, osteoblasts and rat hippocampal cells (Kim *et al.*, 2014; Seo *et al.*, 2014; Tajés *et al.*, 2014; Chan *et al.*, 2016).

During this study, the potential benefits of using SAC and/or NAC derived from natural sources were assessed in a lysozyme-MG system *in vitro*. The formation of cross-linked AGEs was induced by incubation of proteins with MG (Klöpfer *et al.*, 2010). The results obtained from cross-linking assays suggested that cross-linking between the binding of reducing sugars to protein occurred during AGE formation. Using SAC and/or NAC displayed potent inhibitory effects on AGE formation. Furthermore, findings from the present study also indicate that these inhibitors have the potent ability to prevent protein glycation by MG. The inhibition of MG-derived AGEs by SAC/NAC produce a synergistic effect when compared with SAC or NAC alone. This inhibitory effect may occur at any stage in the glycation reaction such as to compete for the amino groups on the protein, bind to the protein or to the glycation

intermediates to stop the progression up to the AGE formation stage (Brownson and Hipkiss, 2000; Harding and Ganea, 2006; Younus and Anwar, 2016). This is in agreement with previous work by Ahmad *et al.* (2007) who demonstrated that aged garlic extract and SAC effectively inhibit AGEs formation *in vitro*.

In this study, synthetic mimic compounds A, B and C were tested for their antiglycation activities. These compounds are small molecules inhibitor- mimics of SAC and NAC. This is the first study to evaluate the effect of these compounds on AGE formation. Incubation of lysozyme glycosylated with MG in the presence and /or absence of compounds A, B and C showed potent inhibitory effect on the formation of AGEs. The basic structure of compounds A, B and C have many functional groups. Therefore, they may have excellent antiglycation and MG trapping ability.

Structurally, compound A [(R) S-Benzyl-L-cysteine] with one benzene ring, an amino group and carbonyl group showed better ability to inhibit AGE formation than compounds B and C. However, its antiglycation ability may have been dependent upon its unique phenolic structure and the number and position of the hydroxyl and amino groups. Despite the fact that compound B does not possess the essential functional groups like benzene ring, its antiglycation activity was stronger than compound C. Compound C [(R) S-triphenylmethyl cysteine] is more fat-soluble compound than compound A. Theoretically, compound C with three benzene rings, amino group and carbonyl group should produce the highest antiglycation activity. Therefore, it may be that the three benzene rings in compound C do not have the required structure, which attributed to these results. In addition, it is thought that acidic and /or basic amino acids play an important role in the antiglycation activity and different positions of the carboxylic group may produce different effects. Therefore, compound A was used in future experiments. However, to our knowledge, this is the first study demonstrating the ability of SAC/NAC as a mixture and compound A to inhibit the formation of cross-linked AGE *in vitro*.

The detection of fluorescence to study the effects of different glucose concentrations on AGE production also confirmed the previous findings with SDS-PAGE techniques. The measurement of fluorescence intensity as a parameter to study the effects of

SAC/NAC on cross-linked AGE formation was not possible because SAC/NAC do not exhibit satisfactory absorption at visible or ultraviolet wavelengths, nor do they exhibit fluorescence (Lee *et al.*, 2014). Other limitations are in terms of sensitivity or procedures being time-consuming (Ercal *et al.*, 1996). Therefore, other methods were used to study the effects of SAC/NAC on the formation of cross-linked AGEs. Furthermore, comparative studies were conducted between SAC/NAC and compound A using ELISA. Since MG is an important reactive intermediate of AGEs' generation, its elimination may hinder AGE production in biological systems.

As shown in the ELISA assay, after BAECs were exposed to 300 μ M MG, the AGEs formation was significantly increased in the cell medium. However, the MG-induced AGE formation was markedly inhibited by the treatment with SAC/NAC and compound A, with the results being comparable to the positive control. Furthermore, a recent study tested the effect of 200 μ M NAC on HaCaT exposed to 400 μ M MG for 48 hours, and showed that NAC inhibited MG-induced AGE formation (Yang *et al.*, 2017).

Different strategies have been proposed to reverse the effect of AGEs, focusing on the prevention of the formation of AGE cross-links or even the development of AGEs (Elosta *et al.*, 2012). The results obtained from both SDS-PAGE-silver stain and Western blot assays showed that SAC/NAC and compound A inhibited the formation of AGEs and this is in agreement with previous studies demonstrating that aged garlic extract and SAC effectively inhibit AGE formation *in vitro* in dose-dependent (Ahmad *et al.*, 2007).

Analysis of SDS-PAGE revealed the abilities of SAC/NAC and compound A to inhibit AGE formation decreased in the order of compound A > SAC/NAC > SAC > NAC. In all tested concentrations, compound A has more potent effects when compared with SAC/NAC against glycation-derived protein cross-linking. These results suggest that other functional groups may be present in compound A, which gives its antiglycation activity, although these groups have not yet been determined.

It was further suggested that the antiglycation activity of aged garlic extract is mainly due to its organosulphur compounds. The latter is derived from garlic; DAS, SEC, SAC and NAC, and have been found to protect LDL against oxidation and glycation. This may, therefore, explain why garlic protects against cardiovascular disease in healthy individuals (Ou *et al.*, 2003).

In addition, organosulphur compounds, including SAC and NAC, are well known to exhibit free-radical scavenging effects (Colín-González *et al.*, 2012,; Dewi *et al.*, 2017). This antioxidant property of aged garlic extract may be, at least in part, involved in the AGE-inhibitory mechanisms. For this reason, various comparative studies between SAC, NAC and compound A were conducted in this study. However, the antioxidant properties of SAC, NAC and compound A have not been elucidated in this study. Chemically, NAC is derived from L-cysteine, whose amino-group is acetylated. It was reported that L-cysteine, as well as its metabolite H₂S, is decreased in African Americans with Type 2 DM (Jain *et al.*, 2015). Although NAC is a well-known thiol compound used in chronic obstructive pulmonary disease because it possesses a free sulphhydryl group through which it reduces disulfide bonds conferring antioxidant effects; NAC possesses other beneficial effects on glucose and lipid metabolism (Yongjie Ma *et al.*, 2016).

The possible reason for the inhibition of AGE formation in samples treated with different concentrations of SAC/NAC and compound A was that such inhibitors might have the ability to modify the carbonyl or amino groups in the glycation reaction, which therefore results in the inhibition of AGE formation.

4.2 Angiogenesis

The angiogenic process is tightly regulated and can be triggered by some pathological processes such as diabetic angiogenesis. The prevalence of diabetes mellitus and diabetic vascular complications are largely associated with mortality and disability. The formation of tube-like structures in endothelial cells is another crucial step of angiogenesis (Xie *et al.*, 2016). The tube formation assay is a rapid and quantitative method for determining genes or pathways involved in angiogenesis. In the later stages

of angiogenesis, endothelial cells differentiate into tubular-like structures, which eventually form the lumen of new blood vessels. Tube formation occurs quickly with most tubes forming in this assay within 2 - 6 hours, depending on the quantity and type of angiogenic stimuli (DeCicco-Skinner *et al.*, 2014).

This study has mainly examined the effect of glucose, AGEs, SAC/NAC and compound A on the paradoxical phenomena of angiogenesis and its underlying mechanism of migration and capillary loop formation of endothelial cells. FGF-2 is a pro-angiogenic factor that stimulates the proliferation, migration and tube formation of the endothelial cell at the concentration of 25ng/ml (Hussain *et al.*, 2009). Hence, in the current study, it was used as a positive control. Although the migration and tube formation results show that FGF-2 greatly increased cell invasion compared to untreated cells, its effect has not been examined in the presence of the inhibitors including, glucose, AGEs, SAC/NAC and compound A.

It is well established in DM, that hyperglycaemia usually ranges from 6 to 30mM glucose and, in severe conditions the levels may reach at 55mM (Facchiano *et al.*, 2006). In this study, concentrations of 15 - 100mM of glucose have been chosen to represent a range corresponding to moderate to severe diabetic conditions (J. Zhang *et al.*, 2006). Although these concentrations approach the upper limit of those seen in physiological conditions, this takes into account that the normal ideal growth conditions for endothelial cells *in vitro* include medium supplementation with 25mM glucose. This concentration is similar to that used in similar studies investigating the effects of glucose on protein glycation and oxidative stress in macrovessel and microvessel endothelial cells (Paget *et al.*, 1998; Padayatti *et al.*, 2001).

The effect of high glucose on BAEC migration was evaluated using the *in vitro* wound healing assay. The results demonstrated that 25 - 100mM glucose inhibits the migratory abilities of endothelial cells and that these effects occurred in a dose-dependent manner compared to controls (Fig. 3.42). The effect of glucose on BAEC may induce oxidative stress through inactivation of antioxidant enzymes and glycation (Buranasin *et al.*, 2018). Moreover, these results were in agreement with those of other studies showing that high glucose concentration (75mM) significantly inhibited cell

migration (Buranasin *et al.*, 2018). However, Lamers *et al.* (2011) found that glucose, at lower concentration 25mM, impairs cell migration in Chinese hamster ovary (CHO) cells (CHO.K1) and mouse embryonic fibroblasts (NIH-3T3) due to an increase in oxidative stress that causes polarity loss, deficient adhesion and protrusion.

Sustained high glucose environments can cause abrogation of the cell migration and tube formation as well (Qiu *et al.*, 2018). In accordance with previous studies, this work also showed that glucose inhibits tube formation by endothelial cells *in vitro*. When BAECs were cultured on polymerised Matrigel, they were organised into such tube like-structures. However, when BAECs were cultured on polymerised Matrigel in the presence of glucose (25 - 100mM), the cells failed to organise into capillary-like structures. These effects occurred in a dose-dependent manner compared to controls. Song *et al.* (2017) found that the ability of HUVECs to form vascular-like structures was inhibited under high glucose or in the presence of AGEs. By mean of RNA interference, the expression of inhibitory genes can promote neovascularisation in the diabetic environment. The abnormal activation mechanism of barriers to angiogenesis in refractory diabetic wounds.

The migration of endothelial cells is one of the critical features in the formation of new blood vessels and in the repair of injured vessels. Therefore, another approach in this study was to determine whether SAC/NAC and compound A induce or inhibit the migration process of BAECs. The *in vitro* wound-healing assay showed that both SAC/NAC and compound A, at concentrations of between 0.1 - 2µg/ml, inhibited BAEC migration in a dose-response manner. The involvement of aged garlic extract in cell migration had already investigated by Nariaki Matsuura *et al.* (2006) who tested its effects on cell functions associated with migration. Their data showed that aged garlic extract is able to enhance the adhesion of endothelial cells to collagen and fibronectin. Furthermore, suppressed cell motility and invasion in the wound-healing assay. SAC suppressed the migration of human epithelial ovarian cancer cell line A2780 in a dose-dependent manner (Xu *et al.*, 2014), HUVEC (Lee *et al.*, 2015) and T24 bladder cancer cells (Supabphol *et al.*, 2009).

Aged garlic extract produces several pharmacological effects, including the inhibition of tumour cell growth and chemopreventive effects (Kyo *et al.*, 2001). It could prevent tumour formation by inhibiting angiogenesis through the suppression of endothelial cell motility, proliferation, and tube formation (Matsuura *et al.*, 2006). This study found that in the *in vitro* tube formation assay, SAC/NAC and compound A, at concentrations of between 0.1 - 2µg/ml, are also capable of destroying vascular networks formed on Matrigel. Recently, SAC (100µM) was found to enhance the formation of new blood vessels derived from EPCs (Syu *et al.*, 2017). Alliin was shown to induced-tube formation and angiogenesis in HUVECs and *ex vivo* in the CAM assay (Matsuura *et al.*, 2006). NAC reduced VEGF-induced tube formation of endothelial cells (Lee *et al.*, 2015). However, previous studies showed that SAC (Matsuura *et al.*, 2006; Pandrangi, 2015; Haghi *et al.*, 2017) and NAC (Cai *et al.*, 1999; Zafarullah *et al.*, 2003; Zhang *et al.*, 2018) promote cellular migration. Thus, further studies are required to determine the underlying mechanisms of these inhibitors.

In this study, SAC/NAC and compound A (0.01 - 2µg/ml) incubated with glucose (75mM) were found to dramatically inhibit BAECs to undergo cell migration at all concentrations *in vitro*. Lamers *et al.* (2011) showed that the 25mM glucose effects were partially or completely reversed in CHO.K1 and NIH-3T3 cell migration by treatment with 10mM NAC. These results could be due to the high NAC concentration used and the concentration at which NAC is effective, varying on the cell type (Sadowska *et al.*, 2007; Buranasin *et al.*, 2018). Exposure of HaCaT cells to 400µM MG markedly suppressed cell migration. However, this was alleviated by pretreatment with 200µM NAC (Yang *et al.*, 2017).

It has been reported that hyperglycaemia-induced oxidative stress increases ROS formation in type 2 diabetic mouse model (Furukawa *et al.*, 2017). Furthermore, It has been shown that treatment with a high concentration of NAC (1mM) could restore cell migration and proliferation in human gingival fibroblast cells (HGFs) grown at high glucose concentrations (50mM), while lower concentrations of NAC (100µM and 500µM) produce the opposite effects (Buranasin *et al.*, 2018). However, the mechanism through which excess glucose results in endothelial damage has not been

well elucidated. Incubation of SAC/NAC and compound A (0.01-2 μ g/ml) with glucose (75mM) was found to inhibit BAEC tube formation *in vitro*. This study has shown that prolonged exposure to elevated glucose reduced endothelial-dependent relaxation and delayed cell migration in cultured endothelial cells. This was coincident to other findings in normal blood vessels (Control and Group, 1993; Guo *et al.*, 2000; J. Zhang *et al.*, 2006). The results obtained from cell migration and tube formation showed that SAC/NAC and compound A in combination with glucose showed more inhibition effect than glucose alone.

Increasing evidence from *in vitro* and *in vivo* studies have shown that the biochemical process of AGE formation, which is accelerated in diabetes as a result of chronic hyperglycaemia, is responsible for the development of diabetic complications (Yamagishi and Imaizumi, 2005; Goh and Cooper, 2008; Saeidnia and Abdollahi, 2013; Aljohi *et al.*, 2018; Rhee and Kim, 2018). This has, accordingly, led to the hypothesis that protein glycation, through the formation of AGEs, may play a role in angiogenesis (Stitt *et al.*, 2005; Oak *et al.*, 2009). AGE-modified BSA (BSA-AGE) has been used for studying AGE toxicity on a number of cell types (McCarthy *et al.*, 1997; Yui *et al.*, 1994) and shown to be toxic to mesangial cells (Trachtman *et al.*, 1994), BAECs (Duraisamy *et al.*, 2003) and retinal pericytes (Yamagishi *et al.*, 1995). This toxicity is mediated via the production of free radicals, particularly when AGEs interact with their receptors on the cell surface (Naka *et al.*, 2004; Rojas and Morales, 2004).

In the present study, the results showed that BSA-AGEs at concentrations of 15 – 50 μ g/ml, inhibited the number of migrated cells. This range was selected as it may represent the lowest plasma AGE level found in diabetic patients (Xu *et al.*, 2003). BSA-AGEs were used at 50 μ g/ml for the study, which is considered not toxic to BAECs, in agreement with Chibber *et al.* (1997) who show that BSA-AGEs are toxic to BAECs only at concentrations higher than 62.5 μ g/ml. Also, Makita *et al.* (1992) stated that human serum AGE levels were elevated more than two-fold in diabetic patients (~25 μ g/ml), and almost eight-fold in diabetic patients on haemodialysis (~80 μ g/ml) in comparison with normal patients. Moreover, BSA-AGEs have been used extensively in order to study the changes induced by protein glycation on several

cell lines and tissues (McCance *et al.*, 1993; McCarthy *et al.*, 1997; Franke *et al.*, 2009). In addition, a recent study showed that high concentrations of BSA-AGEs have been reported to impair cell migration by bone marrow-derived endothelial progenitor cells (Aljohi *et al.*, 2018). Another study by Sharaf *et al.* (2015) showed that the concentration range between 25–200µg/ml of MG-BSA-AGEs significantly increased the distance of cell migration of the MDA-MB-231 breast cancer cell line in a dose-dependent manner, with a peak at 50µg/ml.

AGEs have been observed to accumulate around vessels in the skin, which leads to impaired angiogenesis. Angiogenesis, including endothelial proliferation, migration and capillary tube-like formation, is regulated by many angiogenic factors (Song *et al.*, 2017). HUVECs exposed to high glucose and AGE concentration, have an impaired ability to form capillary-like assemblies in the tube formation assay was observed (Song *et al.*, 2017; Wang *et al.*, 2017). This study confirms that a high concentration of BSA-AGEs has been reported to inhibit tube formation. This is in agreement with previous studies who showed the same inhibitory effect of BSA-AGEs on tube formation (Wang *et al.*, 2005; Aljohi *et al.*, 2018).

The angiogenic effect of AGEs on ECs has been elucidated for several decades. It has been shown that the accumulation of serum AGEs in diabetes increases the severity of vascular complications (Goh and Cooper, 2008). Previous studies have confirmed that the interaction of AGEs and receptor RAGE is correlated with angiogenesis (Yamagishi *et al.*, 2008; Ko *et al.*, 2014). However, previous reports have debated whether AGEs exert pro-angiogenic or anti-angiogenic effects. Devi and Sudhakaran (2011) have demonstrated that different cell environments exert opposite effects on AGE-induced angiogenesis, while Wang *et al.* (2016) confirmed pro-angiogenic effects of AGEs in HUVECs by showing that BSA-AGEs induced increased angiogenesis.

In the present study, it has been shown that 25 - 50µg/ml of BSA-AGEs inhibited tube formation by BAECs. Moreover, BSA-AGEs caused a modest, but consistent, decrease in tube formation, the same BSA-AGEs concentration (50µg/ml) giving a maximal effect. This concentration of BSA-AGEs was comparable with that of the *in*

vivo situation in diabetes (Chen *et al.*, 2009). Reduced formation of tube-like structures by BAECs incubated under hyperglycaemic conditions suggests that the endothelial cell dysfunction in hyperglycaemia may contribute to decreased angiogenesis, which is mediated by glycation of cellular proteins (Ahmed *et al.*, 2008). The inhibition of tube formation in BAECs clearly shows that the effects observed with BSA-AGEs are due to their glycated moiety (Gallicchio *et al.*, 2006).

Previous studies report that BSA-AGEs may produce several biological effects in terms of the cultured cell including endothelial cell migration and tube formation (Tezuka *et al.*, 1993). Different cell environments exert opposite effects on AGE-induced angiogenesis. In a study by Wang *et al.* (2016) on HUVECs, they confirmed the pro-angiogenic effects of AGEs by showing that BSA-AGEs induced increased angiogenesis. The increase of hydroimidazolone, one of the components of AGEs, in the vitreous humour and serum has been demonstrated to be associated with proliferative diabetic retinopathy (PDR). In addition, Matsuura *et al.* (2006) reported that AGEs potently inhibited the tube formation of endothelial cells. The ability of HUVECs to form vascular-like structures was inhibited under high glucose and AGEs environments. The inhibition is relative to the factors Ang-2 and VEGF; Tie-2 receptor differential expression in cells also has a certain effect on the regulation of angiogenesis under high glucose and AGEs environments (Song *et al.*, 2017).

Surprisingly, this study also illustrated that the addition of 1-2 μ g/ml SAC/NAC and 0.5-2 μ g/ml compound A reversed the BSA-AGE anti-angiogenic effect on cell migration. This reactivity is justified because the AGE formation's being arrested by SAC/NAC and compound A may occur through blocking of AGE formation. A similar finding was obtained when the *Momordica charantia* (MC) was used in combination with AGEs (Aljohi *et al.*, 2018). NAC, an intracellular radical scavenger, completely prevented the inhibitory effects of AGEs on protein synthesis (Yamagishi *et al.*, 2003).

Similarly, the addition of 0.5-2 μ g/ml SAC/NAC and 0.5-2 μ g/ml compound A, combined with BSA-AGEs in BAEC showed an increase in angiogenesis. They formed short, thick capillary-like networks that seemed to be indicative of an early stage of angiogenic development. One explanation for these speculative results may

be that SAC/NAC and compound A act as AGE inhibitors by blocking AGE formation. A similar finding using MC was illustrated by Aljohi *et al.* (2018). The *in vitro* administration of NAC inhibited MG-induced AGE generation in skin keratinocytes. Importantly, the treatment with NAC significantly reduced MG-triggered inflammatory injury, mitochondrial dysfunction and impairment of cellular behavioural action. Further results revealed that the blockage of NAC on MG-induced inflammatory injury was mediated by RAGE, which indicates that the administration of NAC can attenuate DM-related dermal injury through the inhibition of AGE/RAGE signals (Yang *et al.*, 2017).

In the present study, the results demonstrated that SAC/NAC (500 μ g/ml) and compound A (250 μ g/ml) were not toxic and induced hADMSCs to release these inhibitory drugs in the dosage sufficient to inhibit the glycation induced by MG in endothelial cells. Therefore, SAC/NAC- and compound A-loaded hADMSCs CM might be employed to protect endothelial cells from AGE hyperactivity-induced toxicity caused by intracellular AGEs under the exposure to stress, such as oxidative stress and inflammation.

4.3 HPLC

Several studies have focused on HPLC with the fluorometric detection of derivatives of NAC (Gabard and Mascher, 1991). Several methods have been proposed for the measurement of NAC, but they have practical limitations in terms of sensitivity or time-consuming procedures (Ercal *et al.*, 1996). In this study, the development of a new HPLC method for measuring biological thiols, which incorporated the derivatising agent NMP (Winters *et al.*, 1995). NPM readily reacts with free sulphhydryl groups to form fluorescent derivatives. This method afforded substantial improvements in rapidity of analysis and ease of use. However, the NAC assay described in the present study may prove useful to the extent that it can be run under ambient conditions, requires only about 18 min per sample to run, is susceptible to automation being an HPLC method, but linearity for the NAC standards was obtained only between 100-300 μ g/ml ($r=0.9871$). The results obtained from HPLC indicated the quantity of NAC released from hADMSCs were enough for the protection against

the ECs damage from AGEs. However, the HPLC method to detect NAC still needs to be developed for further study.

The use of hADMSCs as an active targeted-delivery vehicle for therapeutic agents is especially attractive because they have proven to be permissive to small compound incorporation, and are immune-protective and pathotrophic. Considering the limited number of hADMSCs which can be delivered *in vivo*, it is important to have enough drug incorporated into them in order to achieve a therapeutic drug concentration in the targeted tissues (Janowski *et al.*, 2015). Numerous studies on the uptake of nanoparticles in hADMSCs have shown that the internalisation of nanoparticles can be improved by their modification, size control, proper incubation time and concentration (Auffinger *et al.*, 2013). To be effective, a therapeutic vehicle must primarily be stably loaded inside the cell carrier and then be released into the extracellular space gradually and steadily, instead of instant release into the systemic circulation prior to the cells' reaching the target site. Thereby, it gives time for the cell carrier to migrate towards the wound regions and reach as many target cells as possible after the systemic delivery.

It is also critical to ensure that drug loading does not affect the viability of hADMSCs and endothelial cells or their native properties, especially their pathotrophic ones. Several studies have proved that loading anticancer-drug nanoparticles, or even chemotherapeutic drugs, does not affect the short-term or long-term viability of MSCs (Auffinger *et al.*, 2013; Pascucci *et al.*, 2014; Fang *et al.*, 2016). This work also confirmed that neither SAC/NAC nor compound A loading affects the viability of hADMSCs. *In vitro* transwell experiments have demonstrated that nanoparticle-loaded MSCs still possess the migration capacity towards chemoattractant and endothelial cells (Huang *et al.*, 2013; Landázuri *et al.*, 2013; Sadhukha *et al.*, 2014; Fang *et al.*, 2016).

In the present study, the combination of SAC/NAC, compound A, SAC/NAC- and compound A-loaded hADMSCs CM were examined by SDS-PAGE-silver stain and Western blot to show whether these inhibited the glycation activity in endothelial cells. The results showed that SAC/NAC, compound A, SAC/NAC- and compound A-

loaded hADMSCs CM potent effective at inhibiting the formation of cross-linked AGEs *in vitro*. In addition, the uptake of SAC/NAC and compound A in hADMSCs increased in a time-dependent manner, starting from 24-hour incubation and gradually enriching the cytoplasm up to 48 hours of priming. After internalisation, SAC/NAC and compound A-loaded hADMSCs continuously released SAC/NAC and compound A into the medium for 4 days, with the peak release within the first 24 hours. The incorporation and release kinetics of nanoparticles in MSCs for the treatment of malignant glioma revealed that nanoparticles demonstrated an initial burst of release from cells within the first 4 hours followed by a steady release over 9 days (Sadhukha *et al.*, 2014). These findings were supported by a previous study conducted on BAECs to determine the effect of another inhibitor, P5, and P5-primed MSCs. The results from this study showed that the P5 was able to significantly inhibit calcium-induced CDK5 activity, reduce cell number and apoptosis markers (Fang *et al.*, 2016). In addition, a recent study tested the effect of 200 μ M NAC on HaCaT cells exposed to 400 μ M MG for 48 hours showed that NAC inhibited MG-induced AGE (Yang *et al.*, 2017).

Parekkadan and Milwid (2010) confirmed the therapeutic hypothesis that collection of bioactive molecules could be used as treatment. This can be done by collecting the molecules secreted in MSC-conditioned medium (MSC-CM) and administering them intravenously in a concentrated form in a single bolus dose to animals after the induction of disease. They also engineered a delivery platform for the continuous and dynamic administration of these molecules into the bloodstream. It was found that this treatment method provided an improved survival benefit of 71% compared with 14% in controls. In addition, other studies have suggested that pre-treatment of target cells, such as by gene editing, can change the secretion characteristics and function of the exosomes. It is believed that, after pre-treatment, MSCs may be the ideal drug or gene delivery media (Kim *et al.*, 2007; Yu *et al.*, 2013).

The important novel findings from the current study demonstrate that SAC/NAC- and compound A-loaded hADMSCs CM was able to promote cell migration and tube formation considerably. This could mean that the secretions from hADMSCs contain diverse cytokines, such as EGF, VEGF, HGF, bFGF, GDNF, angiogenin and IL-8, which have shown their capabilities in promoting angiogenesis (Du *et al.*, 2016).

Notably, drugs released from hADMSCs are capable of keeping their bioactivities. The findings described herein make these cells interesting candidates for drug delivery vehicles. Also, they are able to play protective roles against endothelial cell damage by AGEs under specific culture condition *in vitro*. In addition, SAC/NAC and compound A incubated with SCM have been shown to induce the migration and tube formation abilities of endothelial cells compared to control. In this study, used hADMSCs as a drug carrier in order to release SAC/NAC and compound A which provide to protect the cells against AGEs damage.

Wu *et al.* (2007) reported that injection of BMSCs significantly enhanced the wound closure and strength in a diabetic mouse model for wound healing. PARK *et al.* (2008) showed that used ASC-CM increased collagen synthesis leading to improve the outcome of wound healing. Further analysis revealed increased collagen production and altered gene expression with CM obtained from ASCs (Kim *et al.*, 2007; Lee *et al.*, 2009). Barcelos *et al.* (2009) demonstrated the efficacy of local therapy with human fetal aorta-derived CD133⁺ progenitor cells and their CM in a preclinical model of DFU. Taken together, the above findings indicate that ASCs release effective factors and can stimulate recruitment, migration, and proliferation of endogenous cells in the wound environment. Consequently, Paracrine factors' secretion from ASCs was related to promote angiogenesis, epithelialization, and tissue remodelling through during wound repair (Hassan *et al.*, 2014).

Chapter 5 – Conclusion and Future work

5.1 Conclusion

The findings of the current study have demonstrated that protein glycation causes cross-linked that fundamentally influence the physical and chemical properties of proteins. The degree of protein glycation is concentration-dependent. These data support the contribution of protein glycation in the development of diabetic complications. However, the process of glycation and the damage caused by AGEs may be reduced with the use of antiglycation agents. The present study was conducted to evaluate the antiglycation activities of several inhibitors including SAC, NAC and compound A. The data presented in this study clearly indicate that both SAC/NAC and compound A can effectively protect against MG-mediated protein modification *in vitro*, possibly due to their interaction with α -oxoaldehydes generated during the glycation process. The work contained within this thesis has highlighted the potential of hADMSCs as an applied therapy for wound healing.

The most promising area of this section of the study is the development towards a successful methodology for the quantification of drug release from hADMSCs by HPLC. If this methodology can be finalised, the possible applications in the development of stem cells as a means of drug delivery would be extremely significant.

In conclusion, hADMSCs provide a highly attractive option for the treatment of diabetic wound healing due to their many natural characteristics and their potential to be applied as a combinational therapy. The successful delivery of drugs such as SAC/NAC and compound A in combination and using a target method, could be an effective way to stimulate wound healing.

5.2 Limitations

1. An *in vivo* study on the effect of SAC/NAC and compound A on diabetic patients wound healing was not included. Further investigation into the effect of SAC/NAC and compound A *in vivo* is certainly required
2. Unavailable detector for SAC and compound A
3. To our limited knowledge, there has been no report relevant to the effects of SAC/NAC- loaded hADMSCs CM on wound healing

5.3 Future work

1. Further studies relating to the current work that can be pursued include:
 - New techniques, such as mass spectrometry or nuclear magnetic resonance, may be used for the structural determination of AGEs
 - The bioavailability of SAC/NAC and compound A, and their ability to inhibit AGE formation require further investigation using specific biomarkers
 - The examination of the effects of BSA-AGEs, SAC/NAC and compound A on FGF-2-induced BAEC modification
 - A further, more in-depth, study with greater focus on the quantification of AGEs in diabetic tissues, and their functional effects on cell signalling
 - Further HPLC methodology for NAC development
 - SAC/NAC, compounds A, B and C could be further studied for their antioxidant activity
2. Investigate the anti-inflammation of IL-1RA-primed MSCs
 - Assess the mRNA and protein synthesis of cytokines and chemokines (IL-1 β , TNF α , CRP, IL-6, IL-10, MCP) in monocytes and macrophages by real-time PCR and Western blotting
 - Analyse the release of cytokines and chemokines by monocytes and macrophages using ELISA
3. Investigate the effectiveness of dressing coated with drug-primed MSCs
 - Optimise the dressing conditions, including materials, the amounts of drug-primed MSCs
 - Investigate the effectiveness of the dressing coated with drug-primed MSCs on wound healing

References

- Abdullah, T. (1989) 'Enhancement of natural killer cell activity in AIDS with garlic.' *J. Oncol.*, 21 pp. 52-53.
- Adisakwattana, S., Sompong, W., Meeprom, A., Ngamukote, S. and Yibchok-anun, S. (2012) 'Cinnamic acid and its derivatives inhibit fructose-mediated protein glycation.' *International Journal of Molecular Sciences*, 13(2) pp. 1778-1789.
- Agarwal, A., Munoz-Najar, U., Klueh, U., Shih, S. C. and Claffey, K. P. (2004) 'N-acetyl-cysteine promotes angiostatin production and vascular collapse in an orthotopic model of breast cancer.' *Am J Pathol*, 164(5), May, 2004/04/28, pp. 1683-1696.
- Agunloye, O. M. and Oboh, G. (2018) 'Caffeic acid and chlorogenic acid: Evaluation of antioxidant effect and inhibition of key enzymes linked with hypertension.' *Journal of Food Biochemistry*, p. e12541.
- Ahmad, M. S., Pischetsrieder, M. and Ahmed, N. (2007) 'Aged garlic extract and S-allyl cysteine prevent formation of advanced glycation endproducts.' *European journal of pharmacology*, 561(1-3) pp. 32-38.
- Ahmed, N. (2005) 'Advanced glycation endproducts—role in pathology of diabetic complications.' *Diabetes Research and Clinical Practice*, 67(1) pp. 3-21.
- Ahmed, N. and Thornalley, P. (2007) 'Advanced glycation endproducts: what is their relevance to diabetic complications?' *Diabetes, Obesity and Metabolism*, 9(3) pp. 233-245.
- Ahmed, N., Balamash, K., Albar, O. and Wang, Q. (2012) 'Effect of Kyolic® aged garlic extract on glycaemia, lipidaemia and oxidative stress in patients with type 2 diabetes mellitus.' *Journal of Diabetes Research and Clinical Metabolism*, 1(1) p. 18.
- Ahmed, U., Dobler, D., Larkin, S. J., Rabbani, N. and Thornalley, P. J. (2008) 'Reversal of Hyperglycemia-Induced Angiogenesis Deficit of Human Endothelial Cells by Overexpression of Glyoxalase 1In Vitro.' *Annals of the New York Academy of Sciences*, 1126(1) pp. 262-264.
- Ajandouz, E., Tchiakpe, L., Ore, F. D., Benajiba, A. and Puigserver, A. (2001) 'Effects of pH on caramelization and Maillard reaction kinetics in fructose-lysine model systems.' *Journal of Food Science*, 66(7) pp. 926-931.
- Akita, S., Akino, K., Hirano, A., Ohtsuru, A. and Yamashita, S. (2010) 'Noncultured autologous adipose-derived stem cells therapy for chronic radiation injury.' *Stem Cells International*, 2010

Aljohi, A., Matou-Nasri, S. and Ahmed, N. (2016) 'Antiglycation and antioxidant properties of Momordica charantia.' *PloS one*, 11(8) p. e0159985.

Aljohi, A., Matou-Nasri, S., Liu, D., Al-Khafaji, N., Slevin, M. and Ahmed, N. (2018) 'Momordica charantia extracts protect against inhibition of endothelial angiogenesis by advanced glycation endproducts in vitro.' *Food & Function*, 9(11) pp. 5728-5739.

Amagase, H., Petesch, B. L., Matsuura, H., Kasuga, S. and Itakura, Y. (2001) 'Recent advances on the nutritional effects associated with the use of garlic as a supplement.' *J. Nutr*, 131(3) pp. 955S-962S.

Ames, J. M. (1990) 'Control of the Maillard reaction in food systems.' *Trends in Food Science & Technology*, 1 pp. 150-154.

Andrews, A. M. (2015) *Human mesenchymal stem cell loading as a novel targeting and drug delivery system for stroke*. Manchester Metropolitan University.

Ankeny, D. P., McTigue, D. M. and Jakeman, L. B. (2004) 'Bone marrow transplants provide tissue protection and directional guidance for axons after contusive spinal cord injury in rats.' *Experimental Neurology*, 190(1) pp. 17-31.

Ankrum, J. and Karp, J. M. (2010) 'Mesenchymal stem cell therapy: Two steps forward, one step back.' *Trends in Molecular Medicine*, 16(5) pp. 203-209.

Appiah, D., Schreiner, P. J., Gunderson, E. P., Konety, S. H., Jacobs, D. R., Nwabuo, C. C., Ebong, I. A., Whitham, H. K., Goff, D. C. and Lima, J. A. (2016) 'The Association of Gestational Diabetes Mellitus With Left Ventricular Structure and Function: The CARDIA Study.' *Diabetes Care*, p. dc151759.

Arreola, R., Quintero-Fabián, S., López-Roa, R. I., Flores-Gutiérrez, E. O., Reyes-Grajeda, J. P., Carrera-Quintanar, L. and Ortuño-Sahagún, D. (2015) 'Immunomodulation and anti-inflammatory effects of garlic compounds.' *Journal of Immunology Research*, 2015

Arya, A. K., Garg, S., Kumar, S., Meena, L. P. and Tripathi, K. (2013) 'Estimation of lymphocyte apoptosis in patients with chronic non-healing diabetic foot ulcer.' *Int J Med Sci Pub Health*, 2(4) pp. 766-768.

Arzanlou, M. and Bohlooli, S. (2010) 'Introducing of green garlic plant as a new source of allicin.' *Food Chemistry*, 120(1) pp. 179-183.

Ashraf, R., Khan, R. A. and Ashraf, I. (2011) 'Garlic (*Allium sativum*) supplementation with standard antidiabetic agent provides better diabetic control in type 2 diabetes patients.' *Pak J Pharm Sci*, 24(4) pp. 565-570.

Association, A. D. (2015) 'Standards of medical care in diabetes—2015 abridged for primary care providers.' *Clinical diabetes: a publication of the American Diabetes Association*, 33(2) p. 97.

Auffinger, B., Morshed, R., Tobias, A., Cheng, Y., Ahmed, A. U. and Lesniak, M. S. (2013) 'Drug-loaded nanoparticle systems and adult stem cells: a potential marriage for the treatment of malignant glioma?' *Oncotarget*, 4(3) p. 378.

Baglio, S. R., Pegtel, D. M. and Baldini, N. (2012) 'Mesenchymal stem cell secreted vesicles provide novel opportunities in (stem) cell-free therapy.' *Frontiers in Physiology*, 3 p. 359.

Balakumar, P., Rohilla, A., Krishan, P., Solairaj, P. and Thangathirupathi, A. (2010) 'The multifaceted therapeutic potential of benfotiamine.' *Pharmacological Research*, 61(6) pp. 482-488.

Barcelos, L. S., Duplaa, C., Kränkel, N., Graiani, G., Invernici, G., Katare, R., Siragusa, M., Meloni, M., Campesi, I. and Monica, M. (2009) 'Human CD133+ progenitor cells promote the healing of diabetic ischemic ulcers by paracrine stimulation of angiogenesis and activation of Wnt signaling.' *Circulation Research*, 104(9) pp. 1095-1102.

Barry, F. P. and Murphy, J. M. (2004) 'Mesenchymal stem cells: clinical applications and biological characterization.' *The International Journal of Biochemistry & Cell Biology*, 36(4) pp. 568-584.

Bassama, J., Brat, P., Bohuon, P., Hocine, B., Boulanger, R. and Günata, Z. (2011) 'Acrylamide kinetic in plantain during heating process: Precursors and effect of water activity.' *Food Research International*, 44(5) pp. 1452-1458.

Basta, G., Schmidt, A. M. and De Caterina, R. (2004) 'Advanced glycation end products and vascular inflammation: implications for accelerated atherosclerosis in diabetes.' *Cardiovascular Research*, 63(4) pp. 582-592.

Beisswenger, P. J., Howell, S. K., Russell, G. B., Miller, M. E., Rich, S. S. and Mauer, M. (2013) 'Early progression of diabetic nephropathy correlates with methylglyoxal-derived advanced glycation end products.' *Diabetes Care*, p. DC_122689.

Bianchi, E., Ripandelli, G., Taurone, S., Feher, J., Plateroti, R., Kovacs, I., Magliulo, G., Orlando, M. P., Micera, A. and Battaglione, E. (2016) 'Age and diabetes related changes of the retinal capillaries: an ultrastructural and immunohistochemical study.' *International Journal of Immunopathology and Pharmacology*, 29(1) pp. 40-53.

Bianco, P., Robey, P. G. and Simmons, P. J. (2008) 'Mesenchymal stem cells: revisiting history, concepts, and assays.' *Cell Stem Cell*, 2(4) pp. 313-319.

Bierhaus, A., Humpert, P. M., Morcos, M., Wendt, T., Chavakis, T., Arnold, B., Stern, D. M. and Nawroth, P. P. (2005) 'Understanding RAGE, the receptor for advanced glycation end products.' *Journal of Molecular Medicine*, 83(11) pp. 876-886.

Bohlender, J. r. M., Franke, S., Stein, G. n. and Wolf, G. (2005) 'Advanced glycation end products and the kidney.' *American Journal of Physiology-Renal Physiology*, 289(4) pp. F645-F659.

Bommer, C., Sagalova, V., Heesemann, E., Manne-Goehler, J., Atun, R., Bärnighausen, T., Davies, J. and Vollmer, S. (2018) 'Global economic burden of diabetes in adults: projections from 2015 to 2030.' *Diabetes Care*, 41(5) pp. 963-970.

Bose, R. J., Kim, B. J., Arai, Y., Han, I.-b., Moon, J. J., Paulmurugan, R., Park, H. and Lee, S.-H. (2018) 'Bioengineered stem cell membrane functionalized nanocarriers for therapeutic targeting of severe hindlimb ischemia.' *Biomaterials*, 185 pp. 360-370.

Böttcher-Haberzeth, S., Biedermann, T., Klar, A. S., Pontiggia, L., Rac, J., Nadal, D., Schiestl, C., Reichmann, E. and Meuli, M. (2014) 'Tissue engineering of skin: human tonsil-derived mesenchymal cells can function as dermal fibroblasts.' *Pediatric Surgery International*, 30(2) pp. 213-222.

Bozin, B., Mimica-Dukic, N., Samojlik, I., Goran, A. and Igic, R. (2008) 'Phenolics as antioxidants in garlic (*Allium sativum* L., Alliaceae).' *Food Chemistry*, 111(4) pp. 925-929.

Branco, M. C. and Schneider, J. P. (2009) 'Self-assembling materials for therapeutic delivery.' *Acta Biomaterialia*, 5(3) pp. 817-831.

Brem, H., Stojadinovic, O., Diegelmann, R. F., Entero, H., Lee, B., Pastar, I., Golinko, M., Rosenberg, H. and Tomic-Canic, M. (2007) 'Molecular markers in patients with chronic wounds to guide surgical debridement.' *Molecular Medicine*, 13(1-2) p. 30.

Brownlee, M. (2001) 'Biochemistry and molecular cell biology of diabetic complications.' *Nature*, 414(6865) p. 813.

Brownlee, M. (2005) 'The pathobiology of diabetic complications: a unifying mechanism.' *Diabetes*, 54(6) pp. 1615-1625.

Brownson, C. and Hipkiss, A. R. (2000) 'Carnosine reacts with a glycosylated protein.' *Free Radical Biology and Medicine*, 28(10) pp. 1564-1570.

Buranasin, P., Mizutani, K., Iwasaki, K., Mahasarakham, C. P. N., Kido, D., Takeda, K. and Izumi, Y. (2018) 'High glucose-induced oxidative stress impairs proliferation and migration of human gingival fibroblasts.' *PloS one*, 13(8) p. e0201855.

Cai, T., Fassina, G., Morini, M., Aluigi, M. G., Masiello, L., Fontanini, G., D'Agostini, F., De, S. F., Noonan, D. M. and Albin, A. (1999) 'N-acetylcysteine inhibits endothelial cell invasion and angiogenesis.' *Laboratory Investigation; A Journal of Technical Methods and Pathology*, 79(9) pp. 1151-1159.

Calcutt, N. A., Cooper, M. E., Kern, T. S. and Schmidt, A. M. (2009) 'Therapies for hyperglycaemia-induced diabetic complications: from animal models to clinical trials.' *Nature Reviews Drug Discovery*, 8(5) p. 417.

Caliceti, C., Calabria, D., Roda, A. and Cicero, A. (2017) 'Fructose intake, serum uric acid, and cardiometabolic disorders: a critical review.' *Nutrients*, 9(4) p. 395.

Caplan, A. I. (1991) 'Mesenchymal stem cells.' *Journal of Orthopaedic Research*, 9(5) pp. 641-650.

Cardelle-Cobas, A., Soria, A. C., Corzo, N. and Villamiel, M. (2010) 'A comprehensive survey of garlic functionality.'

Cashman, C. R. and Höke, A. (2015) 'Mechanisms of distal axonal degeneration in peripheral neuropathies.' *Neuroscience Letters*, 596 pp. 33-50.

Cervantes-Laurean, D., Schramm, D. D., Jacobson, E. L., Halaweish, I., Bruckner, G. G. and Boissonneault, G. A. (2006) 'Inhibition of advanced glycation end product formation on collagen by rutin and its metabolites.' *The Journal of Nutritional Biochemistry*, 17(8) pp. 531-540.

Chan, C. M., Huang, D. Y., Huang, Y. P., Hsu, S. H., Kang, L. Y., Shen, C. M. and Lin, W. W. (2016) 'Methylglyoxal induces cell death through endoplasmic reticulum stress-associated ROS production and mitochondrial dysfunction.' *Journal of Cellular and Molecular Medicine*, 20(9) pp. 1749-1760.

Charbord, P., Livne, E., Gross, G., Häupl, T., Neves, N. M., Marie, P., Bianco, P. and Jorgensen, C. (2011) 'Human bone marrow mesenchymal stem cells: a systematic reappraisal via the genostem experience.' *Stem Cell Reviews and Reports*, 7(1) pp. 32-42.

Chaudhury, A., Duvoor, C., Dendi, R., Sena, V., Kraleti, S., Chada, A., Ravilla, R., Marco, A., Shekhawat, N. S. and Montales, M. T. (2017) 'Clinical review of antidiabetic drugs: Implications for type 2 diabetes mellitus management.' *Frontiers in Endocrinology*, 8 p. 6.

Chawla, A., Chawla, R. and Jaggi, S. (2016) 'Microvascular and macrovascular complications in diabetes mellitus: distinct or continuum?' *Indian Journal of Endocrinology and Metabolism*, 20(4) p. 546.

Chen, C.-P., Chen, Y.-Y., Huang, J.-P. and Wu, Y.-H. (2014) 'The effect of conditioned medium derived from human placental multipotent mesenchymal stromal cells on neutrophils:

possible implications for placental infection.' *Molecular Human Reproduction*, 20(11) pp. 1117-1125.

Chen, Q., Dong, L., Wang, L., Kang, L. and Xu, B. (2009) 'Advanced glycation end products impair function of late endothelial progenitor cells through effects on protein kinase Akt and cyclooxygenase-2.' *Biochemical and Biophysical Research Communications*, 381(2) pp. 192-197.

Chibber, R., Molinatti, P., Rosatto, N., Lambourne, B. and Kohner, E. (1997) 'Toxic action of advanced glycation end products on cultured retinal capillary pericytes and endothelial cells: relevance to diabetic retinopathy.' *Diabetologia*, 40(2) pp. 156-164.

Chiossone, L., Conte, R., Spaggiari, G. M., Serra, M., Romei, C., Bellora, F., Becchetti, F., Andaloro, A., Moretta, L. and Bottino, C. (2016) 'Mesenchymal stromal cells induce peculiar alternatively activated macrophages capable of dampening both innate and adaptive immune responses.' *Stem Cells*, 34(7) pp. 1909-1921.

Cho, S. O., Lim, J. W. and Kim, H. (2013) 'Red ginseng extract inhibits the expression of MCP-1 and iNOS in Helicobacter pylori-infected gastric epithelial cells by suppressing the activation of NADPH oxidase and Jak2/Stat3.' *Journal of Ethnopharmacology*, 150(2) pp. 761-764.

Chulpanova, D. S., Kitaeva, K. V., Tazetdinova, L. G., James, V., Rizvanov, A. A. and Solovyeva, V. V. (2018) 'Application of mesenchymal stem cells for therapeutic agent delivery in anti-tumor treatment.' *Frontiers in Pharmacology*, 9 p. 259.

Clavreul, A., Pourbaghi-Masouleh, M., Roger, E., Lautram, N., Montero-Menei, C. N. and Menei, P. (2017) 'Human mesenchymal stromal cells as cellular drug-delivery vectors for glioblastoma therapy: a good deal?' *Journal of Experimental & Clinical Cancer Research*, 36(1) p. 135.

Coghe, S., Gheeraert, B., Michiels, A. and Delvaux, F. R. (2006) 'Development of Maillard reaction related characteristics during malt roasting.' *Journal of the Institute of Brewing*, 112(2) pp. 148-156.

Colín-González, A. L., Santana, R. A., Silva-Islas, C. A., Chánez-Cárdenas, M. E., Santamaría, A. and Maldonado, P. D. (2012) 'The antioxidant mechanisms underlying the aged garlic extract- and S-allylcysteine-induced protection.' *Oxidative Medicine and Cellular Longevity*, 2012

Collawn, S. S., Banerjee, N. S., de la Torre, J., Vasconez, L. and Chow, L. T. (2012) 'S. S. Collawn, N. S. Banerjee, J. de la Torre, L. Vasconez, and L. T. Chow, "Adipose-derived stromal cells accelerate wound healing in an organotypic raft culture model," *Annals of Plastic Surgery*, vol. 68, no. 5, pp. 501–504, 2012.' *Annals of plastic surgery*, 68(5) p. 501.

Control, D. and Group, C. T. R. (1993) 'The effect of intensive treatment of diabetes on the development and progression of long-term complications in insulin-dependent diabetes mellitus.' *New England Journal of Medicine*, 329(14) pp. 977-986.

Couture, P., Paradis-Massie, J., Oualha, N. and Thibault, G. (2009) 'Adhesion and transcellular migration of neutrophils and B lymphocytes on fibroblasts.' *Experimental Cell Research*, 315(13) pp. 2192-2206.

Cui, H., Kong, Y. and Zhang, H. (2012) 'Oxidative stress, mitochondrial dysfunction, and aging.' *Journal of Signal Transduction*, 2012

Cunha, B. A. (2000) 'Antibiotic selection for diabetic foot infections: a review.' *The Journal of Foot and Ankle Surgery*, 39(4) pp. 253-257.

Dart, A. B., Martens, P. J., Rigatto, C., Brownell, M. D., Dean, H. J. and Sellers, E. A. (2014) 'Earlier onset of complications in youth with type 2 diabetes.' *Diabetes Care*, 37(2) pp. 436-443.

de Oliveira, S., Rosowski, E. E. and Huttenlocher, A. (2016) 'Neutrophil migration in infection and wound repair: going forward in reverse.' *Nature Reviews Immunology*, 16(6) p. 378.

de Vos, L. C., Lefrandt, J. D., Dullaart, R. P., Zeebregts, C. J. and Smit, A. J. (2016) 'Advanced glycation end products: An emerging biomarker for adverse outcome in patients with peripheral artery disease.' *Atherosclerosis*, 254 pp. 291-299.

DeCicco-Skinner, K. L., Henry, G. H., Cataisson, C., Tabib, T., Gwilliam, J. C., Watson, N. J., Bullwinkle, E. M., Falkenburg, L., O'Neill, R. C. and Morin, A. (2014) 'Endothelial cell tube formation assay for the in vitro study of angiogenesis.' *Journal of Visualized Experiments: JoVE*, (91)

Demidova-Rice, T. N., Hamblin, M. R. and Herman, I. M. (2012) 'Acute and impaired wound healing: pathophysiology and current methods for drug delivery, part 1: normal and chronic wounds: biology, causes, and approaches to care.' *Advances in Skin & Wound Care*, 25(7) p. 304.

Devi, M. S. and Sudhakaran, P. R. (2011) 'Differential modulation of angiogenesis by advanced glycation end products.' *Experimental Biology and Medicine*, 236(1) pp. 52-61.

Dewi, A. D. R., Kusnadi, J. and Shih, W.-L. (2017) 'Comparison of the main bioactive compounds and antioxidant activity from garlic water-soluble and garlic oil.' *KnE Life Sciences*, 3(5) pp. 20-34.

Di Loreto, S., Zimmiti, V., Sebastiani, P., Cervelli, C., Falone, S. and Amicarelli, F. (2008) 'Methylglyoxal causes strong weakening of detoxifying capacity and apoptotic cell death in

rat hippocampal neurons.' *The International Journal of Biochemistry & Cell Biology*, 40(2) pp. 245-257.

Diabetes, U. (2011) Diabetes in the UK 2010: key statistics on diabetes. March 2010.

DiPietro, L. A. (2013) 'Angiogenesis and scar formation in healing wounds.' *Current Opinion in Rheumatology*, 25(1) pp. 87-91.

Dolan, J. W. (2002) 'The importance of temperature.' *LC GC NORTH AMERICA*, 20(6) pp. 524-531.

Dominici, M., Paolucci, P., Conte, P. and Horwitz, E. M. (2009) 'Heterogeneity of multipotent mesenchymal stromal cells: from stromal cells to stem cells and vice versa.' *Transplantation*, 87(9S) pp. S36-S42.

Doob Jr, H., Willmann, A. and Sharp, P. F. (1942) 'Influence of moisture on browning of dried whey and skim milk.' *Industrial & Engineering Chemistry*, 34(12) pp. 1460-1468.

Driskell, R. R., Clavel, C., Rendl, M. and Watt, F. M. (2011) 'Hair follicle dermal papilla cells at a glance.' *J Cell Sci*, 124(8) pp. 1179-1182.

Du, W. J., Chi, Y., Yang, Z. X., Li, Z. J., Cui, J. J., Song, B. Q., Li, X., Yang, S. G., Han, Z. B. and Han, Z. C. (2016) 'Heterogeneity of proangiogenic features in mesenchymal stem cells derived from bone marrow, adipose tissue, umbilical cord, and placenta.' *Stem Cell Research & Therapy*, 7(1) p. 163.

Duraisamy, Y., Gaffney, J., Slevin, M., Smith, C. A., Williamson, K. and Ahmed, N. (2003) 'Aminosalicic acid reduces the antiproliferative effect of hyperglycaemia, advanced glycation endproducts and glycosylated basic fibroblast growth factor in cultured bovine aortic endothelial cells: comparison with aminoguanidine.' *In Vascular Biochemistry*. Springer, pp. 143-153.

Durstine, J. L., Gordon, B., Wang, Z. and Luo, X. (2013) 'Chronic disease and the link to physical activity.' *Journal of Sport and Health Science*, 2(1) pp. 3-11.

Echavarría, A., Pagán, J. and Ibarz, A. (2012) 'Melanoidins formed by Maillard reaction in food and their biological activity.' *Food Engineering Reviews*, 4(4) pp. 203-223.

Edwards, J. F., Casellini, C. M., Parson, H. K., Obrosova, I. G., Yorek, M. and Vinik, A. I. (2015) 'Role of peroxynitrite in the development of diabetic peripheral neuropathy.' *Diabetes Care*, 38(7) pp. e100-e101.

Eidi, A., Eidi, M. and Esmaeili, E. (2006) 'Antidiabetic effect of garlic (*Allium sativum* L.) in normal and streptozotocin-induced diabetic rats.' *Phytomedicine*, 13(9-10) pp. 624-629.

Elosta, A., Ghous, T. and Ahmed, N. (2012) 'Natural products as anti-glycation agents: possible therapeutic potential for diabetic complications.' *Current Diabetes Reviews*, 8(2) pp. 92-108.

Eming, S. A., Martin, P. and Tomic-Canic, M. (2014) 'Wound repair and regeneration: mechanisms, signaling, and translation.' *Science Translational Medicine*, 6(265) pp. 265sr266-265sr266.

Ercal, N., Oztezcan, S., Hammond, T. C., Matthews, R. H. and Spitz, D. R. (1996) 'High-performance liquid chromatography assay for N-acetylcysteine in biological samples following derivatization with N-(1-pyrenyl) maleimide.' *Journal of Chromatography B: Biomedical Sciences and Applications*, 685(2) pp. 329-334.

Erices, A., Conget, P. and Minguell, J. J. (2000) 'Mesenchymal progenitor cells in human umbilical cord blood.' *British Journal of Haematology*, 109(1) pp. 235-242.

Facchiano, F., D'Arcangelo, D., Russo, K., Fogliano, V., Mennella, C., Ragone, R., Zambruno, G., Carbone, V., Ribatti, D. and Peschle, C. (2006) 'Glycated fibroblast growth factor-2 is quickly produced in vitro upon low-millimolar glucose treatment and detected in vivo in diabetic mice.' *Molecular Endocrinology*, 20(11) pp. 2806-2818.

Falanga, V. (2005) 'Wound healing and its impairment in the diabetic foot.' *The Lancet*, 366(9498) pp. 1736-1743.

Fang, W.-H., Kumar, S., McDowell, G., Smith, D., Krupinski, J., Olah, P., Al-Baradie, R. S., Al-Rukban, M. O., Petcu, E. B. and Slevin, M. (2016) 'Mesenchymal Stem Cells Loaded with p5, Derived from CDK5 Activator p35, Inhibit Calcium-Induced CDK5 Activation in Endothelial Cells.' *Stem Cells International*, 2016

Fattori, V., Hohmann, M. S., Rossaneis, A. C., Pinho-Ribeiro, F. A. and Verri, W. A. (2016a) 'Capsaicin: current understanding of its mechanisms and therapy of pain and other pre-clinical and clinical uses.' *Molecules*, 21(7) p. 844.

Fattori, V., Hohmann, M., Rossaneis, A., Pinho-Ribeiro, F. and Verri, W. (2016b) 'Capsaicin: current understanding of its mechanisms and therapy of pain and other pre-clinical and clinical uses.' *Molecules*, 21(7) p. 844.

Feng, B., Ruiz, M. A. and Chakrabarti, S. (2012) 'Oxidative-stress-induced epigenetic changes in chronic diabetic complications.' *Canadian Journal of physiology and pharmacology*, 91(3) pp. 213-220.

FINOT, P. A. (2005) 'Historical perspective of the Maillard reaction in food science.' *Annals of the New York Academy of Sciences*, 1043(1) pp. 1-8.

Formigli, L., Paternostro, F., Tani, A., Mirabella, C., Quattrini Li, A., Nosi, D., D'asta, F., Saccardi, R., Mazzanti, B. and Lo Russo, G. (2015) 'MSCs seeded on bioengineered scaffolds improve skin wound healing in rats.' *Wound Repair and Regeneration*, 23(1) pp. 115-123.

Fowler, M. J. (2008) 'Microvascular and macrovascular complications of diabetes.' *Clinical Diabetes*, 26(2) pp. 77-82.

Fowler, M. J. (2011) 'Microvascular and macrovascular complications of diabetes.' *Clinical Diabetes*, 29(3) pp. 116-122.

Franke, S., Sommer, M., Rüster, C., Bondeva, T., Marticke, J., Hofmann, G., Hein, G. and Wolf, G. (2009) 'Advanced glycation end products induce cell cycle arrest and proinflammatory changes in osteoarthritic fibroblast-like synovial cells.' *Arthritis Research & Therapy*, 11(5) p. R136.

Frey, R. S., Ushio-Fukai, M. and Malik, A. B. (2009) 'NADPH oxidase-dependent signaling in endothelial cells: role in physiology and pathophysiology.' *Antioxidants & Redox Signaling*, 11(4) pp. 791-810.

Fu, Z., R Gilbert, E. and Liu, D. (2013) 'Regulation of insulin synthesis and secretion and pancreatic Beta-cell dysfunction in diabetes.' *Current Diabetes Reviews*, 9(1) pp. 25-53.

Funk, S. D., Yurdagul, A. and Orr, A. W. (2012) 'Hyperglycemia and endothelial dysfunction in atherosclerosis: lessons from type 1 diabetes.' *International Journal of Vascular Medicine*, 2012

Furukawa, S., Fujita, T., Shimabukuro, M., Iwaki, M., Yamada, Y., Nakajima, Y., Nakayama, O., Makishima, M., Matsuda, M. and Shimomura, I. (2017) 'Increased oxidative stress in obesity and its impact on metabolic syndrome.' *The Journal of Clinical Investigation*, 114(12) pp. 1752-1761.

Gabard, B. and Mascher, H. (1991) 'Endogenous plasma N-acetylcysteine and single dose oral bioavailability from two different formulations as determined by a new analytical method.' *Biopharmaceutics & Drug Disposition*, 12(5) pp. 343-353.

Gaens, K. H., Stehouwer, C. D. and Schalkwijk, C. G. (2013) 'Advanced glycation endproducts and its receptor for advanced glycation endproducts in obesity.' *Current Opinion in Lipidology*, 24(1) pp. 4-11.

Galkowska, H., Wojewodzka, U. and Olszewski, W. L. (2006) 'Chemokines, cytokines, and growth factors in keratinocytes and dermal endothelial cells in the margin of chronic diabetic foot ulcers.' *Wound Repair and Regeneration*, 14(5) pp. 558-565.

Gallicchio, M. A., McRobert, E. A., Tikoo, A., Cooper, M. E. and Bach, L. A. (2006) 'Advanced glycation end products inhibit tubulogenesis and migration of kidney epithelial cells in an ezrin-dependent manner.' *Journal of the American Society of Nephrology*, 17(2) pp. 414-421.

Galván-Peña, S. and O'Neill, L. A. (2014) 'Metabolic reprogramming in macrophage polarization.' *Frontiers in Immunology*, 5 p. 420.

Ganeshkumar, M., Ponrasu, T., Krithika, R., Iyappan, K., Gayathri, V. S. and Suguna, L. (2012) 'Topical application of *Acalypha indica* accelerates rat cutaneous wound healing by up-regulating the expression of Type I and III collagen.' *Journal of Ethnopharmacology*, 142(1) pp. 14-22.

Garg, R. K., Rennert, R. C., Duscher, D., Sorkin, M., Kosaraju, R., Auerbach, L. J., Lennon, J., Chung, M. T., Paik, K. and Nimpf, J. (2014) 'Capillary Force Seeding of Hydrogels for Adipose-Derived Stem Cell Delivery in Wounds.' *Stem Cells Translational Medicine*, 3(9) pp. 1079-1089.

Genuth, S., Sun, W., Cleary, P., Gao, X., Sell, D. R., Lachin, J., Monnier, V. M. and Group, D. E. R. (2015) 'Skin advanced glycation end products glucosepane and methylglyoxal hydroimidazolone are independently associated with long-term microvascular complication progression of type 1 diabetes.' *Diabetes*, 64(1) pp. 266-278.

Gerrard, J. A. (2006) 'The Maillard reaction in food: Progress made, challenges ahead—Conference Report from the Eighth International Symposium on the Maillard Reaction.' *Trends in Food Science & Technology*, 17(6) pp. 324-330.

Ghani, M. J. A. (2010) 'Determination of alliin and allicin in different types garlic using high performance liquid chromatography.' *Journal of University of Anbar for Pure Science*, 4(2) pp. 16-23.

Giacco, F. and Brownlee, M. (2010) 'Oxidative stress and diabetic complications.' *Circulation Research*, 107(9) pp. 1058-1070.

Gibran, N. S., Jang, Y.-C., Isik, F. F., Greenhalgh, D. G., Muffley, L. A., Underwood, R. A., Usui, M. L., Larsen, J., Smith, D. G. and Bunnett, N. (2002) 'Diminished neuropeptide levels contribute to the impaired cutaneous healing response associated with diabetes mellitus.' *Journal of Surgical Research*, 108(1) pp. 122-128.

Goffin, U. (2012) 'Master bioingénieur: chimie et bioindustries.'

Goh, S.-Y. and Cooper, M. E. (2008) 'The role of advanced glycation end products in progression and complications of diabetes.' *The Journal of Clinical Endocrinology & Metabolism*, 93(4) pp. 1143-1152.

Goldberg, M., Langer, R. and Jia, X. (2007) 'Nanostructured materials for applications in drug delivery and tissue engineering.' *Journal of Biomaterials Science, Polymer Edition*, 18(3) pp. 241-268.

Griffioen, A. W. and Molema, G. (2000) 'Angiogenesis: potentials for pharmacologic intervention in the treatment of cancer, cardiovascular diseases, and chronic inflammation.' *Pharmacological Reviews*, 52(2) pp. 237-268.

Guest, J. F., Ayoub, N., McIlwraith, T., Uchegbu, I., Gerrish, A., Weidlich, D., Vowden, K. and Vowden, P. (2015) 'Health economic burden that wounds impose on the National Health Service in the UK.' *BMJ open*, 5(12) p. e009283.

Guo, X., Liu, W.-L., Chen, L.-W. and Guo, Z.-G. (2000) 'High glucose enhances H₂O₂-induced apoptosis in bovine aortic endothelial cells.' *Acta pharmacologica Sinica*, 21(1) pp. 41-45.

Haghi, A., Azimi, H. and Rahimi, R. (2017) 'A Comprehensive Review on pharmacotherapeutics of three phytochemicals, curcumin, quercetin, and Allicin, in the treatment of gastric cancer.' *Journal of Gastrointestinal Cancer*, 48(4) pp. 314-320.

Hallam, K. M., Li, Q., Ananthakrishnan, R., Kalea, A., Zou, Y. S., Vedantham, S., Schmidt, A. M., Yan, S. F. and Ramasamy, R. (2010) 'Aldose reductase and AGE–RAGE pathways: central roles in the pathogenesis of vascular dysfunction in aging rats.' *Aging Cell*, 9(5) pp. 776-784.

Haller, H., Ji, L., Stahl, K., Bertram, A. and Menne, J. (2017) 'Molecular Mechanisms and Treatment Strategies in Diabetic Nephropathy: New Avenues for Calcium Dobesilate—Free Radical Scavenger and Growth Factor Inhibition.' *BioMed Research International*, 2017

Harding, J. J. and Ganea, E. (2006) 'Protection against glycation and similar post-translational modifications of proteins.' *Biochimica et Biophysica Acta (BBA)-Proteins and Proteomics*, 1764(9) pp. 1436-1446.

Hassan, W. U., Greiser, U. and Wang, W. (2014) 'Role of adipose-derived stem cells in wound healing.' *Wound Repair and Regeneration*, 22(3) pp. 313-325.

Hellwig, M. and Henle, T. (2014) 'Baking, ageing, diabetes: a short history of the Maillard reaction.' *Angewandte Chemie International Edition*, 53(39) pp. 10316-10329.

Hima Bindu, A. and Srilatha, B. (2011) 'Potency of various types of stem cells and their transplantation.' *J Stem Cell Res Ther*, 1 p. 115.

Hocking, A. M. (2012) 'Mesenchymal stem cell therapy for cutaneous wounds.' *Advances in Wound Care*, 1(4) pp. 166-171.

Hocking, A. M. and Gibran, N. S. (2010) 'Mesenchymal stem cells: paracrine signaling and differentiation during cutaneous wound repair.' *Experimental Cell Research*, 316(14) pp. 2213-2219.

Hodge, J. E. (1953) 'Dehydrated foods, chemistry of browning reactions in model systems.' *Journal of Agricultural and Food Chemistry*, 1(15) pp. 928-943.

Hu, M. S.-M., Rennert, R. C., McArdle, A., Chung, M. T., Walmsley, G. G., Longaker, M. T. and Lorenz, H. P. (2014) 'The role of stem cells during scarless skin wound healing.' *Advances in Wound Care*, 3(4) pp. 304-314.

Hu, M. S., Borrelli, M. R., Lorenz, H. P., Longaker, M. T. and Wan, D. C. (2018) 'Mesenchymal Stromal Cells and Cutaneous Wound Healing: A Comprehensive Review of the Background, Role, and Therapeutic Potential.' *Stem Cells International*, 2018

Huang, S.-P., Hsu, C.-C., Chang, S.-C., Wang, C.-H., Deng, S.-C., Dai, N.-T., Chen, T.-M., Chan, J. Y.-H., Chen, S.-G. and Huang, S.-M. (2012) 'Adipose-derived stem cells seeded on acellular dermal matrix grafts enhance wound healing in a murine model of a full-thickness defect.' *Annals of Plastic Surgery*, 69(6) pp. 656-662.

Huang, X., Zhang, F., Wang, H., Niu, G., Choi, K. Y., Swierczewska, M., Zhang, G., Gao, H., Wang, Z. and Zhu, L. (2013) 'Mesenchymal stem cell-based cell engineering with multifunctional mesoporous silica nanoparticles for tumor delivery.' *Biomaterials*, 34(7) pp. 1772-1780.

Hudson, B. I. and Schmidt, A. M. (2004) 'RAGE: a novel target for drug intervention in diabetic vascular disease.' *Pharmaceutical Research*, 21(7) pp. 1079-1086.

Hussain, S., Slevin, M., Ahmed, N., West, D., Choudhary, M. I., Naz, H. and Gaffney, J. (2009) 'Stilbene glycosides are natural product inhibitors of FGF-2-induced angiogenesis.' *BMC Cell Biology*, 10(1) p. 30.

Igura, K., Zhang, X., Takahashi, K., Mitsuru, A., Yamaguchi, S. and Takahashi, T. (2004) 'Isolation and characterization of mesenchymal progenitor cells from chorionic villi of human placenta.' *Cytotherapy*, 6(6) pp. 543-553.

Jain, S. K., Kahlon, G., Bass, P., Levine, S. N. and Warden, C. (2015) Can L-Cysteine and Vitamin D Rescue Vitamin D and Vitamin D Binding Protein Levels in Blood Plasma of African American Type 2 Diabetic Patients? : Mary Ann Liebert, Inc. 140 Huguenot Street, 3rd Floor New Rochelle, NY 10801 USA.

Janowski, M., Wagner, D.-C. and Boltze, J. (2015) 'Stem cell-based tissue replacement after stroke: factual necessity or notorious fiction?' *Stroke*, 46(8) pp. 2354-2363.

Jeetah, R., Bhaw-Luximon, A. and Jhurry, D. (2014) 'Nanopharmaceutics: phytochemical-based controlled or sustained drug-delivery systems for cancer treatment.' *Journal of Biomedical Nanotechnology*, 10(9) pp. 1810-1840.

Jeng, C.-J., Hsieh, Y.-T., Yang, C.-M., Yang, C.-H., Lin, C.-L. and Wang, I.-J. (2018) 'Development of diabetic retinopathy after cataract surgery.' *PloS one*, 13(8) p. e0202347.

Jeon, Y. K., Jang, Y. H., Yoo, D. R., Kim, S. N., Lee, S. K. and Nam, M. J. (2010) 'Mesenchymal stem cells' interaction with skin: Wound-healing effect on fibroblast cells and skin tissue.' *Wound Repair and Regeneration*, 18(6) pp. 655-661.

Jinfeng, L., Yunliang, W., Xinshan, L., Shanshan, W., Chunyang, X., Peng, X., Xiaopeng, Y., Zhixiu, X., Honglei, Y. and Xia, C. (2016) 'The effect of MSCs derived from the human umbilical cord transduced by fibroblast growth factor-20 on Parkinson's disease.' *Stem Cells International*, 2016

Jun, E. K., Zhang, Q., Yoon, B. S., Moon, J.-H., Lee, G., Park, G., Kang, P. J., Lee, J. H., Kim, A. and You, S. (2014) 'Hypoxic conditioned medium from human amniotic fluid-derived mesenchymal stem cells accelerates skin wound healing through TGF- β /SMAD2 and PI3K/Akt pathways.' *International Journal of Molecular Sciences*, 15(1) pp. 605-628.

Kaewkamson, T., Pannangpetch, P., Kongyingyoes, B. and Kukongvirayapan, U. A. (2007) 'Antiplatelet Aggregation Activities of Some Thai Medicinal Plants.' *Thai J Pharmacol*, 29 pp. 40-43.

Karmakar, P. S. and Goswami, R. P. (2012) 'Advanced glycation end products (AGEs): It's role in the pathogenesis of diabetic complications.' *MEDICINE*, 22

Kato, Y., Iwata, T., Washio, K., Yoshida, T., Kuroda, H., Morikawa, S., Hamada, M., Ikura, K., Kaibuchi, N. and Yamato, M. (2017) 'Creation and Transplantation of an Adipose-derived Stem Cell (ASC) Sheet in a Diabetic Wound-healing Model.' *Journal of Visualized Experiments: JoVE*, (126)

Keating, A. (2012) 'Mesenchymal stromal cells: new directions.' *Cell Stem Cell*, 10(6) pp. 709-716.

Kiho, T., Usui, S., Hirano, K., Aizawa, K. and Inakuma, T. (2004) 'Tomato paste fraction inhibiting the formation of advanced glycation end-products.' *Bioscience, Biotechnology, and Biochemistry*, 68(1) pp. 200-205.

Kim, J. W., Lee, J. H., Lyoo, Y. S., Jung, D. I. and Park, H. M. (2013) 'The effects of topical mesenchymal stem cell transplantation in canine experimental cutaneous wounds.' *Veterinary Dermatology*, 24(2) pp. 242-e253.

Kim, S. H., Bianco, N. R., Shufesky, W. J., Morelli, A. E. and Robbins, P. D. (2007) 'Effective treatment of inflammatory disease models with exosomes derived from dendritic cells genetically modified to express IL-4.' *The Journal of Immunology*, 179(4) pp. 2242-2249.

Kim, W.-S., Park, B.-S., Sung, J.-H., Yang, J.-M., Park, S.-B., Kwak, S.-J. and Park, J.-S. (2007) 'Wound healing effect of adipose-derived stem cells: a critical role of secretory factors on human dermal fibroblasts.' *Journal of Dermatological Science*, 48(1) pp. 15-24.

Kim, Y. S., Lee, I. S. and Kim, J. S. (2014) 'Protective effects of Puerariae radix extract and its single compounds on methylglyoxal-induced apoptosis in human retinal pigment epithelial cells.' *Journal of Ethnopharmacology*, 152(3) pp. 594-598.

King, A., Balaji, S., Keswani, S. G. and Crombleholme, T. M. (2014) 'The role of stem cells in wound angiogenesis.' *Advances in Wound Care*, 3(10) pp. 614-625.

Kirana, S., Stratmann, B., Prante, C., Prohaska, W., Koerperich, H., Lammers, D., Gastens, M., Quast, T., Negrean, M. and Stirban, O. (2012) 'Autologous stem cell therapy in the treatment of limb ischaemia induced chronic tissue ulcers of diabetic foot patients.' *International Journal of Clinical Practice*, 66(4) pp. 384-393.

Kishabongo, A. S., Katchunga, P., Van Aken, E. H., Speeckaert, R., Lagniau, S., Coopman, R., Speeckaert, M. M. and Delanghe, J. R. (2015) 'Glycation of nail proteins: from basic biochemical findings to a representative marker for diabetic glycation-associated target organ damage.' *PLoS one*, 10(3) p. e0120112.

Kislinger, T., Humeny, A. and Pischetsrieder, M. (2004) 'Analysis of protein glycation products by matrix-assisted laser desorption ionization time-of-flight mass spectrometry.' *Current Medicinal Chemistry*, 11(16) pp. 2185-2193.

Klöpfer, A., Spanneberg, R. and Glomb, M. A. (2010) 'Formation of arginine modifications in a model system of N α -tert-butoxycarbonyl (Boc)-arginine with methylglyoxal.' *Journal of Agricultural and Food Chemistry*, 59(1) pp. 394-401.

Ko, S.-Y., Ko, H.-A., Shieh, T.-M., Chang, W.-C., Chen, H.-I., Chang, S.-S. and Lin, I.-H. (2014) 'Cell migration is regulated by AGE-RAGE interaction in human oral cancer cells in vitro.' *PLoS One*, 9(10) p. e110542.

Kodera, Y., Ushijima, M., Amano, H., Suzuki, J.-i. and Matsutomo, T. (2017) 'Chemical and Biological Properties of S-1-Propenyl-L-Cysteine in Aged Garlic Extract.' *Molecules*, 22(4) p. 570.

Kolaczowska, E. and Kubes, P. (2013) 'Neutrophil recruitment and function in health and inflammation.' *Nature Reviews Immunology*, 13(3) p. 159.

Kolset, S., Reinholt, F. and Jenssen, T. (2012) 'Diabetic nephropathy and extracellular matrix.' *Journal of Histochemistry & Cytochemistry*, 60(12) pp. 976-986.

Kong, X., Ma, M. z., Huang, K., Qin, L., Zhang, H. m., Yang, Z., Li, X. y. and Su, Q. (2014) 'Increased plasma levels of the methylglyoxal in patients with newly diagnosed type 2 diabetes 初诊 2 型糖尿病患者血浆甲基乙二醛水平升高.' *Journal of Diabetes*, 6(6) pp. 535-540.

Kraehenbuehl, K., Davidek, T., Devaud, S. and Mauroux, O. (2008) *Basic and acidic sugars as flavour precursors in the Maillard reaction*. Institut Für Chemie und Biologische Chemie.

Kyo, E., Uda, N., Kasuga, S. and Itakura, Y. (2001) 'Immunomodulatory effects of aged garlic extract.' *The Journal of Nutrition*, 131(3) pp. 1075S-1079S.

Laakso, M. (2010) 'Cardiovascular disease in type 2 diabetes from population to man to mechanisms: the Kelly West Award Lecture 2008.' *Diabetes Care*, 33(2) pp. 442-449.

Laemmli, U. K. (1970) 'Cleavage of structural proteins during the assembly of the head of bacteriophage T4.' *Nature*, 227 pp. 680-685.

Lamers, M. L., Almeida, M. E., Vicente-Manzanares, M., Horwitz, A. F. and Santos, M. F. (2011) 'High glucose-mediated oxidative stress impairs cell migration.' *PloS one*, 6(8) p. e22865.

Landázuri, N., Tong, S., Suo, J., Joseph, G., Weiss, D., Sutcliffe, D. J., Giddens, D. P., Bao, G. and Taylor, W. R. (2013) 'Magnetic targeting of human mesenchymal stem cells with internalized superparamagnetic iron oxide nanoparticles.' *Small*, 9(23) pp. 4017-4026.

Landén, N. X., Li, D. and Stähle, M. (2016) 'Transition from inflammation to proliferation: a critical step during wound healing.' *Cellular and Molecular Life Sciences*, 73(20) pp. 3861-3885.

Lee, C. and Park, C. (2017) 'Bacterial responses to glyoxal and methylglyoxal: reactive electrophilic species.' *International Journal of Molecular Sciences*, 18(1) p. 169.

Lee, D.-H., Kim, Y.-J., Kim, H.-H., Cho, H.-J., Ryu, J.-H., Rhee, M. H. and Park, H.-J. (2013) 'Inhibitory effects of epigallocatechin-3-gallate on microsomal cyclooxygenase-1 activity in platelets.' *Biomolecules & Therapeutics*, 21(1) p. 54.

Lee, D. E., Ayoub, N. and Agrawal, D. K. (2016) 'Mesenchymal stem cells and cutaneous wound healing: novel methods to increase cell delivery and therapeutic efficacy.' *Stem Cell Research & Therapy*, 7(1) p. 37.

Lee, E. Y., Xia, Y., Kim, W. S., Kim, M. H., Kim, T. H., Kim, K. J., Park, B. S. and Sung, J. H. (2009) 'Hypoxia-enhanced wound-healing function of adipose-derived stem cells: Increase in stem cell proliferation and up-regulation of VEGF and bFGF.' *Wound Repair and Regeneration*, 17(4) pp. 540-547.

Lee, K. Y. and Yuk, S. H. (2007) 'Polymeric protein delivery systems.' *Progress in Polymer Science*, 32(7) pp. 669-697.

Lee, P. C., Yang, Y. Y., Huang, C. S., Hsieh, S. L., Lee, K. C., Hsieh, Y. C., Lee, T. Y. and Lin, H. C. (2015) 'Concomitant inhibition of oxidative stress and angiogenesis by chronic hydrogen-rich saline and N-acetylcysteine treatments improves systemic, splanchnic and hepatic hemodynamics of cirrhotic rats.' *Hepatology Research*, 45(5) pp. 578-588.

Lee, S., Yoo, M., Kim, S. and Shin, D. (2014) 'Identification and quantification of S-allyl-l-cysteine in heated garlic juice by HPLC with ultraviolet and mass spectrometry detection.' *LWT-Food Science and Technology*, 57(2) pp. 516-521.

Lee, S. H., Jeong, S. K. and Ahn, S. K. (2006) 'An update of the defensive barrier function of skin.' *Yonsei Medical Journal*, 47(3) pp. 293-306.

Lee, S. H., Jin, S. Y., Song, J. S., Seo, K. K. and Cho, K. H. (2012) 'Paracrine effects of adipose-derived stem cells on keratinocytes and dermal fibroblasts.' *Annals of Dermatology*, 24(2) pp. 136-143.

Levinson, H. (2013) 'A paradigm of fibroblast activation and dermal wound contraction to guide the development of therapies for chronic wounds and pathologic scars.' *Advances in Wound Care*, 2(4) pp. 149-159.

Li, M. D., Atkins, H. and Bubela, T. (2014) 'The global landscape of stem cell clinical trials.' *Regenerative Medicine*, 9(1) pp. 27-39.

Li, P., Gong, Z., Shultz, L. D. and Ren, G. (2019) 'Mesenchymal stem cells: From regeneration to cancer.' *Pharmacology & Therapeutics*,

Lim, A. K. (2014) 'Diabetic nephropathy—complications and treatment.' *International Journal of Nephrology and Renovascular Disease*, 7 p. 361.

Lin, C.-Y., Chen, C.-S., Shieh, M.-S., Wu, C.-H. and Lee, H.-M. (2002) 'Development of an automated immunoassay for advanced glycosylation end products in human serum.' *Clinical Biochemistry*, 35(3) pp. 189-195.

Lindsay, S. (1992) *Analytical Chemistry by Open Learning High Performance Liquid Chromatography*. John Willey and Sons, London.

Liu, L., Yu, Y., Hou, Y., Chai, J., Duan, H., Chu, W., Zhang, H., Hu, Q. and Du, J. (2014) 'Human umbilical cord mesenchymal stem cells transplantation promotes cutaneous wound healing of severe burned rats.' *PloS one*, 9(2) p. e88348.

Lobmann, R., Ambrosch, A., Schultz, G., Waldmann, K., Schiweck, S. and Lehnert, H. (2002) 'Expression of matrix-metalloproteinases and their inhibitors in the wounds of diabetic and non-diabetic patients.' *Diabetologia*, 45(7) pp. 1011-1016.

Lobo Júnior, J. P., Brescansin, C. P., Santos-Weiss, I. C., Welter, M., Souza, E. M. d., Rego, F. G. d. M., Picheth, G. and Alberton, D. (2017) 'Serum Fluorescent Advanced Glycation End (F-AGE) products in gestational diabetes patients.' *Archives of Endocrinology and Metabolism*, 61(3) pp. 233-237.

Lu, F., Mizuno, H., Uysal, C. A., Cai, X., Ogawa, R. and Hyakusoku, H. (2008) 'Improved viability of random pattern skin flaps through the use of adipose-derived stem cells.' *Plastic and Reconstructive Surgery*, 121(1) pp. 50-58.

Luevano-Contreras, C. and Chapman-Novakofski, K. (2010) 'Dietary advanced glycation end products and aging.' *Nutrients*, 2(12) pp. 1247-1265.

Lukomska, B., Stanaszek, L., Zuba-Surma, E., Legosz, P., Sarzynska, S. and Drela, K. (2019) 'Challenges and controversies in human mesenchymal stem cell therapy.' *Stem Cells International*, 2019

Luo, G., Cheng, W., He, W., Wang, X., Tan, J., Fitzgerald, M., Li, X. and Wu, J. (2010) 'Promotion of cutaneous wound healing by local application of mesenchymal stem cells derived from human umbilical cord blood.' *Wound Repair and Regeneration*, 18(5) pp. 506-513.

Ma, T. (2010) 'Mesenchymal stem cells: From bench to bedside.' *World Journal of Stem Cells*, 2(2) p. 13.

Ma, Y., Gao, M. and Liu, D. (2016) 'N-acetylcysteine protects mice from high fat diet-induced metabolic disorders.' *Pharmaceutical Research*, 33(8) pp. 2033-2042.

Ma, Y., Song, D., Wang, Z., Jiang, J., Jiang, T., Cui, F. and Fan, X. (2011) 'Effect of ultrahigh pressure treatment on volatile compounds in garlic.' *Journal of Food Process Engineering*, 34(6) pp. 1915-1930.

MacLeod, A. S., Rudolph, R., Corriden, R., Ye, I., Garijo, O. and Havran, W. L. (2014) 'Skin-resident T cells sense ultraviolet radiation-induced injury and contribute to DNA repair.' *The Journal of Immunology*, p. 1303297.

Macpherson, L. J., Geierstanger, B. H., Viswanath, V., Bandell, M., Eid, S. R., Hwang, S. and Patapoutian, A. (2005) 'The pungency of garlic: activation of TRPA1 and TRPV1 in response to allicin.' *Current Biology*, 15(10) pp. 929-934.

Maggini, J., Mirkin, G., Bognanni, I., Holmberg, J., Piazzón, I. M., Nepomnaschy, I., Costa, H., Cañones, C., Raiden, S. and Vermeulen, M. (2010) 'Mouse bone marrow-derived mesenchymal stromal cells turn activated macrophages into a regulatory-like profile.' *PLoS one*, 5(2) p. e9252.

Majors, R. E. and Przybyciel, M. (2002) 'Columns for reversed-phase LC separations in highly aqueous mobile phases.' *LC GC NORTH AMERICA*, 20(7) pp. 584-593.

Makita, Z., Vlassara, H., Cerami, A. and Bucala, R. (1992) 'Immunochemical detection of advanced glycosylation end products in vivo.' *Journal of Biological Chemistry*, 267(8) pp. 5133-5138.

Mallipattu, S. K. and Uribarri, J. (2014) 'Advanced glycation end product accumulation: a new enemy to target in chronic kidney disease?' *Current opinion in nephrology and hypertension*, 23(6) p. 547.

Mane, P., Mayee, R. and Atre, K. (2011) 'Medicinal properties of allium sativum (garlic): A review.' *International Journal of Pharma Research and Development*, 3(2) pp. 17-27.

Mariño, L., Maya-Aguirre, C. A. s., Pauwels, K., Vilanova, B., Ortega-Castro, J., Frau, J., Donoso, J. and Adrover, M. (2017) 'Glycation of Lysozyme by Glycolaldehyde Provides New Mechanistic Insights in Diabetes-Related Protein Aggregation.' *ACS Chemical Biology*, 12(4) pp. 1152-1162.

Martins, S. I. and Van Boekel, M. A. (2005a) 'Kinetics of the glucose/glycine Maillard reaction pathways: influences of pH and reactant initial concentrations.' *Food Chemistry*, 92(3) pp. 437-448.

Martins, S. I. and Van Boekel, M. A. (2005b) 'A kinetic model for the glucose/glycine Maillard reaction pathways.' *Food Chemistry*, 90(1-2) pp. 257-269.

Maruyama, K., Asai, J., Ii, M., Thorne, T., Losordo, D. W. and D'Amore, P. A. (2007) 'Decreased macrophage number and activation lead to reduced lymphatic vessel formation and contribute to impaired diabetic wound healing.' *The American Journal of Pathology*, 170(4) pp. 1178-1191.

Mashilpa, C., Wang, Q., Slevin, M. and Ahmed, N. (2011) 'Antiglycation and antioxidant properties of soy sauces.' *Journal of Medicinal Food*, 14(12) pp. 1647-1653.

Matsuura, N., Miyamae, Y., Yamane, K., Nagao, Y., Hamada, Y., Kawaguchi, N., Katsuki, T., Hirata, K., Sumi, S.-I. and Ishikawa, H. (2006) 'Aged garlic extract inhibits angiogenesis and proliferation of colorectal carcinoma cells.' *The Journal of Nutrition*, 136(3) pp. 842S-846S.

Matthay, M. A., Goolaerts, A., Howard, J. P. and Lee, J. W. (2010) 'Mesenchymal stem cells for acute lung injury: preclinical evidence.' *Critical Care Medicine*, 38(10 Suppl) p. S569.

Maxson, S., Lopez, E. A., Yoo, D., Danilkovitch-Miagkova, A. and LeRoux, M. A. (2012) 'Concise review: role of mesenchymal stem cells in wound repair.' *Stem Cells Translational Medicine*, 1(2) pp. 142-149.

Mayadas, T. N., Cullere, X. and Lowell, C. A. (2014) 'The multifaceted functions of neutrophils.' *Annual Review of Pathology: Mechanisms of Disease*, 9 pp. 181-218.

McCance, D. R., Dyer, D. G., Dunn, J. A., Bailie, K. E., Thorpe, S. R., Baynes, J. W. and Lyons, T. J. (1993) 'Maillard reaction products and their relation to complications in insulin-dependent diabetes mellitus.' *The Journal of Clinical Investigation*, 91(6) pp. 2470-2478.

McCarthy, A. D., Etcheverry, S. B., Bruzzone, L. and Cortizo, A. M. (1997) 'Effects of advanced glycation end-products on the proliferation and differentiation of osteoblast-like cells.' *Molecular and Cellular Biochemistry*, 170(1-2) pp. 43-51.

Mei, S. H., Haitsma, J. J., Dos Santos, C. C., Deng, Y., Lai, P. F., Slutsky, A. S., Liles, W. C. and Stewart, D. J. (2010) 'Mesenchymal stem cells reduce inflammation while enhancing bacterial clearance and improving survival in sepsis.' *American Journal of Respiratory and Critical Care Medicine*, 182(8) pp. 1047-1057.

Mittal, R. (2011) 'Mesenchymal stem cells: the new players in the pathogenesis of tuberculosis.' *J Microbial Biochem Technol*, 3(3)

Morais, M. P. P., Marshall, D., Flower, S. E., Caunt, C. J., James, T. D., Williams, R. J., Waterfield, N. R. and Van Den Elsen, J. M. (2013) 'Analysis of protein glycation using fluorescent phenylboronate gel electrophoresis.' *Scientific Reports*, 3 p. 1437.

Moraru, A., Wiederstein, J., Pfaff, D., Fleming, T., Miller, A. K., Nawroth, P. and Teleanu, A. A. (2018) 'Elevated levels of the reactive metabolite methylglyoxal recapitulate progression of type 2 diabetes.' *Cell Metabolism*, 27(4) pp. 926-934. e928.

Murray, P. J. and Wynn, T. A. (2011) 'Protective and pathogenic functions of macrophage subsets.' *Nature Reviews Immunology*, 11(11) p. 723.

Mustoe, T. A., O'shaughnessy, K. and Kloeters, O. (2006) 'Chronic wound pathogenesis and current treatment strategies: a unifying hypothesis.' *Plastic and Reconstructive Surgery*, 117(7S) pp. 35S-41S.

Muthenna, P., Akileshwari, C. and Reddy, G. B. (2012) 'Ellagic acid, a new antiglycating agent: its inhibition of Nε-(carboxymethyl) lysine.' *Biochemical Journal*, 442(1) pp. 221-230.

Naka, Y., Bucciarelli, L. G., Wendt, T., Lee, L. K., Rong, L. L., Ramasamy, R., Yan, S. F. and Schmidt, A. M. (2004) 'RAGE axis: animal models and novel insights into the vascular complications of diabetes.' *Arteriosclerosis, Thrombosis, and Vascular Biology*, 24(8) pp. 1342-1349.

Neeper, M., Schmidt, A., Brett, J., Yan, S., Wang, F., Pan, Y., Elliston, K., Stern, D. and Shaw, A. (1992) 'Cloning and expression of a cell surface receptor for advanced glycosylation end products of proteins.' *Journal of Biological Chemistry*, 267(21) pp. 14998-15004.

Newman, R. E., Yoo, D., LeRoux, M. A. and Danilkovitch-Miagkova, A. (2009) 'Treatment of inflammatory diseases with mesenchymal stem cells.' *Inflammation & Allergy-Drug Targets (Formerly Current Drug Targets-Inflammation & Allergy)*, 8(2) pp. 110-123.

Newton, A. E., Fairbanks, A. J., Golding, M., Andrewes, P. and Gerrard, J. A. (2012) 'The role of the Maillard reaction in the formation of flavour compounds in dairy products—not only a deleterious reaction but also a rich source of flavour compounds.' *Food & Function*, 3(12) pp. 1231-1241.

Nie, C., Yang, D., Xu, J., Si, Z., Jin, X. and Zhang, J. (2011) 'Locally administered adipose-derived stem cells accelerate wound healing through differentiation and vasculogenesis.' *Cell Transplantation*, 20(2) pp. 205-216.

Nishikawa-Ogawa, M., Wanibuchi, H., Morimura, K., Kinoshita, A., Nishikawa, T., Hayashi, S., Yano, Y. and Fukushima, S. (2005) 'N-acetylcysteine and S-methylcysteine inhibit MeIQx rat hepatocarcinogenesis in the post-initiation stage.' *Carcinogenesis*, 27(5) pp. 982-988.

Nita, M. and Grzybowski, A. (2016) 'The role of the reactive oxygen species and oxidative stress in the pathomechanism of the age-related ocular diseases and other pathologies of the anterior and posterior eye segments in adults.' *Oxidative Medicine and Cellular Longevity*, 2016

Novak, M. L. and Koh, T. J. (2013) 'Macrophage phenotypes during tissue repair.' *Journal of Leukocyte Biology*, 93(6) pp. 875-881.

Nursten, H. E. (2005) *The Maillard reaction: chemistry, biochemistry, and implications*. Royal Society of Chemistry.

O'sullivan, E. P. and Dinneen, S. F. (2009) 'Benefits of early intensive glucose control to prevent diabetes complications were sustained for up to 10 years.' *Evidence-Based Medicine*, 14(1) p. 9.

Oak, J.-H., Youn, J.-Y. and Cai, H. (2009) 'Aminoguanidine inhibits aortic hydrogen peroxide production, VSMC NOX activity and hypercontractility in diabetic mice.' *Cardiovascular Diabetology*, 8(1) p. 65.

Ogony, J., Mare, S., Wu, W. and Ercal, N. (2006) 'High performance liquid chromatography analysis of 2-mercaptoethylamine (cysteamine) in biological samples by derivatization with N-(1-pyrenyl) maleimide (NPM) using fluorescence detection.' *Journal of Chromatography B*, 843(1) pp. 57-62.

Oh, J. Y., Ko, J. H., Lee, H. J., Yu, J. M., Choi, H., Kim, M. K., Wee, W. R. and Prockop, D. J. (2014) 'Mesenchymal stem/stromal cells inhibit the NLRP3 inflammasome by decreasing mitochondrial reactive oxygen species.' *Stem Cells*, 32(6) pp. 1553-1563.

Ojeh, N. O. and Navsaria, H. A. (2014) 'An in vitro skin model to study the effect of mesenchymal stem cells in wound healing and epidermal regeneration.' *Journal of Biomedical Materials Research Part A*, 102(8) pp. 2785-2792.

Omar, S. and Al-Wabel, N. (2010) 'Organosulfur compounds and possible mechanism of garlic in cancer.' *Saudi Pharmaceutical Journal*, 18(1) pp. 51-58.

Ott, C., Jacobs, K., Haucke, E., Santos, A. N., Grune, T. and Simm, A. (2014) 'Role of advanced glycation end products in cellular signaling.' *Redox biology*, 2 pp. 411-429.

Ou, C.-c., Tsao, S.-m., Lin, M.-c. and Yin, M.-c. (2003) 'Protective action on human LDL against oxidation and glycation by four organosulfur compounds derived from garlic.' *Lipids*, 38(3) pp. 219-224.

Ourouadi, S., Moumene, H., Zaki, N., Boulli, A.-A., Ouattmane, A. and Hasib, A. (2016) 'Garlic (*Allium Sativum*): A Source of Multiple Nutraceutical and Functional Components.' *Journal of Chemical, Biological and Physical Sciences (JCBPS)*, 7(1) p. 9.

Ozougwu, J., Obimba, K., Belonwu, C. and Unakalamba, C. (2013) 'The pathogenesis and pathophysiology of type 1 and type 2 diabetes mellitus.' *Journal of Physiology and Pathophysiology*, 4(4) pp. 46-57.

Padayatti, P. S., Jiang, C., Glomb, M. A., Uchida, K. and Nagaraj, R. H. (2001) 'High concentrations of glucose induce synthesis of argpyrimidine in retinal endothelial cells.' *Current Eye Research*, 23(2) pp. 106-115.

Paget, C., Lecomte, M., Ruggiero, D., Wiernsperger, N. and Lagarde, M. (1998) 'Modification of enzymatic antioxidants in retinal microvascular cells by glucose or advanced glycation end products.' *Free Radical Biology and Medicine*, 25(1) pp. 121-129.

Panche, A., Diwan, A. and Chandra, S. (2016) 'Flavonoids: an overview.' *Journal of Nutritional Science*, 5

Pandurangi, A. (2015) 'Cancer chemoprevention by garlic-A review.' *Hereditary Genet*, 4(2) pp. 1-7.

Pang, C., Ibrahim, A., Bulstrode, N. W. and Ferretti, P. (2017) 'An overview of the therapeutic potential of regenerative medicine in cutaneous wound healing.' *International Wound Journal*, 14(3) pp. 450-459.

Parekkadan, B. and Milwid, J. M. (2010) 'Mesenchymal stem cells as therapeutics.' *Annual Review of Biomedical Engineering*, 12 pp. 87-117.

PARK, B. S., Jang, K. A., SUNG, J. H., PARK, J. S., Kwon, Y. H., Kim, K. J. and KIM, W. S. (2008) 'Adipose-derived stem cells and their secretory factors as a promising therapy for skin aging.' *Dermatologic Surgery*, 34(10) pp. 1323-1326.

Parsons, J., Sparrow, K., Ismail, K., Hunt, K., Rogers, H. and Forbes, A. (2018) 'Experiences of gestational diabetes and gestational diabetes care: a focus group and interview study.' *BMC Pregnancy and Childbirth*, 18(1) p. 25.

Parveen, A., Jin, M. and Kim, S. Y. (2017) 'Bioactive phytochemicals that regulate the cellular processes involved in diabetic nephropathy.' *Phytomedicine*,

Pascucci, L., Coccè, V., Bonomi, A., Ami, D., Ceccarelli, P., Ciusani, E., Viganò, L., Locatelli, A., Sisto, F. and Doglia, S. M. (2014) 'Paclitaxel is incorporated by mesenchymal stromal cells and released in exosomes that inhibit in vitro tumor growth: a new approach for drug delivery.' *Journal of Controlled Release*, 192 pp. 262-270.

Pastar, I., Stojadinovic, O., Yin, N. C., Ramirez, H., Nusbaum, A. G., Sawaya, A., Patel, S. B., Khalid, L., Isseroff, R. R. and Tomic-Canic, M. (2014) 'Epithelialization in wound healing: a comprehensive review.' *Advances in Wound Care*, 3(7) pp. 445-464.

Penn, J. W., Grobbelaar, A. O. and Rolfe, K. J. (2012) 'The role of the TGF- β family in wound healing, burns and scarring: a review.' *International Journal of Burns and Trauma*, 2(1) p. 18.

Pescosolido, N., Barbato, A., Giannotti, R., Komaiha, C. and Lenarduzzi, F. (2016) 'Age-related changes in the kinetics of human lenses: prevention of the cataract.' *International Journal of Ophthalmology*, 9(10) p. 1506.

Poulsen, M. W., Hedegaard, R. V., Andersen, J. M., de Courten, B., Bügel, S., Nielsen, J., Skibsted, L. H. and Dragsted, L. O. (2013) 'Advanced glycation endproducts in food and their effects on health.' *Food and Chemical Toxicology*, 60 pp. 10-37.

Prasad, V. K., Lucas, K. G., Kleiner, G. I., Talano, J. A. M., Jacobsohn, D., Broadwater, G., Monroy, R. and Kurtzberg, J. (2011) 'Efficacy and safety of ex vivo cultured adult human mesenchymal stem cells (Prochymal™) in pediatric patients with severe refractory acute graft-versus-host disease in a compassionate use study.' *Biology of Blood and Marrow Transplantation*, 17(4) pp. 534-541.

Procházka, V., Gumulec, J., Jalůvka, F., Šalounová, D., Jonszta, T., Czerný, D., Krajča, J., Urbanec, R., Klement, P. and Martinek, J. (2010) 'Cell therapy, a new standard in management of chronic critical limb ischemia and foot ulcer.' *Cell Transplantation*, 19(11) pp. 1413-1424.

Qader, S. W., Abdulla, M. A., Chua, L. S., Najim, N., Zain, M. M. and Hamdan, S. (2011) 'Antioxidant, total phenolic content and cytotoxicity evaluation of selected Malaysian plants.' *Molecules*, 16(4) pp. 3433-3443.

Qi, Y., Jiang, D., Sindrilaru, A., Stegemann, A., Schatz, S., Treiber, N., Rojewski, M., Schrezenmeier, H., Vander Beken, S. and Wlaschek, M. (2014) 'TSG-6 released from intradermally injected mesenchymal stem cells accelerates wound healing and reduces tissue fibrosis in murine full-thickness skin wounds.' *Journal of Investigative Dermatology*, 134(2) pp. 526-537.

Qiu, F., Tong, H., Wang, Y., Tao, J., Wang, H. and Chen, L. (2018) 'Recombinant human maspin inhibits high glucose-induced oxidative stress and angiogenesis of human retinal microvascular endothelial cells via PI3K/AKT pathway.' *Molecular and Cellular Biochemistry*, pp. 1-10.

Quittet, M.-S., Touzani, O., Sindji, L., Cayon, J., Fillesoye, F., Toutain, J., Divoux, D., Marteau, L., Lecocq, M. and Roussel, S. (2015) 'Effects of mesenchymal stem cell therapy, in association with pharmacologically active microcarriers releasing VEGF, in an ischaemic stroke model in the rat.' *Acta Biomaterialia*, 15 pp. 77-88.

Rahman, K. (2007) 'Effects of garlic on platelet biochemistry and physiology.' *Molecular nutrition & Food Research*, 51(11) pp. 1335-1344.

Rai, A. K., Chandra, S., Singh, S. P. and Parveen, A. (2016) 'Atherosclerosis: a life changing phenomenon.' *Pharmaceutical and Biological Evaluations*, 3(2) pp. 154-164.

Raman, B., Krishna, N., Rao, N., Saradhi, P. and Rao, B. (2012) 'Plants with antidiabetic activities and their medicinal values.' *Int Res J Pharm*, 3(3) pp. 11-15.

Raposeiras-Roubín, S., Rodiño-Janeiro, B. K., Paradelo-Dobarro, B., Grigorian-Shamagian, L., García-Acuña, J. M., Aguiar-Souto, P., Jacquet-Hervet, M., Reino-Maceiras, M. V., González-Juanatey, J. R. and Álvarez, E. (2013) 'Fluorescent advanced glycation end products and their soluble receptor: the birth of new plasmatic biomarkers for risk stratification of acute coronary syndrome.' *PLoS One*, 8(9) p. e74302.

Rhee, S. Y. and Kim, Y. S. (2018) 'The Role of Advanced Glycation End Products in Diabetic Vascular Complications.' *Diabetes & Metabolism Journal*, 42(3) pp. 188-195.

Richarme, G., Mihoub, M., Dairou, J., Bui, L. C., Leger, T. and Lamouri, A. (2015) 'Parkinsonism-associated protein DJ-1/Park7 is a major protein deglycase that repairs

methylglyoxal-and glyoxal-glycated cysteine, arginine, and lysine residues.' *Journal of Biological Chemistry*, 290(3) pp. 1885-1897.

Rivlin, R. S. (2001) 'Historical perspective on the use of garlic.' *The Journal of Nutrition*, 131(3) pp. 951S-954S.

Roby, M. H. H., Sarhan, M. A., Selim, K. A.-H. and Khalel, K. I. (2013) 'Evaluation of antioxidant activity, total phenols and phenolic compounds in thyme (*Thymus vulgaris* L.), sage (*Salvia officinalis* L.), and marjoram (*Origanum majorana* L.) extracts.' *Industrial Crops and Products*, 43 pp. 827-831.

Rodriguez-Menocal, L., Shareef, S., Salgado, M., Shabbir, A. and Van Badiavas, E. (2015) 'Role of whole bone marrow, whole bone marrow cultured cells, and mesenchymal stem cells in chronic wound healing.' *Stem Cell Research & Therapy*, 6(1) p. 24.

Rojas, A. and Morales, M. A. (2004) 'Advanced glycation and endothelial functions: a link towards vascular complications in diabetes.' *Life Sciences*, 76(7) pp. 715-730.

Rustad, K. C., Wong, V. W., Sorkin, M., Glotzbach, J. P., Major, M. R., Rajadas, J., Longaker, M. T. and Gurtner, G. C. (2012) 'Enhancement of mesenchymal stem cell angiogenic capacity and stemness by a biomimetic hydrogel scaffold.' *Biomaterials*, 33(1) pp. 80-90.

Saad, B. and Said, O. (2011) *Greco-Arab and Islamic herbal medicine: Traditional System, Ethics, Safety, Efficacy, and Regulatory Issues*. John Wiley & Sons.

Saap, L. J. and Falanga, V. (2002) 'Debridement performance index and its correlation with complete closure of diabetic foot ulcers.' *Wound Repair and Regeneration*, 10(6) pp. 354-359.

Sadhukha, T., O'brien, T. D. and Prabha, S. (2014) 'Nano-engineered mesenchymal stem cells as targeted therapeutic carriers.' *Journal of Controlled Release*, 196 pp. 243-251.

Sadowska, A., Manuel-Y-Keenoy, B. and De Backer, W. (2007) 'Antioxidant and anti-inflammatory efficacy of NAC in the treatment of COPD: discordant in vitro and in vivo dose-effects: a review.' *Pulmonary Pharmacology & Therapeutics*, 20(1) pp. 9-22.

Saeidnia, S. and Abdollahi, M. (2013) 'Toxicological and pharmacological concerns on oxidative stress and related diseases.' *Toxicology and Applied Pharmacology*, 273(3) pp. 442-455.

Samakradhamrongthai, R. (2017) 'Effect of drying condition of Thai garlic (*Allium sativum* L.) on physicochemical and sensory properties.'

Santhosha, S. G., Jamuna, P. and Prabhavathi, S. N. (2013) 'Bioactive components of garlic and their physiological role in health maintenance: A review.' *Food Bioscience*, 3 pp. 59-74.

Schäfer, M. and Werner, S. (2008) 'Oxidative stress in normal and impaired wound repair.' *Pharmacological Research*, 58(2) pp. 165-171.

Sen, C. K., Gordillo, G. M., Roy, S., Kirsner, R., Lambert, L., Hunt, T. K., Gottrup, F., Gurtner, G. C. and Longaker, M. T. (2009) 'Human skin wounds: a major and snowballing threat to public health and the economy.' *Wound Repair and Regeneration*, 17(6) pp. 763-771.

Seo, K., Ki, S. and Shin, S. (2014) *Methylglyoxal induces mitochondrial dysfunction and cell death in liver. Toxicol Res 30: 193–198. doi: 10.5487. TR. 2014.30. 3.193.*

Serra, M. B., Barroso, W. A., Silva, N. N. d., Silva, S. d. N., Borges, A. C. R., Abreu, I. C. and Borges, M. O. d. R. (2017) 'From inflammation to current and alternative therapies involved in wound healing.' *International Journal of Inflammation*, 2017

Sharaf, H., Matou-Nasri, S., Wang, Q., Rabhan, Z., Al-Eidi, H., Al Abdulrahman, A. and Ahmed, N. (2015) 'Advanced glycation endproducts increase proliferation, migration and invasion of the breast cancer cell line MDA-MB-231.' *Biochimica et Biophysica Acta (BBA)-Molecular Basis of Disease*, 1852(3) pp. 429-441.

Sharma, C., Kaur, A., Thind, S., Singh, B. and Raina, S. (2015) 'Advanced glycation end-products (AGEs): an emerging concern for processed food industries.' *Journal of Food Science and Technology*, 52(12) pp. 7561-7576.

Sharma, G. and Prasad, S. (2006) 'Optimization of process parameters for microwave drying of garlic cloves.' *Journal of Food Engineering*, 75(4) pp. 441-446.

Shimomura, H. and Spiro, R. G. (1987) 'Studies on macromolecular components of human glomerular basement membrane and alterations in diabetes: decreased levels of heparan sulfate proteoglycan and laminin.' *Diabetes*, 36(3) pp. 374-381.

Singh, V. P., Bali, A., Singh, N. and Jaggi, A. S. (2014) 'Advanced glycation end products and diabetic complications.' *The Korean Journal of Physiology & Pharmacology*, 18(1) pp. 1-14.

Siviero, F. (2013) 'Biologia celular: bases moleculares e metodologia de pesquisa.' *In Biologia Celular: Bases Moleculares e Metodologia de Pesquisa.*

Slavich, G. M. and Irwin, M. R. (2014) 'From stress to inflammation and major depressive disorder: a social signal transduction theory of depression.' *Psychological Bulletin*, 140(3) p. 774.

Smith, A. N., Willis, E., Chan, V. T., Muffley, L. A., Isik, F. F., Gibran, N. S. and Hocking, A. M. (2010) 'Mesenchymal stem cells induce dermal fibroblast responses to injury.' *Experimental Cell Research*, 316(1) pp. 48-54.

Snyder, L. R., Kirkland, J. J. and Glajch, J. L. (2012) *Practical HPLC method development*. John Wiley & Sons.

Sollazzo, V., Palmieri, A., Girardi, A., Farinella, F. and Carinci, F. (2011) 'Trabecular titanium induces osteoblastic bone marrow stem cells differentiation.' *J Biotechnol Biomaterial*, 1(102) p. 2.

Soloviev, A., Stefanov, A., Tishkin, S., Khromov, A., Parshikov, A., Ivanova, I. and Gurney, A. (2002) 'SALINE CONTAINING PHOSPHATIDYLCHOLINE LIPOSOMES.' *Journal of physiology and pharmacology*, 53(4) pp. 701-712.

Song, F., Yuan, B., Li, X., Huang, X., Zhou, Z., Dong, J., Yang, H. and Qiao, L. (2017) 'High glucose and AGEs inhibit tube formation of vascular endothelial cells by sustained Ang-2 production.' *International Journal of Clinical and Experimental Pathology*, 10(3) pp. 3786-3793.

Sottile, V., Halleux, C., Bassilana, F., Keller, H. and Seuwen, K. (2002) 'Stem cell characteristics of human trabecular bone-derived cells.' *Bone*, 30(5) pp. 699-704.

Squillaro, T., Peluso, G. and Galderisi, U. (2016) 'Clinical trials with mesenchymal stem cells: an update.' *Cell Transplantation*, 25(5) pp. 829-848.

Srikanth, V., Maczurek, A., Phan, T., Steele, M., Westcott, B., Juskiw, D. and Münch, G. (2011) 'Advanced glycation endproducts and their receptor RAGE in Alzheimer's disease.' *Neurobiology of Aging*, 32(5) pp. 763-777.

Stadler, R. H., Blank, I., Varga, N., Robert, F., Hau, J., Guy, P. A., Robert, M.-C. and Riediker, S. (2002) 'Acrylamide from Maillard reaction products.' *Nature*, 419, 10/03/online, p. 449.

Steiner, M. and Li, W. (2001) 'Aged garlic extract, a modulator of cardiovascular risk factors: a dose-finding study on the effects of AGE on platelet functions.' *The Journal of Nutrition*, 131(3) pp. 980S-984S.

Stinghen, A. E., Massy, Z. A., Vlassara, H., Striker, G. E. and Boullier, A. (2015) 'Uremic toxicity of advanced glycation end products in CKD.' *Journal of the American Society of Nephrology*, p. ASN. 2014101047.

Stitt, A. W., McGoldrick, C., Rice-McCaldin, A., McCance, D. R., Glenn, J. V., Hsu, D. K., Liu, F.-T., Thorpe, S. R. and Gardiner, T. A. (2005) 'Impaired retinal angiogenesis in diabetes: role of advanced glycation end products and galectin-3.' *Diabetes*, 54(3) pp. 785-794.

Stitt, A. W., Curtis, T. M., Chen, M., Medina, R. J., McKay, G. J., Jenkins, A., Gardiner, T. A., Lyons, T. J., Hammes, H.-P. and Simo, R. (2016) 'The progress in understanding and treatment of diabetic retinopathy.' *Progress in Retinal and Eye Research*, 51 pp. 156-186.

Stojadinovic, O., Brem, H., Vouthounis, C., Lee, B., Fallon, J., Stallcup, M., Merchant, A., Galiano, R. D. and Tomic-Canic, M. (2005) 'Molecular pathogenesis of chronic wounds: the role of β -catenin and c-myc in the inhibition of epithelialization and wound healing.' *The American Journal of Pathology*, 167(1) pp. 59-69.

Supabphol, A., Muangman, V., Chavasiri, W., Supabphol, R. and Gritsanapan, W. (2009) 'N-acetylcysteine inhibits proliferation, adhesion, migration and invasion of human bladder cancer cells.' *Medical Journal of the Medical Association of Thailand*, 92(9) p. 1171.

Syu, J.-N., Yang, M.-D., Tsai, S.-Y., Chiang, E.-P. I., Chiu, S.-C., Chao, C.-Y., Rodriguez, R. L. and Tang, F.-Y. (2017) 'S-allylcysteine Improves Blood Flow Recovery and Prevents Ischemic Injury by Augmenting Neovasculogenesis.' *Cell Transplantation*, 26(10) pp. 1636-1647.

Tadokoro, M., Kanai, R., Taketani, T., Uchio, Y., Yamaguchi, S. and Ohgushi, H. (2009) 'New bone formation by allogeneic mesenchymal stem cell transplantation in a patient with perinatal hypophosphatasia.' *The Journal of pediatrics*, 154(6) pp. 924-930.

Tajes, M., Eraso-Pichot, A., Rubio-Moscardó, F., Guivernau, B., Bosch-Morató, M., Valls-Comamala, V. and Munoz, F. J. (2014) 'Methylglyoxal reduces mitochondrial potential and activates Bax and caspase-3 in neurons: Implications for Alzheimer's disease.' *Neuroscience letters*, 580 pp. 78-82.

Takahashi, H., Sakata, N., Yoshimatsu, G., Hasegawa, S. and Kodama, S. (2019) 'Regenerative and Transplantation Medicine: Cellular Therapy Using Adipose Tissue-Derived Mesenchymal Stromal Cells for Type 1 Diabetes Mellitus.' *Journal of Clinical Medicine*, 8(2) p. 249.

Tang, W., Martin, K. A. and Hwa, J. (2012) 'Aldose reductase, oxidative stress, and diabetic mellitus.' *Frontiers in pharmacology*, 3 p. 87.

Tezuka, M., Koyama, N., Morisaki, N., Saito, Y., Yoshida, S., Araki, N. and Horiuchi, S. (1993) 'Angiogenic effects of advanced glycation end products of the Maillard reaction on cultured human umbilical cord vein endothelial cells.' *Biochemical and Biophysical Research Communications*, 193(2) pp. 674-680.

Thornalley, P. J. (2008) 'Protein and nucleotide damage by glyoxal and methylglyoxal in physiological systems-role in ageing and disease.' *Drug Metabolism and Drug Interactions*, 23(1-2) pp. 125-150.

Todd, G. P., LeRoux, M. A. and Danilkovitch-Miagkova, A. (2011) 'Mesenchymal stem cells as vehicles for targeted therapies.' *In Drug Discovery and Development-Present and Future*. InTech,

Torres, C., Picó, Y. and Manes, J. (1996) 'Determination of pesticide residues in fruit and vegetables.' *Journal of Chromatography A*, 754(1-2) pp. 301-331.

Towbin, H., Staehelin, T. and Gordon, J. (1979) 'Electrophoretic transfer of proteins from polyacrylamide gels to nitrocellulose sheets: procedure and some applications.' *Proceedings of the National Academy of Sciences*, 76(9) pp. 4350-4354.

Trachtman, H., Futterweit, S., Prenner, J. and Hanon, S. (1994) 'Antioxidants reverse the antiproliferative effect of high glucose and advanced glycosylation end products in cultured rat mesangial cells.' *Biochemical and Biophysical Research Communications*, 199(1) pp. 346-352.

Troise, A. D. and Fogliano, V. (2013) 'Reactants encapsulation and Maillard reaction.' *Trends in Food Science & Technology*, 33(1) pp. 63-74.

Tsekovska, R., Sredovska-Bozhinov, A., Niwa, T., Ivanov, I. and Mironova, R. (2016) 'Maillard reaction and immunogenicity of protein therapeutics.' *World*, 1 p. 003.

Uribarri, J. (2017) *Dietary AGEs and Their Role in Health and Disease*. CRC Press.

Velnar, T., Bailey, T. and Smrkolj, V. (2009) 'The wound healing process: an overview of the cellular and molecular mechanisms.' *Journal of International Medical Research*, 37(5) pp. 1528-1542.

Villa, M., Parravano, M., Micheli, A., Gaddini, L., Matteucci, A., Mallozzi, C., Facchiano, F., Malchiodi-Albedi, F. and Pricci, F. (2017) 'A quick, simple method for detecting circulating fluorescent advanced glycation end-products: Correlation with in vitro and in vivo non-enzymatic glycation.' *Metabolism*, 71 pp. 64-69.

Walter, M., Wright, K. T., Fuller, H., MacNeil, S. and Johnson, W. E. B. (2010) 'Mesenchymal stem cell-conditioned medium accelerates skin wound healing: an in vitro study of fibroblast and keratinocyte scratch assays.' *Experimental Cell Research*, 316(7) pp. 1271-1281.

Wang, I.-H., Moorman, R. and Bureson, J. (2003) 'Isocratic reversed-phase liquid chromatographic method for the simultaneous determination of (S)-methoprene, MGK264, piperonyl butoxide, sumithrin and permethrin in pesticide formulation.' *Journal of Chromatography A*, 983(1-2) pp. 145-152.

Wang, J., Sun, B., Cao, Y. and Tian, Y. (2009) 'Protein glycation inhibitory activity of wheat bran feruloyl oligosaccharides.' *Food Chemistry*, 112(2) pp. 350-353.

Wang, Q., Fan, A., Yuan, Y., Chen, L., Guo, X., Huang, X. and Huang, Q. (2016) 'Role of moesin in advanced glycation end products-induced angiogenesis of human umbilical vein endothelial cells.' *Scientific Reports*, 6 p. 22749.

Wang, X., Ackermann, M., Neufurth, M., Wang, S., Li, Q., Feng, Q., Schröder, H. C. and Müller, W. E. (2017) 'Restoration of Impaired Metabolic Energy Balance (ATP Pool) and Tube Formation Potential of Endothelial Cells under "high glucose", Diabetic Conditions by the Bioinorganic Polymer Polyphosphate.' *Polymers*, 9(11) p. 575.

Wang, Y., Friedrichs, U., Eichler, W., Hoffmann, S. and Wiedemann, P. (2005) 'Advanced glycation endproducts enhance pro-liferation, but not tube formation in choroidal microvascular endothelial cells.' *International Journal of Ophthalmology*, 5(2)

Waterman, R. and Betancourt, A. (2011) 'Treating chronic pain with mesenchymal stem cells: A therapeutic approach worthy of continued investigation.' *J Stem Cell Res Ther*, p. S2.

Wikramanayake, T. C., Stojadinovic, O. and Tomic-Canic, M. (2014) 'Epidermal differentiation in barrier maintenance and wound healing.' *Advances in Wound Care*, 3(3) pp. 272-280.

Wilgus, T. A., Roy, S. and McDaniel, J. C. (2013) 'Neutrophils and wound repair: positive actions and negative reactions.' *Advances in Wound Care*, 2(7) pp. 379-388.

Williamson, J. and Ido, Y. (2012) 'Linking diabetic complications to sorbitol oxidation, oxidative stress and metabolic suppression.' *Journal of Diabetes Metabolism*, 3

Winters, R. A., Zukowski, J., Ercal, N., Matthews, R. H. and Spitz, D. R. (1995) 'Analysis of glutathione, glutathione disulfide, cysteine, homocysteine, and other biological thiols by high-performance liquid chromatography following derivatization by n-(1-pyrenyl) maleimide.' *Analytical Biochemistry*, 227(1) pp. 14-21.

Wu, J.-W., Hsieh, C.-L., Wang, H.-Y. and Chen, H.-Y. (2009) 'Inhibitory effects of guava (*Psidium guajava* L.) leaf extracts and its active compounds on the glycation process of protein.' *Food Chemistry*, 113(1) pp. 78-84.

Wu, S. C., Marston, W. and Armstrong, D. G. (2010) 'Wound care: the role of advanced wound-healing technologies.' *Journal of the American Podiatric Medical Association*, 100(5) pp. 385-394.

Wu, Y., Chen, L., Scott, P. G. and Tredget, E. E. (2007) 'Mesenchymal stem cells enhance wound healing through differentiation and angiogenesis.' *Stem Cells*, 25(10) pp. 2648-2659.

Wu, Y., Ding, Y., Tanaka, Y. and Zhang, W. (2014) 'Risk factors contributing to type 2 diabetes and recent advances in the treatment and prevention.' *International Journal of Medical Sciences*, 11(11) p. 1185.

Xie, C., Liu, N., Long, J., Tang, C., Li, J., Huo, L., Wang, X., Chen, P. and Liang, S. (2011) 'Blue native/SDS-PAGE combined with iTRAQ analysis reveals advanced glycation end-product-

induced changes of synaptosome proteins in C57 BL/6 mice.' *Electrophoresis*, 32(16) pp. 2194-2205.

Xie, D., Ju, D., Speyer, C., Gorski, D. and Kosir, M. A. (2016) 'Strategic Endothelial Cell Tube Formation Assay: Comparing Extracellular Matrix and Growth Factor Reduced Extracellular Matrix.' *Journal of Visualized Experiments: JoVE*, (114)

Xu, B., Chibber, R., Ruggiero, D., Kohner, E., Ritter, J. and Ferro, A. (2003) 'Impairment of vascular endothelial nitric oxide synthase activity by advanced glycation end products.' *The FASEB journal*, 17(10) pp. 1289-1291.

Xu, J., Wu, W., Zhang, L., Dorset-Martin, W., Morris, M. W., Mitchell, M. E. and Liechty, K. W. (2012) 'The role of microRNA-146a in the pathogenesis of the diabetic wound-healing impairment: correction with mesenchymal stem cell treatment.' *Diabetes*, 61(11) pp. 2906-2912.

Xu, Y.-s., Feng, J.-g., Zhang, D., Zhang, B., Luo, M., Su, D. and Lin, N.-m. (2014) 'S-allylcysteine, a garlic derivative, suppresses proliferation and induces apoptosis in human ovarian cancer cells in vitro.' *Acta Pharmacologica Sinica*, 35(2) p. 267.

Yagihashi, S., Mizukami, H. and Sugimoto, K. (2011) 'Mechanism of diabetic neuropathy: where are we now and where to go?' *Journal of Diabetes Investigation*, 2(1) pp. 18-32.

Yamagishi, S.-i. (2011) 'Role of advanced glycation end products (AGEs) and receptor for AGEs (RAGE) in vascular damage in diabetes.' *Experimental Gerontology*, 46(4) pp. 217-224.

Yamagishi, S.-i. and Imaizumi, T. (2005) 'Diabetic vascular complications: pathophysiology, biochemical basis and potential therapeutic strategy.' *Current Pharmaceutical Design*, 11(18) pp. 2279-2299.

Yamagishi, S.-i., Inagaki, Y., Okamoto, T., Amano, S., Koga, K. and Takeuchi, M. (2003) 'Advanced glycation end products inhibit de novo protein synthesis and induce TGF- β overexpression in proximal tubular cells.' *Kidney International*, 63(2) pp. 464-473.

Yamagishi, S.-i., Matsui, T., Nakamura, K., Inoue, H., Takeuchi, M., Ueda, S., Fukami, K., Okuda, S. and Imaizumi, T. (2008) 'Olmesartan blocks advanced glycation end products (AGEs)-induced angiogenesis in vitro by suppressing receptor for AGEs (RAGE) expression.' *Microvascular Research*, 75(1) pp. 130-134.

Yamagishi, S., Hsu, C.-C., Taniguchi, M., Harada, S., Yamamoto, Y., Ohsawa, K., Kobayashi, K. and Yamamoto, H. (1995) 'Receptor-mediated toxicity to pericytes of advanced glycosylation end products: a possible mechanism of pericyte loss in diabetic microangiopathy.' *Biochemical and Biophysical Research Communications*, 213(2) pp. 681-687.

Yan, L.-J. (2014) 'Pathogenesis of chronic hyperglycemia: from reductive stress to oxidative stress.' *Journal of Diabetes Research*, 2014

Yang, C.-t., Meng, F.-h., Chen, L., Li, X., Cen, L.-J., Wen, Y.-h., Li, C.-c. and Zhang, H. (2017) 'Inhibition of methylglyoxal-induced AGEs/RAGE expression contributes to dermal protection by N-acetyl-L-cysteine.' *Cellular Physiology and Biochemistry*, 41(2) pp. 742-754.

Yazdanpanah, L., Nasiri, M. and Adarvishi, S. (2015) 'Literature review on the management of diabetic foot ulcer.' *World Journal of Diabetes*, 6(1) p. 37.

Yin, M.-c. and Cheng, W.-s. (2003) 'Antioxidant and antimicrobial effects of four garlic-derived organosulfur compounds in ground beef.' *Meat Science*, 63(1) pp. 23-28.

Yolanda, M.-M., Maria, A.-V., Amaia, F., Marcos, P., Silvia, P., Dolores, E. and Jesús, O. (2014) 'Adult stem cell therapy in chronic wound healing.' *J Stem Cell Res Ther*, 4(162) p. 2.

You, H.-J. and Han, S.-K. (2014) 'Cell therapy for wound healing.' *Journal of Korean Medical Science*, 29(3) pp. 311-319.

Younus, H. and Anwar, S. (2016) 'Prevention of non-enzymatic glycosylation (glycation): Implication in the treatment of diabetic complication.' *International Journal of Health Sciences*, 10(2) p. 261.

Yu, A.-N. and Zhang, A.-D. (2010) 'The effect of pH on the formation of aroma compounds produced by heating a model system containing L-ascorbic acid with L-threonine/L-serine.' *Food Chemistry*, 119(1) pp. 214-219.

Yu, L., Yang, F., Jiang, L., Chen, Y., Wang, K., Xu, F., Wei, Y., Cao, X., Wang, J. and Cai, Z. (2013) 'Exosomes with membrane-associated TGF- β 1 from gene-modified dendritic cells inhibit murine EAE independently of MHC restriction.' *European Journal of Immunology*, 43(9) pp. 2461-2472.

Yui, S., Sasaki, T., Araki, N., Horiuchi, S. and Yamazaki, M. (1994) 'Induction of macrophage growth by advanced glycation end products of the Maillard reaction.' *The Journal of Immunology*, 152(4) pp. 1943-1949.

Zafarullah, M., Li, W., Sylvester, J. and Ahmad, M. (2003) 'Molecular mechanisms of N-acetylcysteine actions.' *Cellular and Molecular Life Sciences CMLS*, 60(1) pp. 6-20.

Zhang, J., Slevin, M., Duraisamy, Y., Gaffney, J., Smith, C. A. and Ahmed, N. (2006) 'Comparison of protective effects of aspirin, D-penicillamine and vitamin E against high glucose-mediated toxicity in cultured endothelial cells.' *Biochimica et Biophysica Acta (BBA)-Molecular Basis of Disease*, 1762(5) pp. 551-557.

Zhang, P., Zhong, S., Wang, G., Zhang, S.-y., Chu, C., Zeng, S., Yan, Y., Cheng, X., Bao, Y. and Hoher, B. (2018) 'N-Acetylcysteine Suppresses LPS-Induced Pathological Angiogenesis.' *Cellular Physiology and Biochemistry*, 49(6) pp. 2483-2495.

Zhao, Y., Vanhoutte, P. M. and Leung, S. W. (2015) 'Vascular nitric oxide: Beyond eNOS.' *Journal of Pharmacological Sciences*, 129(2) pp. 83-94.

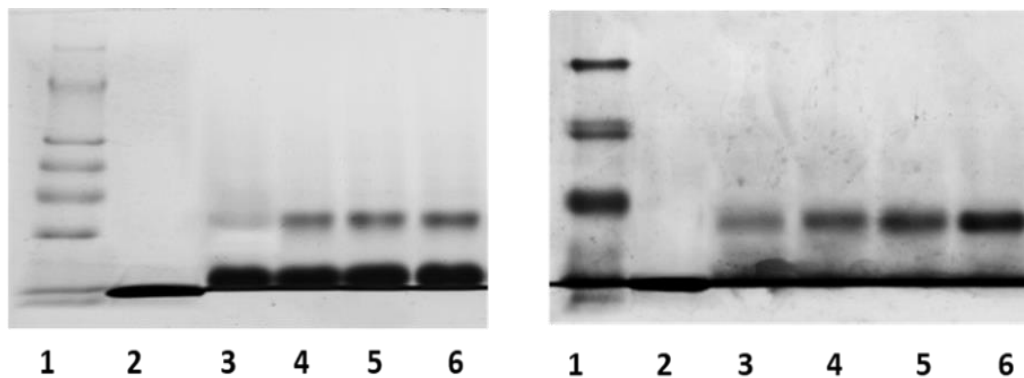
Zvaifler, N. J., Marinova-Mutafchieva, L., Adams, G., Edwards, C. J., Moss, J., Burger, J. A. and Maini, R. N. (2000) 'Mesenchymal precursor cells in the blood of normal individuals.' *Arthritis Research & Therapy*, 2(6) p. 477.

Appendices

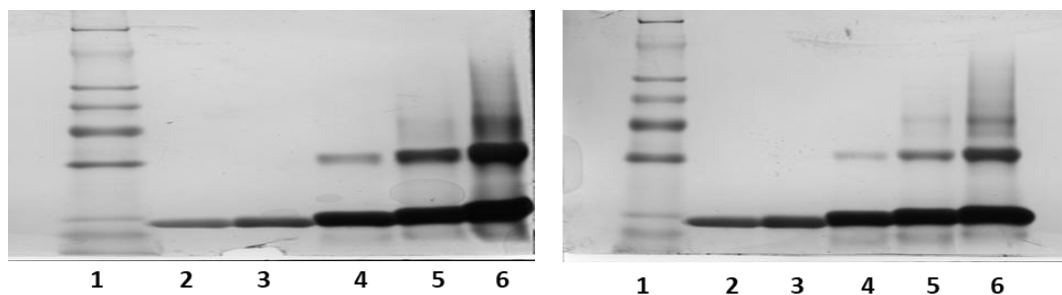
Appendix A

1. AGE formation of lysozyme induced by MG

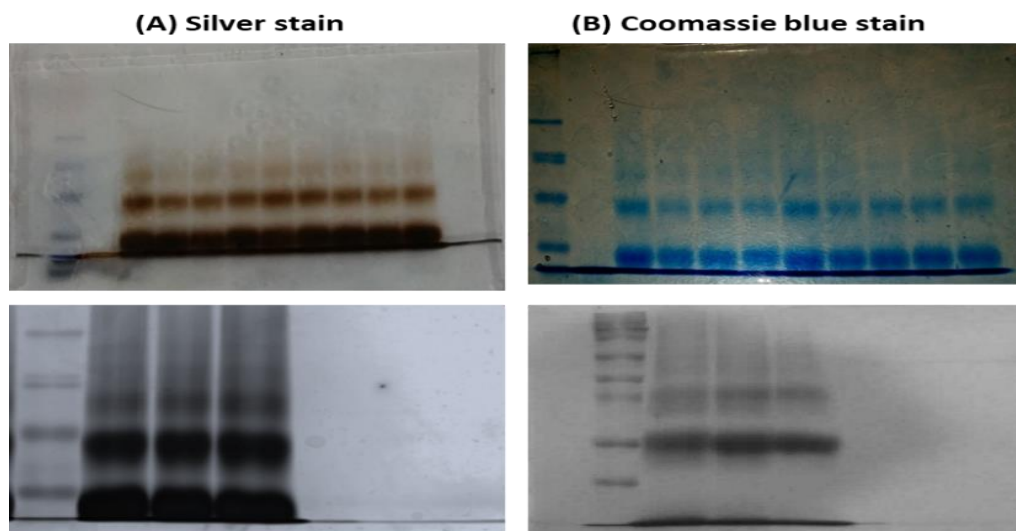
Lysozyme glycation by MG after 24 hours



Lysozyme glycation by MG after 72 hours

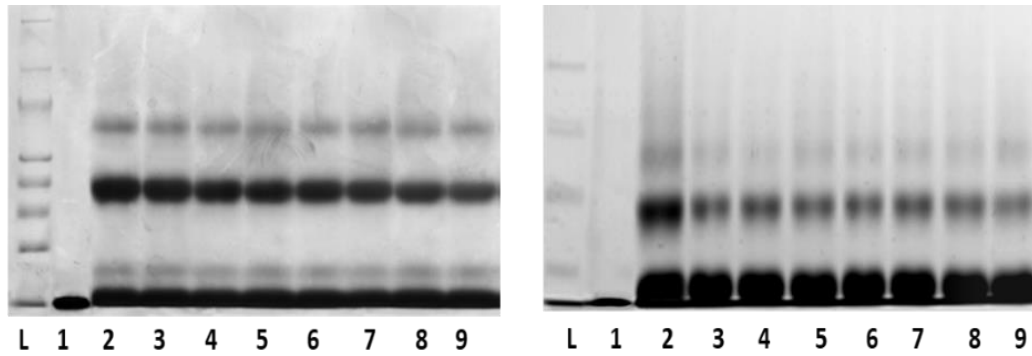


Compartion between stains

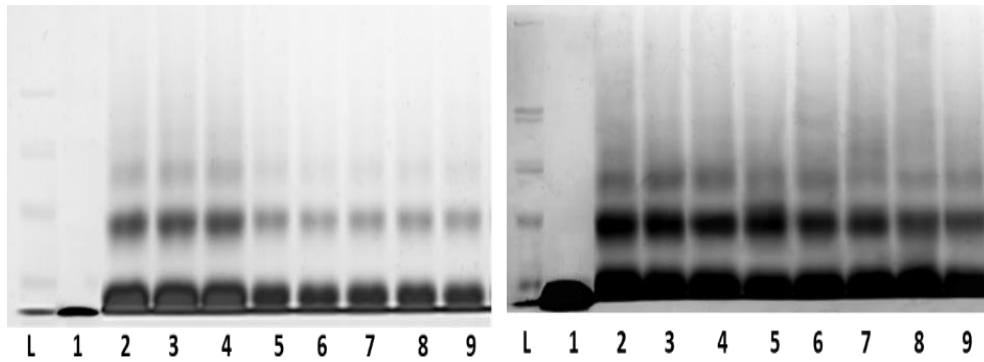


2. Detection of AGEs by SDS-PAGE-silver stain

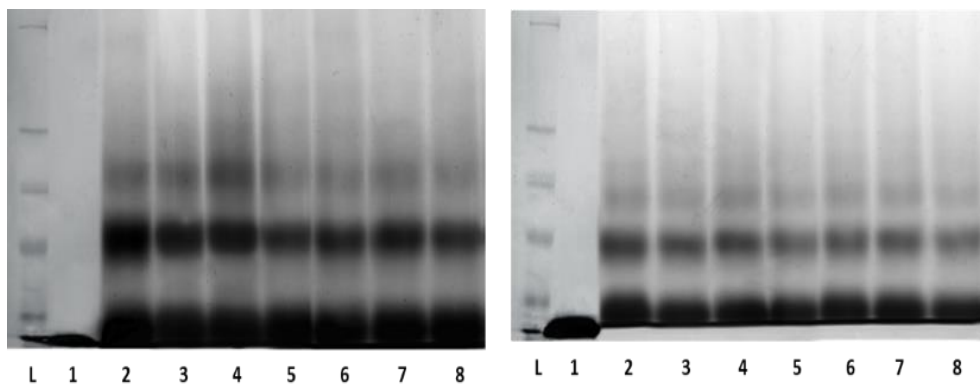
The effect of SAC on MG-derived AGE formation



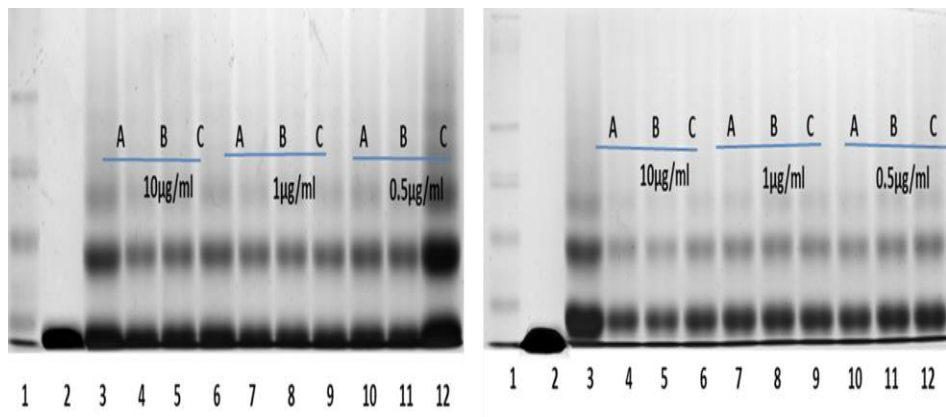
The effect of NAC on MG-derived AGE formation



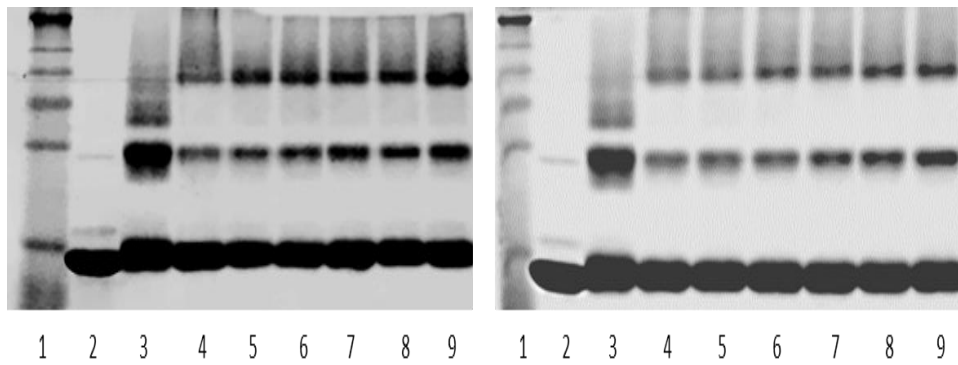
The effect of SAC/NAC on the cross-linked AGE formation



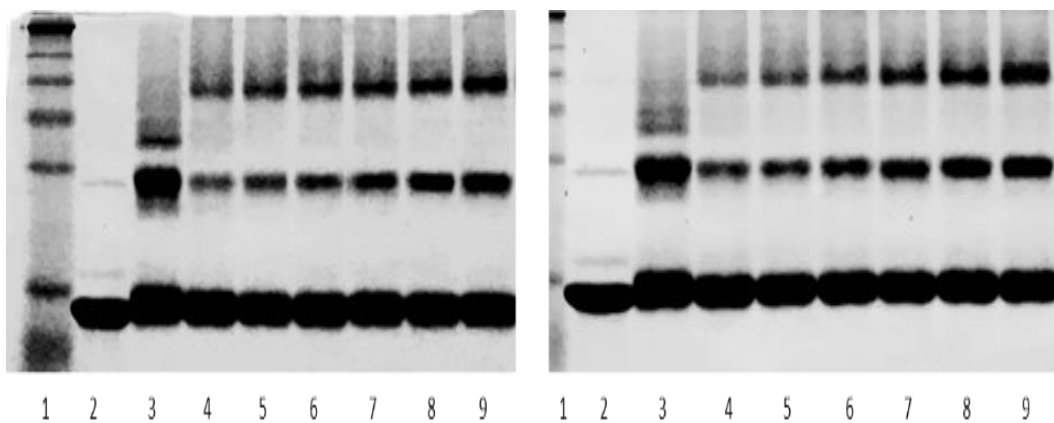
Comparison between mimic compounds A, B and C on MG-induced AGE formation



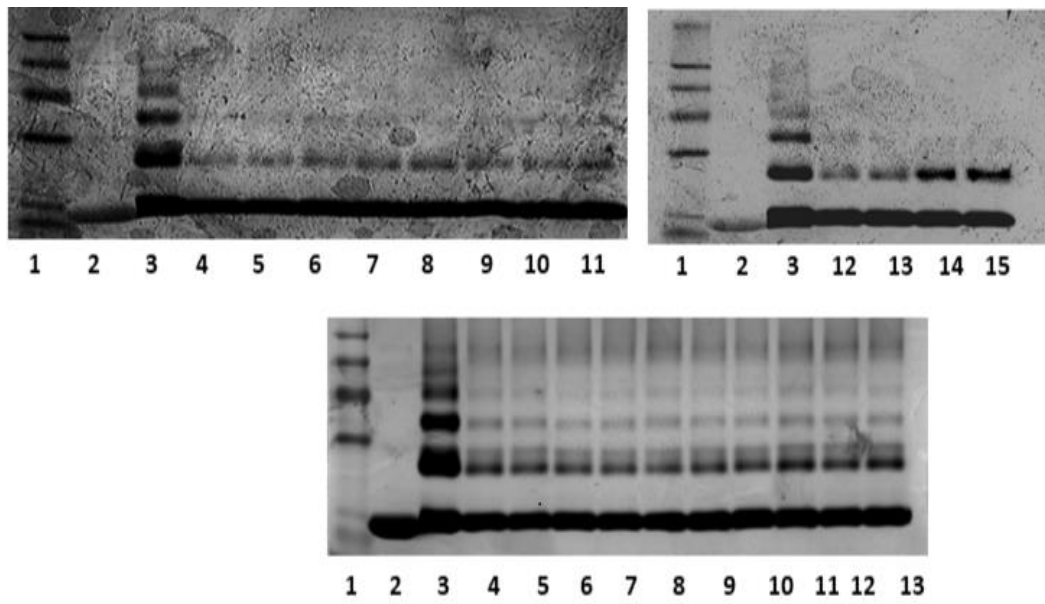
The effect of SAC/NAC on MG-induced AGE formation



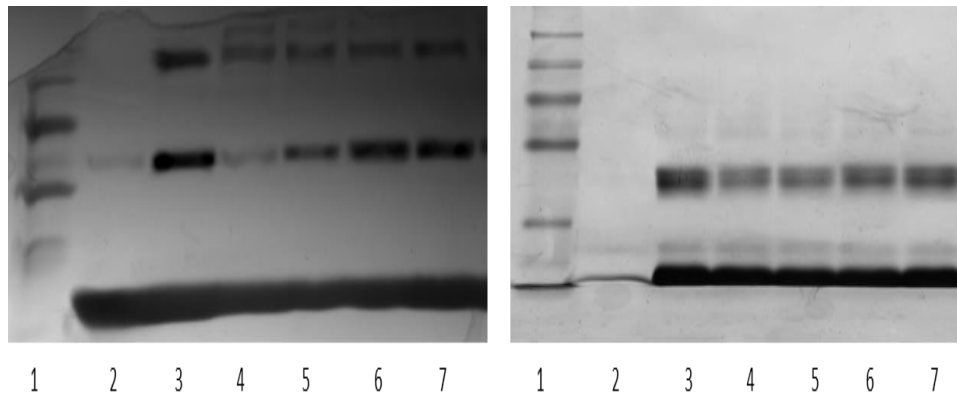
The effect of compound A on MG-induced AGE formation



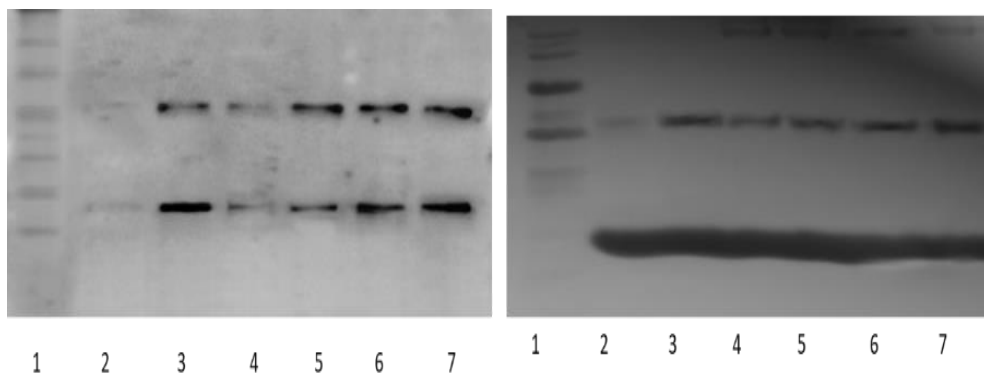
Effect of SAC/NAC and compound A on MG-induced AGE formation



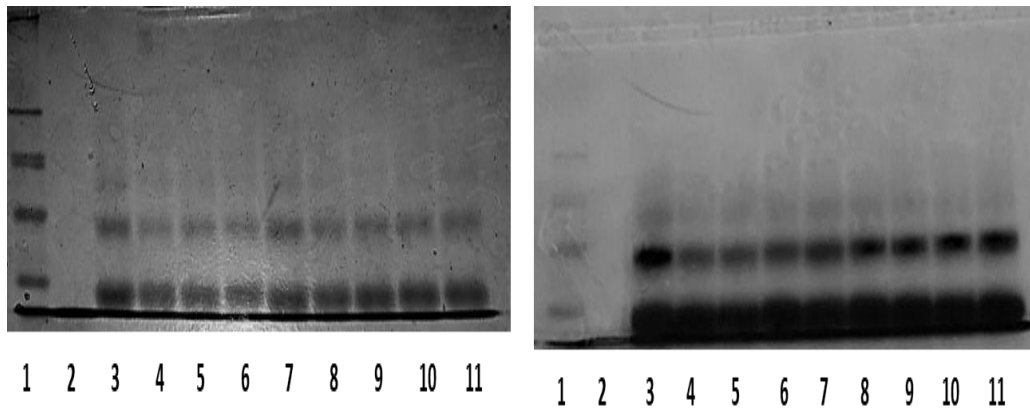
Effect of SAC/NAC-primed hADMSCs CM on MG-induced AGE formation



Effect of compound A-primed hADMSCs CM on MG-induced AGE formation

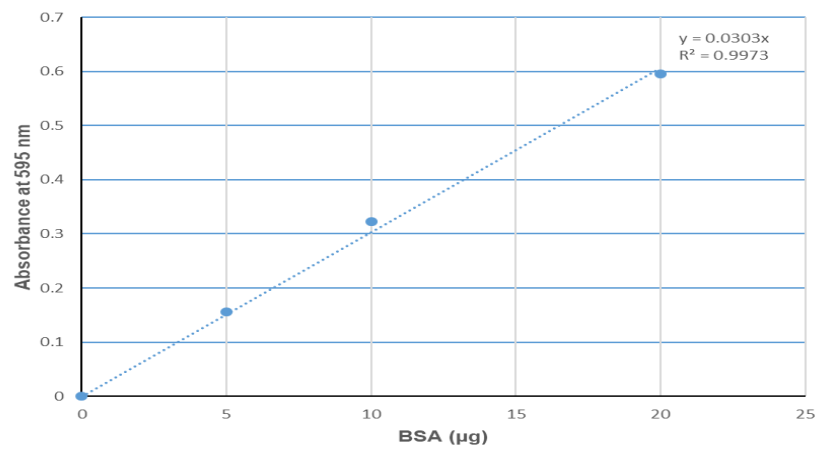


Effect of SAC/NAC- and compound A-loaded hADMSCs CM on MG-induced AGE formation

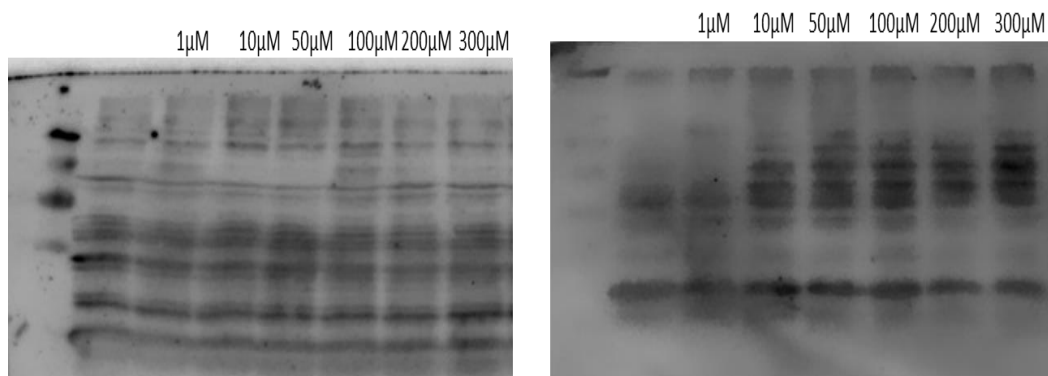


3. Detection of AGEs by Western blot

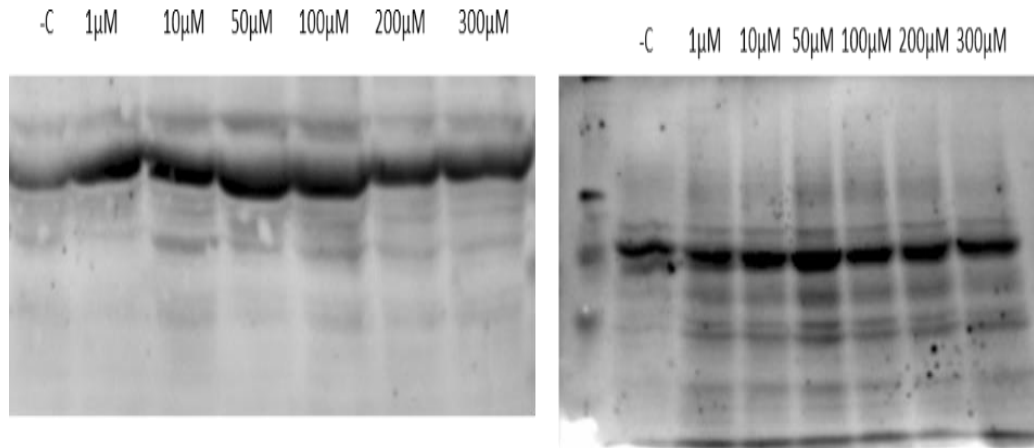
Protein determination



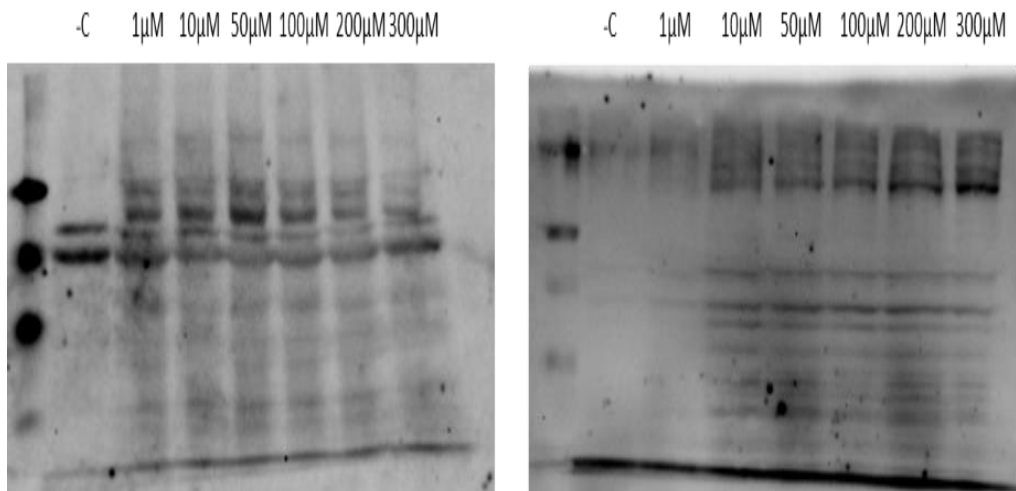
The effect of MG on BAEC glycation after 1 day



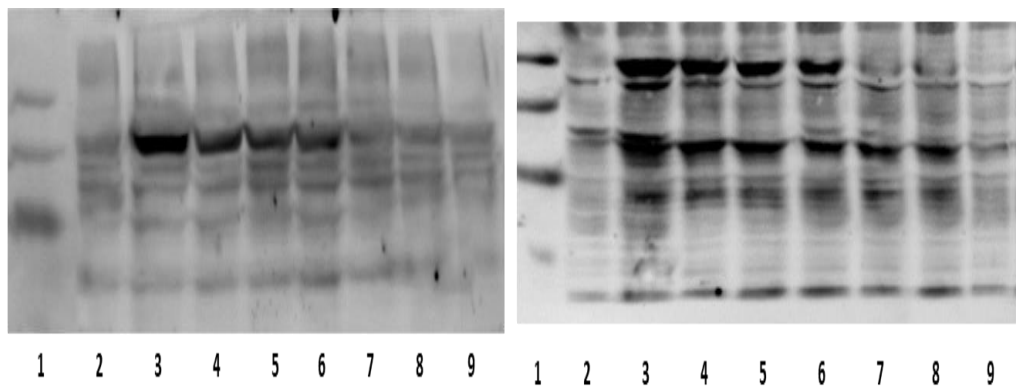
The effect of MG on BAEC glycation after 72 hours.



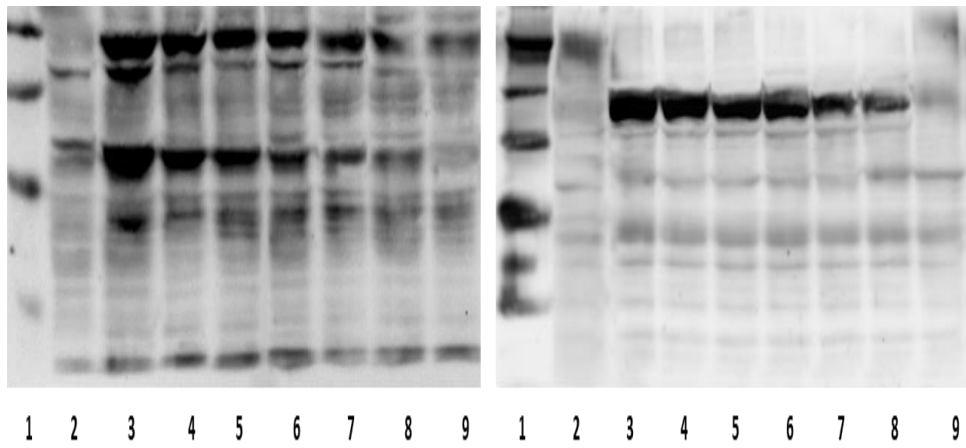
The effect of MG on BAEC glycation after 5 days.



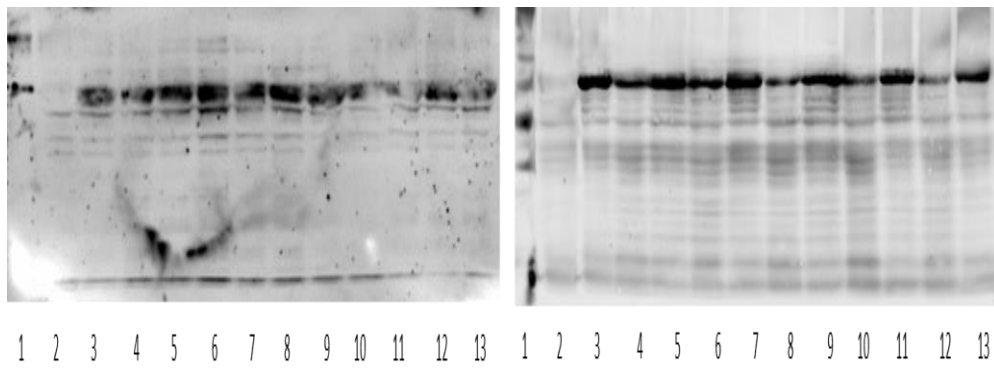
The effect of compound A on BAEC glycation.



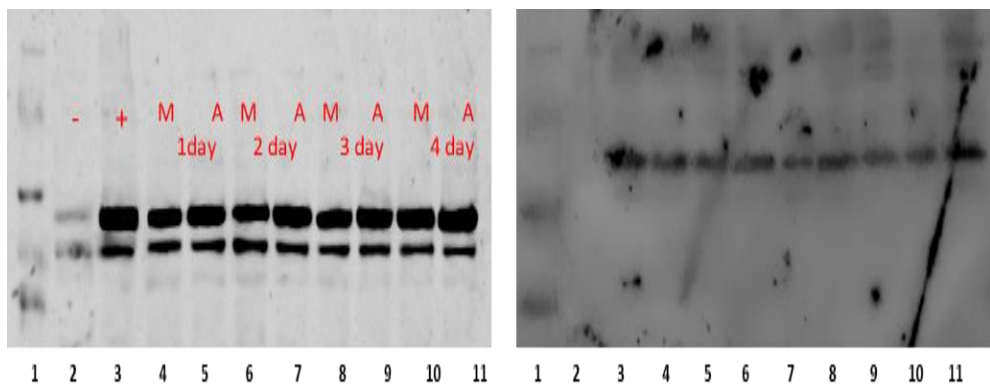
The effect of SAC/NAC on BAEC glycation.



The effect SAC/NAC and compound A of BAEC glycation.

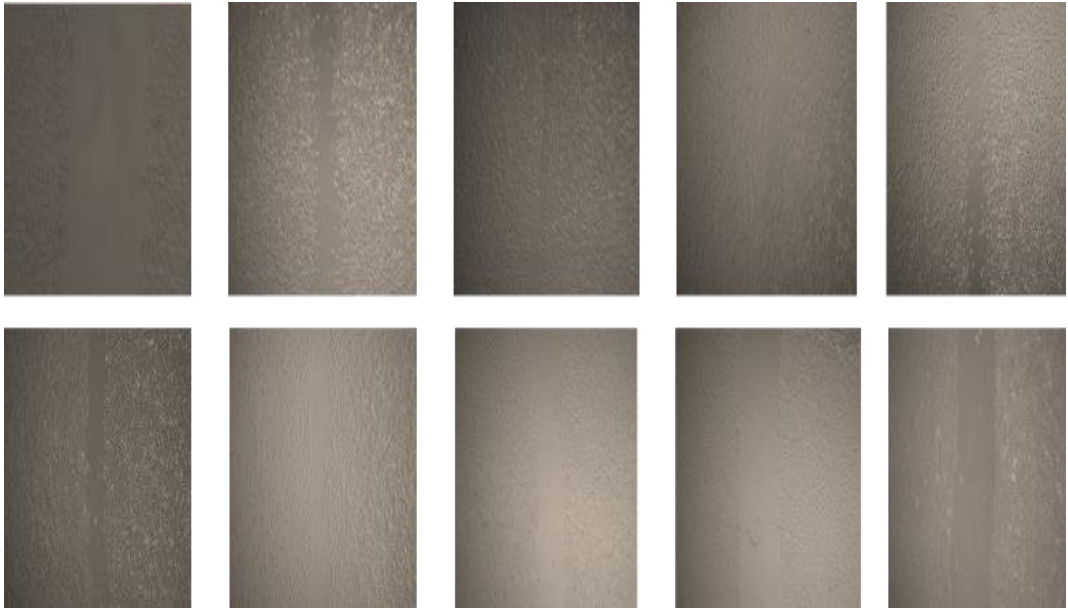


The effect of (SAC/NAC and compound A) - loaded hADMSCs CM

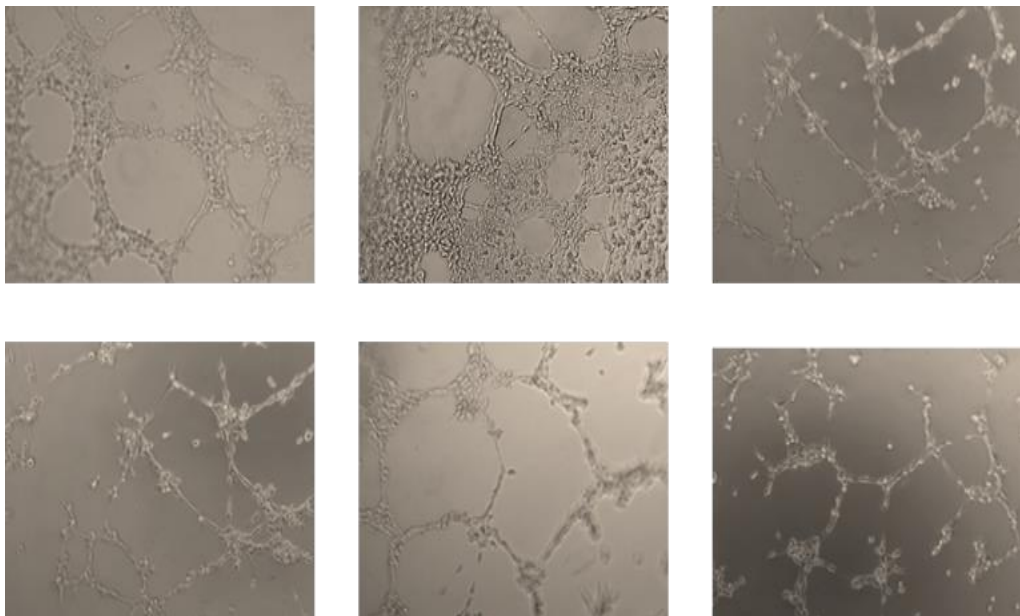


Appendix B: Angiogenesis

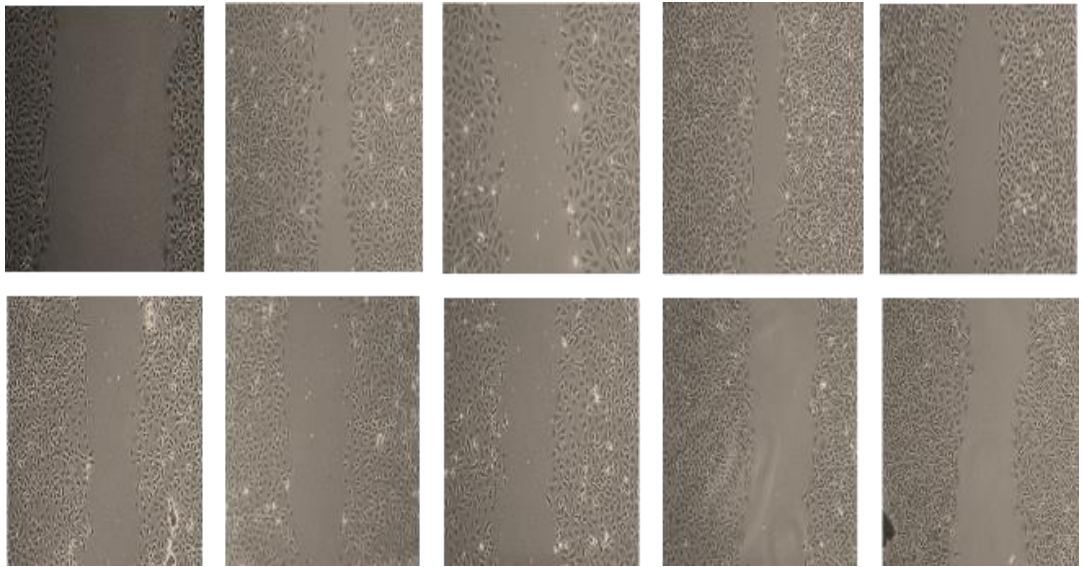
Effect of glucose on BAEC wound healing



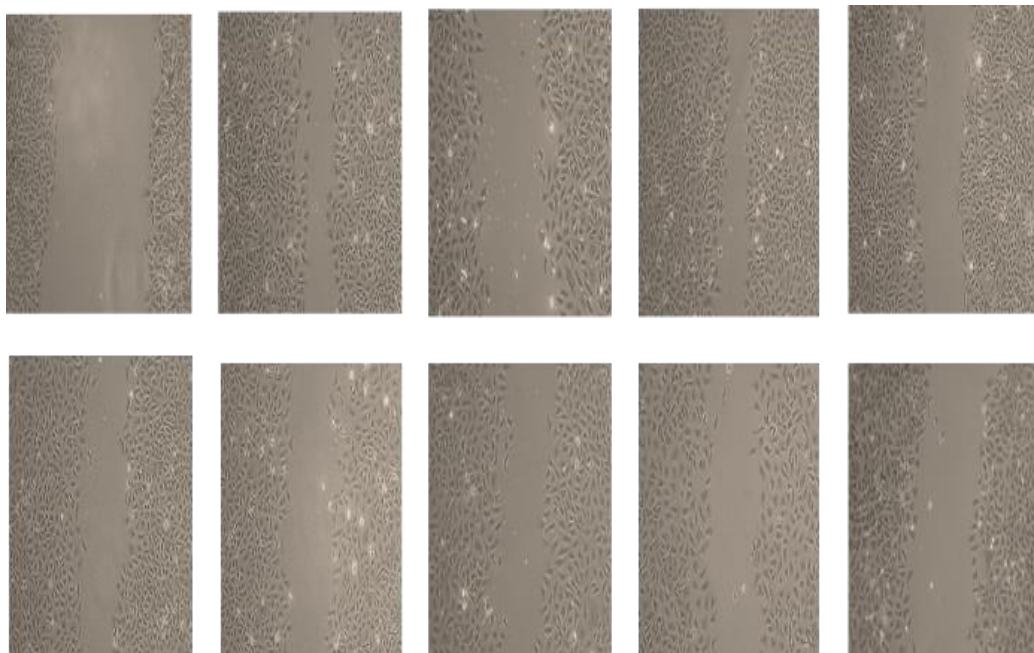
Effect of glucose on tube formation



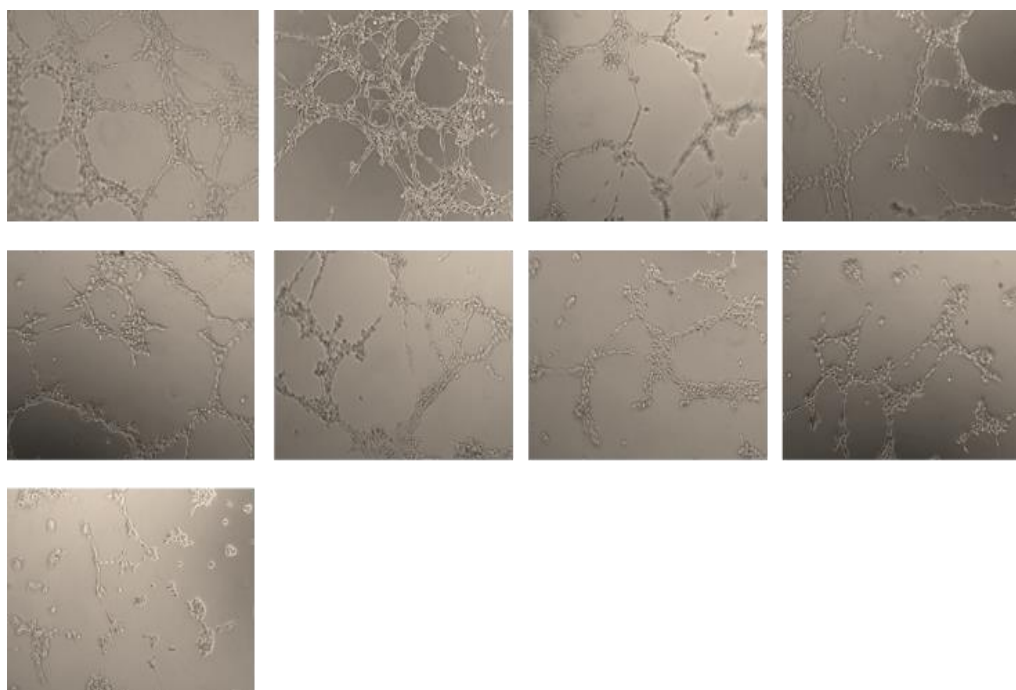
Effect of SAC/NAC pre-incubation in the presence of glucose on BAECs wound healing



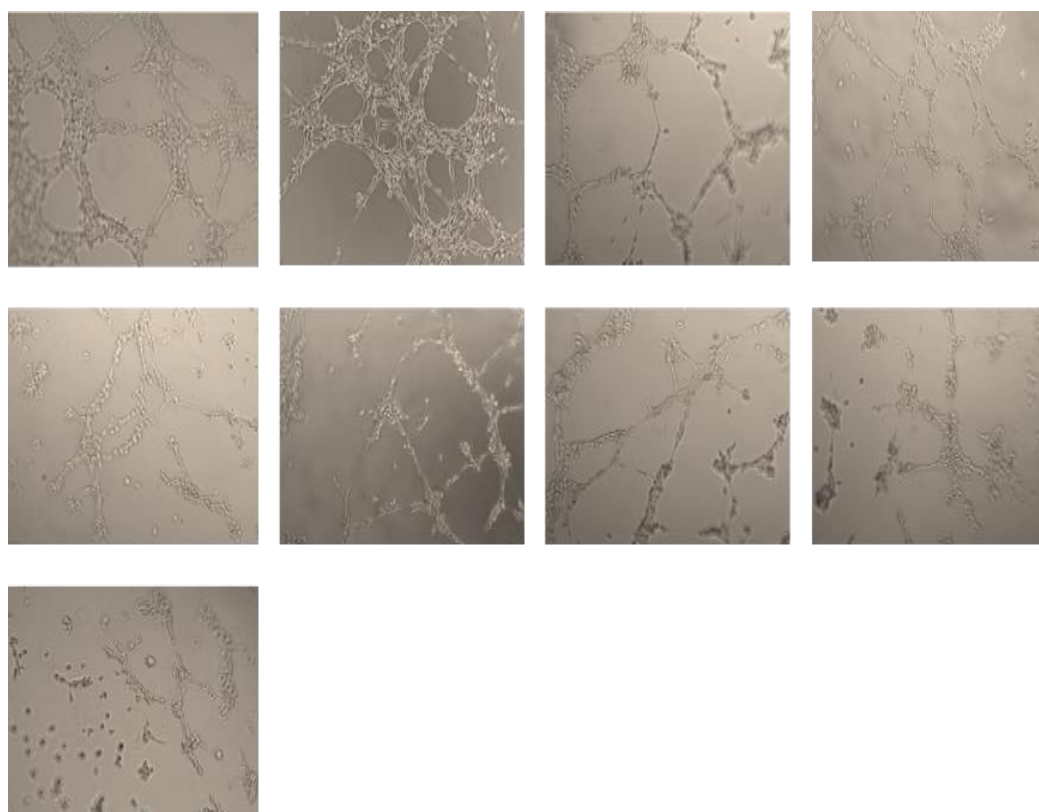
Effect of compound A pre-incubation in the presence of glucose on BAECs wound healing



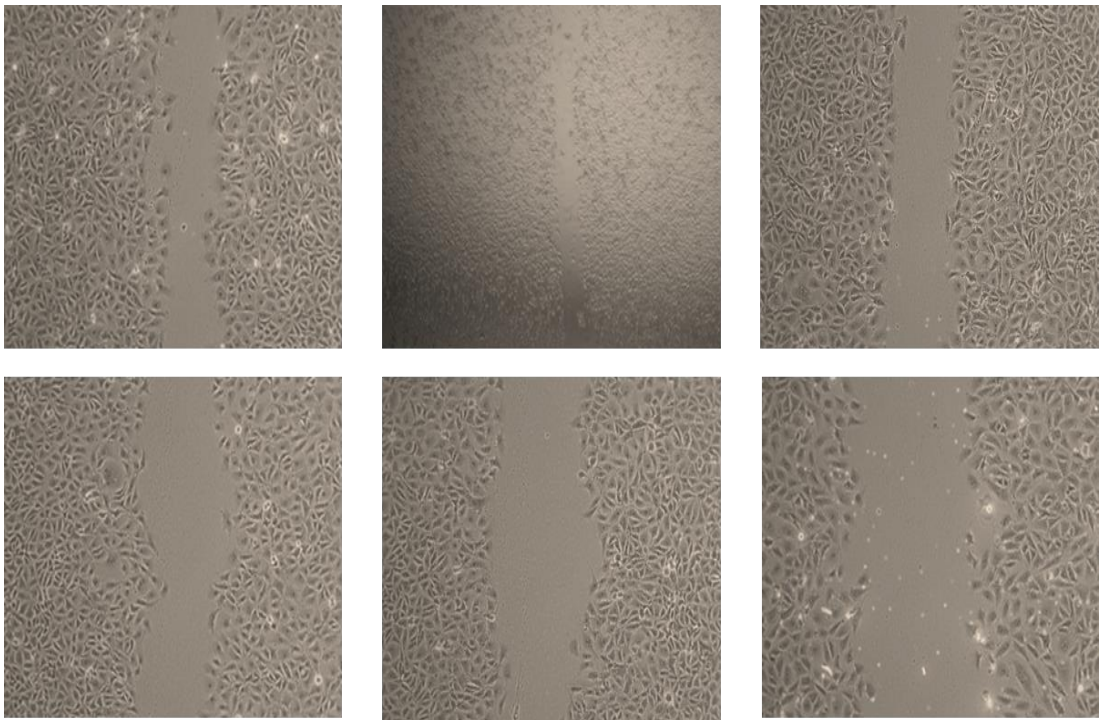
Effect of SAC/NAC in the presence of glucose on BAECs tube formation



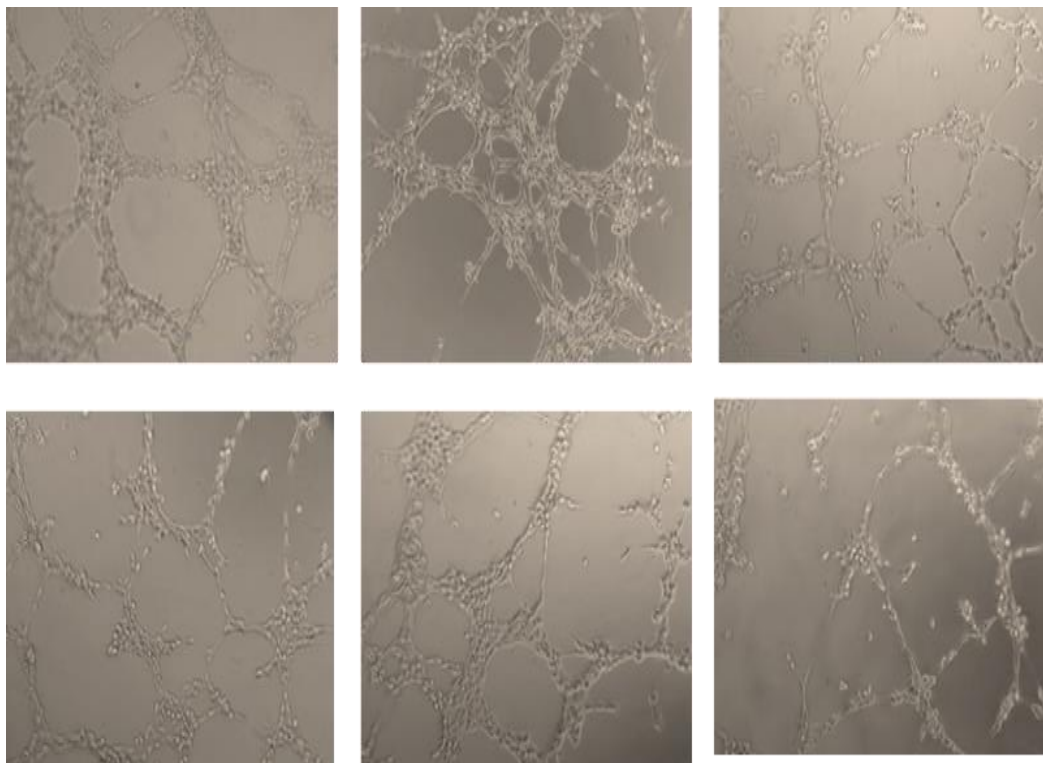
Effect of compound A pre-incubation in the presence of glucose on BAECs tube formation



Effect of BSA-AGE on BAECs wound healing



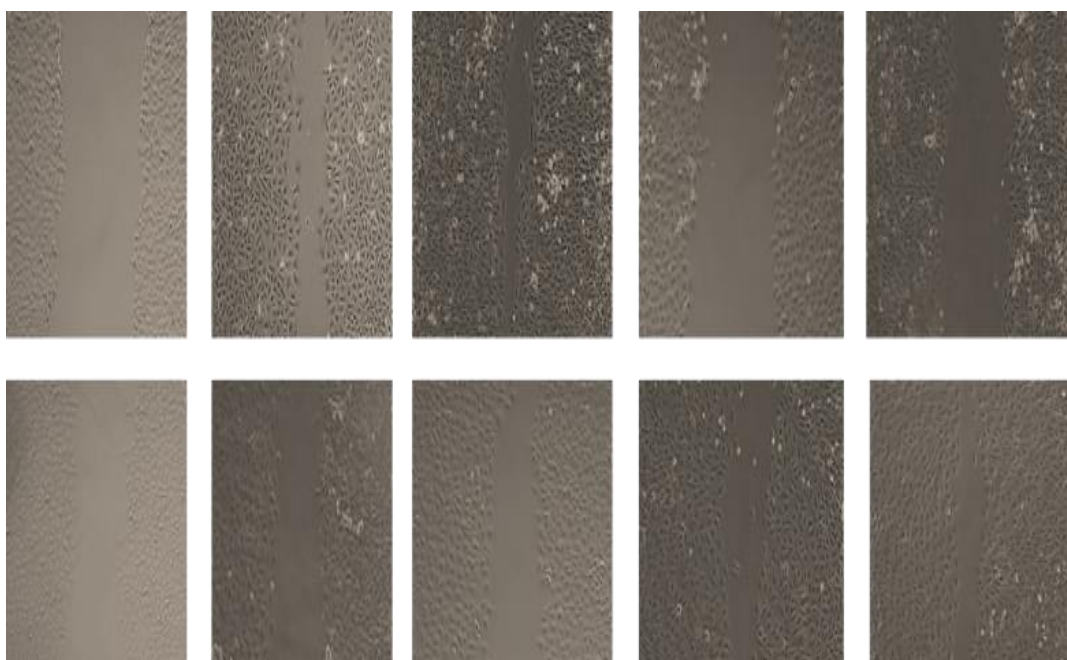
Effect of BSA-AGEs on BAEC tube formation



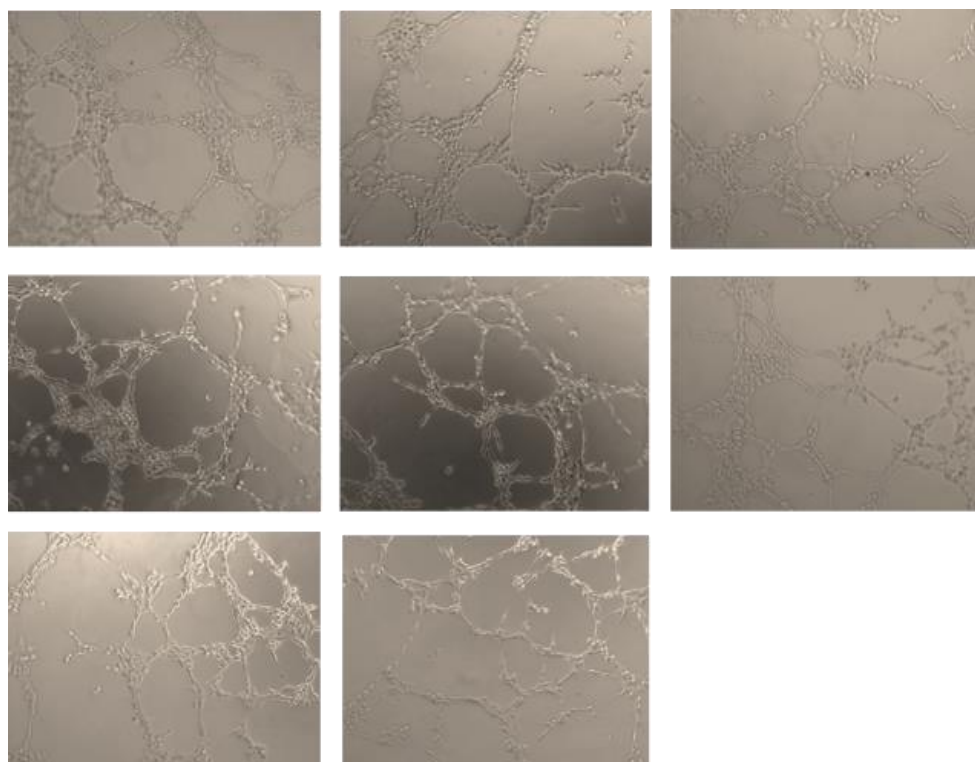
Effect of SAC/NAC in presence of BSA-AGE on BAEC wound healing



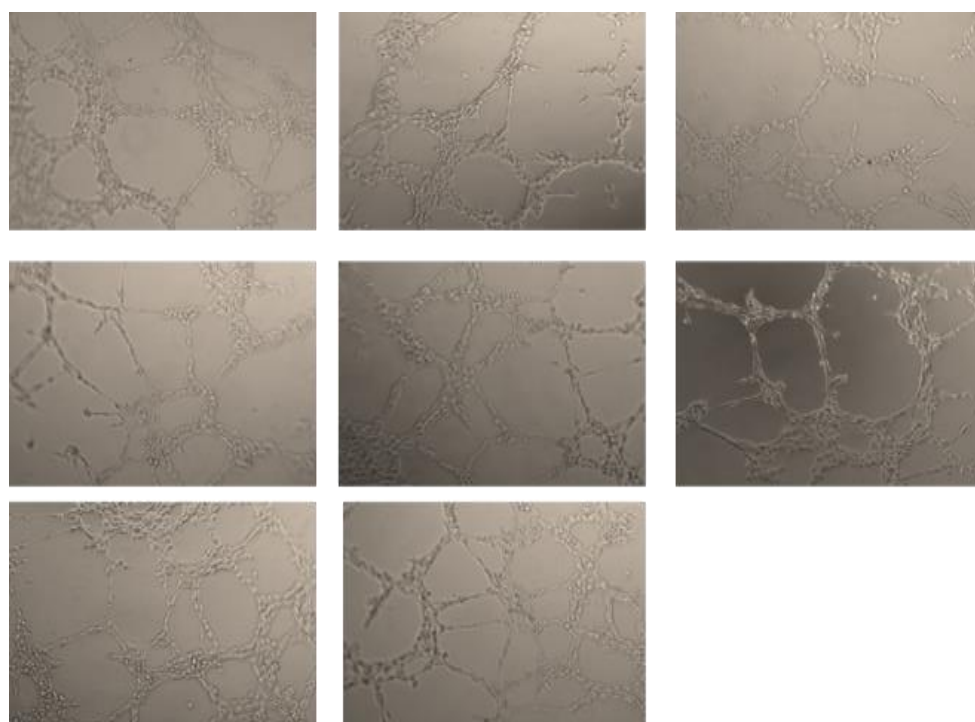
Effect of compound A in presence of BSA-AGE on BAEC wound healing



Effect of SAC/NAC in presence of BSA-AGE on BAEC tube formation



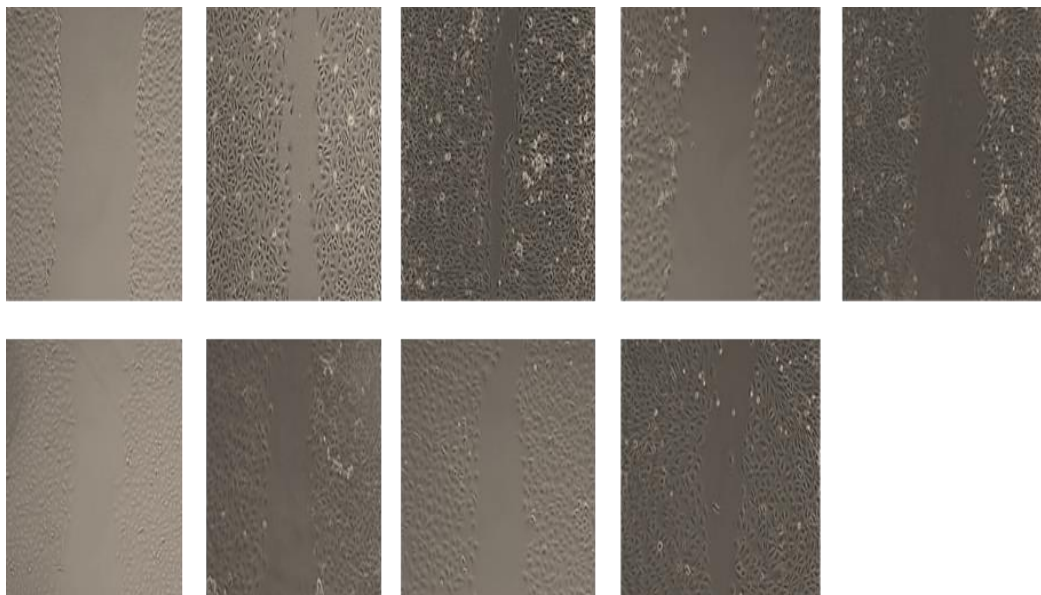
Effect of compound A in presence of BSA-AGE on BAEC tube formation



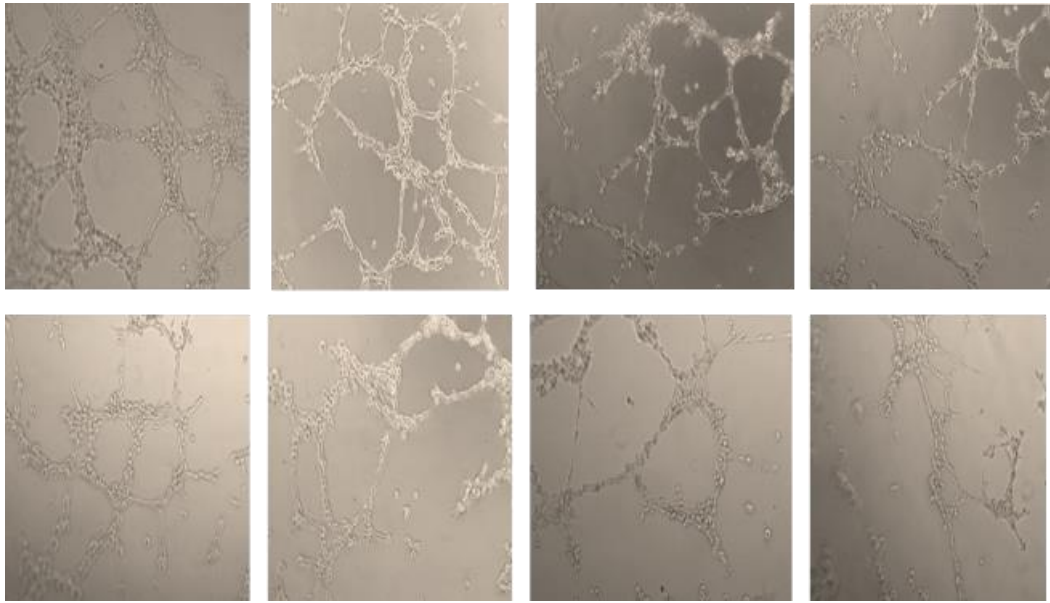
Effect of SAC/NAC on BAEC wound healing



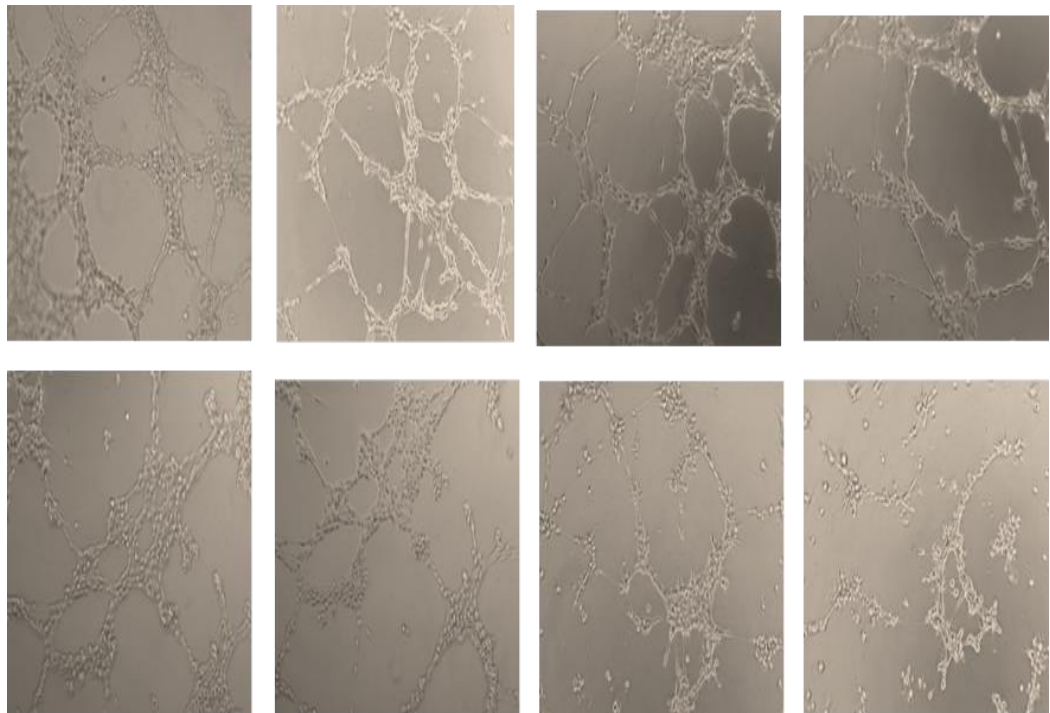
Effect of compound A on BAEC wound healing



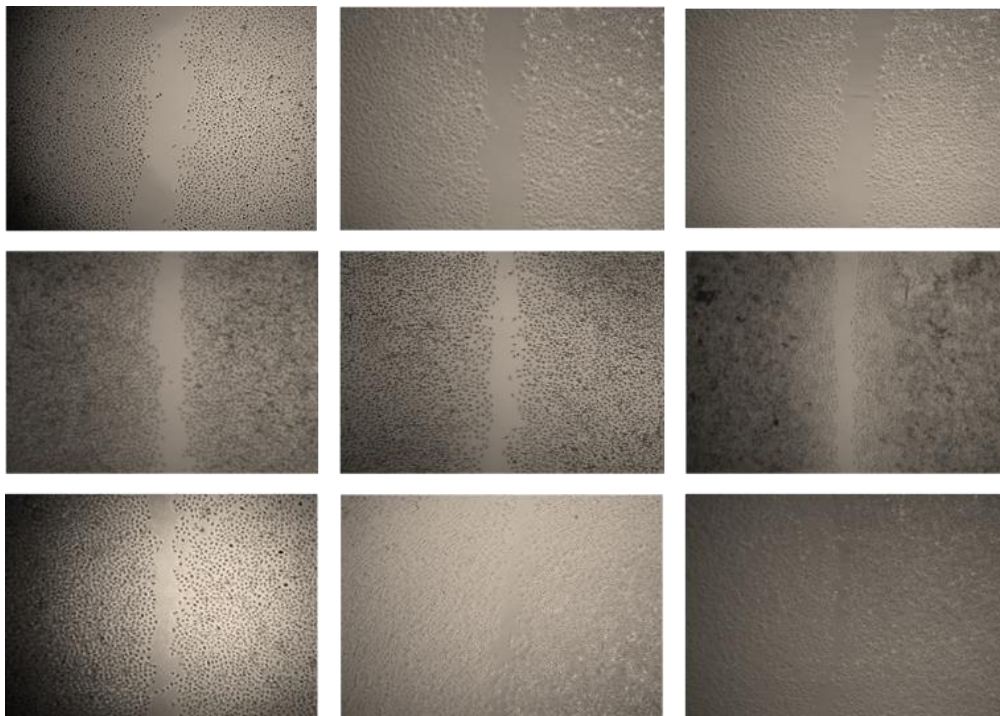
Effect of SAC/NAC on BAEC tube formation



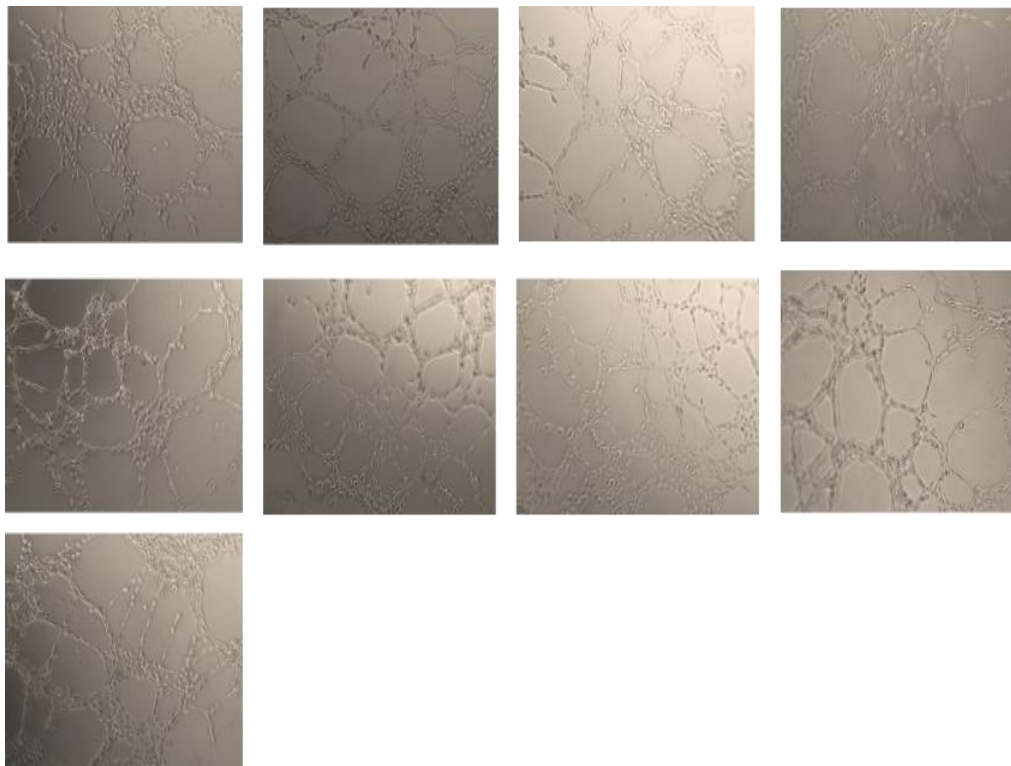
Effect of compound A on BAEC tube formation



Effect of SAC/NAC- and compound A-loaded hADMSCs CM on BEAC wound healing

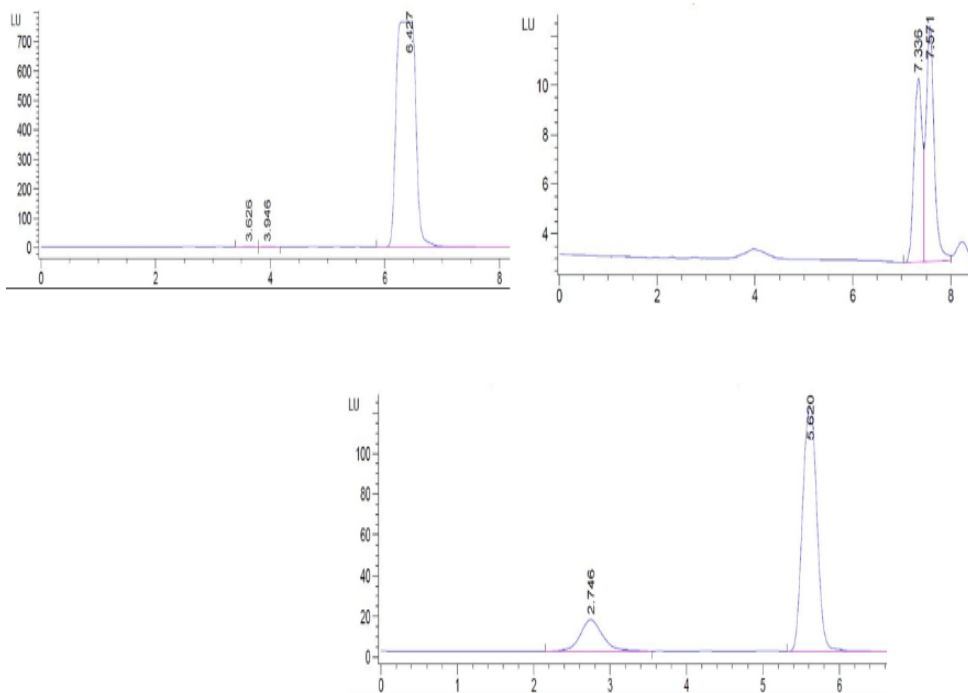


Effect of SAC/NAC- and compound A-loaded hADMSCs CM on BAEC tube formation

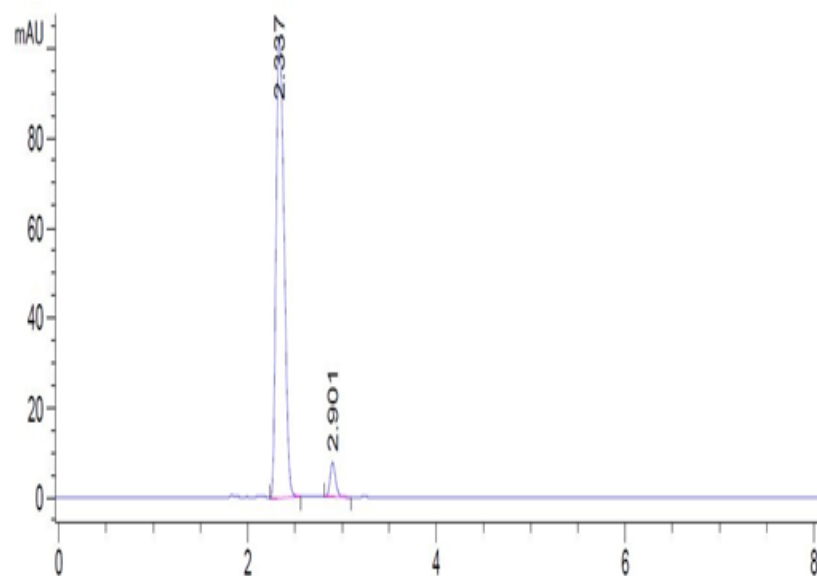


Appendix C: HPLC

Analysis of NAC hADMSCs-loaded CM with high performance liquid chromatography (HPLC)



Detection of NAC by UV –DAD



HPLC analysis of NAC

